APRIL 2019 Ph.D. in Civil Engineering MUHAMMET ÇINAR

HASAN KALYONCU UNIVERSITY

GRADUATE SCHOOL OF

NATURAL AND APPLIED SCIENCES

AN INVESTIGATION OF FRESH AND HARDENED PROPERTIES OF CEMENTITIOUS GROUT MADE WITH COMBINED USE OF WASTE MARBLE POWDER AND FLY ASH

Ph.D. THESIS

IN

CIVIL ENGINEERING

BY

MUHAMMET ÇINAR

APRIL 2019

An investigation of fresh and hardened properties of cementitious grout made with combined use of waste marble powder and fly ash

Ph.D. Thesis

In

Civil Engineering

Hasan Kalyoncu University

Supervisor

Prof. Dr. Mehmet KARPUZCU

By

Muhammet Çınar

April 2019

GRADUATE SCHOOL OF NATURAL & APPLIED SCIENCES INSTITUTE
PhD ACCEPTANCE AND APPROVAL FORM

Civil Engineering Department, Civil Engineering PhD (Philosophy of Doctorate) programme student **Muhammet ÇINAR** prepared and submitted the thesis titled **"An Investigation of Fresh and Hardened Properties of Cementitious Grout Made with Combined Use of Waste Marble Powder and Fly Ash"** defened successfully at the VIVA on the date of 04/04/2019 and accepted by the jury as a PhD thesis.

Position	**Title, Name and Surename Department/University**	**Signature**
Supervisor	Prof. Dr. Mehmet KARPUZCU Civil Engineering Department/ Hasan Kalyoncu University	
Jury Member	Prof. Dr. Hanifi ÇANAKCI Civil Engineering Department/ Gaziantep University	
Jury Member	Prof. Dr. Fevziye AKÖZ Civil Engineering Department/ Hasan Kalyoncu University	
Jury Member	Assist. Prof. Dr. Adem YURTSEVER Civil Engineering Department/ Hasan Kalyoncu University	
Jury Member	Assist. Prof. Dr. Fatih ÇELİK Civil Engineering Department/ Niğde Ömer Halisdemir University	

This thesis is accepted by the jury members selected by the institute management board and approved by the institute management board.

Prof. Dr. Mehmet KARPUZCU
Director

I hereby declare that all information in this docement has been obtained and presented in accordance with academic rules and ethical conduct. I also declare that, as required by these rules and conduct, I have fully cited and referenced all material and results that are not original to this work.

Muhammet ÇINAR

ABSTRACT

AN INVESTIGATION OF FRESH AND HARDENED PROPERTIES OF CEMENTITIOUS GROUT MADE WITH COMBINED USE OF WASTE MARBLE POWDER AND FLY ASH

ÇINAR, Muhammet

Ph.D. in Civil Engineering

Supervisor: Prof. Dr. Mehmet KARPUZCU

April 2019

171 pages

The main objective of this thesis study is to investigate the effect of Waste Marble Powder (WMP) and Fly Ash (FA) on the rheology, workability, fresh and hardened properties of cementitious grout with respect to higher water/ binder (w/b) ratios.

Due to the rapid increase in the demand for marble, which is a natural stone, the number of enterprises and factories related to marble sector is increasing. Depending on the capacity of these factories, mud, powder and pieces of marble waste are exposed; waste amount reaches up to 75%. Emptying the marble wastes to the usable agricultural land, the mixing of the very fine powdered part into the air and the water causes environmental pollution, has a negative effect on the health, covering the agricultural land in a long time and damages the soil and the products.

Fly Ash is a silica-based powdery substance originating from the flue-gas of thermal power plants. Because of its pozzolanic effect, it binds free lime from cement hydration. This feature caused by fly ash in concrete production are widely used, but the rapid increase in the demand for electrical energy in Turkey, inadequacy of existing plants necessitates the creation of new thermal power plants, which in our country annually about 13 million tons, which will further increase the amount of this waste it means.

The use of marble dust and fly ash from the solid wastes, which is an environmental problem in the world, in the improvement of the ground, which is a very important area of the construction sector, will provide the economic value of these wastes and will contribute to the prevention of environmental pollution by the removal of solid wastes. In this thesis; In order to contribute to the solution of the waste problem, it is aimed to use marble dust and fly ash in the production of cement based grout which is used for the treatment of soils. In the experimental study planned for this purpose, waste marble powder (WMP) and fly ash (FA) were replaced with cement; in this study, the fresh and hardened properties of cement based grout mixtures were

investigated by experimental study. The investigation of the effects of these mixtures on the ground by model experiments was excluded.

Four series of mixtures were prepared for the production of cement based injection mortars. In the first series prepared, 5, 10, 15, 20, 25% by weight of the marble was added to the cement. In the second series 25% (fixed) by weight of fly ash, 10, 15, 20, 25, 30% of the amount of waste marble dust was added to the cement. In the third and fourth batch mix, 20% by weight of clay is added to the whole mixture ratio provided that the ratios in the first two series remain constant. The ratio of water to the binder in each series was chosen as 0.75, 1.00, 1.25, and 1.5. A total of 48 (forty-eight) different injection mixtures were prepared with these materials and ratios. In each of the mixtures, a series of tests, such as plate cohesion, marsh funnel flow time, mini slump flow diameter, and cylindrical rotating rheometer, were carried out, including freshness and rheology tests. Specifically prepared series of 432 cylindrical specimens with a diameter of 5.5 cm, 11 cm in height, with three and four series identified; unconfined compressive strength test (UCS) were performed on 3, 7, 28 days. In each series, control sample was prepared by considering water-binding ratios. Control samples ingredient included first and second series water and cement, thirth and fourth series water, cement and clay. No additives were added to the cntrol samples.

The test results were compared with the control samples and the literature; It has been concluded that mixtures of cement based grout prepared using waste marble dust and fly ash can be injected and used in the treatment of weak soils.

Keywords: Cement grout, Waste marble powder, Fly ash, Rheology, Workability, Fresh and hardened properties, Soilcrete.

ÖZET

ATIK MERMER TOZU VE UÇUCU KÜLÜN BİRLEKTE KULLANIMIYLA ÜRETİLEN ÇİMENTO ESASLI ENJEKSİYON HARCININ TAZE VE SERTLEŞMİŞ ÖZELLİKLERİNİN ARAŞTIRILMASI

ÇINAR, Muhammet

Doktora Tezi, İnşaat Mühendisliği

Tez Yöneticisi: Prof. Dr. Mehmet KARPUZCU

Nisan 2019

171 sayfa

Bu tez çalışmasının temel amacı, Atık Mermer Tozu (WMP) ve Uçucu Kül (FA) ikame edilmiş çimento bazlı enjeksiyon karışımlarının yüksek su / bağlayıcı (w / b) oranlarında reolojik, işlenebilirlik, taze ve sertleştirilmiş özellikleri üzerindeki etkisini araştırmaktır.

Doğal taş olan mermer talebi hızlı artışa bağlı olarak mermer ile ilgili işletme ve fabrika sayısı da artmaktadır. Bu fabrikaların kapasitesine bağlı olarak çamur, toz ve mermer atıkları ortaya çıkmakta; atık miktarı %75'e kadar ulaşmaktadır. Mermer atıklarının kullanılabilir tarımsal alanlara boşaltılması, çok ince toz şeklinde olan kısmının havaya ve suya karışması çevre kirliliğine neden olur, sağlığa olumsuz etki yapar, uzun sürede tarım arazilerini kaplayarak toprağa ve ürünlere zarar verir.

Uçucu Kül, termik santrallerin baca gazından kaynaklanan silika esaslı toz halinde bir maddedir. Puzolanik etkisi olduğu için çimento hidratasyonundan açığa çıkan serbest kireci bağlar. Bu özelliği nedeni ile uçucu kül, beton üretiminde yaygın olarak kullanılmaktadır, ancak Türkiye'de elektrik enerjisine olan ihtiyacın hızla artması, mevcut santralların yetersiz kalması yeni termik santralların kurulmasını zorunlu kılmaktadır, bu da ülkemizde yıllık yaklaşık 13 milyon ton olan bu atık miktarının daha da artacağı anlamına gelmektedir.

Günümüzde tüm dünyada çevresel bir sorun olan katı atıklardan mermer tozu ve uçucu külün inşaat sektörünün çok önemli bir alanı olan zeminin iyileştirilmesinde kullanılması, bu atıkların ekonomik değer kazanmasını sağlayacak, katı atıkların bertaraf edilmesi ile çevre kirliliğinin önlenmesinde önemli katkıda bulunacaktır. Bu tez çalışmasında; atık sorununun çözümüne katkıda bulunmak için mermer tozu ve uçucu külün zeminlerin iyileştirilmesinde kullanılan çimento esaslı enjeksiyon harcının üretiminde kullanılması amaçlanmıştır. Bu amaçla planlanan deneysel çalışmada atık mermer tozu (WMP) ve uçucu kül (FA) çimentoya ikame edilmiş; yüksek su / bağlayıcı (w / b) oranlarındaki çimento esaslı enjeksiyon karışımlarının reolojik ve işlenebilirlik gibi taze, basınç dayanımı gibi sertleştirilmiş özellikleri deneysel çalışma ile araştırılmıştır. Bu karışımların zemine yapacağı etkilerin model deneyler ile araştırılması kapsam dışı bırakılmıştır.

Çimento esaslı enjeksiyon harçlarının üretiminde dört seri karışım hazırlanmıştır. Hazırlanan ilk seride çimentoya ağırlıkça %5, 10, 15, 20, 25 oranında atık mermer tozu ilave edilmiştir. İkinci seride çimentoya ağırlıkça %25 (sabit) oranında uçucu kül, %10, 15, 20, 25, 30 oranlarında atık mermer tozu ilave edilmiştir. Üçüncü ve dördüncü seri karışımda ise ilk iki serideki oranlar sabit kalmak koşulu ile tüm karışım oranınına ağırlıkca %20 oranında kil eklenmiştir. Her seride suyun bağlayıcıya oranı 0.75, 1.00, 1.25, ve 1.5 olarak seçilmiştir. Bu malzemeler ve oranları ile toplam 48 (kırk sekiz) farklı enjeksiyon karışımı hazırlanmıştır. Karışımların her birinde taze halde iken işlenebilirlik ve reoloji testlerini içeren plaka kohezyon, marsh hunisi akış zamanı, mini slump akış çapı ve silindirik dönen rheometre gibi bir dizi test yapılmıştır. Özellikleri belirlenen seri üç ve dört karışımlar ile çapı 5.5 cm, yüksekliği 11 cm olan 432 adet silindir numune hazırlanmış; 3, 7, 28 günlerde basınç deneyleri yapılmıştır. Her seride su / bağlayıcı oranları göz önüne alınarak kontrol numunesi hazırlanmıştır. Kontrol numunelerinin içine seri bir ve ikide sadece su ve çimento, seri üç ve dörtte çimento, kil ve su katılmış herhangi bir katkı maddesi ilave edilmemiştir.

Deney sonuçları kontrol numuneleri ve literatür sonuçları ile karşılaştırılmış; atık mermer tozu ve uçucu kül kullanılarak hazırlanan çimento bazlı enjeksiyonun karışımlarının zayıf zeminlerin iyileştirilmesinde enjekte edilebilir ve kullanılabilir olduğu kanaatine varılmıştır.

Anahtar Kelimeler: Çimento enjeksiyonu, Atık mermer tozu, Uçucu kül, Reoloji, İşlenebilirlik, Taze ve Sertleşmiş özellikler, Soilcrete

To My Parents

ACKNOWLEDGEMENTS

In the name of Allah, the most benevolent, the most merciful. First of all, I wish to record immeasurable gratitude and thankful fullness to the one and the almighty creator, the Lord and sustainer of the universe, and the mankind, in particular. It is only through His mercy and help that this work could be completed, and it is ardently desired that this little effort be accepted by Him to be of some service to the cause of humanity.

This dissertation has been completed under the guidance of my advisor, Prof. Dr. Mehmet KARPUZCU. I dedicate the greatest and sincere thanks to my supervisor for his advice, guidance and help throughout the preparation of this work.

I would like to thank to Prof. Dr. Hanifi ÇANAKCI and Prof. Dr. Ömer ARIÖZ for their helps and valuable suggestion.

Also, I would like to thank to Res. Assist. Mehmet SAKİN, Res. Assist. İbrahim Halil DEGER, and Assist. Prof. Dr. Mehmet Eren GÜLŞAN for supporting me during my research.

My thanks are also expressed to my parents (Hüseyin ÇINAR and Şefika ÇINAR) for their appreciable toil and supports upto now.

I would like to extend special thanks to my wife, Zamire ÇINAR, my sons, Hüseyin ÇINAR and Said ÇINAR for helps, patience and encouragement during this work.

Finally, I would also like to specially thanks to everyone who I cannot remember and tell their names and who have big toils on my success and life upto now.

TABLE OF CONTENTS

LIST OF TABLES

LIST OF FIGURE

LIST OF SYMBOLS / ABBREVIATIONS

ASTM	American standard for testing materials
ASTM C-143	Standard Test Method for Slump of Hydraulic Cement Concrete
C	Constant
CBG	Cement Based Grout
CG	Cement Grout
CL	Low Plasticity Clay
Cp	Centipoises
FA	Fly Ash
JG	Jet Grouting
LL	Liquid Limit
MCD	Microfine Cement Dust
MCFT	Marsh Cone Flow Time
MDD	Maximum Dry Density
MS	Marble Slurry
OMC	Optimum Moisture Content
PC	Portland Cement
PCM	Plate Cohesion Meter
PFI	Particle Flow Interaction Model
PL	Plastic Limit
RH	Rice Husk
RHP	Rice Husk Powder
R^2	The coefficients of correlation
SCC	Self Compacting Concrete
UCS	Unconfined Compressive Strength
USCS	Unified Soil Classification System
WMP	Waste Marble Powder
WMS	Waste Marble Sluge
w/c	water-cement ratio
w/b	water-binder ratio

CHAPTER 1

INTRODUCTION

1.1. Overview

Cement Based Grout (CBG) is a widely used method for many applications in the geotechnical area. Some examples of CBG applications are suspension grouting, emulsion grouting, solution grouting, compaction grouting, permeation grouting, displacement grouting and replacement grouting. The rheological and permeability properties of the CBG are straightly involved with the penetrability and pumpability in cracks and soil voids.

Because of the need for underground improvement (e.g. metro, tunnel, canal, basement etc.) over the last twenty years, practice of grouting method in solving problems related to groundwater leekage, insufficient foundation soil and precision existing construction have been commonly applied in the infrastructure construction works in around the world. Permeation grouting by injecting CBG into the ground via a pressure system, e.g. pump, was found mostly applied in the construction industry for decreasing leakage impact induced by diggings in permeable media, e.g. sand of high permeability and improving the steady and bearing resistance of soil in diggings and foundation works, separately.

Because of the complication of the rheological characters (e.g. viscosity and yield stress) of CBG and its uncertain flow movement (i.e. injectability or groutability) in permeable media undersoil, specially, in the regional sandy soil usually found with the high ingredient of fines normally used by using chemical grout or superfine cement grout overseas, the influence of permeation grouting using standard Portland cement with high w/c rate in excess of 3.0 by some regional researcher is not clear. For this reason, it appears that it is still substantially a trial and error process in the present practice, particularly in the local construction industry. If it is not satisfactorily completed, it could lead to wastege or failed performance (e.g. weak water impermabilty) of the soil improvement work.

In the present situation of the grouting, the movement of a viscous fluid injected from the borehole into the ground was examined by considering the laminar flow from inside a cylindrical or spherical cavity into the mass of granular soil completly homogeneous.

In accordance with Tomiolo (1982), these 2 current flow types (Raffle and Greenwood, 1961) consider the flow of viscous fluids through the soil follows the similir laws ruling the flow of water, all worths (e.g. coefficient of permeability to grout, kG) being amplified proportionally to the rate of grout viscosity to water viscosity as display in Eq. (1.1).

It is the idea of the author that such importance may not be suitable for CBG with water/cement ratio (w/c, by weight) below 1.5 in view of the important Bingham's fluid characteristics possessed by these CBG mixes and also the very high injection pressure applied in the CBG permeation grouting works, which may effect the validity of Darcy's law.

$$k/k_G = \eta/\eta_w \quad \text{(after Muller-Kirchenbauer, 1968)} \qquad (1.1)$$

Where, η_w = viscosity of water, Pas, η = viscosity of Newtonian grout, Pas ($N.s/m^2$), k = permeability of soil to water, m/s, k_G = permeability of soil to grout, m/s

For improve the practice of CBG using the existing flow models in the local construction industry, proper understanding of the characteristics of CBG, including the effects of the handling process to the viscosity measurement of CBG and grout flow properties taking into take into account the effect of high injection pressure on the coefficient of permeability for CBG (kG) in permeable area, i.e. the validity of constant kG based on Darcy's law, existing flow models require a default value is needed.

Literature review and reginoal application reveals the limited rheology work for CBG in published research studies and uncertainties regarding CBG implementation like:

•Porous flow of Bingham's fluid;

•Rheological characteristics (e.g. yield stress and viscosity) of CBG with w/c between 0.6 and 1.5 not available in research work in the past, specially for the normal Portland cement mostly used in the local construction industry, taking into importance of dependence on time and shear history dependence on several mixing and measurement programs;

•Effect of injection pressure in flow properties of CBG in permeable area.

1.2. Use of Grouting for Ground Engineering

Due to the rapid development of underground urban infrastructure, the utilization of grouting has been more favored in last decade, underground space for commercial (e.g. carpark) and civil protection building (e.g. storage and shelter) and underground facilities (e.g. tunnel system and common services channel) uses and the need in place control during construction. The grouting could be utilized to develop the construction area against potential construction problems as follows:

• To decrease the porosity of ground for reduce leakage effect

• To strengthen soils to make better its resistance in against liquefaction effect, excavation stability and load carrying capacity.

• Increasing the stability of existing buildings

• Fixing the soil to facilitate tunnel opening or shaft excavation.

• Create an obstacle or cut against water or contaminant flow on the soil.

1.3. Rheology of Grout

Rheology is the examination of the materials flow. The major characteristics of grouts are viscosity, stability and setting time. The measured stability properties contain pressure filtration and bleed. Bleed is the free water amount that improves with duration at a grout column top at rest, expressed as its total volume percentage. If the bleeding is below five percent after two hours, a mortar is considered stable. Pressure filtration is a leakage measurement under pressure. The pressure filtration coefficient is a measure of how much water is taken from of a sample under pressure in a given time period.

Grout requires setting time for hardening. CBG usually setting within four to twenty-four hours which depending on the additives used. For chemical groups that can be adjusted very quickly in minutes, setting or gel time can be critical. Viscosity (μ) is defined by Newton's law of viscosity, which is the proportionality factor that relating the shear resistance (τ) in a fluid to the speed gradient (dv/dz), it represents the ratio at which a fluid layer moves relative to an adjacent layer.(Eq. 1.2)

$$\tau = \mu . dv/dz \quad (1.2)$$

The above equation hold for laminar flow. The SI unit for viscosity is the pascal-second (Pa.s). The viscosity μ is also called the dynamic viscosity or absolute viscosity. When dynamic viscosity is divided by mass density ρ, it becomes the kinematic viscosity (υ). (Eq. 1.3)

$$\upsilon = \mu / \rho = (\mu . g) / \gamma \quad (1.3)$$

The units of kinematic viscosity are square meters per second. Another unit name which may be used is the centistoke (cSt) where 1 cSt $=E^{-6}$ m^2/s.For turbulent flow dynamic eddy viscosity η is used.(Eq. 1.4)

$$\tau = (\mu+\eta).dv/dz \quad (1.4)$$

Turbulent flow is important as far as maintaining the stability of the grout during pumping is concerned. When it comes to evaluating the extent of grout penetration into the ground, laminar conditions are generally assumed. The transition from laminar to turbulent flow is usually described in terms of dimensionless Reynold's number Re . (Eq. 1.5)

$$Re = (\rho \upsilon L)/\mu \quad (1.5)$$

υ is the flow velocity and L is the characteristic length. Normally, a grout must have low viscosity, a controllable setting time and high strength when it enters the ground. It should not be toxic, permanent and inexpensive.

Viscosity of grout can be estimated directly or indirectly. Rheologic properties of grouts can be calculated by using several test methods. Some of them are given below.

1. Viscometer

2. Marsh cone test
3. Plate cohesion test
4. Mini slump test.

In Newtonian fluid the shear stress varies proportionally to the velocity gradient dv/dz. A fluid which has a non-linear relationship between dv/dz and shear stress is classified as non-Newtonian. Bingham body is not a fluid, but rather a visco-plastic solid. Nevertheless the term Bingham fluid. The rheological attitude of a Bingham body is expressed by;

$$\tau=\tau_o+\mu(dv/dz) \quad (1.6)$$

The initial yield stress (τ_o) is also called rigidity. (Eq. 1.6) Some engineers refers to it as cohesion or flow limit. Water behaves as a newtonian fluid. Clay particles in suspension represent a non-newtonian substance. A cement or clay grout might be almost as Bingham body is treated.

1.4. Waste Marble Powder(WMP), Fly Ash (FA) and Soilcretes Prperties

CBG is mixed of water, cement and admixture. For CBG mix design, different range of water-cement (w/c) ratio can be utilized. For the applications of permeation grout, w/c ratio of CBG range between 0.5 and 1 (Danot and Derache, 2007). The w/c rate of injectable grout ranges from 1 to 2. Also, the grout should be similar to the liquid that can be injected into the rock and soil (Baltazar et al., 2012). CBG mixes have usually water-cement ratios of 1.00 by volume.

Mineral and chemical admixtures are used to develop the properties of CBG like durability, permeability, rheological and fresh properties. Adding mineral admixtures to the CBG at different amount modify the rheological and fresh properties of injections. For various types of grout applications, various additions (Cement kiln dust, silica fume, rice husk ash, metakaolin and bentonite) have been applied (Miltiadou, 1991; Ruggiero, 1984; Weaver, 1990).

Some recent studies showed that additive, like rice husk ash, have increased the durability, long-term performance and workability of CBG mix (Sonebi et. al., 2013; Rosquoe et al., 2003). Consequently, the additives usage in CBG applications reduce the charge of the application but increment the flowability and the strength.

Marble is a very important material for construction, particularly for decoration reasons. %25 percent of marble turns to powder and dust due to shaping, polishing, and sawing. Turkey has 40 percent of the world's total marble and produces 7 million tons of marble were manufactured every year. Five thousand processing factories are used for marble production in Turkey. It is clear that these waste products reach millions of tons; so it is too difficult to store this amount of wastes (Alyamaç and Ince, 2009; Pooja and Prof, 2014).

FA is a divided siliceous tailing from the burning up of powdered coal and can be used an admixture. Fa has the same fineness like Portland cement (PC). It can also react easily chemically with cement. Also, the average annual FA production in Turkey has about 13 million tons and half of it was utilized.

The disposal of WMP and FA are one of the most environmental concerns all over the world nowadays. On the other hand, WMP and FA can be used to increase the fresh properties of cementitious grout.

WMP is used like a complementary cement based material in the concrete. Earlier researches concluded that maximum 10-15 percent of WMP can be conveniently mixed into the concrete without negatively impacting the durability, hardness and strength of the resulting concrete (Shirule et al., 2012; Aliabdo et al., 2014). Another researches investigated the usage of WMP as a cement substitution. Also, Study showed that combining of WMP in self-compacting concrete (SCC) with concrete reduce the splitting tensile strength, compressive strength, bulk weight, slump flow, ultrasonic pulse velocity, porosity and cost (Aliabdo et al., 2014).

Usually, the percentage of FA usage is 10-35% in concrete(Yao et al., 2015). The usage of FA in concretes and SCC have also been investigated and have been well developed in the last decade(Uysal and Yılmaz, 2011). On the other hand, there is limited knowledge available concerning the fresh characteristics of cement based grout containing FA. The replacement of Portland Cement with FA is important for decreasing the viscosity, increasing passing ability and flowability of cement based grout materials(Sadati et al., 2016). The aim of this experimental study is to research the impact of water-binder (w/b) rate (1.00) and different percentage of WMP, FA and WMP+FA content on the workability, fluidity, and rheological characteristics of CBG.

1.5. Objectives of The Thesis Study

The goal of the thesis study is to research the effect of Waste Marble Powder (WMP) and Fly Ash (FA) on the rheology, mechanical and workability characteristics of cement base grouts with respect to higher water/binder (w/b) rations. Based on this modeling process, following studies are aimed;

- ✓ To investigate the effect of using WMP and FA as an additive on rheological properties (yield stress and viscosity) of cement base grout at different range of w/b rations that are generally used for jet grouting applications.
- ✓ Also to find the effect of WMP and FA on cement base grouts depending on workability properties such as mini slump diameter, marsh cone flow time and plate cohesion meter.
- ✓ Then, to evaluate the impact of WMP and FA on compressive strength of soilcretes obtained by mixing WMP, FA, cement, clay, and water at different w/b rations ranges.
- ✓ In addition, to examine the bleeding features of grout mixtures prepared by mixing WMP, FA, cement, clay and water at different w/b rations ranges.
- ✓ Finally, to compare the results with control samples and literature to show the injectibility, workability and usability of the cement base grout obtained by using WMP and FA, which is waste materials.

1.6. Organization of The Thesis Study

The organisation of the thesis study was presented as following;

In Chapter 1: general background and introduction of the study were given. General information about the grouting techniques, grouting materials cement base grouts, rhelogical and mechanical properties of the cement base grouts were discused in this chapter

In Chapter 2: detailed literature informations related with rheological and mechanical properties of cement base grouts were given and discussed.

In Chapter 3: detailed overview and theoretical background of cement base grouts were investigated and the methods and models were discussed.

In Chapter 4: experimental study of rheological and workability properties of cement base grouts mixing with WMP prepared for this study were presented. And also test results obtained from the thesis study were discussed.

In Chapter 5: experimental study of rheological and workability properties of cement base grouts mixing with WMP and FA prepared for this study were presented. And also test results obtained from the thesis study were discussed.

In Chapter 6: evaluation of unconfined compressive strength, stability and failure creteria of the soilcretes samples obtained from mixing of cement base grout with WMP and FA and clay soil were investigated and test results were given and debated.

In Chapter 7: conclusions and recommendations extracted from the thesis study were explained.

CHAPTER 2

LITERATURE SURVEY

2.1 Studies on Rheological Properties of CBG

The rheological characteristic (e.g. viscosity and yield stress) of grout with the inclusion of different influence types like as stability (bleeding), mixing duration, additives and the degree of saturation have been worked by a lot of researchers until now. Although, the knowledge got from all these works are shown more intensive in the characters of the solution grout, microfine cement grout or ordinary CBG with additives (e.g. bentonite, etc.) owing to weak penetration of arrant CBG because of its short setting time and high viscosity, and the grout mixtures considered in these works are found not to cover the proper range of CBG mixtures, i.e. water /cement = 0.6 to 1.5, for efficient implementation of penetration grouting in sand using ordinary Portland cement as accepted in the experimental program of the present work. Some of the findings / comments obtained from previous studies are summed up as below.

Cambefort (1964) clarified that CBG has good-defined shear stress that improves directly later mixing and is qualified by its viscosity function.

Klein and Polivka (1958) schematically interpreted the cement grout stages after mixing as dormant, hardening and setting with a grout strength increasing with curing time nearly in function of power or exponential.

Caron (1963) entitle CBG as Bingham's grouts, as owning hardness and viscosity at the same time, both increment with time and displacement could only start beyond a specific pressure or so called yield stress.

Raffle and Greenwood (1961) improved a graphical relationship between the rheological properties of grout (Figure 1.1) and its capacity to pass on the soil and remarked that injection of fresh cement grout is controlled by shear strength and viscosity in order of in the early and later phases. Significant increases in shear strength and viscosity have been reported for the CBG not exceeding 0.6, as shown in Figure 1.1 with the water/cement ratio (w / c).

Little John (1975) made an observation that a w/c rates between 0.4 and 0.45 give a grout with adequate fluidity to be pumped and placed easily in a small diameter borehole and yet keep enough continuity and strength after injection to act as a strengthening area. He reported a rapid increment in shear strength and viscosity for CBG with w/c rate below from 0.9 which is different from the rate of 0.6 noticed by both Burgin (1979) and the author.

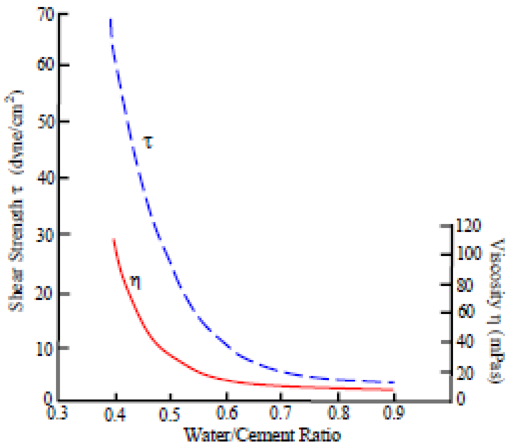

Figure 2. 1: Shear Strength and Viscosities for Cement Pastes with Different w/c Rate (after Raffle and Greenwood, 1961)

Deere (1982) were classified as cement grout as fixed grout due to bleeding not passing over five percent after two hours from finishing of mixing and commented that little amount of bentonite appears to be sufficient, preferable to decrease bleeding and sedimentation but not large enough to develop the penetrability and pumpability.

Banfill (2003) indicated that a mixing time of about five min is enough in order to get stable characteristics for both the plastic viscosity and the yield value. On the other hand, the blended grout volume is unknown.

Lombardi (1985) analyzed the flow terms of a mixture through a smooth stone crack and finalized that the yield stress detects the maximum distance the grout can reach and the viscosity determines the flow ratio and for this reason the time essential to fulfill the injection.

Paoli et al. (1992) debated the basic finding on CBG and commented that penetration is controlled by the particles size more than by yield stress and the grout viscosity ingredients. The grout penetrability can be developed by decreasing the size of the cement particle grains and development the grout’s rheological characters, increment the stability under pressure percolation and decreasing the yield stress.

Vipulanandan et al. (1992) examined the CBG characteristics and grouted sands with additives and stated that the maximum particle size should not exceed 1/3 to 1/10 the void size to penetrate a formation at a reasonable rate and pressure.

Helal & Krizek (1992) stated the orientation of the porous structure in CBG sand indicated that porous structure injected with a CBG is a w/c rate function and the suspended materials sedimentation attitude.

Shroff et al. (1996) studied the microfine cement dust (MCD) grouts rheological characteristics and reported that MCD grout could penetrate into the permeable medium sand and also sand have to permeability value, k= 7.89 x 10^{-3} cm/sec. In addition, He stated that MCD grout possesses not only penetration capability in medium to fine sand comparable to many chemical grouts but also to provide higher adhesion strength to the mass in the grout.

Perret et al. (2000) investigated the impact of the sand saturation degree on groutability and finalized that the grout spreading through permeable area is affected not only by the particle size dispersion of the cement and soil, the water penetrability of the soil and rheological properties of the grout but also the sand saturation degree. The grout water dilution is higher in the unsaturated soil than in the saturated soil, where the grout may be replaced by the water, resulting in a grout layer mixed and diluted with water. In the case of unsaturated sand, the suction resulting from capillary pressure and the non-continuous aqueous medium of the pore water in the soil are led to further water dilution in the unsaturated sand case.

2.2 Marble Powder (MP)

Marble is a very important material for construction, particularly for decoration reasons. 25 percent of marble turns to powder and dust due to shaping, polishing, and sawing. The wastes of the marble factory have turned into a main environmental issue onwards the early of the 1990s. This problem is not only a local issue but also direct anxiety for all at of countries. In many countries, like Turkey, Italy, Iran, India, China, Brazil, Spain, Portugal, South Africa, USA, Pakistan, Finland, and Egypt, export the marble products, many other countries, like Germany, Japan, South Korea, and Taiwan, import them (Alyamac et al., 2017). Turkey has forty percent of the world reserves of marble, and the storage of waste generated during production is of great significance. Turkey has approximately marble reserves of 3.872 million m^3, of which close to 125 * 10^3 t/year are produced in Afyon City. (Singh et al., 2019). Five thousand processing factories are used for marble production in Turkey. It is clear that these waste products reach millions of tons; so it is too difficult to store this amount of wastes (Alyamac and Ince, 2009).

2.3 Fly Ash (FA)

Fly ash is a waste product of coal-fired thermic power plants and has been successfully used as embankment material for road construction projects or a structural filler around the world. Compared to the classic soils used in the filling, fly ash has a matchless engineering material. When dried, the fly ash is incompatible and is considered by many to be a dusty disturbance. If it is saturated, fly ash becomes an uncontrollable mess. However, as with most fine-grained soils, fly ash can be easily used and compressed in more moderate-medium contents and exhibits some amount of cohesion.

The use, storage, and disposal of fly ash produced by coal-burning power plants continue to be the main problem in all over the world. Although it is used in significant quantities in a variety of applications, and especially as a substitute for cement in concrete, large quantities are not used and must be disposed of at high cost in waste collection facilities.

Effective utilization of waste materials decreases the need for large disposal areas, while providing a cheap mineral resource for construction applications. Geotechnical engineering became a key profession in evaluation of the engineering performance of byproduct materials, and in finding new applications.

2.4 The Previous Studies Related with Marble Powder and Fly Ash

Various research studies have been conducted to find the usability of WMP and FA. It has been concluded from these studies that WMP can beneficial for low cost construction material as pozzolonic additive material.

Shirule et al. (2012) replaced the cement with MP and researched how MP impacts the mechanical characteristics of the concrete. They finalized that the marble powder replacement percentage was 10% and the compressive strength of 28 days increased by 17% and the tensile strength was increased 11.5%.

Uysal and Sumer (2011) examined the impacts of different additives, with the inclusion of marble powder, on the self-compacting (SCC) concrete performance. MP replacement were used in 10, 20, and 30% cement percentage. In compression tests performed on days 7, 28, 90 and 400, the control sample performance was matched with the best 10% MP replacement. On the 400th day, the compressive strengths of samples replacement percentage of 10, 20, and 30 MP were measured to be 97.6, 96.8 and 93.4 MPa, while the control sample was found to be 100 MPa. The loss of UCS (according to the control sample) was recorded as 12.3%, 20% and 8.5% in samples with 10%, 12 and 20% marble powder replacement in 10% magnesium sulfate solution, respectively.

Uysal and Yılmaz (2011) studied the impacts of various mineral additives on SCC performance. Samely to Uysal and Sumer (2011), they substituted cement with MP percentage of 10, 20, and 30. On day 90, they found the UCS at 82 MPa in the control sample and 84, 81, and 80 MPa in samples changed with MP percentage of 10, 20, and 30, respectively. In addition, they performed cost analysis according to the compressive strength of 28 days, obtaining 0.52, 0.48, and 0.47 US\$/MPa/m^3 for replacement sample with 10, 20, and 30% MP and US\$0.58/MPa/m^3 for the control sample.

Rana et al. (2015) examined the usage of marble slurry (MS) in concrete manufacture. For this reason, 5, 10, 15, 20 and 25% MS were replaced instead of cement. On days 7, 28 and 90, the UCS of the control sample was 36, 43 and 51 MPa, respectively. The strength of the specimen containing 5% MS was 50, 42.5 and 35.5 MPa. The UCS reduces with an enhancement replacement percentage of MS on all 3 test days. On days 90, 28, and 7 the flexural strength was 6.8, 6.5, and 5.4 MPa, respectively, in the control specimen, and almost 6.5, 6.4, and 5.3 MPa, respectively, in the sample replacement with 5% MS.

Rodrigues et al. (2015) cement was replaced by 5, 10 and 20% MP and investigated the concrete mechanical characteristics. To this end, they produced a no chemical complement, a hyper plasticizer supplement, and a superplasticizer complement. Among the mechanical characteristics, the ultrasonic pulse rate was the least sensitive to the substitution rate and the wear resistance was changed to the maximum rate of 20% substitution (decreased by 4.4%).

Rodrigues et al. (2015) claimed that the replacement of MP compensated for decreased compressive strength. MP substitution rate of up to 10% did not find a decrease in compressive strength; But, at a 20 replacement percentage, the compressive strength was reduced by 25%. From the UCS on days 7, 28, and 56 in every group, they concluded that UCS is a reducing function of the MP replacement percentage. The largest recorded decrease was 33.9%. Accompanied by the rejected compressive strength, they measured a decrease in the 28 day splitting tensile strength, which was incremented to a maximum of 30.9%. These rates were proximate from the graphics shown in their experiment.

Aliabdo et al. (2014) substituted natural sand and cement with MP and studied how the replacement influenced the characterizes of concrete. They contain MP at replacement percentage of 5, 7.5, 10 and 15.

Rodrigues et al. (2015) found that replacing 15% of sand or cement with MP didn't importantly impact the ultrasonic pulse ratio. In addition, substituting 10% of the sand with MP incremented the UCS of concrete by 14%. In the low water/cement range, the strength was increment by 22%. In contrast, in the example substituted with 15% MP, the compressive strength was the same to or less than that of the control sample, but the steele concrete bond strength (adherence) was developed. Adhesion showed a maximum improvement in the 10% substitute specimen.

Aliabdo et al. (2014), it was also found that 10% of natural sand or cement substituted MP with a 15% increment in splitting tensile strength. Raising the rate of replacement percentage to 15% decreased the tensile strength but gave better performance than the control specimens. In the study, specimens with low water/cement rates have consistently ensured good results.

Ergun (2011) substitute the cement with MP percentage of 5, 7.5 and 10 and found the characters of the ordinary concrete.

Corinaldesi et al. (2010) found that MP served as filler. Substitute the 5% MP increased the flexural and compressive strength of the concrete by 5% and 12 %, respectively, and reduced the porosity. The addition of superplasticizers has had a positive impact on a small percentage of MP substitute. The MP improved the mechanical characteristics of the concrete at a substitute rate of 5% and incremented the compressive strength because of the filling effect.

Topçu et al. (2009) studied the impacts of MP on the mechanical characteristics of SCC. They substituted cement with MP at rates of 30%, 40%, 50%, and 60%. Too much amount of cement was substituted with MP, the bending and compressive the concrete strengths reduced. MP substitute at 300 kg/m^3 decreased the splitting tensile and compressive strengths by 47 and 51%, respectively. In accordance with these researchers study, increasing the rate of MP cause decreasing in the slump flow (mm).

Belaidi et al. (2012) researched the impacts of MP and natural pozzolan on SCC. They made two experiments; one was substituted portland cement with puzzolana at the percentage of 5 to 25%, while the other was prepared with MP at a percentage of 10 to 40%. In both experiments, a substitute rate of 40% reduced the compressive strength by 50% and increment the slump value.

Gesoglu et al. (2012) examined the mechanical characters of concrete with various substitute rates of MP. According to the control samples, the slump values of samples manufactured with 5, 10, and 20% replacement rates were reduced, and the setting time was an enhancement function of MP rate. The UCS of 28 days was 13.46% lower in the specimen with 20% MP rate compared to the control specimen. The UCS of 90 days changed significantly at 5% replacement but decreased by 3% when the replacement rate to 10%. Also, replacement with 5 and 10% MP decreased the splitting tensile strength by 14 and 5.2%, respectively, according to the control specimen. These data are taken from the graphs shown in the report of Gesoğlu et al. (2012).

Elyamany et al. (2014) studied MP as filler material in SCC and examined the physical and mechanical characters of the modified product. For this purpose, they replaced 7.5%, 10%, and 15% MP into a mixture of 400 kg/m^3 cement and 10% MP, and a preparation of 500 kg/m^3 cement. The 7-day UCS of the mix made with 15% MP and 15% silica fume were almost 36.5 and 31 MPa, respectively. The compressive strengths increment to 47.5 and 46.5 MPa, after 56 days. They deduced that the fill type greatly affects the bleeding and segregation rates. Especially, both values are decreased by non-pozzolanic filler material.

Gencel et al. (2012) researched the usability of MP in concrete pavement blocks. The cement types prepared two series samples based on 32.5 and 42.5 and substituted the fine aggregates with 10%, 20, 30 and 40% MP. Both series also, they found that as the rate of MP incremented, the bulk weight, splitting tensile strength, and compressive strength all reduced. When the 28 day UCS between the test and control specimen were cross-checked, the compressive strength was reduced by 94.3, 91.7, 86, and 76.4% at MP substitution rates of 10, 20, 30, and 40%, respectively.

Gesoglu et al. (2012) indicated that the cement substitute with MP at 20% or higher negatively impacts the mechanical concrete properties of concrete. These different outcomes are opinion to be reasoned by the various C_3A substances of the cement used in the different experiments. Uysal and Sumer (2011), Gesoglu et al. (2012), Uysal and Yılmaz (2011), Ergun (2011), accordingly, the appropriate concrete change rate was determined as 5%. There are two likely comments for this impact. First, the silica in the MP reacts with the $Ca(OH)_2$, which results from the hydration reaction between the water and cement. An additional binding phase occurs from the extra pozzolanic characters. Secondly, the tricalcium aluminate (C_3A) in the cement reacts with the calcium carbonate ($CaCO_3$) in the MP to form calcium carboalumination. This combined increments both the cement compressive strength and hydration rate.

Rodrigues et al. (2015) stated that super-plasticizer additives are required to get the request cement properties, which is partially replaced by MP. In the lack of super-plasticizers, they reported negative effects on the concrete mechanical properties at substitute rates above 10%.

2.5 Workability Tests for Grouts

Marsh cone test is a common technic to evaluate the rheological properties of cement base grouts in field applications. The time it passes one liter of sample to flow through a Marsh cone. This test is defined as marsh cone flow time (MCFT) or marsh viscosity and the rheologic attitude of the grout can be predicted by using this time. But, specific viscosity or yield stress cannot be found by using this test. Lombardi (1985) invented a cohesion meter that can be used in conjunction with the Marsh viscosity to evaluate the apperent viscosity of the grout. With using cohesion and MCFT, apparent viscosity can be estimated by using the chart. The unit of cohesion will be used as millimeters and the unit of MCFT will be taken as seconds and then viscosity value will be divided by unit weight. Finally, this value multiplied by the unit weight and converted centipoises (cP) to find the apperent viscosity. The results obtained from the chart and the results obtained from the rheometer test machine were compared to each other by Lombardi (1985), the results were seen close to each other.

The MCFT is a flowability test used for the properties and quality check of CBG and cement mortars which developed by Bartos et al. The volume of this device has 1500 ml and 5 mm inner cap. The MCFT is used to detect the CBG volume through flow cone at a measured time. The CBG mix was proud in a cone (1250 ml) and bottom outlet was turned on. After that, CBG mix begins to flow and elapsed time was measured providing that 1000 ml of CBG had flowed. Consequently, the elapsed of time gave the MCFT time. The MCFT time of water was found as 24 s in comparison with cement based grout.

The mini-slump test was used to find the spread of grout mixtures. The apparatus shape is same to the slump cone described by ASTM C-143 (Çelik et al., 2015). Dimensions of mini-slump apparatus; 38 mm high with at the top diameters of 57 mm and 19 mm at the bottom (Çelik et al., 2015; Kantro, 1980; Ozawa et al., 1995). In the mini slump test, CBG mix is poured into a cone until it's full. Then, the mixture is allowed to spread by removing the mini slump cone. It is transfer to on a flat glass plate. In the vertical direction the spread diameters are measured and the average spread diameter is calculated.

Lombardi plate cohesion meter (PCM) was used to find the cohesion. PCM consists of a steel plate with rough surfaces on both sides. 10×10×3 mm is a dimension of the PCM. PCM apparatus was used for the calculate of cohesion. The plate was immersed in the CBG mixture. Due to cohesion, the CBG mixture sticks on the plate. After that, the cohesion measured from the control mix was compared with that measured from the CBG mixes. All tests were done two times by preparing a new mixture for control purposes.

2.6 Unconfined Compressive Strength (UCS) of Grouts with Waste Marble Powder (WMP) and Fly Ash (FA)

In order to decrease the use of cement in the construction works, researchers have began to study formation of blended cements pozzolanic agricultural by- products compositions such as WMP and FA that can be replaced with cement at different ratios. While hydration of cement is going on, calcium hydroxide, $Ca(OH)_2$, will start to exist as one of hydration products. The corruption of concrete is directlyrelated with it. After any pozzolanic additive is mixed with cement, calcium-silicate-hydrate as the main cementing component will be produced because of chemical reaction between the pozzolanic material and $Ca(OH)_2$. Howeveri because of the reaction between the pozzolanic material and $Ca(OH)_2$, the amount of harfull $Ca(OH)_2$ decreases and this reaction increase the usefull C-S-H amount.

Research on the use of MP as partial modification of concrete has been the subject of interest is nowadays. According to Ramezanianpour, A.A. (2009) proved that additional cementing materials are economical and environmentally friendly alternatives to ordinary concrete blends. Researchers have recently carried out studies on the use of MP to replace a portion of the concrete as cement. The repetition of previous researches has been about the efficacy and applicability of MP as an effective substitute material.

Rai et al. studied M30 class of concrete by partially substituting cement with 5 different percentages by weight of MP (0–20%) and found that compressive strength increments by 5–10% for below 15% substitute.

Vardhan et al. analysis of the cement mortar mixture, it reported improved workability in the case of partial substitution with 0-50% by weight of MP. The reported results show that 10% MP addition has been achieved to the maximum benefit of improved fluidity. In addition, the compressive strength for the cure of 28 days increased slightly until 10% change; after that, the strength decreases to increment with the substitution percentage. Replacement of cement in various rates by natural puzzolana and MP to prepare SCC was investigated by Belaidi et al. The experimental research illustrated developed rheological characters of concrete mortar by substitution of MP (10– 40%) but illustrated decreased compressive strength with the substitution of natural puzzolana and MP.

Aliabdo, A.A., et al., Arshad, A., et al., Hebhoub, H., et al. and Ergün, A. investigated a reduce in values of slump on incrementing the substitution cement percent by MP which was ascribed to the high amount of fines in MP. Small particles increment the demand for water in concrete. Arshad, A. et al. and Hebhoub, H. et al. had similar studies.

Aliabdo, A.A. et al. investigated the impact of partly substituting cement by MP for 2 w/b rates 0.40 and 0.50. Increase in UCS for up to 7.5% substitution for water binder rate 0.5 and small increment in UCS for up to 10% substitution for water binder rate 0.40 was shown.

Shirulea, P.A. et al. reported an appropriate percentage change of 15% replacement which illustrated an increment in compressive strength as compared to the control mix. The reduce in the quantity of tri-calcium silicate (C_3S) and di-calcium silicate (C_2S) for the fall in strength were stated as the primary contributors.

Ali and Hashmi noticed an increment in split tensile strength on partly substituting cement by MP by 10%. Ergun, A. achieved same results, but with increasingly lower values for higher substitution rates. It was also found that the flexural strength was improved by Ali and Hashmi by replacing the 10% cement by MP, it increased 10.73%. Also, Belaidi et al. found a reduction in the flexural strength of ordinary concrete. Soliman, N.M. found a rise in modulus of elasticity of concrete.

CHAPTER 3

OVERVIEW AND THEORETICAL BACKGROUND OF GROUTING

3.1 Principles of Grouting

3.1.1 Definition and purpose of grouting

The grouting technique is often used to increase soil characteristics and to transfer loads to strong ground layers. Also, it is also used as base stoppers to prevent excess water movements below the level of the excavation and to form a permeable curtain wall in order to ensure the stability of the slope, to prevent liquefaction.

3.1.2 Categories of grouting

Recently, there are 4 different grouting methods types in use; slurry (intrusion), compaction (displacement), jet (replacement), and chemical (permeation) grouting (Welsh, 1986). Figure 3.1 shows these grouting methods. Each one serves several aim and application for various equipment. Compaction and jet grouting are high-pressure applications, while slurry and chemical grouting are low-pressure methods. Jet grouting uses grouting pressure up to 69 Mpa and pressure in compaction grouting is about 2.7 Mpa.

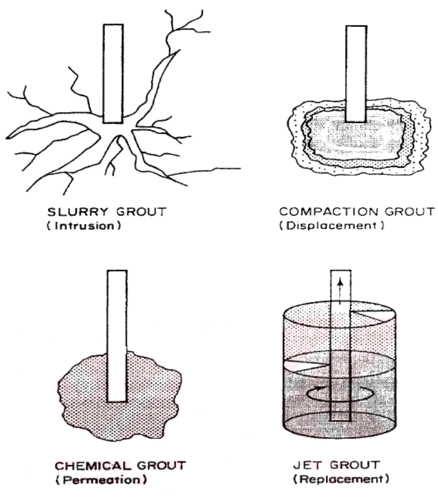

Figure 3. 1: Basic Models ogf Cement Base Grouting (Welsh.JP 1986)

3.1.2.1 Slurry grouting

The slurry grout fills the voids and cracks in the rock and ground passes the granular, coarse soils to create a cemented mass. Widespread uses; underlining the foundations, creating obstacles to groundwater flow, stabilize and strengthening of granular soils, providing excavation support.

The slurry grouting, also known as high mobility grouting or cement grouting, voids in rock/soil or fills pores in granular soil, with flowable particulate grouts. The grout void size and grain size must be suitably matched to allow the CBG to penetrate. According to the circumstances, microfine cement grout or portland cement is injected under pressure through strategic locations through multiple port or single port pipes. The grouted mass reduced permeability and incremented strength, stiffness.

The slurry grouting may provide an economic benefit for underpinning applications over alternative approaches like piling or replacement and removal and can be performed where reach is hard and area is limited. Since the effect of CBG is structural connections independent, this technique can be readily adapted to present foundations and can typically be successful without disrupting normal plant operations.

3.1.2.2 Compaction grouting

The compaction grout (CoG) concentrates the loose-grained soils, strengthens the stabilizes and fine-grained soils the underground sinkholes or voids by the staged injection of low mobility, low-slump aggregate grout. When treating the soil, an injection pipe is typically placed at the maximum processing depth. The grout is then injected as while the pipe is slowly raised in lifts, creating a column of overlapping grout bulbs. The expansion of the low mobility grout bulbs changes the location of surrounding soils. CoG increments the density, friction angle, and hardness of the granular soils around it. The effectiveness of the improvement can be increased by sequencing the low mobility (compression) grouting filling from the first to the secondary. In all ground, high modulus grout column strengthens the treatment site.

CoG was found in the 1950s as a remedial measure for the adjustment of building settlement. In recent years, low mobility grouting technology has improved to use a wide area of subsurface conditions for corrective and new structures. These include poorly placed fills, karst conditions, collapsible or loosened soils, liquefiable soils, and rubble fills. This method has also been utilized in preventing ground settlement while tunneling through soft ground. Groud mix consistency should be under control for successful applications. A low slump very stiff soil cement grout is injected to compact and displace the soil. Grouts with high water content would act same to slurry grout and fracture through the soil skeleton. In general, compaction grout consists of silty sand, fly ash or cement, water and additives (accelerators, fluidifiers). This technique was used in Bolton Hill subway of Baltimore project to prevent settlement (Baker et. al., 1983) and in densification of a liquefiable stratum in West Pinpolis Dam site in South Carolina.

3.1.2.3 Chemical grouting

Chemical grouting (ChG) converts granular grounds into sandstone-like masses by filling gaps with a low viscosity, non-particulate grout. Sands with low fines are most suitable for this technique. The ChG is injected below pressure through the ports. The grout passes through the ground and hardens to form a sandstone-like mass. The grouted soil has decreased permeability and incremented stiffness, strength.

ChG offers the benefits of being well attainable in areas where space and access are limited, and where no structural connection to the foundation being underpinned is required. The application of a ChG is to ensure both underpinnings of existing structures and excavation support adjacent to an excavation. Normally, normal plant work operations can be carried out without interruption.

ChG equipment is suitable for tunneling applications in urban environments, either to balance the soil around separations or separations or to reduce the placement of overlapping structures within the effect of tunnel alignment.

ChG is the injection of appropriately formulated chemicals into sandy soils. The soil fraction passing by No. 200 sieve must be less than 20%. The product obtained is generally a sandstone-like material with UCS above 4.1 MPa. ChG are often used for water control purposes due to their positive properties like good control of set time and low viscosity. ChG is usually an ingredient of sodium bicarbonate and sodium aluminate. Sodium silicate and acrylates (AC-400) sodium silicate are mostly used as grout materials.

3.1.2.4 Jet Grouting

Jet Grouting (JG) uses high-speed fluid jets to build the cemented ground of changing geometries in the soil. General uses; ensure excavation support, underpin foundations, technical details, seal the bottom of planned excavations. JG compose in situ geometries of soilcrete (grouted soil), using a grouting monitor annexed to the end of a drill stem.

JG pursue is advanced to the maximum treatment depth. Then high-velocity jets (CB with optional water and air) are started from ports in the monitor. The jets erode and blend the construction site soil with grout as the drill stem and monitor is rotated and raised.

According as the soil types and application, one of 3 types is used: the triple fluid system (water jet surrounded by an air jet, with a separate grout port), the double fluid system (slurry grout jet surrounded by an air jet) and the single fluid system (slurry grout jet). JG creates soilcrete panels, partial columns, or full columns with designed permeability or strength.

JG is efficient for the widest soil types variety of any grouting system, including most clays and silts. The physical and geometry characteristics of the soilcrete are designed based on the in-situ soils. As a system based on erosion, soil erosion plays an important role in predicting production, quality and, geometry. Cohesionless soils are typically more wear by JG than cohesive soils.

Jet grouting’s capability to build soilcrete in limited areas and around subsurface obstacles like unique, provides, utilities design flexibility. In any case, which requires the groundwater control or requires the unstable soil excavation (water-carrying or otherwise) JG, it is generally a preferred solution.

Generally, JG may be performed without disrupting normal plant operations. The containerized development, highly mobile support equipment has decreased the costs and time of mobilization and demobilization. JG can usually result in saving the construction program time.

3.2 Properties Study on CBG in Porous Media

As the characteristics of the operation / handling procedures of grout injection and grout material are necessary for proving the effective practice of permeation grouting using CB, a correct comprehension of the grouting process and grout material parameters as explained in the following parts are incorporated in the existing study.

3.2.1 Grout material parameters

The particulate grouts permeability in the porous area depends on the various factors.

• Pressure filtration

• Stability

• Grain size distribution

• Rheology (mainly yield stress and viscosity)

As present above, the solution grouts are evolutive Newtonian liquids throughout their period of practical injectability, when penetration occurs in accordance with Darcy's law. Therefore, the main controls on grout properties and penetration distance,

Ground porosity and permeability.

First grout viscosity and evolution.

Deere (1982) stated that cohesion defines the travel distance and states the viscosity flow rate.

•Pressure (relate to flow time)

•Injection practical process

3.2.2 Grouting method parameters

The structure of the French Tunnel Union (AFTES 1991) offers a logical approach that defines the four (4) main parameters:

•Grout volume,

•Injection pressure,

• Injection rate,

• Time of injection,

3.3 Rheology of CBG

The rheological characters of CBG is considered complex (Håkansson, 1993). The grout is consists of yield stress and thixotropic and non-Newtonian. In addition, cement hydration also plays an important role as rheological characters change over time. CBG rheology is a very important factor in the pumping, transportation, spreading and pouring of the material. In reality, CBG with w/c rates of 0.6-1.5, consisting of a solid volume concentration of about 30%-50%, are used (Rosquoe et al., 2003). In concrete, the shear rate increments with total ingredients and a complete breakdown can be accomplished at the end of the mixture. On the other hand, because of the lack of aggregates for the CBG, the surface space of the finer cement grain is higher and the rheology is more complex as a conclusion of the interaction between the suspended grains and the disintegration on shearing. Typical rates of the rheological characters of the cementitious substances are epitomized by Banfill (2003) and are illustrated in Table 3.1.

CBG and cementitious materials are subject to hydration, and the rheological characters vary accordingly. As noticed by Håkansson (1993) and abridged by Banfill (2006) and Sant et al. (2008), hydration proceeds in various phases. The first phase involves a fast effect between the anhydrous water and minerals, which leads to the peak of wetting. It then follows an accelerated phase, which is responsible for locking a slow reaction for two or more hours known as the sleep period. Ultimately, the fourth phase involves the retardation process. As a result, the apparent viscosity of the cementitious materials will change according to the hydration process.

The cementitious materials rheological characters are frequently expressed by a curve fitting a constitutive model to the shear rate vs. shear stress value. Various rheological characteristics are illustrated in Figure 3.2 Newtonian fluids do not have a yield stress and have a constant viscosity.

Pseudoplastic fluids do not have a yield stress but show a shear thinning character with increasing shear rate and can be shown using a power law model. Bingham fluids have a yield stress and stable viscosity. The yield pseudo plastic fluids have a yield stress and illustrate a shear thinning attitude with an incremented shear rate.

Table 3. 1: Typical values of rheological characters of cementitious materials (Banfill, 2003)

Material	Cement paste, Grout	Mortar	Flowing Concrete	Self-Compacting Concrete	Concrete
Yield stress N/m^2	10-100	80-400	400	50-200	500-2000
Plastic viscosity Pa.s	0.01-1	1.0-3.0	20	20-100	50-100
Structural Breakdown	Significant	Slight	None	None	None

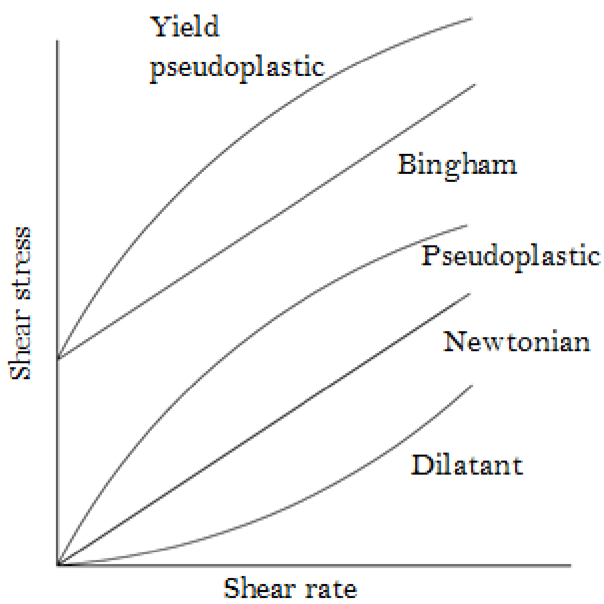

Figure 3. 2: Rheological characters of non-Newtonian fluids and Newtonian

Yield pseudo plastic attitude can be shown by using the Modified Bingham model. Dilatant fluids exhibit a shear thickening attitude in which the shear rate increases. The Bingham model is generally used because of its simplicity and the linear relationship between shear rate and shear stress. However, the dense cementitious materials rheological attitude can be better illustrated with the Modified Bingham model because it can model the observed shear thinning attitude (De Larrard et al., 1998). The Bingham model (Eq. 3.1) and the Modified Bingham model (Eq. 3.2) are illustrated as:

Bingham model ($\tau = \tau_0 + \mu_p \dot{\gamma}$)

(3.1)

Modified Bingham model ($\tau = \tau_0 + \mu_p \dot{\gamma} + c\dot{\gamma}^2$)

(3.2)

where τ = shear stress (Pa), τ_0= yield stress (Pa), μ_p= plastic viscosity (Pa s), $\dot{\gamma}$ = shear rate (s^{-1}) and c = constant. As can be observed, both models contain yield stress. In the Bingham model, the viscosity is uttered in a linear relation with the shear rate in the Modified Bingham model. It shows resistance to the viscosity of the material flow and is defined as the relationship between the shear rate and the stress applied to the material. A change in the apparent viscosity could be found with changes of temperature.

3.3.1 Yield stress

Yield stress is the material property that expresses the transition between fluid-like and solid-like attitude. As a result, it is the minimum stress that allows the fluid to flow like an viscous material. Inter-particle forces between the solids in a suspension effect in yield stress that must be overcome to start the flow and applied stress that is lower than the yield stress will result in a deformation such as a solid instead of flowing. The presence of yield stress has been questioned by some authors, e.g. Barnes and Walters (1985), owing to the fact that dedicated direct measurements at very low shear rates, no yield stress obtained.

The concept of historical yield stress is summarized by Barnes (1999), and the argument on the presence of yield stress was finalized by the fact that it is acceptable to define the material attitude with yield stress over a limited shear rate range; on the other hand, this is shown by limited data.

The problem related to the yield stress is the complexity in deciding it. Theoretically, at the yield stress, the apparent viscosity of the material alters from a finite value to infinity; for this reason, an infinite test period is needed (Barnes 1997; Barnes 1999). Yield stress fluids exhibit an elastic attitude before attaining the yield stress. Before reaching the yield stress, the material attitude alters to non-linearity from linearity and residual stress is monitored after the highest stress. For this reason, the definition of yield stress is also a matter of debate, and a series of yield stress may be used for practical applications (James et al. 1987; Mujumdar et al. 2002).

3.3.2 Viscosity

Viscosity (η) is the proportionality factor that links the shear resistance (τ) in the fluid to the slope velocity or the shear stress rate of the flow rate, which represents the rate at which a fluid layer moves relative to an adjacent layer (Newton's viscosity law). It is also named the absolute viscosity or apparent viscosity.

Viscosity is a significant fluid characteristic when analyzing fluid behavior and liquid motion near solid boundaries. The fluid viscosity is a measure of its reluctant to gradual deformation by shear stress or tensile stress. The slip resistance in a fluid is induced by intermolecular friction when the fluid layers try to slide from each other.

There are two relevant fluid viscosity measurements

- dynamic (or absolute)
- kinematic

3.3.2.1 Dynamic (absolute) viscosity

Absolute viscosity coefficient of absolute viscosity is a measure of internal resistance. The dynamic (absolute) viscosity is the tangent force per unit area needed to move a horizontal plane relative to the other plane in the unit velocity while maintaining a unit distance in the fluid.

The shear stress between the layers of a non-turbulent fluid moving in straight parallel lines can be identified as for a Newtonian fluid.

3.3.2.2 Kinematic viscosity

Kinematic viscosity - the absolute viscosity rate to density - a force-free amount. The kinematic viscosity can be got by dividing the liquid absolute viscosity by the liquid bulk density.

3.3.3 Measurement techniques

The rheological characters of CBG are measured in the field and the laboratory. The instruments used in the laboratory are not robust and the instruments used in the field are quite primitive and their results are not reliable and can be difficult to reproduce (Håkansson and Rahman, 2009).

3.3.3.1 Laboratory measurement

Laboratory measurements are done using various types of rotational and tube viscometers. Rheological characters can be measured by rotational viscometer using direct and indirect techniques. As stated by Nguyen and Boger (1983), indirect methods can be called extrapolation of the rheological shear rate-shear stress data, ie extrapolation of flow curves, assuming various rheological models. The direct methods are, for instance, the loosening the shear stress method and the shear vane method.

Concentric cylinder geometry is often used when measuring the rheological characters of CBG by using the rotational viscometer. This has the advantage that this geometry requires just a small sample that can be illustrated for a longer time period. Also, a measurement must be made with the concentric cylinder geometry, because the thinning phenomenon of the wall is inevitable when measuring a thinner thixotropic fluid (Barnes, 1995). Wall slippage occurs when the dispersion phase (concentrated suspension) slides away from the solid boundary and leaves a low viscous layer next to the smooth wall. Since CBG produce lots, a relatively large gap is required when using the concentric cylinder geometry, which paradoxically results in a greater sliding impact. Also, the wall surfaces can be roughening to reduce the slip.

For the elimination of the effect of wall slip, Nguyen and Boger (1983) introduced the vane technique. Various measurement geometries were used, e.g. the complexity and a concentric cylinder united with the measurement at the model fitted parameters and low shear rates were studied. The importance of measuring the shear stress-shear rate data by a direct method was emphasized. The measurement with the vane geometry is free of the vane dimension and size and has been demonstrate to be more correct for highly concentrated thixotropic suspensions. Another study by Nguyen and Boger (1987) indicated that when the suspension of a concentrated thixotropic material was measured using a concentric cylinder, the sample could be cut partially due to the yield stress. Furthermore, the measured shear stress will also depend on the rotational speed of the bob that is applied. Besides the impact of the applied rotational speed, the measured shear rate will vary owing to the time-dependent attitude of the sample material.

Tube viscometers are the most widely used tools for measuring viscosity because of their simplicity and low cost. When a fluid is pressurized through a pipe, the velocity becomes the maximum at the center, indicating that the speed gradient or shear rate is zero at the maximum and center at the pipe wall. The wall shear stress is got from the pressure difference at a known distance. Shear rate, a Newtonian fluid and a correction factor; Apply Rabinowitsch - Mooney to determine the shear rate of a non-Newtonian fluid. Consequently, the wall shear stress and the wall shear rate curve are got, on condition that pipes of various diameters with the same L / R rate are used.

When pipe viscometers are used, the wall slip event is significant for CBG. A cement layer is depleted at the pipe wall, and the smooth surface provides a lower grout viscosity. Therefore, the wall cutting speed should be corrected due to slip. Further details of the tube viscometer can be found in Mannheimer (1991), Barnes (1999).

3.3.3.2 Field measurement

The rheological characters of CBG are usually measured in the field by basic tools, like a Marsh cone flow time (MCFT) and yield stick. The MCFT is used to find the fluidity of CBG in the field. In fact, this is a workability test to control the properties and control the character of CBG. The longer the time required for the grout to flow out of the cone, the lower the flowability. The the grout flow time may be related with the viscosity assuming a Bingham plastic material, provided that the grout density and yield stress is known. The yield stress can be found by the 'raise pipe'. Here the grout is inserted into a vertical raising tube, and the principle is that the flow stops when the maximum shear stress in the tube wall is below the yield stress. The fluid density should be known for this experiment (Håkansson et al. 1992). Moreover, the yield stress can be found by the yield stick in the field (Axelsson and Gustafson, 2006). Waste marble powder and fly ash type grouting material and water

/ cement rates of 0.75- 1.5, CBG was tested. Compared to rotational rheometers, the yield bar provided slightly lower yield stress values. It has been finalized that the yield stick can be used as a robust technique to find the yield stress of the CBG in the field. Moreover, it can be combined with the MCFT to find the CBG viscosity. Referring to the yield stress as cohesion, a simple tool, called the plate cohesion meter (PCM), was presented by Lombardi (1985).

PCM apparatus was used for the calculate of cohesion. The plate was immersed in the CBG mixture. Due to cohesion, the CBG mixture sticks on the plate. While these techniques are used in the field, the results generally lack accuracy and reliability (Håkansson et al. 1992).

CHAPTER 4

AN INVESTIGATION OF FRESH AND HARDENED PROPERTIES OF CEMENTITIOUS GROUT MADE WITH USE OF WASTE MARBLE POWDER (WMP)

4.1 Introduction

Cement Based Grout (CBG) is a widely used method for many applications in the geotechnical area (Nonveiller, 1989). Some examples of CBG applications are suspension grouting, emulsion grouting, solution grouting, compaction grouting, permeation grouting, displacement grouting and replacement grouting (Stille and Gustafson, 2010; Yeon and Han, 1997; Baltazar et al., 2012; Çınar et al., 2017). The rheological and permeability properties of the CBG are straightly involved with the penetrability and pumpability in cracks and soil voids.

CBG is mixed of water, cement, and admixture. For CBG mix design, different range of water-cement (w/c) ratio could be used. Figure 4.1 illustrates the different usages of CBG with various w/c ratios.

For the applications of permeation grout, w/c ratio of CBG range between 0.5 and 1 (Danot and Derache, 2007). The w/c rate of injectable grout ranges from 1 to 2. Also, the grout should be similar to the liquid that can be injected into the rock and soil (Baltazar et al., 2012). As for consolidation and repair of masonry structures, w/c rates must be between 0.5 and 1.5 (Miltiadou, 1991).

Mineral and chemical admixtures are used to develop the characters of CBG as durability, penetrability, rheological and fresh properties. Adding mineral admixtures to the CBG at different amount modify the rheological and fresh properties of injections. For various types of grout applications, various additions (Cement kiln dust, rice husk ash, FA, silica fume, metakaolin and bentonite) have been applied. (Ruggiero, 1984; Weaver , 1990).

Some recent studies showed that additive, like rice husk ash, have increased the durability, long-term performance and workability of CBG mix

(Sonebi et. al., 2013). Also, Singh et al. (2019) studied the utilization of Portland cement with WMP in concrete. They stated that the binary composition of the binders ensures environmental and economic benefits by decreasing the production of Portland cement (PC) and so CO_2 emissions. Consequently, the additives using in CBG applications reduce the cost of application but increment the flowability and the strength.

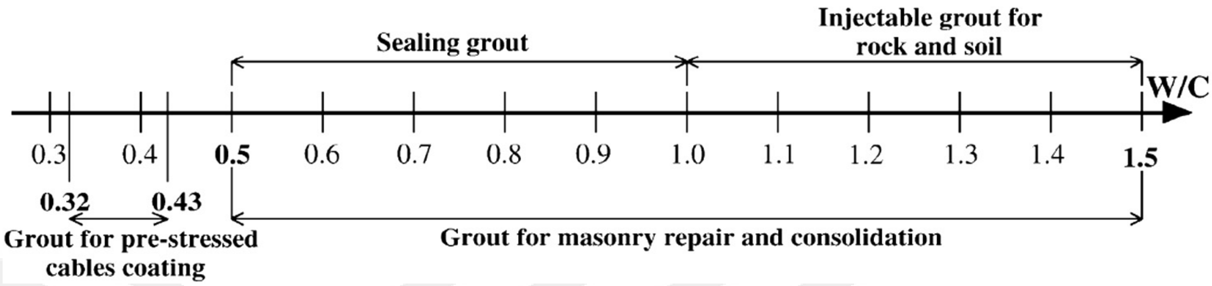

Figure 4. 1: Summary scheme of the various application areas of use of CBG (Rosquoe et al. 2003).

Marble is a very important material for construction, particularly for decoration reasons. %25 percent of marble turns to powder and dust due to shaping, polishing, and sawing. The wastes of the marble factory have turned into a main environmental issue onwards the early of the 1990s. This problem is not only a local issue but also direct anxiety for all at of countries. In many countries, like Turkey, Italy, Iran, India, China, Brazil, Spain, Portugal, South Africa, USA, Pakistan, Finland, and Egypt, export the marble products, many other countries, like Germany, Japan, South Korea, and Taiwan, import them.(Alyamac et al., 2017). Turkey has forty percent of the world reserves of marble, and the storage of waste generated during production is of great significance. Turkey has approximately marble reserves of 3.872 million m^3, of which close to 125 * 10^3 t/year are produced in Afyon City. (Singh et al., 2019). Five thousand processing factories are used for marble production in Turkey. It is clear that these waste products reach millions of tons; so it is too difficult to store this quantity of wastes (Alyamac and Ince, 2009).

The disposal of Waste Marble Powder (WMP) is one of the most environmental concern all over the world nowadays. On the other hand, WMP can be used to increase the fresh and hardened properties of cementitious grout.

WMP is used like a complementary cement based material in the concrete (Pooja and Prof, 2014). Earlier researches concluded that maximum 10-15 percent of WMP can be conveniently mixed into the concrete without negatively impacting the durability, hardness and strength of the resulting concrete (Shirule et al., 2012; Aliabdo et al., 2014; Rodrigues et al., 2015). Another researches investigated the usage of WMP as a cement substitution and showed that combining of WMP in SCC with concrete reduce the splitting tensile strength, compressive strength, bulk weight, slump flow, ultrasonic pulse velocity, porosity and cost (Shirule et al., 2012; Aliabdo et al., 2014; Rodrigues et al., 2015; Yao et al., 2015; Uysal and Yılmaz, 2011; Gencel et al., 2012; Gesoglu et al., 2012; Alyousef et al., 2018).

Moreover, some investigators studied the flowing characteristic of paste and mortar to facilitate the SCC design process according to flow duration and flow spread (Shirule et al., 2012; Aliabdo et al., 2014; Rodrigues et al., 2015; Yao et al., 2015; Uysal and Yılmaz, 2011; Gencel et al., 2012; Gesoglu et al., 2012; Alyousef et al., 2018). Water/cement ratio used in all works were between 0.3 and 0.6. On the other hand, injectable grout is ranged from 1.0 to 1.5 in soil and rock (Çınar et al., 2017). Also, Water/cement can be used maximum 2.0 in jet grout application.

Most of the works cited in the litaratures investigated effect of WMP on fresh and hardened characters of ordinary and SCC. The purpose of this study is to research the impact of high water-binder (w/b) rate and WMP content on the rheological characteristics properties and workability of CBG for geotechnical application such as improving strength, compressibility, and permeability. The studies were done on 24 CBG mixes including different amounts of WMP with the various percentages (5, 10, 15, 20 and 25%), of the total cement based materials weight and with 0.75, 1.00, 1.25 and 1.5 rates of w/c. A series of rheology and workability tests including Marsh cone flow time (MCFT) test, Lombardi Plate cohesion test, a coaxial rotating cylinder rheometer and mini-slump flow diameter test were conducted to observe the fresh characters of CBG mixtures. All study field experiments and modeling were not carried out.

4.2. Experimental Procedure

4.2.1. Materials used in this study

In this study portland cement (PC) (CEM I-42.5R) was used complying with ASTM C150 Type-I cement was used. WMP was used as an additive. Waste marble sludge (WMS) was provided in the form of a wet slurry from marble factory in Gaziantep-Turkey. WMS was dried in an oven at a temperature of 100 ± 10 °C for twentyfour hours and then sieved with 150 µm sieve (Fig. 4.2). Table 4.1 demonstrates the physical and chemical properties of PC and WMP.

Figure 4. 2: Waste Marble Powder

Table 4. 1: The physical and chemical properties of PC, WMP and FA

Chemical composition(%)	Portland Cement(PC)	Waste Marble Powder (WMP)	Fly Ash(FA)*
SiO_2	20.27	3.86	62.35
Al_2O_3	5.32	4.62	21.14
Fe_2O_3	3.56	0.78	7.35
CaO	60.41	54.40	1.57
MgO	2.46	16.9	2.35
SO_3	3.17	–	0.10
Loss on ignition	3.55	20.00	2.07
Physical Properties			
Specific gravity	3.15	2.71	2.30
Spacific surface(blaine) (cm^2/g)	3030	4190	3870

*(Cevik et al., 2018)

4.2.2. Mixture design

Water-binder (w/b) ratio is one of the important parameters that has a prominent impact on the fresh and hardened characteristics of CBG mix. So, in this experimental work four different (0.75, 1.00, 1.25 and 1.50) w/b rates were used to investigate the effect of WMP on the CBG. 24 injection mixtures with various WMP amount and various w/b rates were present to analyze the impact of WMP on the characteristics of CBG mixtures. (Table 4.2).

WMP was replace with cement substitutions of 5, 10, 15, 20, and 25% by volume. The control mix was prepared at each w/b rate. WMP wasn't added to the control mix. The mixture dosages, w/b ratio are shown in Tables 4.2.

Table 4. 2: WMP mix amount for 1.5 L and fresh and fluidity properties of the CBG mixtures.

MIX ID	**CEMENT (kg/m^3)**	**MP (kg/m^3)**	**WATER (kg/m^3)**	**W/b**	**MP (%)**	**Mini Slump (cm)**	**Marsh Cone (s)**	**Plate Cohesion (mm)**
MP0WB075	1396	0	1047	0.75	0	175	32	3
MP5WB075	1323	70	1044	0.75	5	171	33	3
MP10WB075	1250	139	1042	0.75	10	180	33	4
MP15WB075	1178	208	1039	0.75	15	183	32	5
MP20WB075	1106	276	1037	0.75	20	176	33	6
MP25WB075	1034	345	1034	0.75	25	174	33	6
MP0WB100	1131	0	1131	1	0	203	27	3
MP5WB100	1072	56	1129	1	5	202	27	3
MP10WB100	1014	113	1127	1	10	204	27	3
MP15WB100	956	169	1124	1	15	205	27	3
MP20WB100	898	224	1122	1	20	199	27	4
MP25WB100	840	280	1120	1	25	202	27	4
MP0WB125	951	0	1188	1.25	0	225	26	3
MP5WB125	902	47	1186	1.25	5	222	26	4
MP10WB125	853	95	1184	1.25	10	221	27	3
MP15WB125	804	142	1182	1.25	15	226	26	4
MP20WB125	755	189	1180	1.25	20	205	27	4
MP25WB125	707	236	1179	1.25	25	204	27	4
MP0WB150	820	0	1230	1.5	0	230	26	2
MP5WB150	778	41	1228	1.5	5	223	26	3
MP10WB150	736	82	1226	1.5	10	229	26	3
MP15WB150	694	122	1225	1.5	15	218	26	3
MP20WB150	652	163	1223	1.5	20	214	26	4
MP25WB150	611	204	1221	1.5	25	209	27	4

4.2.3 Mixing procedures

In preparation for the grout mixtures, five-liter laboratory mixer was used (Figure 4.3). The mixing procedure was applied in the experiment as following; WMP, cement and water were mixed at slow speed (120 rpm) for 1 min. The mixer was stopped and the paste remained on the sides of the bowl was scraped down. Also, grout mixtures were mixed by hand for 1 min. Eventually, the mixer was restarted at 240 rpm and the grout mixture mixed for 3 min.

Figure 4. 3: Laboratory mixer

Temperature and humidity of the laboratory for all tests were checked and measured as 50-60% and 20±3 $^{\circ}$C respectively. All CBG mixtures were obtained by using the same mixing procedures.

4.2.4. Test apparatus

4.2.4.1. Rheometer

Rotational viscometer (rheometer) was used to find the yield stress and the plastic viscosity (proRheo R180 Instrument, Germany) at 20 ± 3 $^{\circ}$C. The viscosity of the grout can be measured at various rotational speeds. The rheometer determines viscosity according to the searle-principle; The proRheo R180 is a standard rotational model viscometer which uses a motor-driven bob turning in a fixed measuring tube (Figure 4.4). The specimen is sheared in the gap between the bob the tube and the measured shear stress is used with the shear rate to compute the viscosity (Mezger, 2011).

Figure 4. 4: Rotational viscometer (Rheometer)

4.2.4.2. Mini-slump test, marsh cone flow test (MCFT) and plate cohesion test

The mini-slump test, MCFT and PCM test were used for evaluating the fluidity or workability of fresh grout mixtures. These tests were very easy to identify the flowability and workability characteristics of the grout prepared in the construction area.

The mini-slump test was used to find the spread of grout mixtures. The apparatus shape is same to the slump cone described by ASTM C-143 (Çelik et al., 2015). Dimensions of mini-slump apparatus; 38 mm high with at the top diameters of 57 mm and 19 mm at the bottom (Çelik et al., 2015; Kantro, 1980; Ozawa et al., 1995).

The MCFT is a flowability test used for the properties and quality check of CBG and cement mortars which developed by Bartos et al. The volume of this device has 1500 ml and 5 mm inner cap.

Lombardi PCM was used to find the cohesion. PCM consists of a steel plate with rough surfaces on both sides. 10×10×3mm is a dimension of the PCM.

4.2.5. Procedures

4.2.5.1. Rheometer

Ascending and descending flow curves in the shear stress–shear rate curve was obtained. The shear rates were varied between from 50 to 1000 s^{-1} for every CBG mixture. The apparent viscosity is regarded as a function of the shear rate; therefore, the shear-thickening (dilatant) attitude of the CBG mixtures is obtained with according to the apparent viscosity of GBG (Çelik et al., 2015).

To find the rheological properties of CBG, several types of analytical models exist. Plastic viscosity and yield stress are got by matching shear stress–shear rate curve values into Modified Bingham model. The modified Bingham model gives a preferable solution than the Bingham model for the same mixes (Khayat and Yahia, 1997). Figure 4.5 demonstrates the shear stress–shear rate curve values of MP5WB075 grout mixture by using both modified Bingham and Bingham model.

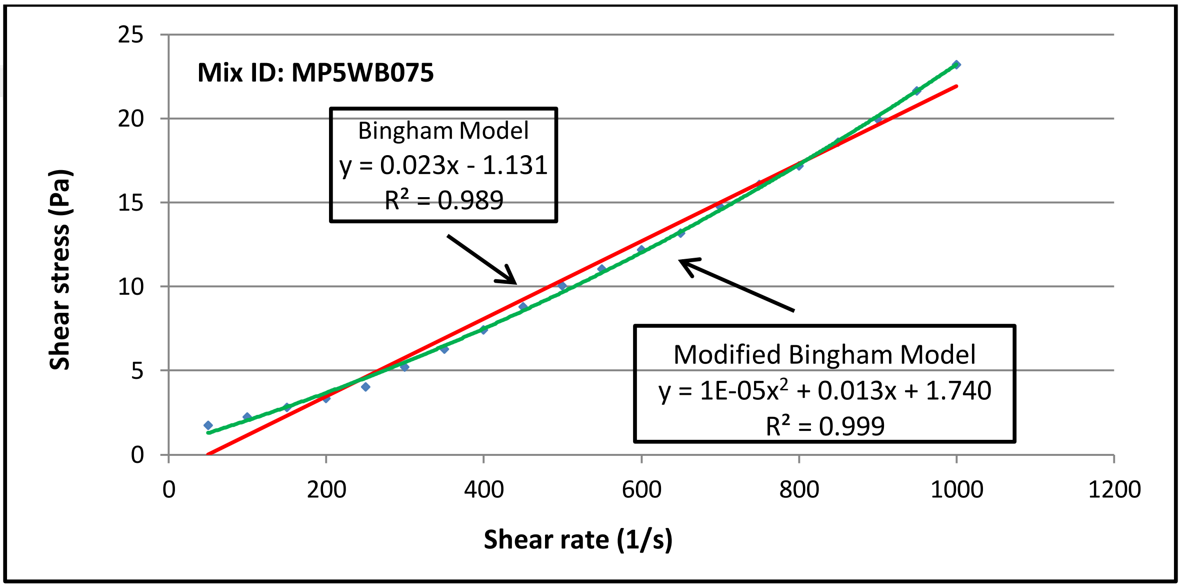

Figure 4. 5: The characteristic flow properties of CBG obtained from Modified Bingham and Bingham Model.

4.2.5.2. Mini-slump test, marsh cone flow test (MCFT) and plate cohesion test

In the mini slump test, CBG mix is poured into a cone until it's full. Then, the mixture is allowed to spread by removing the mini slump cone. It is transfer to on a flat glass plate. In the vertical direction the spread diameters are measured and the average spread diameter is calculated.

The MCFT is used to detect the CBG volume through flow cone at a measured time. The CBG mix was proud in a cone (1250 ml) and bottom outlet was turned on. After that, CBG mix begines to flow and elapsed time was measured providing that 1000 ml of CBG had flowed. Consequently, the elapsed of time gave the MCFT time. The MCFT time of water was found as 24 s in comparison with cement based grout.

PCM apparatus was used for the calculate of cohesion. The plate was immersed in the CBG mixture. Due to cohesion, the CBG mixture sticks on the plate. After that, the cohesion measured from the control mix was compared with that measured from the other mixtures (Weaver and Bruce, 1991).

All tests were done two times by preparing a new mixture for control purposes. The test results were similar and were not indicated in the tables. All tests were made at 8-12 minutes after contact with cement and water.

4.3. Results and Discussions

4.3.1. Rheological properties of CBG

The influence of w/b rate and WMP content on the rheological properties of CBG mixture can be related with between the shear rate and the shear stress. The flow curves of the CBG mixes containing WMP with different w/b rates are illustrated in Figure 4.6.

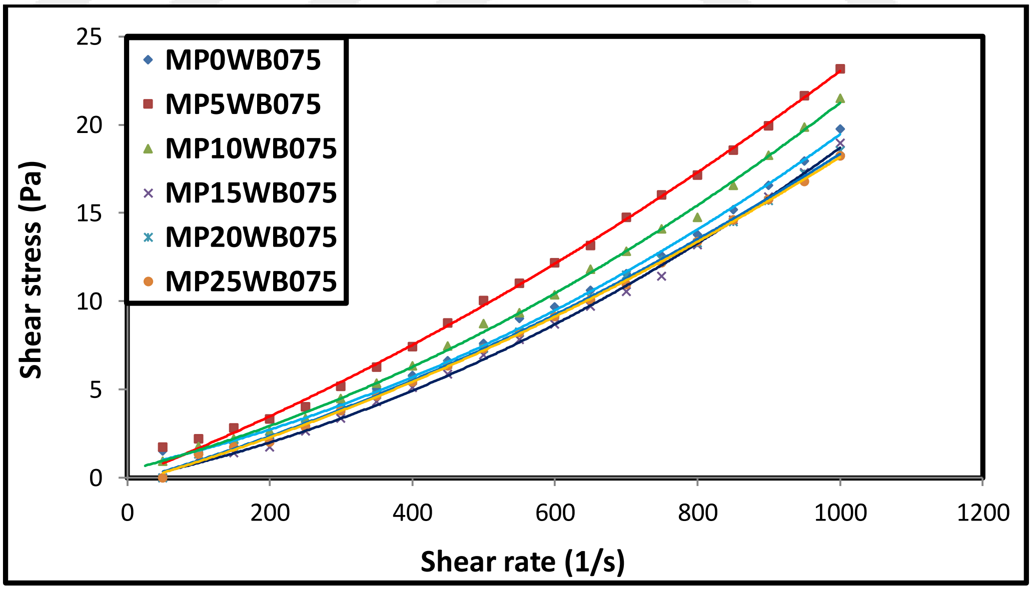

(a)

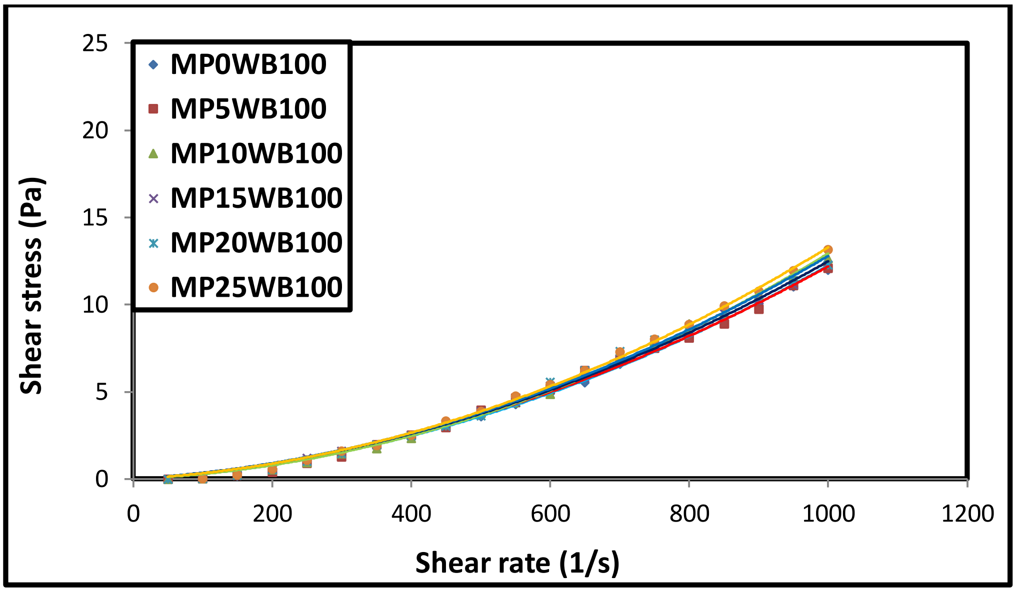
25
20
15
10
5
0
0
200
400
600
800
1000
1200
Shear stress (Pa)
Shear rate (1/s)
MP0WB100
MP5WB100
MP10WB100
MP15WB100
MP20WB100
MP25WB100

(b)

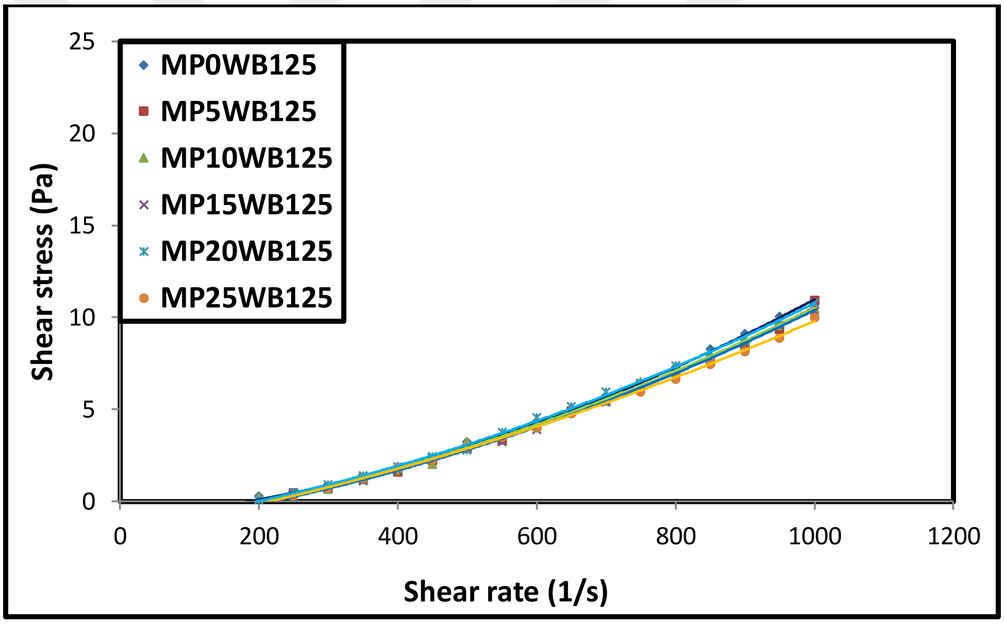
25
20
15
10
5
0
0
200
400
600
800
1000
1200
Shear stress (Pa)
Shear rate (1/s)
MP0WB125
MP5WB125
MP10WB125
MP15WB125
MP20WB125
MP25WB125

(c)

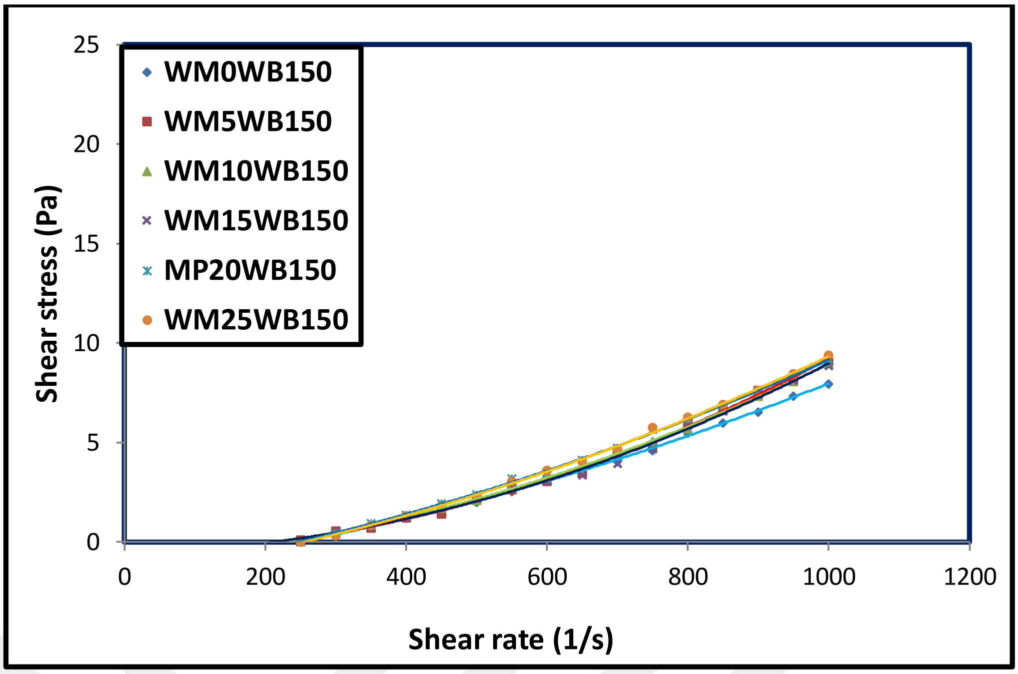

(d)

Figure 4. 6: Flow curves of CBG containing percentage of WMP between 5% to 25% with w/b rate of (a) 0.75; (b) 1.00; (c) 1.25; and (d) 1.5

The shear stress versus the shear rate curves were obtained by using modified Bingham model for grout mixtures. Table 4.3 shows the calculation of modified Bingam Model parameters. Authors used the values obtained from ascending and descending flow curves because it gives more accurate value. In Fig 4.6, the CBG mixtures illustrated shear-thickening attitude at all w/b ratios at all WMP content.

Table 4. 3: Rheological characteristics of the CBG mixture

Mix ID	τ_0 (Pa)	μ_p (Pa.s)	Temperature of the mixture (°C)	R^2
MP0WB075	1.50	0.008	20.0	0.997
MP5WB075	1.74	0.013	19.5	0.998
MP10WB075	2.45	0.010	19.0	0.998
MP15WB075	2.30	0.008	18.5	0.998
MP20WB075	2.69	0.011	18.5	0.999
MP25WB075	3.00	0.011	18.5	0.999
MP0WB100	0.76	0.004	19.0	0.998
MP5WB100	0.66	0.004	18.5	0.997
MP10WB100	0.75	0.003	18.0	0.998
MP15WB100	0.76	0.004	18.5	0.999
MP20WB100	0.46	0.004	18.5	0.997
MP25WB100	0.50	0.004	18.5	0.999
MP0WB125	0.62	0.003	19.0	0.998
MP5WB125	0.49	0.004	19.0	0.997
MP10WB125	0.53	0.005	19.0	0.997
MP15WB125	0.88	0.005	19.0	0.999
MP20WB125	0.68	0.005	19.0	0.999
MP25WB125	0.47	0.006	19.0	0.999
MP0WB150	0.46	0.004	18.7	0.999
MP5WB150	0.80	0.001	19.0	0.997
MP10WB150	0.50	0.015	19.0	0.989
MP15WB150	0.94	0.001	19.1	0.995
MP20WB150	0.87	0.005	19.0	0.999
MP25WB150	0.27	0.005	19.2	0.999

Figure 4.7 demonstrates how the plastic viscosity of different w / b ratios of CBG mixtures containing WMP is affected. It was observed that the increment in WMP amount in the CBG mixture increased the plastic viscosity with 0.75, 1.0, 1.25, 1.5 w/b ratios. Also, for the constant amount of WMP content, the increase in water-binder ratio reduces the plastic viscosity of the CBG mixtures. It can be concluded that the plastic viscosity of the CBG mix made at water-binder rate greater than 1.00 was directly impacted by the substition of WMP.

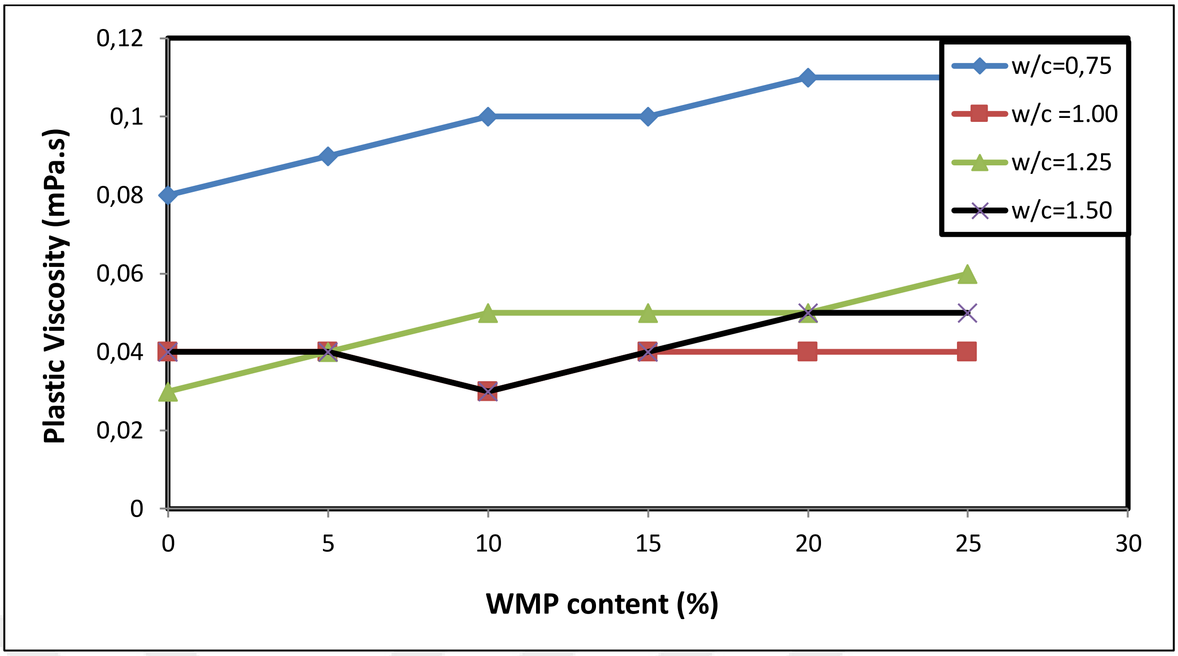

Figure 4. 7: Impact of WMP content at varioust water/binder rates on the plastic viscosity of CBG.

In table 4.3 and Figure 4.6, the apparent viscosity of the CBG mixture at shear rates from 50 to 1000 s^{-1} for WMP addition at different water–binder ratios is listed. The increment in the apparent viscosity of the CBG mixtures showed that the dilatant response incremented with the increment in the percentage of WMP amount. It can be concluded that the high water holding capacity of WMP. All CBG mixtures have showed a shear-thickening attitude, as shear rate increase with the increase in apparent viscosity as shown in Fig. 4.6 and Table 4.

4.3.2.Fluidity properties of CBG

Fig. 4.8 a illustrates the relationship between WMP content and mini-slump flow diameter. It indicates that the increase in the percentage of WMP amount until %15 did not affect, but more than %15 WMP reduced the mini-slump flow diameter because of the angular particle shape of WMP (Gesoğlu et al., 2012). Moreover, the increment in the w/b rate increment the mini slum flow for the constant WMP amount.

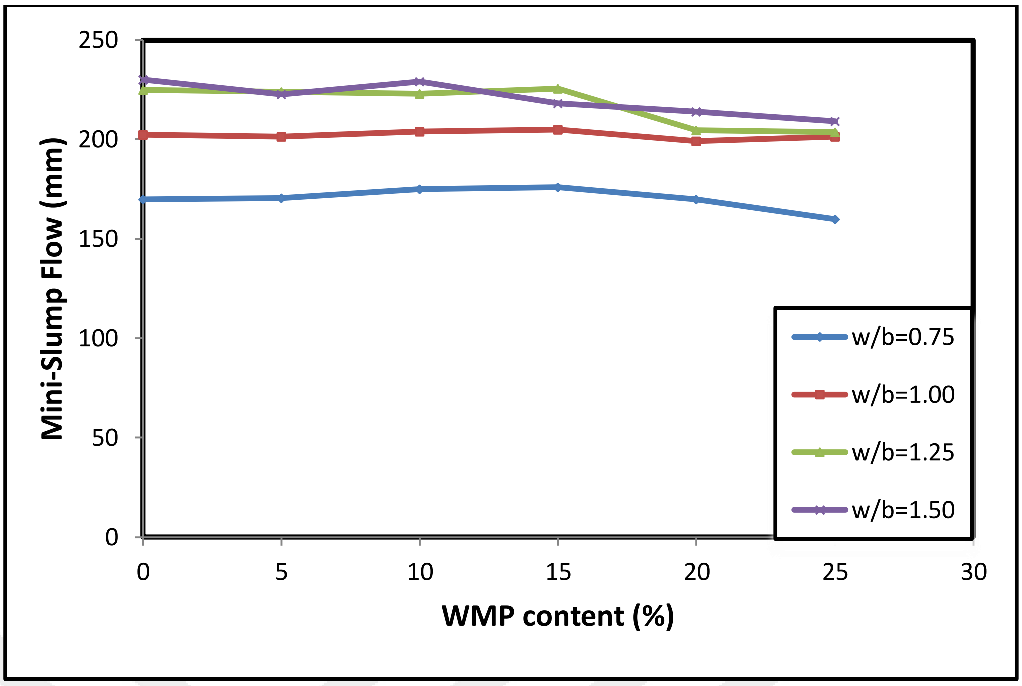

(a)

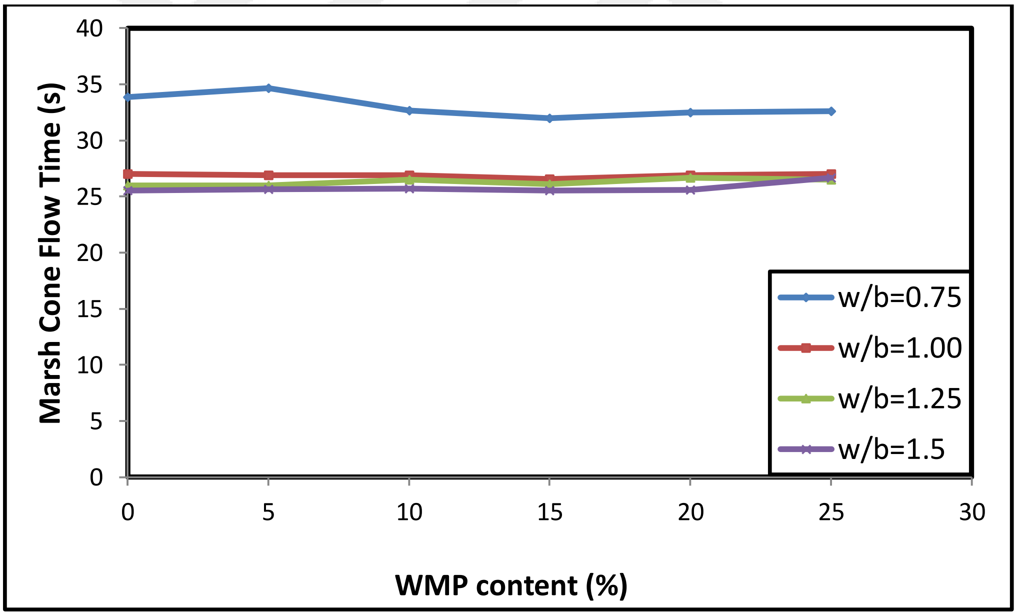

(b)

Figure 4. 8: (a) Impact of WMP on mini-slump flow; (b) Impact of WMP on MCFT.

Fig 4.8b illustrates the impact of WMP amount on MCFT at various w/b ratios. It seems that the increase in WMP amount in the CBG mix, at all water-binder ratios, there is no effect on MCFT. Also, the increase in the w/b rate decrease the MCFT at the constant WMP content because of the water effect. Therefore, it can be concluded that CBG mixtures with WMP reduce fluidity and workability characteristics when w/b is especially smaller than 1.00 in comparisons with w/b ≥ 1.00. Similarly, the increase in WMP amount in the mix spectacularly decreases the deformability and fluidity of the CBG mixture at low water-binder ratios. The decrease in fluidity of grout mixtures, when WMP was added, can be interpreted that WMP has high capacity of water sorption. Similar results were reported by Aliabdo et al. (2014), Ashish (2018), Sing et al. (2017) and Ashish (2019).

4.3.3.The comparisons between fluidity and rheological properties of CBG

The fluidity and the workability characteristics (MCFT, mini-slump flow and PCM) were correlated with two rheological values (yield stress and plastic viscosity) to providing easy and convenient methods for adjusting the rheological control of CBG mixtures. According to Zhang et.al (2016) and Ferraris et al. (2001), a fluid rheometer for cementitious paste is not properly existing in the construction industry for various causes. Like as the experiment device is fairly costly and the significance of using this kind of a device for cement paste was not defended up to lately. For this reason, the authors proposed easy tests like Marsh cone tests and mini-slump. In order to describe the relationship between rheological characters and workability of grout mixes, some graphs were drawn between test results of grout mixes and R^2 value between any of two grout mixtures were accounted. If correlation coefficient (R^2) values are above 0.80, then it can be considered that there is a good correlation between two test outcomes. If R^2 values are below 0.80, it indicates that there is a poor correlation.

Fig. 4.9 displays the relationship between the rheological and the flowability characteristics, meantime Fig. 4.9a illustrates the relationship between the mini-slump flow and the yield stress. As it is known that the slump flow diameter gets some information’s about the deformability of concrete which is associated with the yield stress (Ferraris et al., 2001). For this reason, there is a good correlation between mini-slump flow diameter of fresh mixes and the yield stress found from the modified Bingham model. From the graph, the relation between the yield stress and the mini-slump flow was a very good correlation (R^2 = 0.83). Furthermore, it seemed that the reduction in the yield stress incremented the mini-slump flow diameter. The results are compatible to the literature (Çınar et al., 2017; Çelik et al., 2015).

Figures 4.9b and 4.9c shown the relationship between plastic viscosity and MCFT and yield stress and Lombardi PCM test. Once the yield stress is exceeded, flowing of CBG mixture starts in the marsh cone test. In consequence of this reason, there is a direct relation between the MCFT measured and the viscosity. The marsh cone flow time test is a relatively simple test method to estimate the plastic viscosity value of grout mixture in the field applications (Ferraris et al., 2001; Sahmaran et al., 2008). Fig. 4.9b shown that the increment in plastic viscosity increased the MCFT of the CBG mix. In the figure 4.9b, it can be obtained that there is a good correlation (R^2 = 0.84). Therefore, a well defined demonstration of the plastic viscosity value could be estimated from the marsh cone flow time test.

Also, It seemed that there is weak corelation between yield stress and Lombardi PCM test (R^2 = 0.52) (Fig 4.9c). The reason can be explained that other factors such as friction and shear rate may influence the cohesion of grouts.

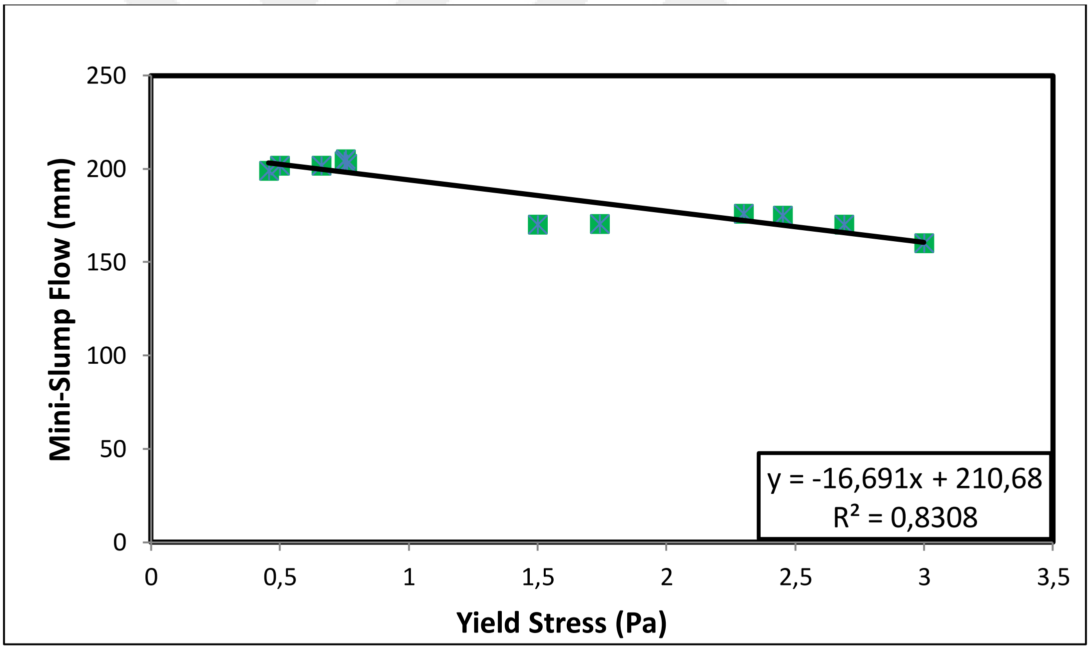

(a)

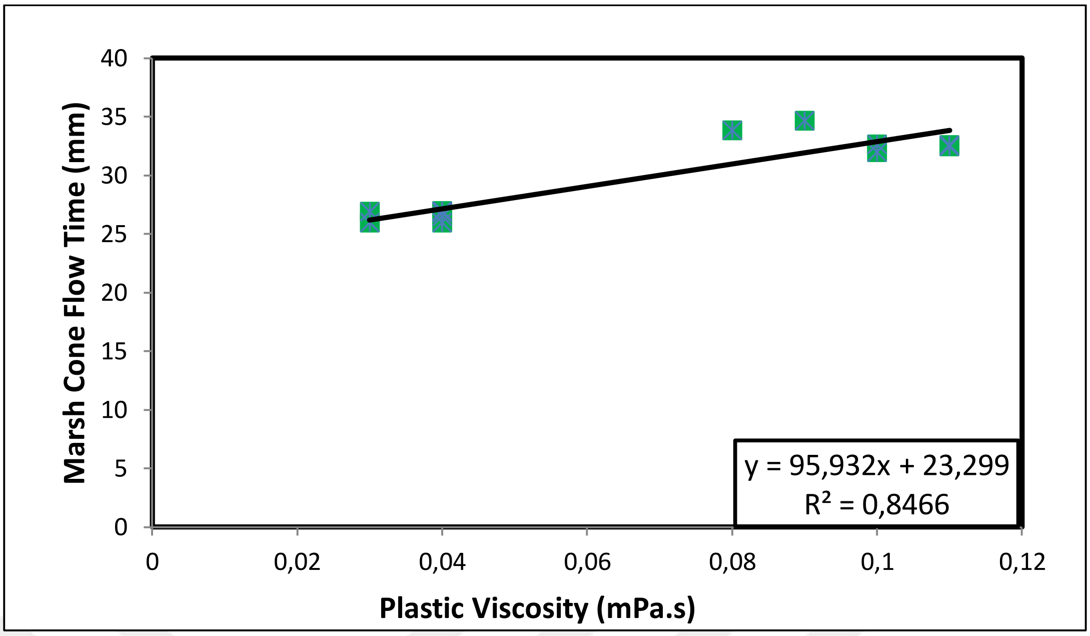

(b)

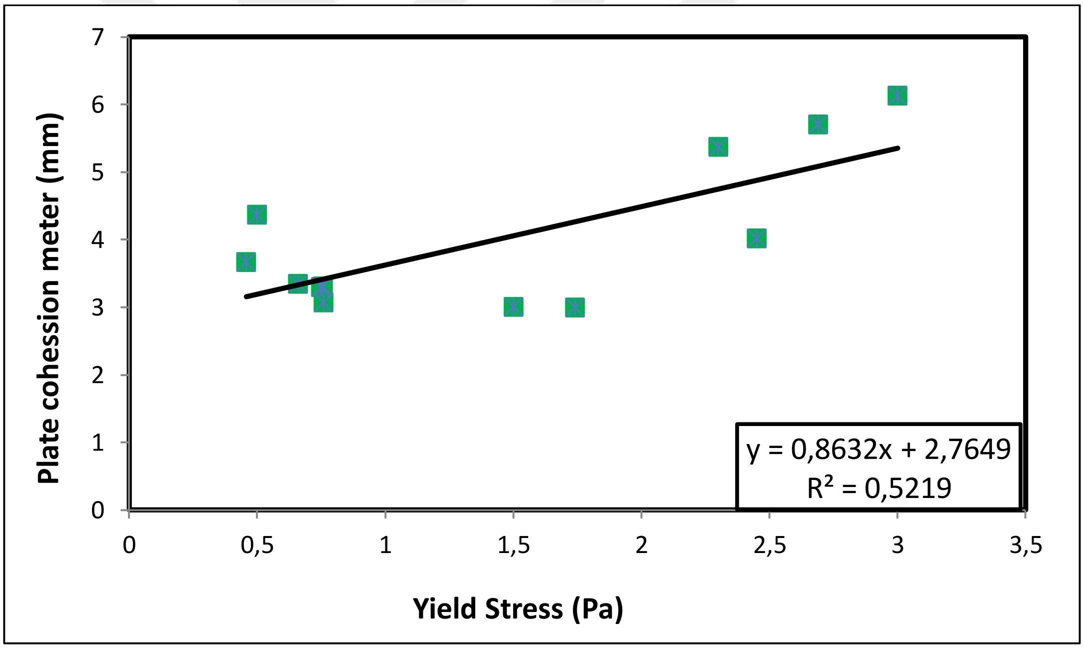

(c)

Figure 4. 9: Correlation between workability and rheological characteristics of a mini-slump flow–yield stress, b MCFT–plastic viscosity and c PCM–yield stres

4.4.Conclusion

1. The rheological properties of the CBGs importantly have been improved by the addition of WMP to grout mix at various w/b ratios. Strongly shear thickening behavior was got from the CBG mixture the all w/b ratios and all WMP content.
2. The increment in the percentage of WMP in the CBG mixture incremented the plastic viscosity at all water–binder proportion. Moreover, the increment in water–binder rate reduced the viscosity of the grout for any given WMP content.
3. The increment in the percentage of WMP in the grout mixture reduced the mini-slump flow diameter. In a constant the percentage of WMP, the increment in water-binder rate incremented the mini-slump flow diameter because of the impact of water. Moreover, the MCFT reduced with an increment in w/b rate for a constant waste marble powder content. The workability and flowability of the CBG importantly changed with the increment in w/b rate in cement based grouts containing WMP.
4. The rheological characteristics (the plastic viscosity and the yield stress) of the CBG got from the modified Bingham model illustrates a good correlation with the MCFT and mini-slump flow of the grout (R^2 = 0.83, R^2=0.84). On the other hand, no correlation was found between yield stress and Lombardi PCM test.
5. According to fresh properties test results; Waste Marble Powder can be suitable for use in substitution cement in proportions up to 15%. For this reason, CO_2 emissions decreased by 15% and cost decreased by this rate.

CHAPTER 5

AN INVESTIGATION OF FRESH AND HARDENED PROPERTIES OF CEMENTITIOUS GROUT MADE WITH COMBINED USE OF WASTE MARBLE POWDER AND FLY ASH

5.1.Introduction

Cement Based Grout (CBG) is a widely used method for many applications in the geotechnical area (Nonveiller, 1989). Some examples of CBG applications are suspension grouting, emulsion grouting, solution grouting, compaction grouting, permeation grouting, displacement grouting and replacement grouting (Stille and Gustafson, 2010; Yeon and Han, 1997; Baltazar et al., 2012; Çınar et al., 2017). The rheological and permeability properties of the CBG are straightly involved with the penetrability and pumpability in cracks and soil voids.

CBG is mixed of water, cement, and admixture. For CBG mix design, different range of water-cement (w/c) ratio could be used. Figure 4.1 illustrates the different usages of CBG with various w/c ratios.

For the applications of permeation grout, w/c ratio of CBG range between 0.5 and 1 (Danot and Derache, 2007). The w/c rate of injectable grout ranges from 1 to 2. Also, the grout should be similar to the liquid that can be injected into the rock and soil (Baltazar et al., 2012). CBG mixes have usually water-cement ratios of 1.00 by volume.

Mineral and chemical admixtures are used to develop the characters of CBG as durability, permeability, rheological and fresh properties. Adding mineral admixtures to the CBG at different amount modify the rheological and fresh properties of injections. For various types of grout applications, various additions (Cement kiln dust, rice husk ash, FA, silica fume, metakaolin and bentonite) have been applied. (Ruggiero, 1984; Weaver, 1990).

Some recent studies showed that additive, like rice husk ash, have increased the durability, long-term performance and workability of CBG mix

(Sonebi et. al., 2013). Also, Singh et al.(2019) investigated the use of Portland cement with WMP in.concrete. They stated that the binary composition of the binders ensures environmental and economic benefits by decreasing the production of Portland cement (PC) and so CO^2 emissions

Marble is a very important material for construction, particularly for decoration reasons. %25 percent of marble turns to powder and dust due to shaping, polishing, and sawing. The wastes of the marble factory have turned into a main environmental issue onwards the early of the 1990s. This problem is not only a local issue but also direct anxiety for all at of countries. In many countries, like Turkey, Italy, Iran, India, China, Brazil, Spain, Portugal, South Africa, USA, Pakistan, Finland, and Egypt, export the marble products, many other countries, like Germany, Japan, South Korea, and Taiwan, import them.(Alyamac et al., 2017). Turkey has forty percent of the world reserves of marble, and the storage of waste generated during production is of great significance. Turkey has approximately marble reserves of 3.872 million m^3, of which close to $125 * 10^3$ t/year are produced in Afyon City. (Singh et al., 2019). Five thousand processing factories are used for marble production in Turkey. It is clear that these waste products reach millions of tons; so it is too difficult to store this amount of wastes (Alyamac and Ince, 2009).

FA is a divided siliceous tailing from the burning up of powdered coal and can be used an admixture. FA has the same fineness like PC. It can also react easily chemically with cement. Also, the average annual FA production in Turkey has about 13 million tons and half of it was utilized.

The disposal of WMP and FA are one of the most environmental concerns all over the world nowadays. On the other hand, WMP and FA can be used to increase the fresh properties of cementitious grout.

WMP is used like a complementary cement based material in the concrete (Pooja and Prof, 2014). Earlier researches concluded that maximum 10-15 percent of WMP can be conveniently mixed into the concrete without negatively impacting the durability, hardness and strength of the resulting concrete (Shirule et al., 2012; Aliabdo et al., 2014; Rodrigues et al., 2015). Another researches investigated the usage of WMP as a cement substitution and showed that combining of WMP in SCC with concrete reduce the splitting tensile strength, compressive strength, bulk weight, slump flow, ultrasonic pulse velocity, porosity and cost (Shirule et al., 2012; Aliabdo et al., 2014; Rodrigues et al., 2015; Yao et al., 2015; Uysal and Yılmaz, 2011; Gencel et al., 2012; Gesoglu et al., 2012; Alyousef et al., 2018).

Usually, the percentage of FA usage is 10-35% in concrete (Yao et al., 2015). The usage of FA in concretes and SCC have also been investigated and have been well developed in the last decade (Uysal and Yılmaz, 2011). On the other hand, there is limited knowledge available concerning the fresh characteristics of cement based grout containing FA. The replacement of Portland Cement with FA is important for decreasing the viscosity, increasing passing ability and flowability of cement based grout materials (Gencel et al., 2012) .

The goal of this work is to illustrate the possible utilization of WMP and FA in preparing the grout mixture and to pursue the impacts of WMP and FA on the workability, fluidity, and rheological characters of CBG. The tests were made on 24 grout mixtures with the inclusion of different amounts of WMP+FA with the percentages of 10-30% + constant 25% (WMP+FA) of the total cement based materials weight and with 0.75 to 1.5 ratios of w/b. A series of rheology and workability tests with the inclusion of MCFT, Lombardi Plate cohesion test, a coaxial rotating cylinder rheometer, and mini-slump flow diameter test were conducted to pursue the fresh characters of CBG mix.

5.2.Materials and Methods

5.2.1. Materials

In this research Portland cement (CEM I-42.5R) was used complying with ASTM C150 Type-I cement. Class F FA was used an additive in CBG according to ASTM C 618. Also, WMP was used as an additive. Waste marble sludge (WMS) was provided in the form of a wet slurry from marble factory in Gaziantep-Turkey. The WMS was dried in an oven at 100 ± 10 °C for 24 hours and then sieved with 150 µm sieve Figure 5.1. Table 4.1 demonstrates the chemical and physical properties of PC, WMP and FA. Also, grain size distributions of PC, WMP and FA are shown in Figure 5.2.

Figure 5. 1: Waste marble powder, cement, fly ash

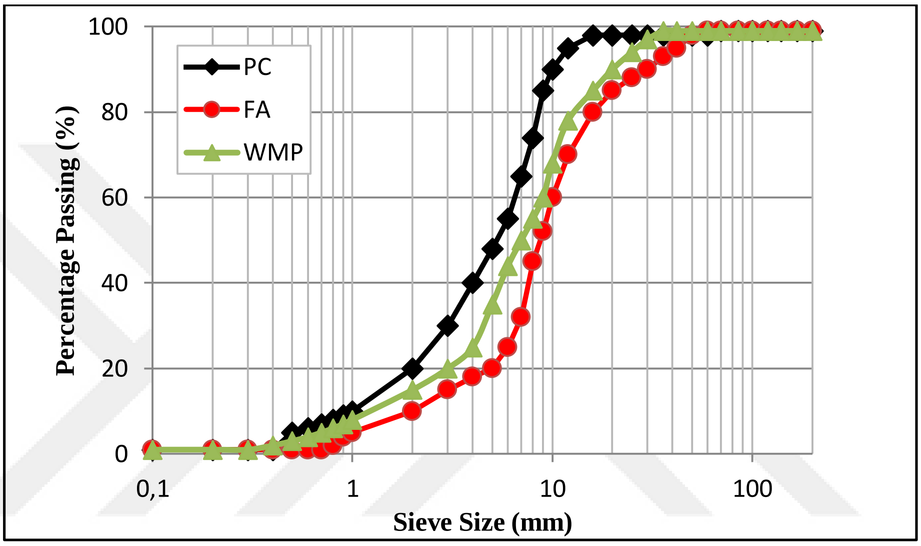

Figure 5. 2: Particle size distributions of PC, WMP and FA

5.2.2. Methods

Water-binder (w/b) rate is one of the significant factors that has a prominent impact on the fresh and hardened characteristics of CBG mixes. So, in this experimental work w/b 0.75, 1.00, 1.25 and 1.5 rates were chosen to research the effect of WMP+FA on the CBG. 24 injection mixtures with various WMP+FA amount were prepared to the impact of WMP, FA on the characteristics of CBG mixtures. (Table 4.1). WMP+FA was replace with cement substitutions of 10-30% + constant 25% by volume. The control mix was prepared with only PC and water at w/b 0.75, 1.00, 1.25, 1,50 rates. WMP and FA weren't added to the control mix. The mixture proportions are illustrated in Tables 5.1.

Table 5. 1: WMP+FA(constant) mix amount for 1.5 L and fresh and fluidity properties of the CBG mixtures.

MIX ID	MIX NO	CEMENT (kg/m^3)	WMP (kg/m^3)	FA (kg/m^3)	WATER (kg/m^3)	w/b	FA(%)	WMP (%)	Mini Slump (cm)	Marsh Cone (s)	Plate Cohesion (mm)
WMP0FA0WB075	M1	1396	0	0	1047	0,75	0	0	175	34	2,99
WMP10FA25WB075	M2	877	135	337	1044	0,75	25	10	188	30	5,32
WMP15FA25WB075	M3	808	202	337	1042	0,75	25	15	187	30	5,49
WMP20FA25WB075	M4	739	269	336	1039	0,75	25	20	185	31	5,26
WMP25FA25WB075	M5	670	335	335	1037	0,75	25	25	183	31	4,74
WMP25FA25WB075	M6	602	401	334	1034	0,75	25	30	180	31	4,29
WMP0FA0WB100	M7	1131	0	0	1131	1,00	0	0	203	27	3,08
WMP10FA25WB100	M8	715	110	275	1129	1,00	25	10	212	26	2,80
WMP15FA25WB100	M9	659	165	275	1127	1,00	25	15	210	27	3,15
WMP20FA25WB100	M10	603	219	274	1124	1,00	25	20	208	26	3,22
WMP25FA25WB100	M11	547	273	273	1122	1,00	25	25	208	26	3,04
WMP30FA25WB100	M12	491	328	273	1120	1,00	25	30	206	27	3,09
WMP0FA0WB125	M13	951	0	0	1188	1,25	0	0	225	27	3,37
WMP10FA25WB125	M14	604	93	232	1186	1,25	25	10	240	26	2,49
WMP15FA25WB125	M15	556	139	232	1184	1,25	25	15	236	26	2,54
WMP20FA25WB125	M16	509	185	231	1182	1,25	25	20	234	26	2,82
WMP25FA25WB125	M17	462	231	231	1180	1,25	25	25	230	26	3,35
WMP30FA25WB125	M18	415	277	231	1179	1,25	25	30	229	26	2,84
WMP0FA0WB150	M19	820	0	0	1230	1,50	0	0	230	26	2,87
WMP10FA25WB150	M20	522	80	201	1228	1,50	25	10	245	25	2,27
WMP15FA25WB150	M21	481	120	201	1226	1,50	25	15	242	25	2,07
WMP20FA25WB150	M22	441	160	200	1225	1,50	25	20	240	25	2,27
WMP25FA25WB150	M23	400	200	200	1223	1,50	25	25	237	25	2,43
WMP30FA25WB150	M24	360	240	200	1221	1,50	25	30	235	26	2,37

In preparation for the grout mixtures, five-liter laboratory mixer was used. The mixing step was applied in the experiment as following; WMP, FA, cement and water was mixed at slow speed (120 rpm) for 1 min. The mixer was paused and the remaining grout mixture on the sides of the container was stripped. Also, grout mixes was blended by hand for one minute. Lastly, the mixer was restarted at high speed (240 rpm) and the grout mixture mixed for three minutes. Temperature and humidity of the laboratory for all tests were checked and measured as 50-60% and 20±3 respectively. All CBG mixtures were obtained by using the same mixing procedures.

Rotational viscometer (rheometer) was used to find the yield stress and the plastic viscosity (proRheo R180 Instrument, Germany) at 20 ± 3 °C. The viscosity of the grout can be measured at various rotational speeds. The rheometer determines viscosity according to the searle-principle; The proRheo R180 is a standard rotational model viscometer which uses a motor-driven bob turning in a fixed measuring tube. The specimen is sheared in the gap between the bob the tube and the measured shear stress is used with the shear rate to compute the viscosity (Mezger, 2011).

Ascending and descending flow curves in the shear stress–shear rate curve were gotten. The shear rates were varied between from 50 to 1000 s^{-1} for every CBG mixture. The apparent viscosity is regarded as a function of the shear rate; for this reason, the shear-thickening (dilatant) behaviour of the CBG mixes is obtained with according to the apparent viscosity of GBG (Çelik et al., 2015).

To find the rheological properties of CBG, several types of analytical models exist. Plastic viscosity and yield stress are got by matching shear stress–shear rate curve values into Modified Bingham model (Eq. 3.2) τ_0 is yielding stress and μ_p is plastic viscosity. The modified Bingham model gives a preferable solution than the Bingham model (Eq. 3.1) for the same mixes (Çelik et al., 2015). Figure 5.3 demonstrates the shear stress–shear rate curve values of MP15FA25 grout mixture by using both modified Bingham and Bingham model.

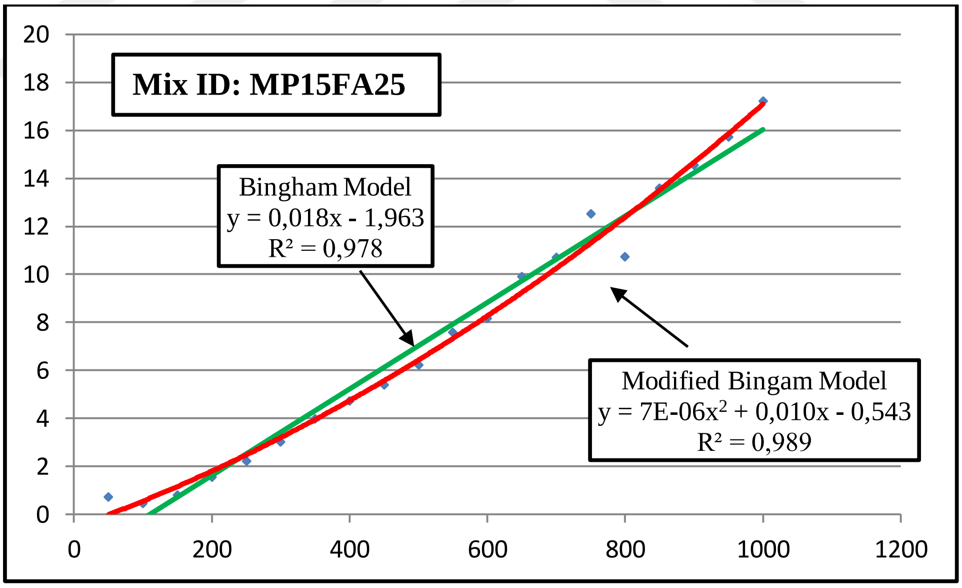

Figure 5. 3: The characteristic flow properties of CBG obtained from Modified Bingham and Bingham Model

The mini-slump test, MCFT and PCM test were used for evaluating the fluidity or workability of fresh grout mixtures. These tests were very easy to identify the flowability and workability characteristics of the grout prepared in the construction site.

The mini-slump test was used to find the spread of grout mixtures. The apparatus shape is same to the slump cone described by ASTM C-143 (Çelik et al., 2015). Dimensions of mini-slump apparatus; 38 mm high with at the top diameters of 57 mm and 19 mm at the bottom (Figure 5.4) (Çelik et al., 2015; Kantro, 1980; Ozawa et al., 1995). In the mini slump test, CBG mix is poured into a cone until it's full. Then, the mixture is allowed to spread by removing the mini slump cone. It is transfer to on a flat glass plate. In the vertical direction the spread diameters are measured and the average spread diameter is found.

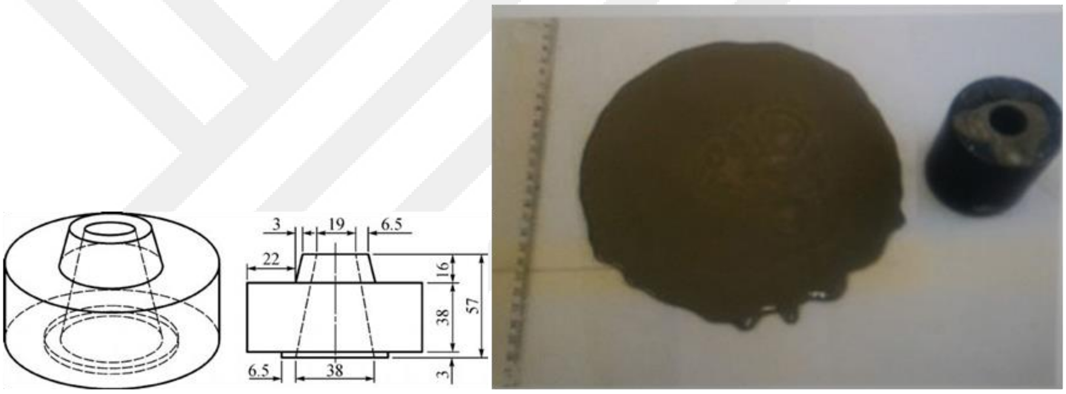

Figure 5. 4: Mini-slump test apparatus

The MCFT is a flowability test used for the properties and quality check of CBG and cement mortars which developed by Bartos et al. The volume of this device has 1500 ml and 5 mm inner cap (Figure 5.5). The MCFT is used to detect the CBG volume through flow cone at a measured time. The CBG mix was proud in a cone (1250 ml) and bottom outlet was turned on. After that, CBG mix begins to flow and elapsed time was measured providing that 1000 ml of CBG had flowed. Consequently, the elapsed of time gave the MCFT time. The MCFT time of water was found as 24 s in comparison with cement based grout.

Figure 5. 5: Marsh cone flow test apparatus

Lombardi PCM was used to find the cohesion. PCM consists of a steel plate with rough surfaces on both sides. 10×10×3 mm is a dimension of the PCM (Figure 5.6). PCM apparatus was used for the calculate of cohesion. The plate was immersed in the CBG mixture. Due to cohesion, the CBG mixture sticks on the plate. After that, the cohesion measured from the control mix was compared with that measured from the CBG mixes. All tests were done two times by preparing a new mixture for control purposes. The test results were similar and were not indicated in the tables. All tests were made at 8-12 minutes after contact with cement and water.

Figure 5. 6: Plate cohesion test apparatus

5.3. Results and Discussions

5.3.1.Rheological properties of CBG

The influence WMP and FA content on the rheological properties of CBG mixture can be related with between the shear rate and the shear stress. The flow curves of the CBG mixes containing WMP (w/b= 0.75, 1.00, 1.25, 1.5), FA (w/b= 1.00) and WMP+FA (w/b= 1.00) rate are shown in Figure 5.7.

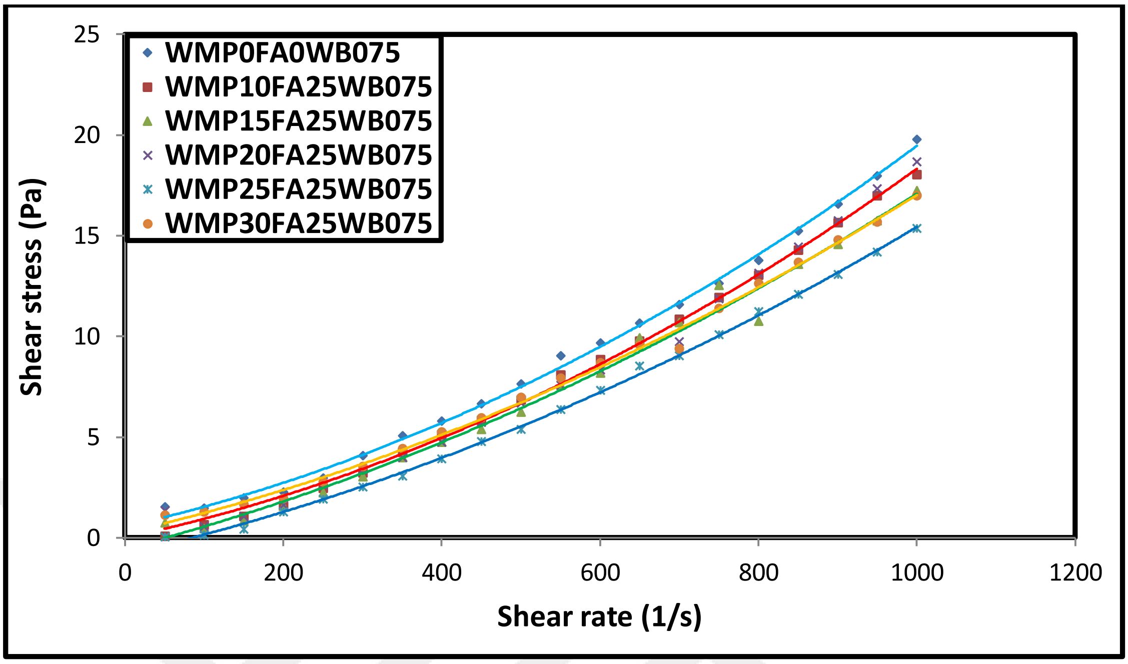

(a)

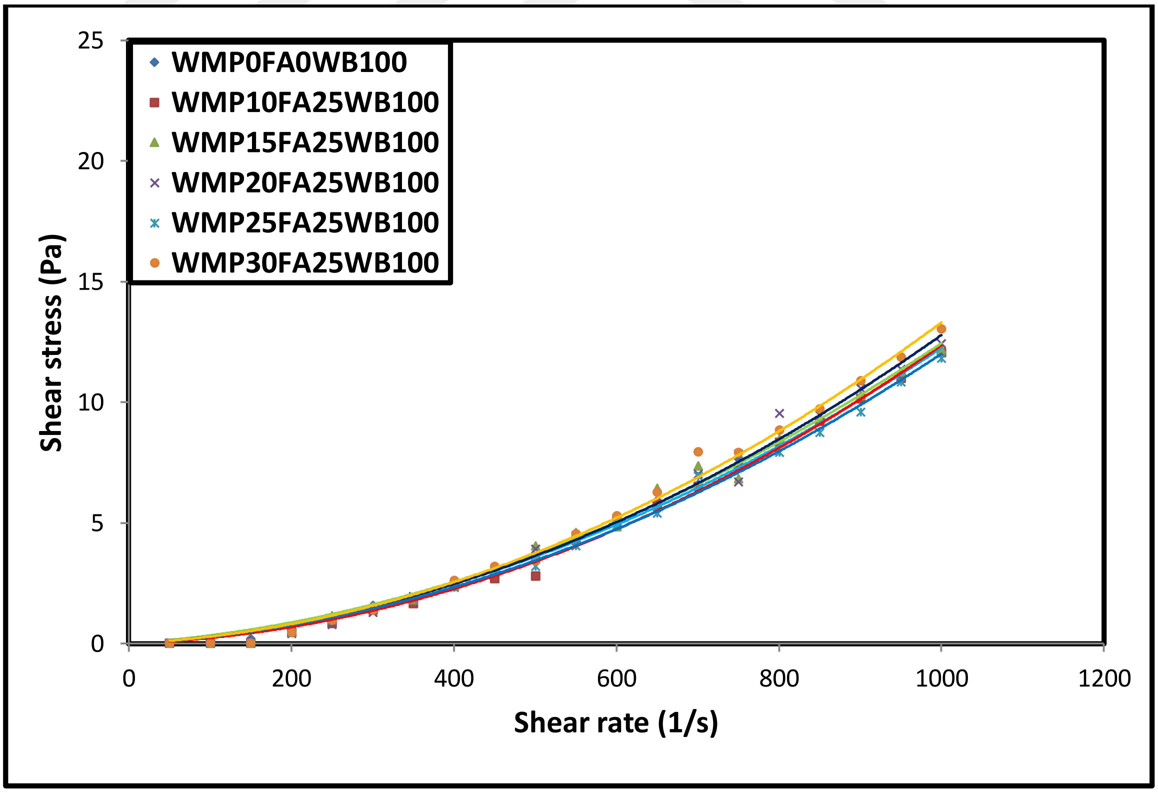

(b)

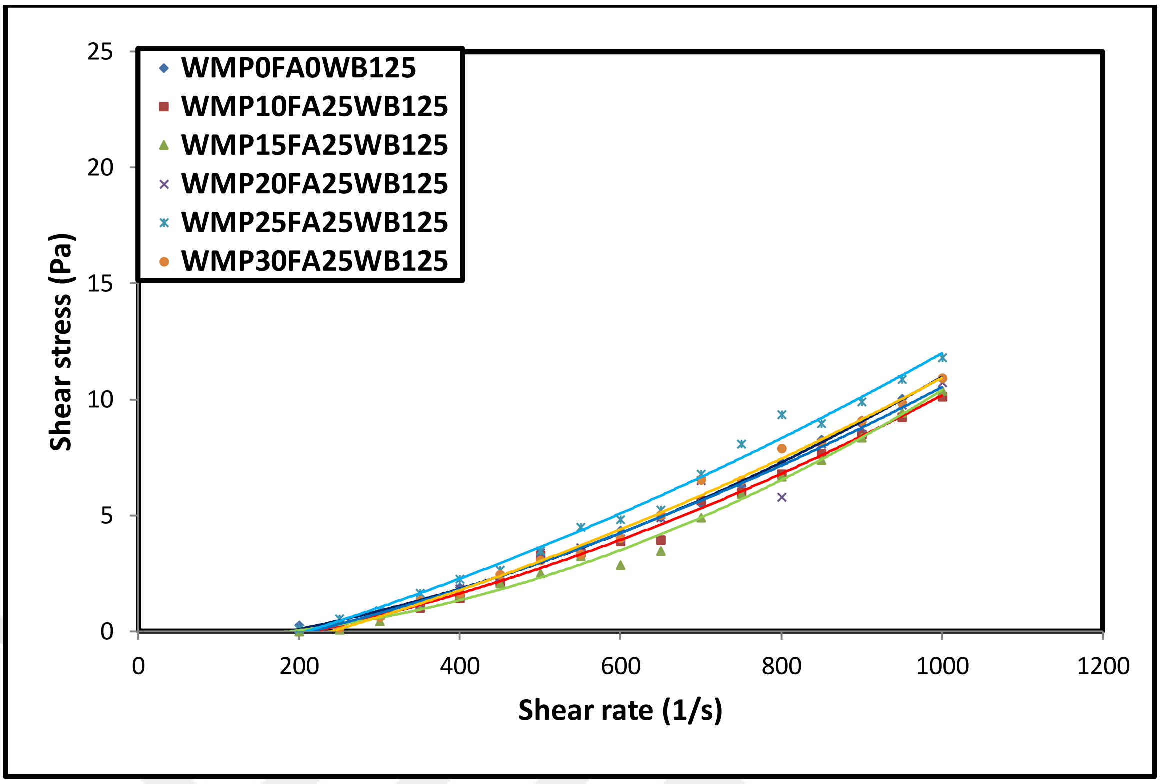

(c)

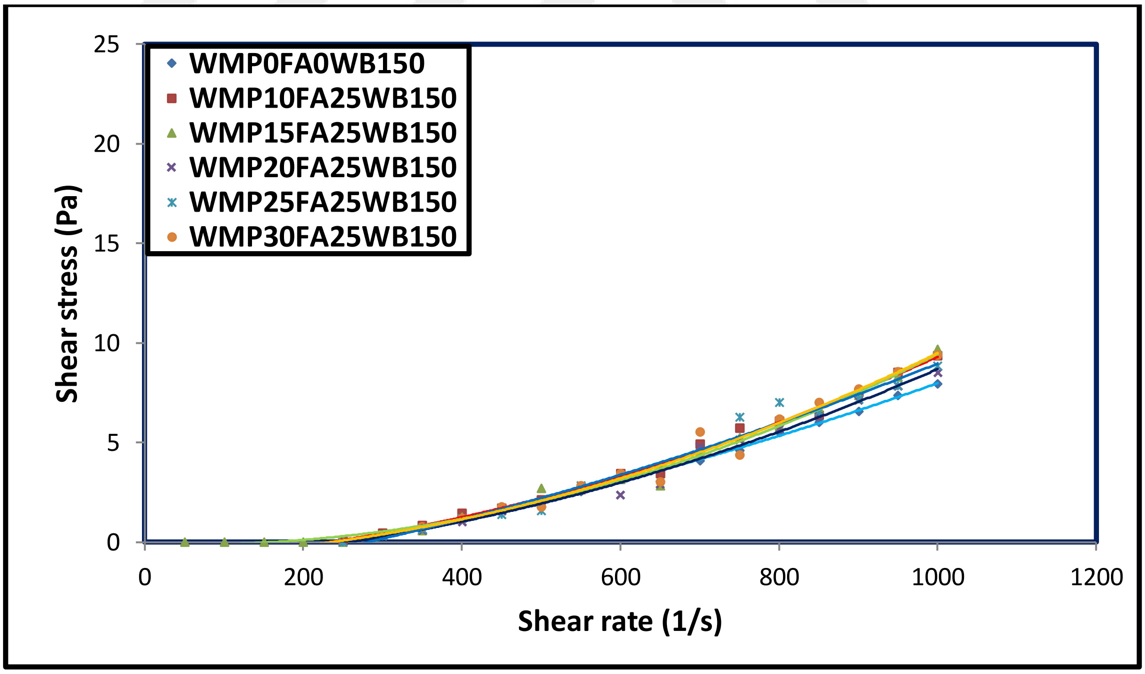

(d)

Figure 5. 7: Flow curves of CBG containing WMP(10-30%)+FA(25%) w/b ratio of (a) 0.75; (b) 1.00; (c) 1.25; and (d) 1.5

The shear stress versus the shear rate curves were obtained by using modified Bingham model for CBG mixes. Table 5.2 shows the calculation of modified Bingam Model parameters. Authors used the values obtained from ascending and descending flow curves because it gives more accurate value. In Figure 5.7, the CBG mixtures illustrated shear-thickening attitude at all WMP+FA contents.

Table 5. 2: Rheological properties of the CBG mixture. WMP (10-30%)+FA(25%) w/b ratio of 0.75; 1.00; 1.25; and 1.5

Rheoleogical Characteristics of The Grout Mixtures

Mix ID	**τ_0 (Pa)**	**μ_p (Pa.s)**	**Grout Temperature (C°)**	**R^2**
M1	1,50	0,008	20,0	0,997
M2	0,53	0,008	19,5	0,999
M3	0,54	0,010	19,0	0,989
M4	0,28	0,006	18,5	0,996
M5	0,83	0,009	18,5	0,998
M6	0,25	0,009	19,0	0,996
M7	0,76	0,004	19,0	0,998
M8	0,46	0,003	19,0	0,996
M9	0,59	0,003	18,1	0,994
M10	0,61	0,002	18,5	0,992
M11	0,51	0,002	18,5	0,995
M12	0,60	0,002	18,8	0,995
M13	0,62	0,003	19,0	0,998
M14	0,50	0,005	19,0	0,993
M15	0,36	0,003	19,0	0,992
M16	0,13	0,004	19,0	0,982
M17	0,63	0,004	19,0	0,990
M18	0,40	0,004	19,0	0,994
M19	0,46	0,004	18,7	0,999
M20	0,21	0,003	19,0	0,993
M21	0,34	0.001	19,0	0,989
M22	0,39	0,003	19,1	0,986
M23	0,25	0,002	19,0	0,972
M24	0,18	0,002	19,2	0,977

Table 5.2 demonstrate how the plastic viscosity (μ_p) of CBG mixtures containing WMP and FA are affected. It was observed that the increment in WMP amount in the

CBG mix increased the plastic viscosity in chapter 4. It can be concluded that the high water holding capacity. Similar result was reported by Singh et al. (2017). However, FA in the CBG mix decreased the plastic viscosity, owing to the spherical shape of the particles of FA (Jiménez et al., 2013; Cevik et al., 2018). Sha F. et al. (2018) found an decrease viscosity, this was primarily for the many amounts of SiO_2 and the "Ball Effects" of FA can evolve rheological characters of grout.

5.3.2. Fluidity properties of GBG

Figure 5.8(a) shows the mini-slump flow diameter of CBG prepared with the different amount of WMP+FA contents. It indicates that the increase in the percentage of WMP (10-25%) amount reduced the mini-slump flow diameter because of the angular particle shape of WMP (Gesoğlu et al., 2012). According to the chapter 4 result, FA positively affected of the mini slump flow. The spherical shape of FA decreases frictional force between the angular particles of PC owing to the ball bearing effect.

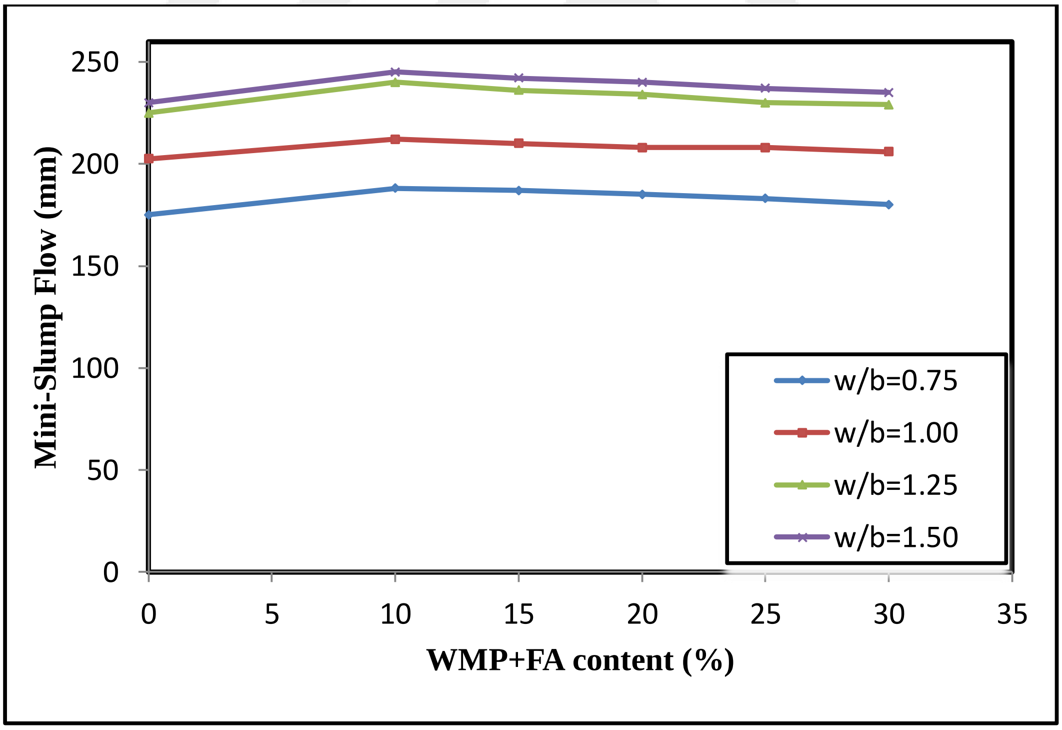

(a)

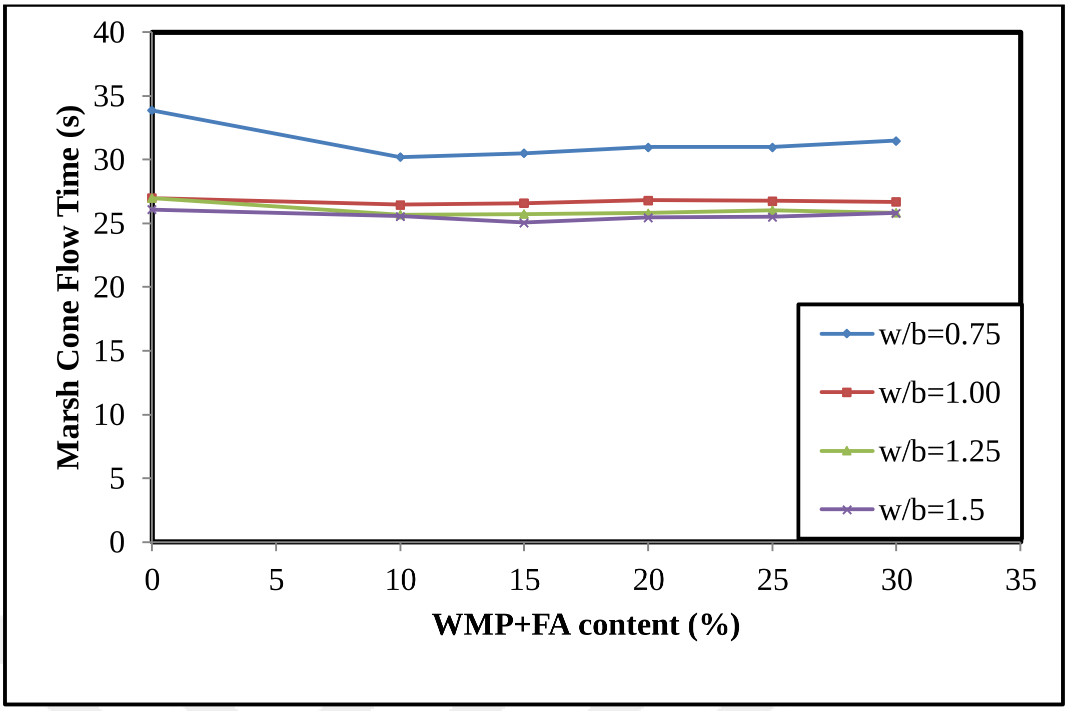

(b)

Figure 5. 8: Effect of WMP and FA on mini-slump flow; (b) impact of WMP and FA on MCFT

Figure 5.8(b) illustrates the impact of WMP and FA amount on MCFT at various w/b rate. It seems that the increase in WMP amount in the CBG mix, there is no effect on MCFT. Also, MCFT decreased with FA amount. It can be said that FA is able to improve the flowability of CBG. Same results were declared by Güllü, H. et al. (2019) and Sha. F. et al. (2018). Especially, FA increased the fluidity of CBG, while the WMP showed negative effect in increase the MCFT in WMP+FA content. Sing et al. (2017) found an decrease flowabilty on enhancement the substitute cement percent by WMP which was based on to the high fines percentage in WMP.

5.3.3. The Comparisons between fluidity and rheological properties of CBG

To descript the relation between two rheological values (plastic viscosity and yield stress) and the flowability and the workability properties (mini-slump flow, MCFT and PCM) of the CBG, the curves were drawn between the test outcomes and the R^2 value. If correlation coefficient (R^2) values are above 0.80, then it can be considered that there is a good correlation between two test outcomes. If R^2 values are below 0.80, it indicates that there is a poor correlation.

Figure 5.9 displays the relationship between the rheological and the flowability properties, meantime Figure 5.9(a) illustrates the relationship between the yield stress and the mini-slump flow. From the graph, the relation between the yield stress and the mini-slump flow was a very good correlation (R^2 = 0.827). Furthermore, it seemed that the reduction in the yield stress incremented the mini-slump flow diameter. Consequently, a well-defined representation of the yield stress value can be estimated from the mini-slump flow diameter test. The results are consistent with the literature (Çelik et al., 2015; Çınar et al., 2017).

Figures 5.9(b) and 5.9(c) shown the relationship between plastic viscosity and MCFT and yield stress and Lombardi PCM test. In the Figure 5.9(b), it can be obtained that there is a good correlation (R^2 = 0.869). Figure 5.9(b) shown that the increment in plastic viscosity increased the MCFT of the CBG mixture. Also, It seemed that there is weak correlation between yield stress and Lombardi PCM test (R^2 = 0.433).

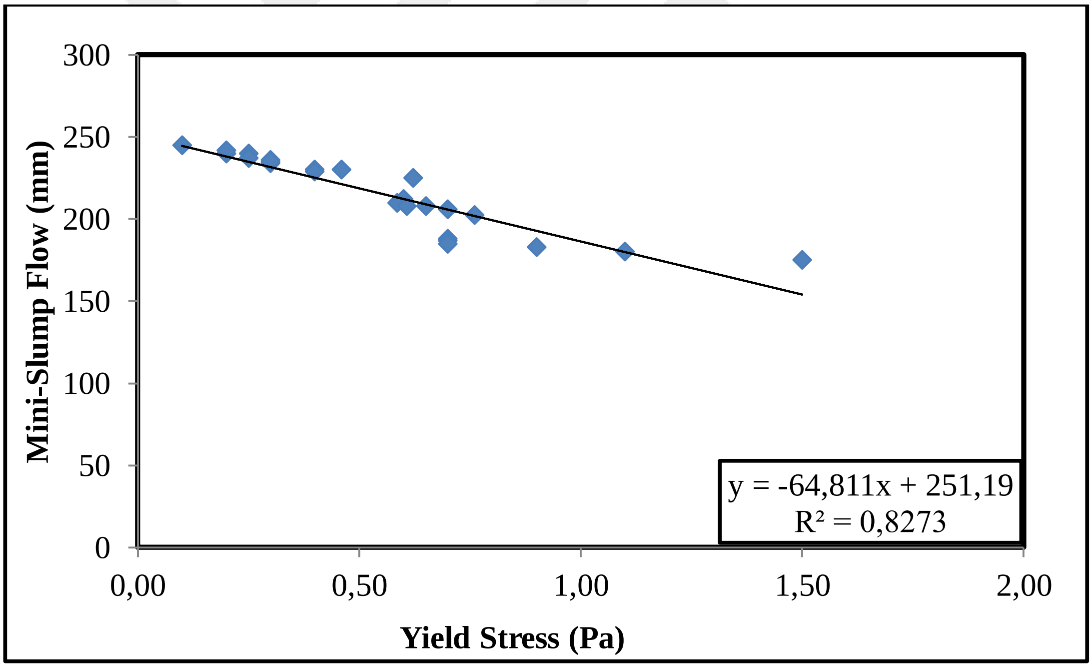

(a)

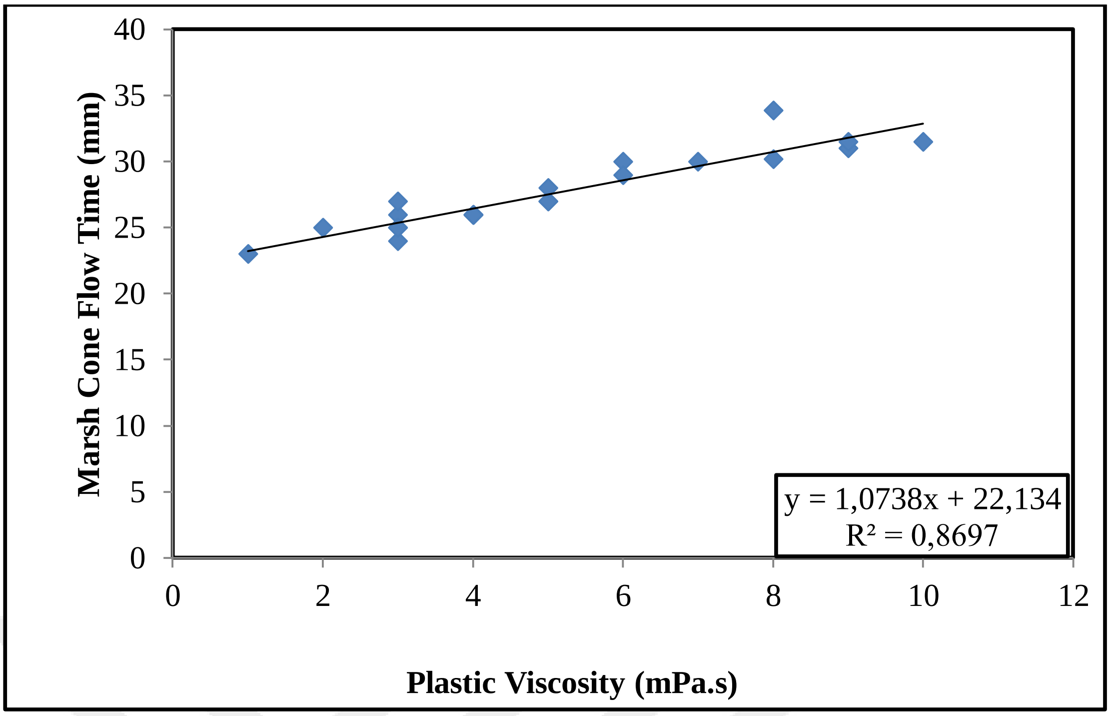

(b)

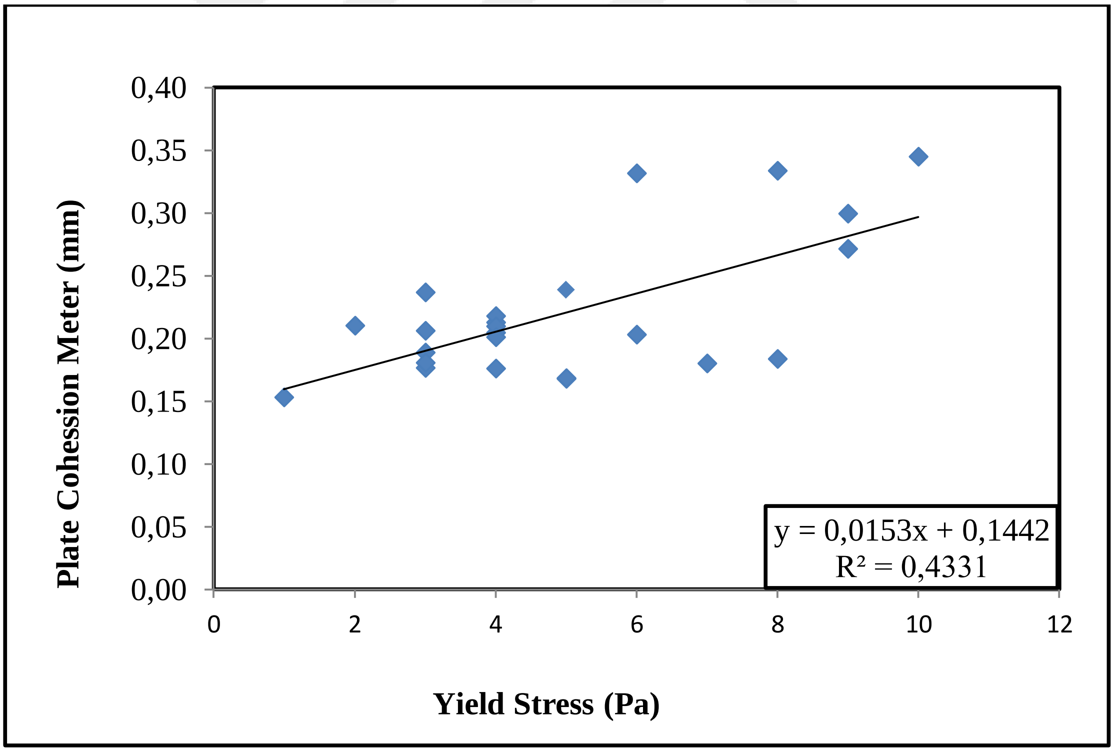

(c)

Figure 5. 9: Correlation between workability and rheological characteristics of a yield stress –mini-slump flow, b plastic viscosity – MCFT and c yield stress –PCM

5.3.Conclusion

Conclusions of this research work are given below.

- The rheological properties of the CBGs importantly have been improved by the addition of WMP+ FA all percentage of to grout mix at all w/b rates. Strongly shear thickening behavior was got from the CBG mixture all mix WMP+ FA contents
- The increment in the percentage of WMP in the CBG mixture incremented the plastic viscosity.
- According to the control sample, the increment in the percentage of WMP (10-25%) amount increased the mini-slump flow diameter for constant FA (25%) content. Especially, FA increased the fluidity of CBG, when the WMP showed negative effect in increase the MCFT in WMP+FA content.
- The rheological properties (the plastic viscosity and the yield stress) of the CBG got from the modified Bingham model also illustrates a good correlation with the MCFT and mini-slump flow of the CBG (R^2 = 0.82, R^2=0.86). On the other hand, no correlation was found between yield stress and Lombardi PCM test.
- According to fresh properties test results; Waste Marble Powder and Fly Ash can be suitable for use in substitution cement in proportions up to 20% and %25. For this reason, CO_2 emissions decreased by 45% and cost decreased by this rate.

CHAPTER 6

MECHANICAL PROPERTIES OF SOILCRETE MIXTURES MODIFIED WITH WASTE MARBLE POWDER (WMP) AND FLY ASH (FA)

6.1.Introduction

Grouting is described as the injection of fluid materials into the cavities of the ground or the space between the floor and adjacent structures. The main purpose of the grouting is to produce a denser, less permeable rock or soil, and/or stronger; it may also simply serve to fill voids, which are otherwise inaccessible and may prevent sufficient stress transmission from the floor or from a structure to the ground. As the cement-based grout especially used for jet grouting applications should have low viscosity to easily penetrate into rock or soil, w/c (water/cement) rate ranges 0.6 to 2 (Moseley,1993). Typical mixes have generally w/c ratios of 1:1 by weight (Coulter and Martin, 2006) to ensure grout of sufficiently low viscosity to fill up the cut soil volume, allowing air voids to escape (Lee et al., 2005). The structural materials obtained by mixing soils with cement slurry from jet-grouting application are called as soilcrete mixtures (Andromalos and Gazaway, 1989).

There have been many studies conducted on jet grouting soilcrete columns prepared with using different types of additives (Clarke et al., 1992; De Paoli et al., 1992; Littlejohn, 1982; Lowe and Standford, 1982; Schwarz and Krizek, 1992; Tinoco et al., 2016). And also, an experimental study has already been conducted by Kolovos, Asteris, Cotsovos, Badogiannis, and Tsivilis (2013) on the mechanical characters of soilcrete mixs improved with metakaolin. For preparing the mixtures, clay was used as binder in moderate and low proportions in order to simulate typical mixing conditions of practice, in soil stabilisation techniques. Moreover, the possible utilisation of metakaolin as a mineral admixture for the synthesis of sand-based binders that can also be used either as grouts in soil applications or for the production of sandcrete was presented by Kolovos, Asteris, and Tsivilis (2016). Overall, the behaviour of cementations sand-based binders (sandcrete) as a potential structures material was experimentally examined in this study. Also, the impact of the metakaolin supplementation on the mechanical characterizes (i.e. deformability, strength elasticity modulus, the uniaxial compressive) of sandcrete was investigated and checked to those of traditional concrete in their study. Similarly, investigation of the mechanical behaviour of metakaolin-based sandcrete mixtures was conducted by Asteris, Kolovos, Athanasopoulou, Plevris, and Konstantakatos (2017). Sandcrete mixture design optimisation and mechanical attitude of the manufactured specimens were experimentally researched in this work.

Rheological and mechanical properties of the grout are changed by adding minerals at different proportions. Several minerals such as cement kiln dust, silica fume, metakaolin, and bentonite have been utilized for many studies (Aitcin, Ballivy, & Parizeau, 1984; Bustamante & Gouvenot, 1983; Deere, 1982; Ruggiero, 1984; Weaver, Evans, & Pancoski, 1990). Therefore, the usage of minerals as an admixture in producing grout mix reduces the cost of production, yet it increases the workability and long term performance. However, the effect of WMP and WMP + FA replaced with cement at different proportions on their strength, stiffness, durability and rheological properties has not been thoroughly investigated for higher w/c ratios (greater than w/b = 0.75).

Marble is a very important material for construction, particularly for decoration reasons. %25 percent of marble turns to powder and dust due to shaping, polishing, and sawing. Turkey has 40 percent of the world's total marble and produces 7 million tons of marble were manufactured every year. Five thousand processing factories are used for marble production in Turkey. It is clear that these waste products reach millions of tons; so it is too difficult to store this amount of wastes (Alyamac and Ince, 2009).

The annihilation of Waste Marble Powder (WMP) is one of the most environmental concern all over the world nowadays. On the other hand, WMP can be used to increase the fresh and hardened properties of cementitious grout.

WMP is used like a complementary cement based material in the concrete (Pooja and Prof, 2014). Earlier researches concluded that maximum 10-15 percent of WMP can be conveniently mixed into the concrete without negatively impacting the durability, hardness and strength of the resulting concrete (Shirule et al., 2012; Aliabdo et al., 2014; Rodrigues et al., 2015). Another researches investigated the usage of WMP as a cement substitution and showed that combining of WMP in self compacting concrete (SCC) with concrete reduce the splitting tensile strength, compressive strength, bulk weight, slump flow, ultrasonic pulse velocity, porosity and cost (Shirule et al., 2012; Aliabdo et al., 2014; Rodrigues et al., 2015; Yao et al., 2015; Uysal and Yılmaz, 2011; Gencel et al., 2012; Gesoglu et al., 2012; Alyousef et al., 2018).

Usually, the percentage of FA usage is 10-35% in concrete (Yao et al., 2015). The usage of FA in concretes and SCC have also been investigated and have been well developed in the last decade (Uysal and Yılmaz, 2011). On the other hand, there is limited knowledge available concerning the fresh characteristics of cement based grout containing FA. The replacement of Portland Cement with FA is important for decreasing the viscosity, increasing passing ability and flowability of cement based grout materials (Gencel et al., 2012).

Their study showed that different replacement level of WMP and FA with cement at different w/b ratios is possible for producing cement base grout. Because of the beneficial effects of WMP and FA have been mentioned above, this waste may be used as an additive for a soilcrete mixture design, to develop the mechanical and rheological behaviour and long term durability of soilcrete as a structural material. Therefore, this study presents the possible utilisation of WMP and FA as an additive for the synthesis of binders that can be used either as grouts in soil applications or for the production of soilcretes that can be utilized in geotechnical applications. And also, the second and third part of this study was conducted on rheological and workability properties of the cement base grout prepared by addition of WMP and FA replaced with cement at same proportions of WMP and WMP+FA and same w/b ratios by. In general, the attitude of soilcrete as a potential construction material has been investigated experimentally. Also, the impact of WMP and WMP+FA on the mechanical characteristics (like the unconfined compressive strength, elasticity modulus, bleeding and failure mechanism) of soilcrete mixtures obtained with different w/b ratios were investigated.

6.2.Experimental procedure

6.2.1. Materials used in this study

In this research Portland cement (CEM I-42.5R) was used complying with ASTM C150 Type-I cement. Class F FA was used an additive in CBG according to ASTM C 618. Also, WMP was utilized as an additive. Waste marble sludge (WMS) was provided in the form of a wet slurry from marble factory in Gaziantep-Turkey. The WMS was dried in an oven at 100 ± 10 °C for 24 hours and then sieved with 150 μm sieve “Fig. 5.1”.

Table 4.1 shows the physical and chemical characteristics of FA, WMP and cement utilized in this study. The clay used in this study was obtained from Gaziantep city in Turkey. The clay soil was collected one meter from the ground surface. The clay was sieved as passing from 75 μm sieve size. Then, laboratory tests related to Atterberg limits, swelling test, standard proctor compaction test made for the clay according to ASTM D4318-05, ASTM D4546-08 and ASTM D698-12, respectively. According to Unified Soil Classification System (USCS) the clay soil is classified as CL (low plasticity clay). Index properties of the clay (including swelling and compaction parameters) are summarised in Table 6.1. The clay had bell-shaped compaction curves obtained from standard compaction test.

Table 6. 1: Index properties and classifications of clay tested.

Properties	Values
Liquid limit (LL)	42%
Plastic limit (PL)	23%
Swell per cent	5%
Degree of expansivity	Medium
Maximum dry density (MDD)	1.65 g/cm³
Optimum moisture content (OMC)	17%
Classification (according to USCS)	CL

6.2.2. Mixture proportions and preparations

Water–binder (w/b) ratio is one of the important parameters that have considerable impact on hardened and fresh characteristics of grout mixs. The ranges of w/c rate that was applied in the past studies were changed among 0.25 to 0.65. On the other hand, this ratio is preferred for injectable grouting in and rock soils at range of 1.0 and 1.5. Furthermore, this ratio sometimes can reach up to 2.0 for jet grouting applications. Because of this situation, 0.75, 1.00, 1.25 and 1.5 were selected as water–binder ratio (w/b) for this study in order to evaluate the impact of WMP and WMP+FA on the grout mixtures. These ratios generally used for geotechnical projects like CBG for rock or soil injection, sealing cement grouts and jet-grouting (Moseley,1993). For research the impact of WMP and WMP+FA at different substitutions on the cement- based grout mixtures prepared for this study, forty eight mixtures were produced at different w/b rates that have been mentioned (see Table 6.2). Not only, replacement level of WMP was selected as important parameter, but also w/b ratio was used as significant variable for this study. WMP was replaced with cement at substitutions of 5, 10, 15, 20 and 25% by mass and WMP+FA were replaced with cement at substitutions of 10, 15, 20, 25 and 30% by mass and FA was replaced constant value (%25) in this study. The control mixture was produced at each w/b ratio without WMP and FA additive due to control purposes. The mix design parameters including all substitutions of WMP, WMP+FA and w/b rates are demonstrated in Table 6.2. Most of the studies considered mixes with 4–10% cement contents, more typical of deep mixing than jet grouting (Lee et al., 2005), where according to Kauschınger et al. (1992), jet grouting may have cement contents (rate of the weight of cement to total weight of the mix) of up to 50%. Because of this situation clay content was selected as 20% of total amount of the mixtures (Table 6.2).

Table 6. 2: Mix design of the samples (a.WMP, b. WMP+FA) for 1 kg mix.

a. WMP

MIX NO	CEMENT (g)	MP (g)	WATER (g)	Clay (g)	W/b	MP (%)
M1	457,1	0	342,9	200	0,75	0
M2	434	22,9	342,9	200	0,75	5
M3	411	45,7	342,9	200	0,75	10
M4	389	68,6	342,9	200	0,75	15
M5	366	91,4	342,9	200	0,75	20
M6	343	114,3	342,9	200	0,75	25
M7	400	0	400	200	1	0
M8	380	20	400	200	1	5
M9	360	40	400	200	1	10
M10	340	60	400	200	1	15
M11	320	80	400	200	1	20
M12	300	100	400	200	1	25
M13	356	0	444	200	1,25	0
M14	338	18	444	200	1,25	5
M15	320	36	444	200	1,25	10
M16	302	53	444	200	1,25	15
M17	284	71	444	200	1,25	20
M18	267	89	444	200	1,25	25
M19	320	0	480	200	1,5	0
M20	304	16	480	200	1,5	5
M21	288	32	480	200	1,5	10
M22	272	48	480	200	1,5	15
M23	256	64	480	200	1,5	20
M24	240	80	480	200	1,5	25

b. WMP+FA

MIX NO	CEMENT (g)	MP (g)	FA (g)	WATER (g)	Clay (g)	W/b	FA(%)	MP (%)
M1	457,1	0	0	342,9	200	0,75	0	0
M2	297	45,7	114,3	342,9	200	0,75	25	10
M3	274	68,6	114,3	342,9	200	0,75	25	15
M4	251	91,4	114,3	342,9	200	0,75	25	20
M5	229	114,3	114,3	342,9	200	0,75	25	25
M6	206	137,1	114,3	342,9	200	0,75	25	30
M7	400	0	0	400	200	1	0	0
M8	260	40	100	400	200	1	25	10
M9	240	60	100	400	200	1	25	15
M10	220	80	100	400	200	1	25	20
M11	200	100	100	400	200	1	25	25
M12	180	120	100	400	200	1	25	30
M13	356	0	0	444	200	1,25	0	0
M14	231	36	89	444	200	1,25	25	10
M15	213	53	89	444	200	1,25	25	15
M16	196	71	89	444	200	1,25	25	20
M17	178	89	89	444	200	1,25	25	25
M18	160	107	89	444	200	1,25	25	30
M19	320	0	0	480	200	1,5	0	0
M20	208	32	80	480	200	1,5	25	10
M21	192	48	80	480	200	1,5	25	15
M22	176	64	80	480	200	1,5	25	20
M23	160	80	80	480	200	1,5	25	25
M24	144	96	80	480	200	1,5	25	30

In order to obtain grout mix samples, the same mixing procedure was used for all samples. Five-litre standard rotary type laboratory mixer is used to produce the grout mixtures. The mixing method that was selected for this study was applied as following; firstly, the binders that consist of cement and WMP and WMP+FA were obtained by mixing with water for 1 min, and then mixer was stopped and the binders mixed by hand for 1 minute. Subsequently, the clay selected for this study was inserted to the binder mix. Eventually, the mixtures including binders and clay were mixed by the mixer at 240 rpm speed for 3 min. Therefore, the total mixing time was applied as 5 min for preparing all samples in this study. Humidity and temperature of the laboratory for all tests were measured as 55–65% and 23 ± 3 °C, respectively.

6.2.3. Unconfined compressive strength (UCS) test

UCS tests were conducted on the soilcretes prepared from the soils, cement, WMP and WMP+FA mixs following ASTM D5102-09b. The shear rate was chosen as 1 mm/min for all experiments. A total of 432 (2x(24 mixtures × 3 day curing × 3 trial for each mixture)) soilcretes samples were prepared for Unconfined compressive strength (UCS) test in this investigation. All mixtures were cured for 3, 7 and 28 days at dry condition. Each case has been tested for three specimens in order to check the results. Test results showed that all results were repetitive. Therefore, the authors used the average values for this study. In order to compose soilcrete samples plastic molds 110 mm high with a height to diameter ratio of 2:1 according to ASTM D2166-13 (Figure 6.1(a)) were used. The problem of bleed was overcome by attaching cardboard plastic collars to the top of the moulds mostly occurring in the first two hours (Lee et al., 2005). Then, the moulds with collars were covered by plastic bags to prevent escaping of the water that is available in the grout samples. The bleed water was siphoned from the top of the sample and the collar was removed after 24 h. Excess grout was then shaved from the top of the sample in order to bring the level of the sample to the top of the mould. The sample was then left in the mould for a further 24 h before being removed. From the latter curves the uniaxial UCS and elasticity modulus of soilcrete also the axial-strain corresponding to the maximum sustained load were detected. The Uni-axial UCS test machine used for this experiments is demonstrated in Figure 6.1(c). Then, these values were compared to control samples and each other's.

6.2.4. Bleeding test for stabilization of fresh grouts

The stability of CBG mix is decided by basic laboratory tests (bleeding test) utilizing 1000 ml CBG contained in a regular glass cylinder with a constant diameter of 60 mm (Figure 6.1(b)). To assess the stability of a suspension, the sedimentation rate (dV / V), which is defined as the volume of the clear water (dV) which is separated on the suspension divided into the actual slurry volume (ie, V = 1000 ml), is recorded. Deere (1982) classified the suspension as a 'stable suspension' based on Kutzner (1996) based on a sedimentation rate of not more than 5% and a rate of less than 10%. High sedimentation ratio is typical of pure CBG and has great practical results because if sedimentation of solids take shape throught grouting, the voids being treated and the grouting pipelines can be plugged and the grout cannot flow any further.

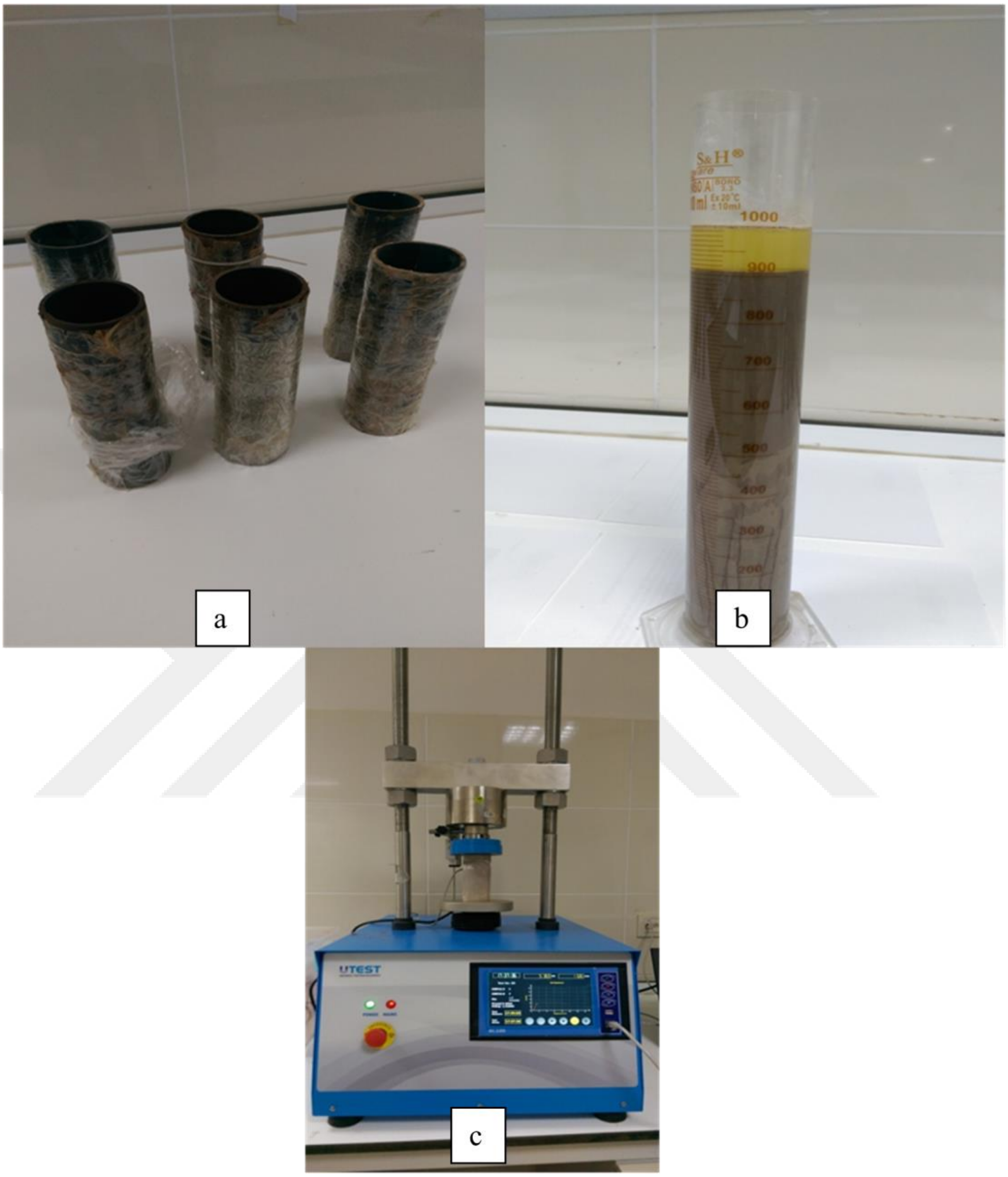

Figure 6. 1: (a) Plastic moulds used for preparing soilcretes. (b) Settlement of M23 mix after bleeding test. (c) The Uni-axial unconfined compressive strength test machine used for this study.

In accordance with to the work on pore structure of CBG sand made by Helal and Krizek (1992) by using microfine CG (i.e. MC-500, MC-300 and MC-100), the ratio of original ungrouted pore space occupied by the hydration products and bleed water was found to be a function of w/c rate of CBG. For the more unbalanced CBG with w/c rate exceeding 1.25 which indicate sedimentation rate greater than 5% during first phase (i.e. <30 min) of test, aggregation and sedimentation of cement grains takes place in soil voids prior to setting with accumulated bleed water occupies the upper parts of the pore void, inducing anisotropic properties in grouted soils.

6.3. Results and Discussions

6.3.1. UCS results for WMP and WMP+FA

UCS results of the mixtures prepared by replacing only 5-25% of WMP and 10-30% of WMP and constant 25% of FA with cement at various water/binder rates (0.75, 1.00, 1.25 and 1.5) for 3, 7 and 28 days curing time are given in Figure 6.2. The average UCS results of the mixtures prepared for this study are ranged between 400 kPa and 5,5 MPa and those are very close to the results (between 1 and 15 MPa in range) that were obtained from the similar works reported in the literature. These studies reported in literature are related with not only soil-based building elements but also grouting practices and repair mortars (Consoli et al., 2011; Mikkelsen, 2002; Morel et al., 2007; Nikbakhtan and Osanloo, 2009; Pavlovic et al., 2010a; Pavlovic et al., 2010b; Sonebi et al., 2013; Yoon and Abu-Farsakh, 2009). According to Figure 6.2, high UCS results were obtained because of the addition of WMP for binders at the lower water/binder ratios in comparison to the higher water/binder ratios. UCS of the soilcretes gradually reduces with increment of water/binder ratio. As expected, the higher water/binder rate is, the higher is the decrease for the calculated average UCS of soilcrete specimens at all curing times (Kolovos et al., 2013). The supplement of WMP in the binder ensued in lower values for the found average compressive strength of soilcrete specimens at all curing times, in comparison to the reference specimens (M1, M7, M13 and M19). The increment in the compressive strength of soilcretes is quick early in the curing time and then slows down over time (Porbaha et al., 2000). As a result it is clearly seen that WMP could be used as an additive for improvement of problematic clay soils.

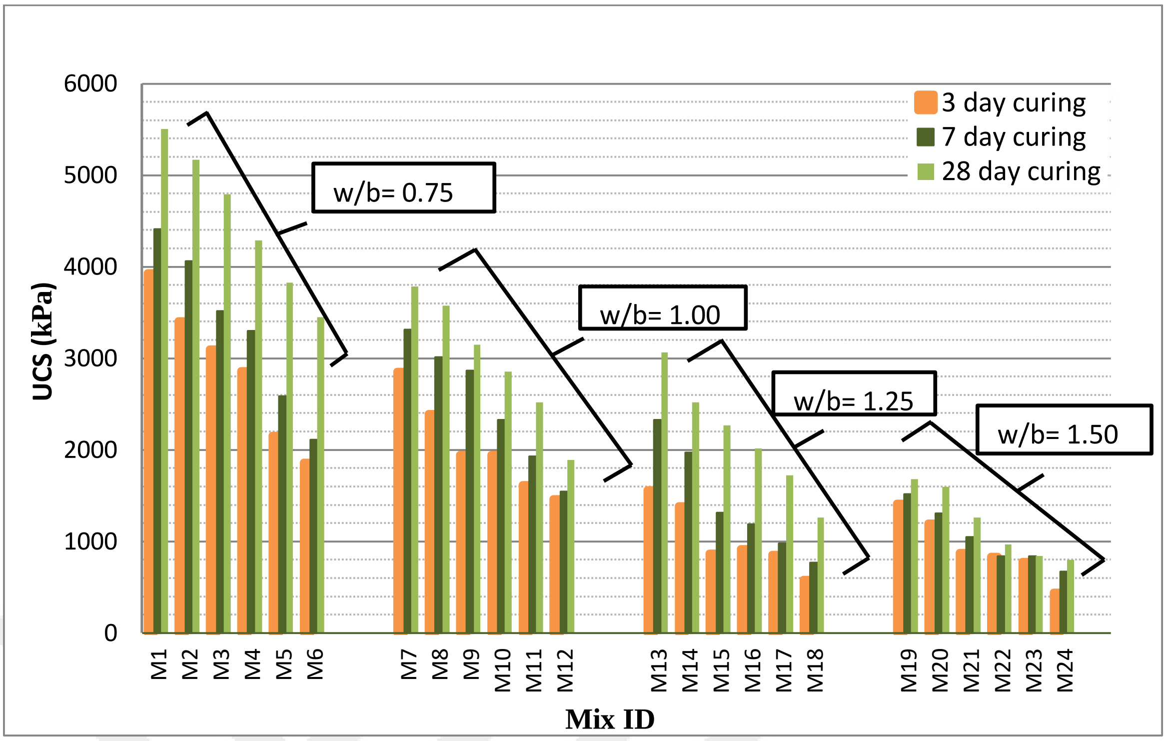

a.WMP

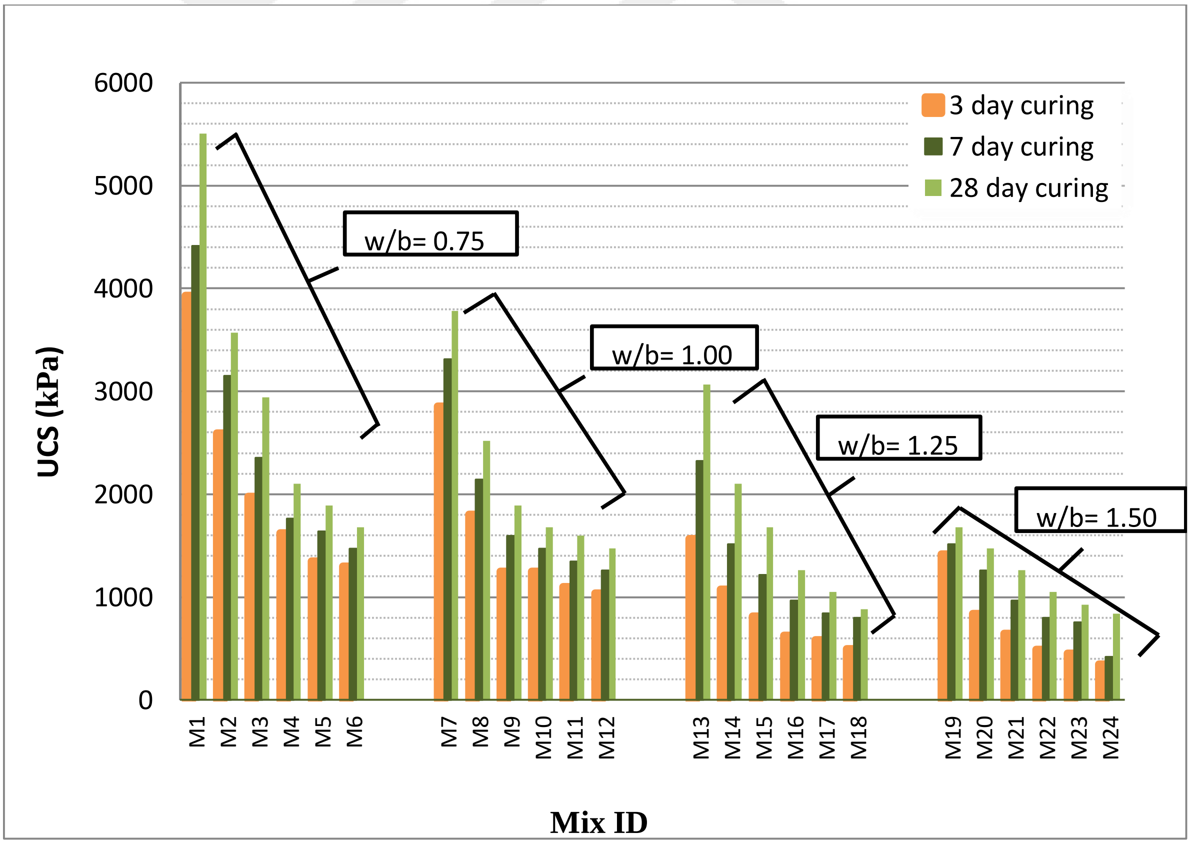

b. WMP+FA

Figure 6. 2: Compressive strength of all soilcrete samples at 3, 7 and 28 days (at different w/b ratios; .75, 1.00 and 1.25, respectively) a.WMP, b. WMP+FA

As it is clearly seen in Figure 6.3, Figure 6.4, Figure 6.5, Figure 6.6, Figure 6.7, Figure 6.8, Figure 6.9, and Figure 6.10 with increasing amount of WMP and WMP+FA in soilcrete sample UCS value of all soilcretes decrease at all curing days and w/b ratios. This consistent model for all the composites is described in Ettu et al. (2013e), as a result of low pozzolanic reaction rate in early ages. The silica from the pozzolans is produced by reacting with the lime produced as the hydration product of ordinary portland cement to produce additional calcium-silicate hydrate, which increases the binder efficiency and strength values at later days of curring (after 50 days curing). The max UCS value in soilcrete sample was observed as 6 Mpa when constitution of WMP and WMP+ FA was 0% at w/b 0.75 and 28 day curing. On the other handthe min UCS of the samples was determined as (WMP) 500 kPa and (WMP+FA) 250 kPa.

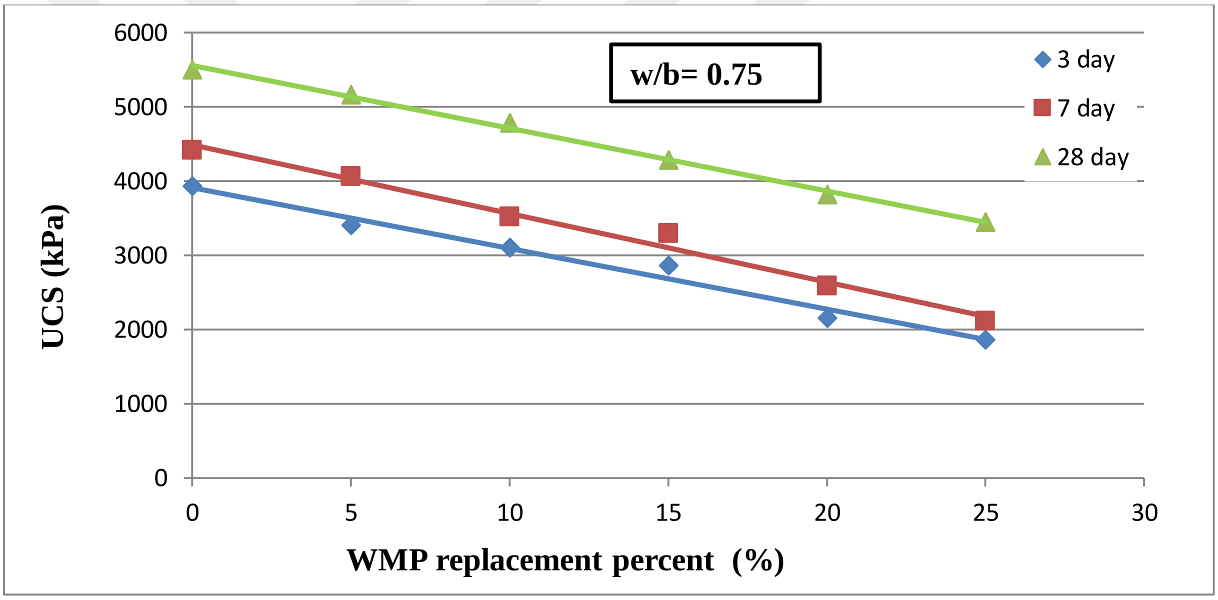

Figure 6. 3: UCS results of soilcrete samples at 3,7 and 28 days for w/b= 0.75 and various WMP replacement levels

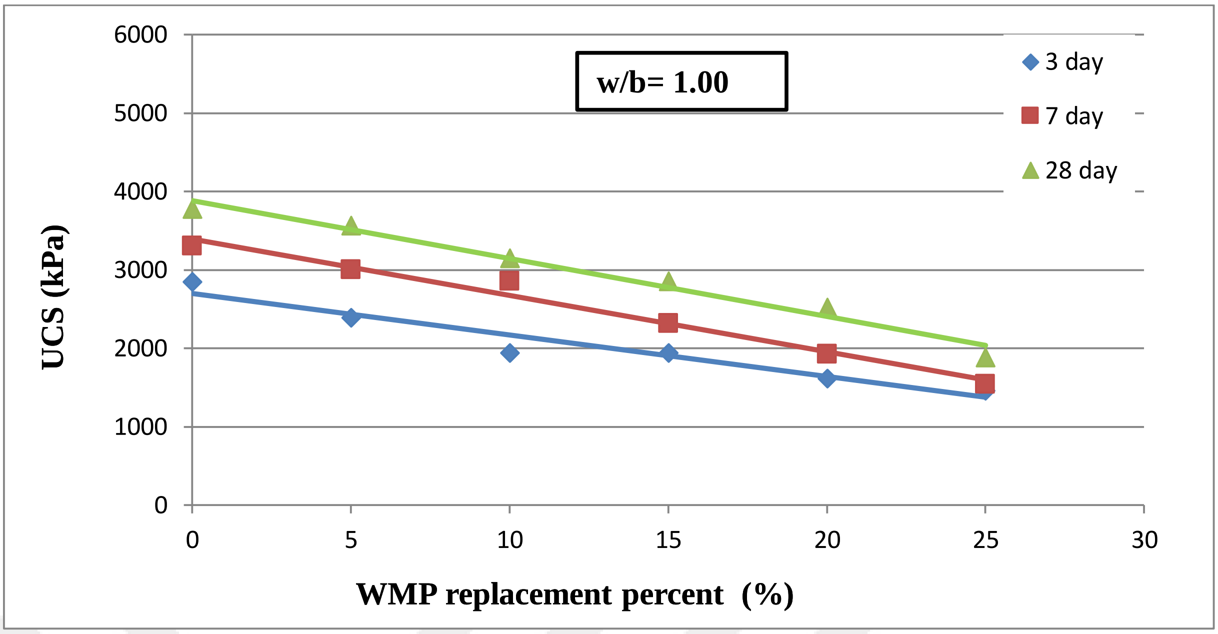

Figure 6. 4: UCS results of soilcrete samples at 3,7 and 28 days for w/b= 1.00 and various WMP replacement levels

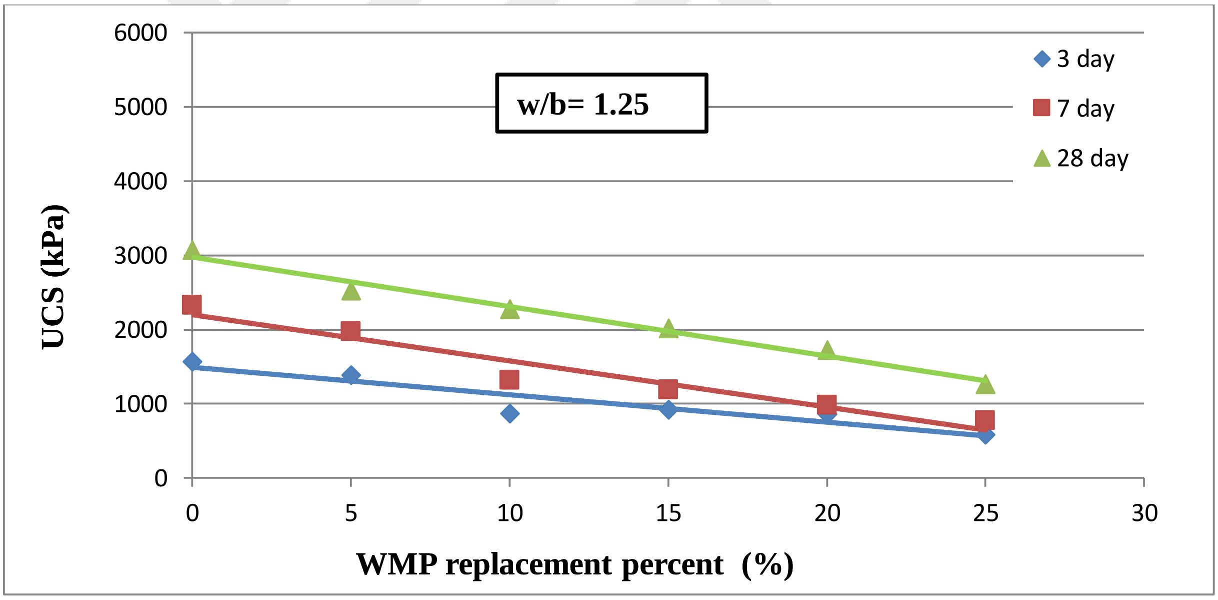

Figure 6. 5: UCS results of soilcrete samples at 3,7 and 28 days for w/b= 1.25 and various WMP replacement levels

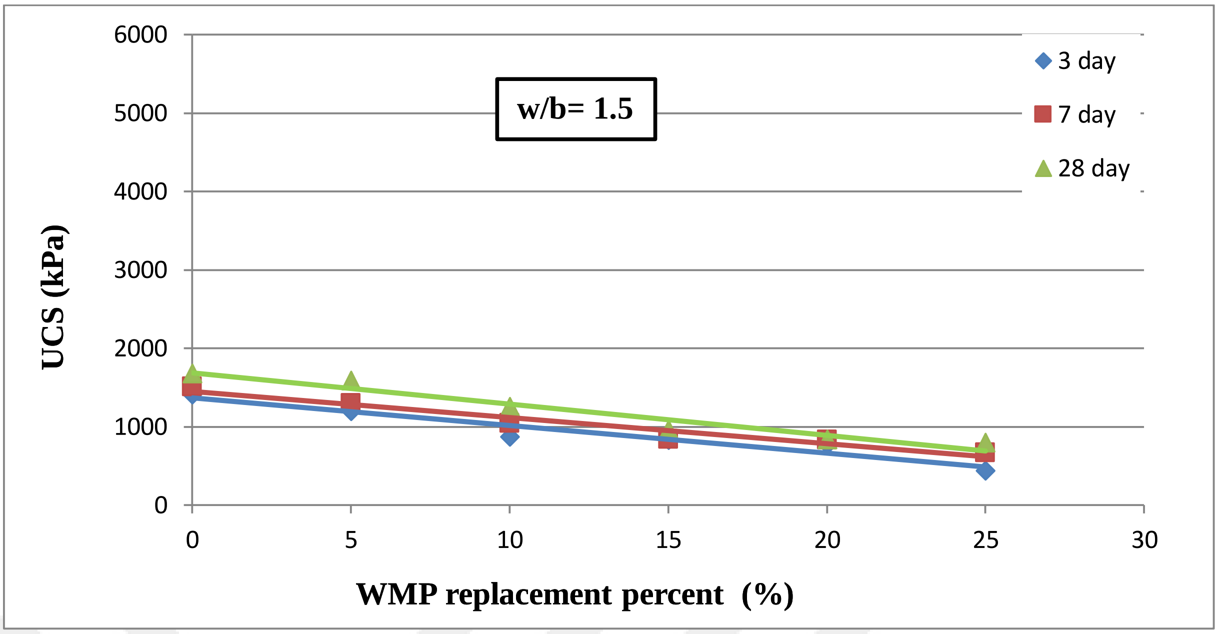

Figure 6. 6: UCS results of soilcrete samples at 3,7 and 28 days for w/b= 1.50 and various WMP replacement levels

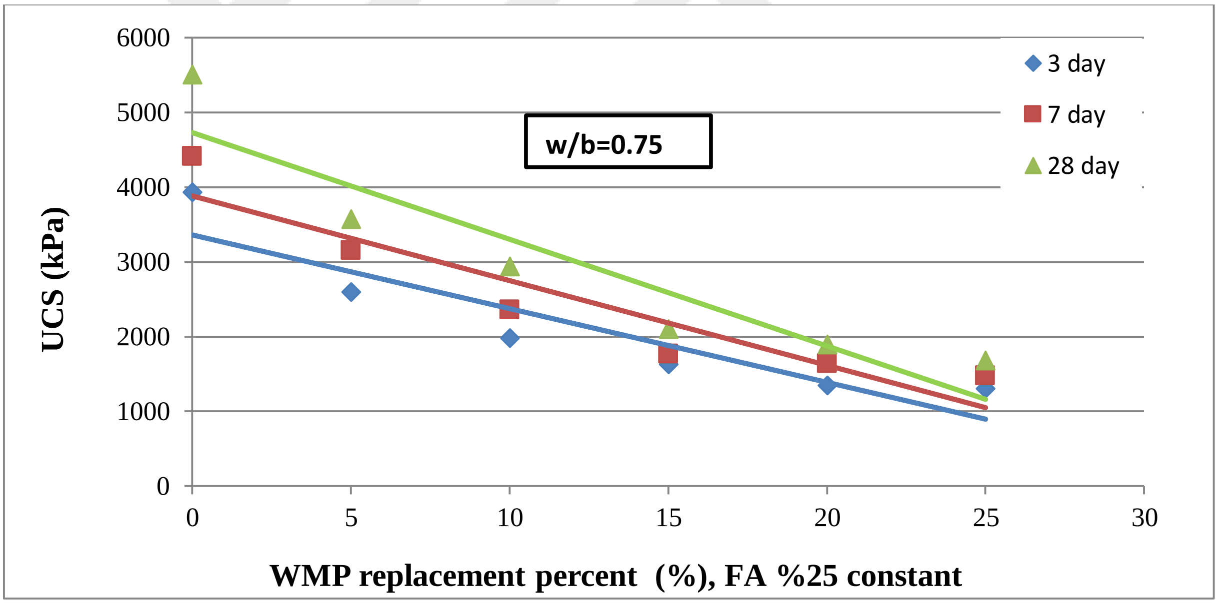

Figure 6. 7: UCS results of soilcrete samples at 3,7 and 28 days for w/b= 0.75 and various WMP+FA (constant %25) replacement levels

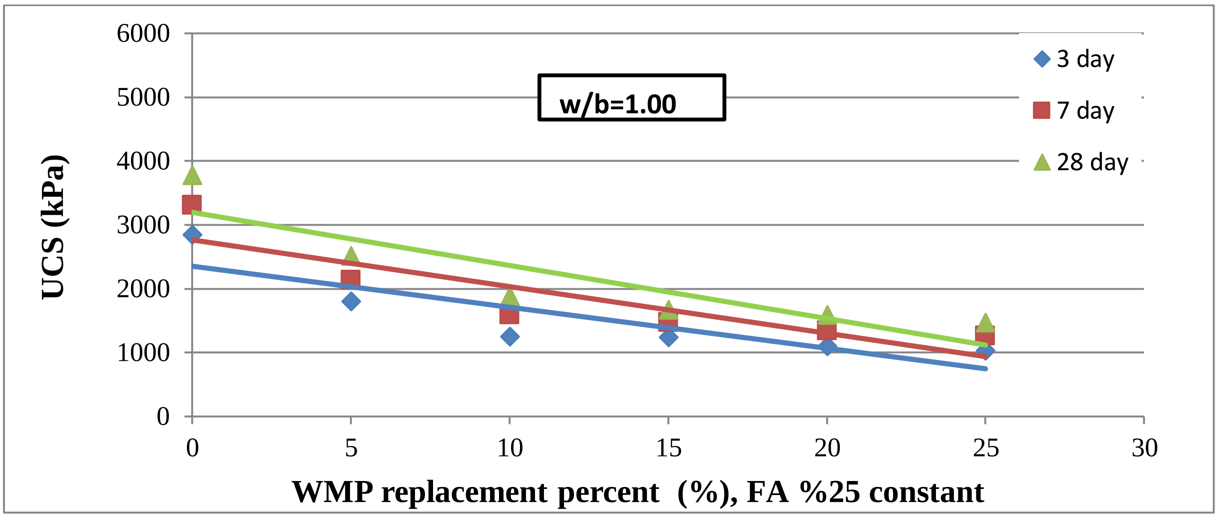

Figure 6. 8: UCS results of soilcrete samples at 3,7 and 28 days for w/b= 1.00 and various WMP+FA (constant %25) replacement levels

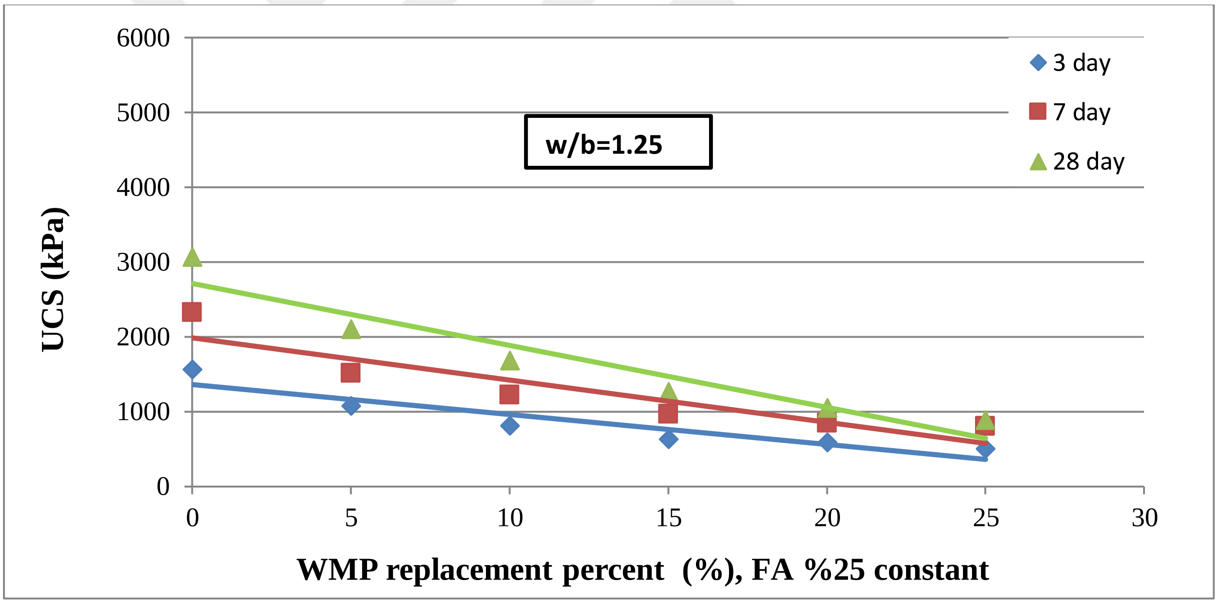

Figure 6. 9: UCS results of soilcrete samples at 3,7 and 28 days for w/b= 1.25 and various WMP+FA (constant %25) replacement levels

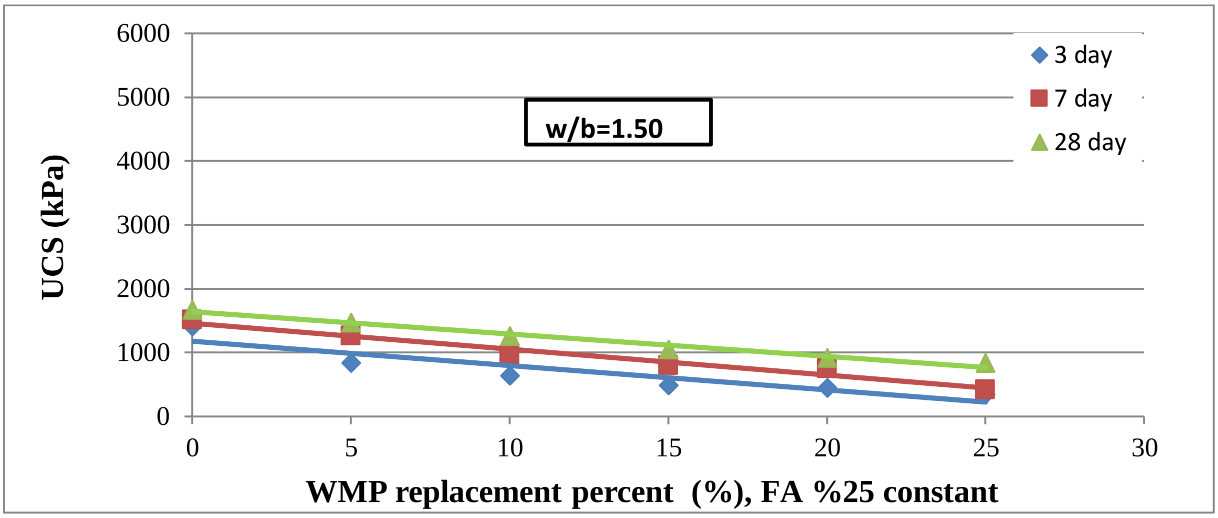

Figure 6. 10: UCS results of soilcrete samples at 3,7 and 28 days for w/b= 1.50 and various WMP+FA (constant %25) replacement levels

The compressive strengths of soilcretes obtained in this study found significantly increased with increasing curing time as it is shown in Figure 6.11, Figure 6.12, Figure 6.13, Figure 6.14, Figure 6.15, Figure 6.16, Figure 6.17, Figure 6.18. (Kawasaki et. al. 1981; Uddin et. al. 1997)

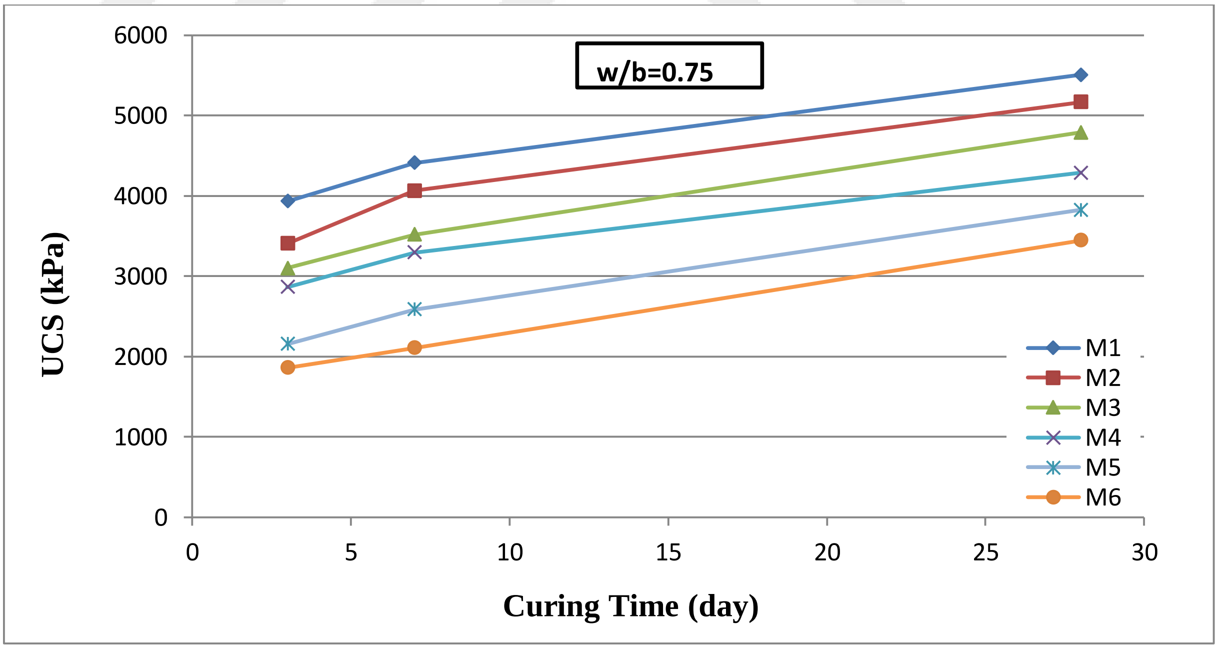

Figure 6. 11: UCS-curing time relations for WMP and w/b= 0.75

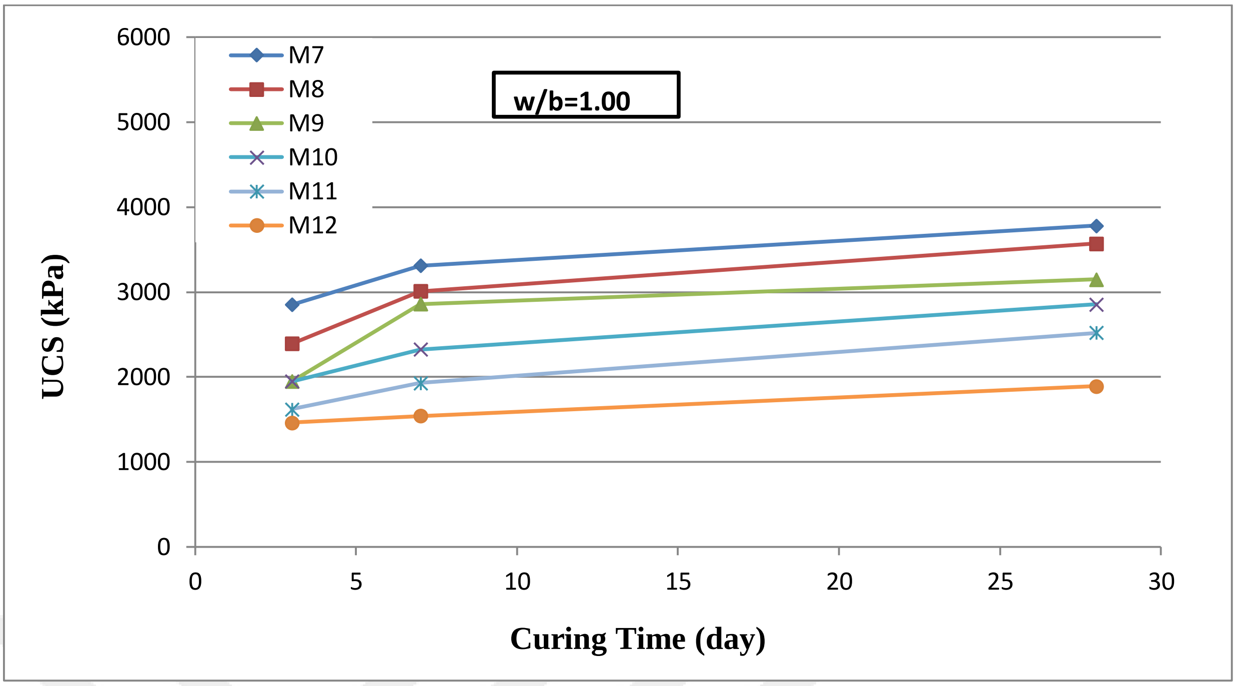

Figure 6. 12: UCS-curing time relations for WMP and w/b= 1.00

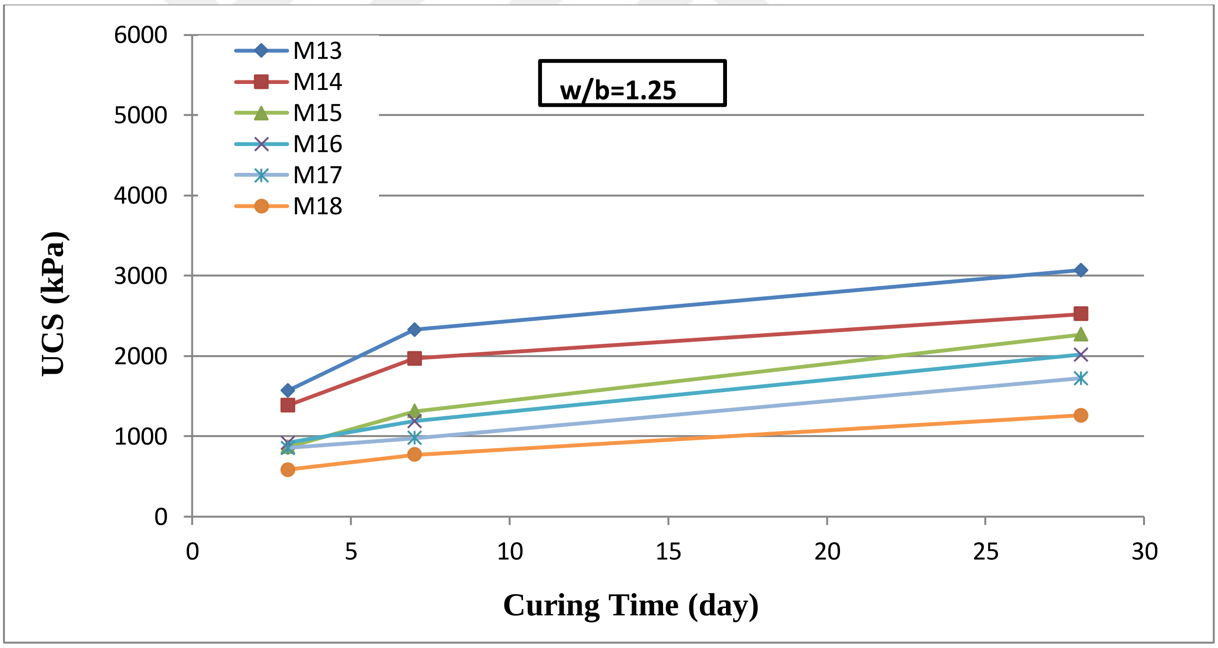

Figure 6. 13: UCS-curing time relations for WMP and w/b= 1.25

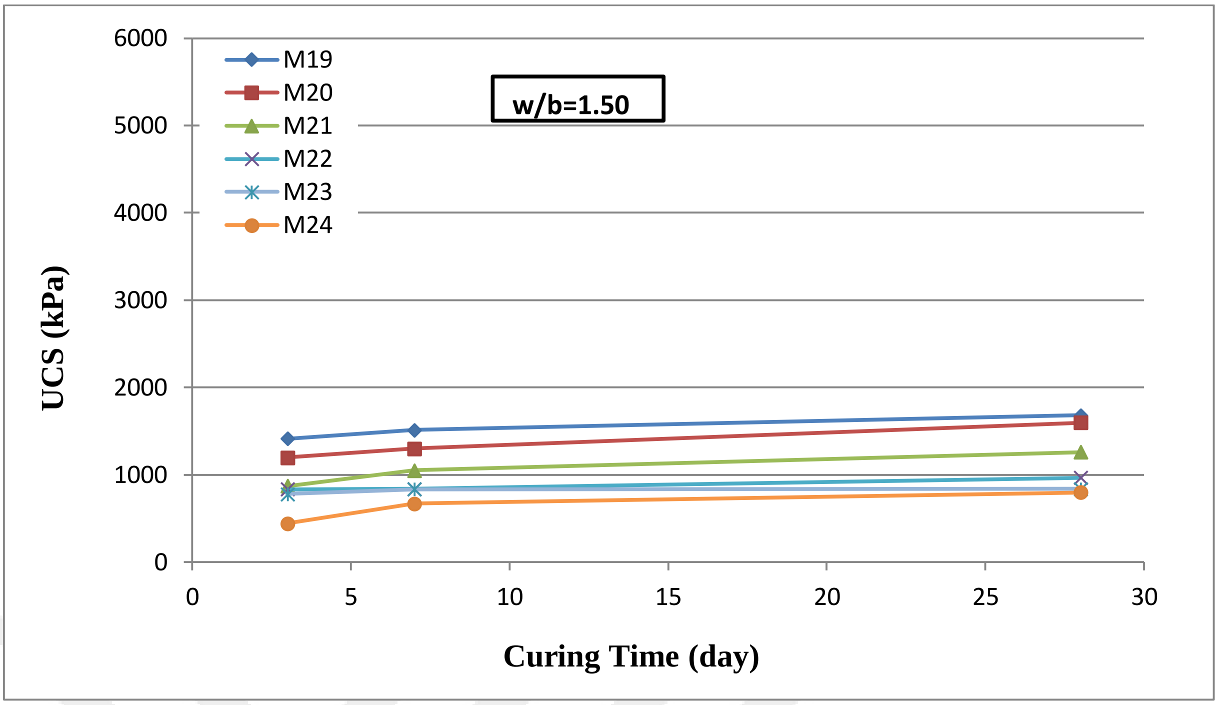

Figure 6. 14: UCS-curing time relations for WMP and w/b= 1.50

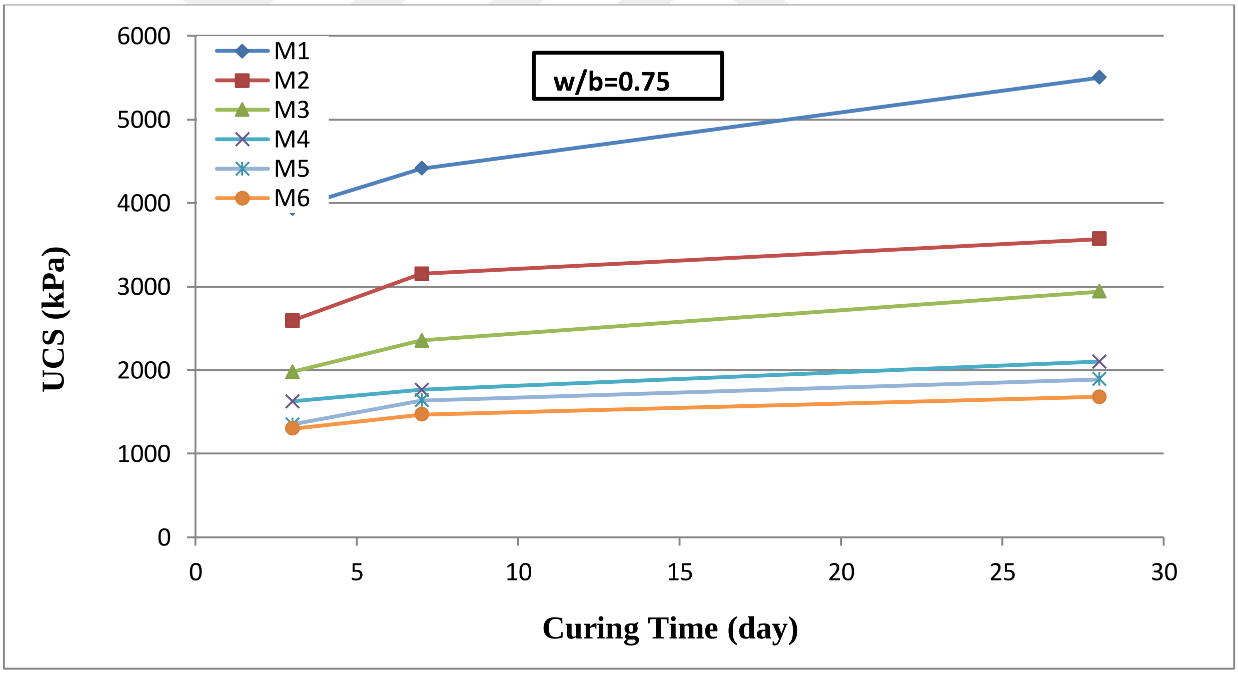

Figure 6. 15: UCS-curing time relations for WMP+FA(constant %25) and w/b= 0.75

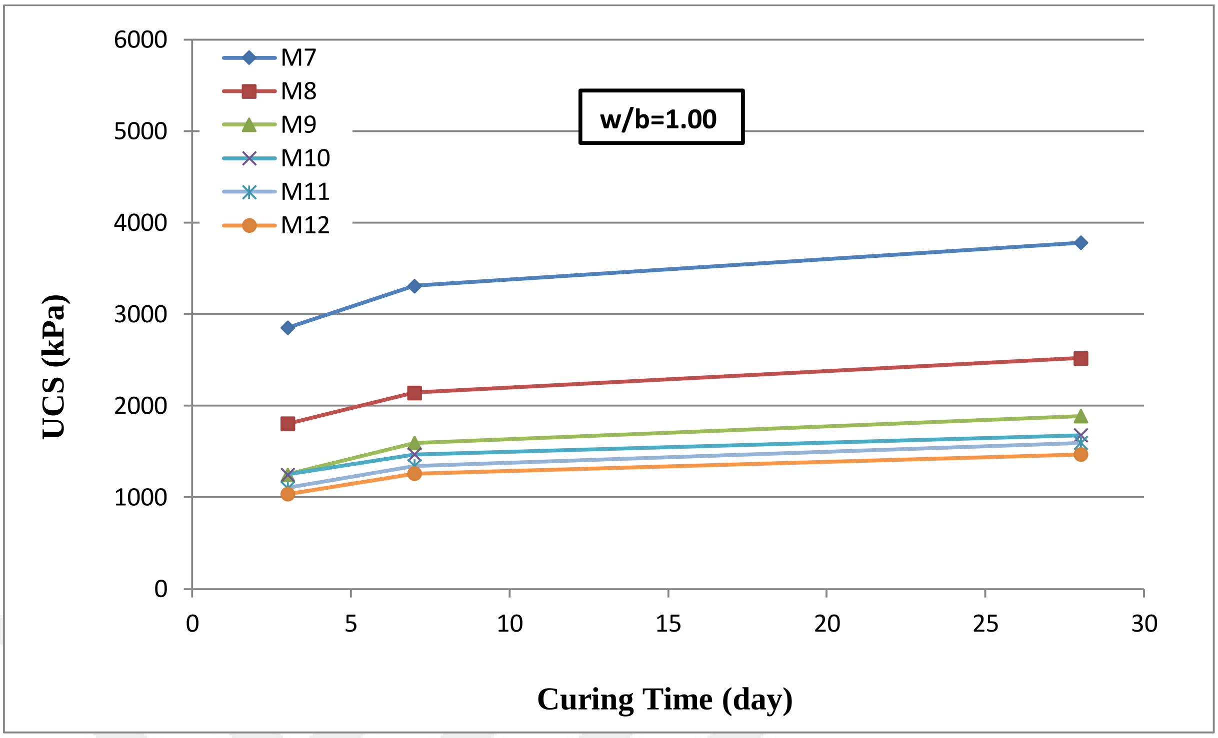

Figure 6. 16: UCS-curing time relations for WMP+FA(constant %25) and w/b= 1.00

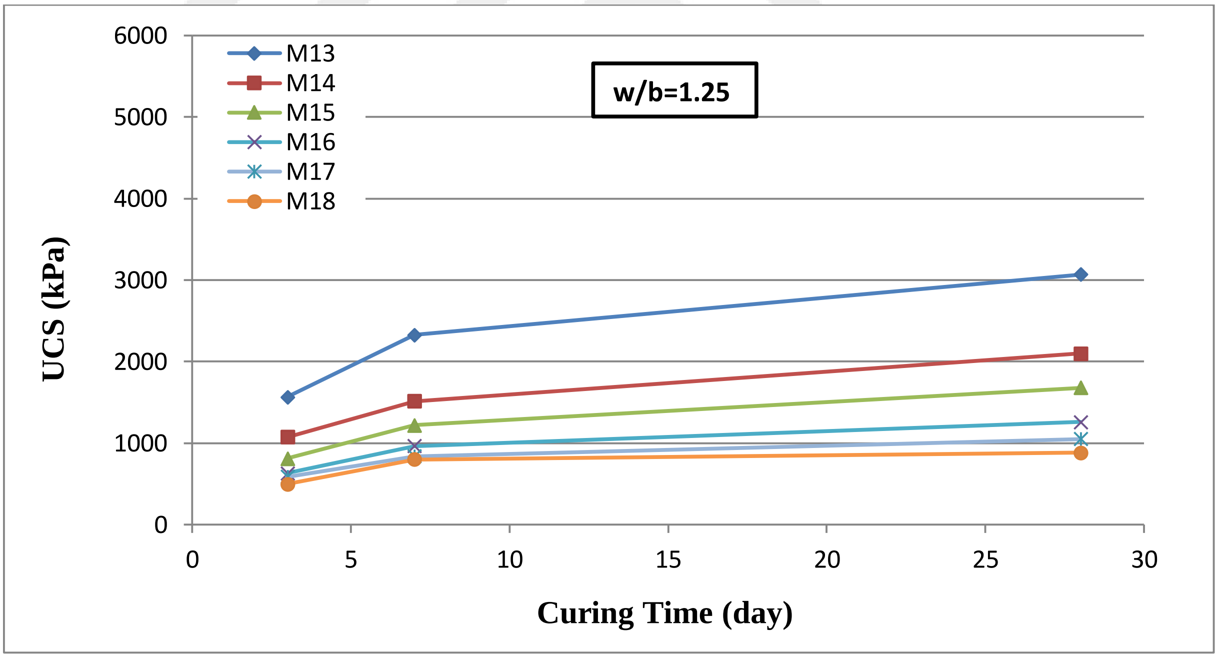

Figure 6. 17: UCS-curing time relations for WMP+FA(constant %25) and w/b= 1.25

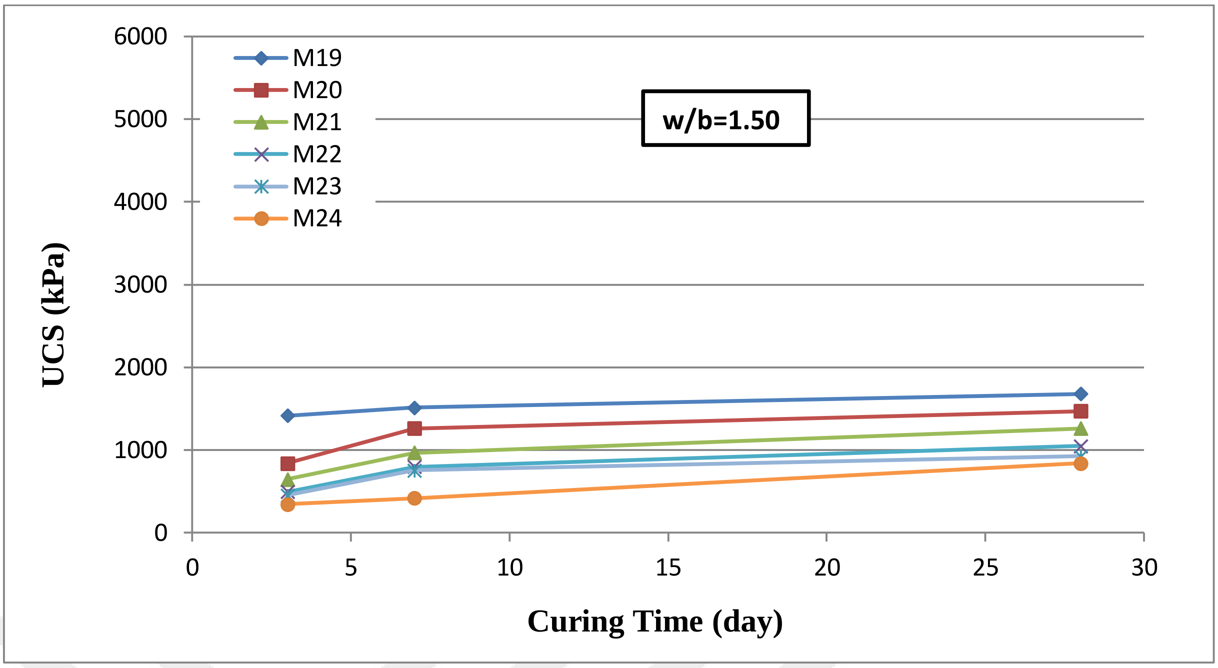

Figure 6. 18: UCS-curing time relations for WMP+FA(constant %25) and w/b= 1.50

The increment in the compressive strength of soilcreates is fast early in the curing time and then slows down over time (Porbaha et al., 2000). For all 28 day curing time ucs values of all soilcretes are greater than 1 Mpa (Figure 6.11, Figure 6.12, Figure 6.13, Figure 6.14, Figure 6.15, Figure 6.16, Figure 6.17, Figure 6.18). Due to the fact that 1 Mpa compressive strength values can be supposed as higher values for stabilizing the problematic soils in geotechnical practices (Hausmann, 1990), it is clearly seen that WMP and WMP+FA could be used as an additive for improvement of problematic clay soils.

As it is known that the compressive strength of a clay–cement mix usually increments because of enhancement the cement ingredient up to a certain percentage, however its strength starts to decrease after which (Uddin et al., 1997). Uni-axial compressive strength of the soilcretes is generally ranged from 10 to 50 times the UCS of the natural soils. The upper and lower limits of the strength enhancement were got for higher cement ingredients and/or non-adhering soils, also for lower cement ingredients and/or adhesive soils, respectively (Jaritngam and Swasdi, 2006). Figure 6.19, Figure 6.20, Figure 6.21, Figure 6.22, Figure 6.23, and Figure 6.24 demonstrates the similar behaviour with respect to increasing of cement content in soilcretes comparing with the literature mentioned above. Test results showed that cement content had an important influence because of increasing compressive strength of the mixs at all w/b ratios and curing time. The increasing ranges are same for all curing time and w/b ratios.

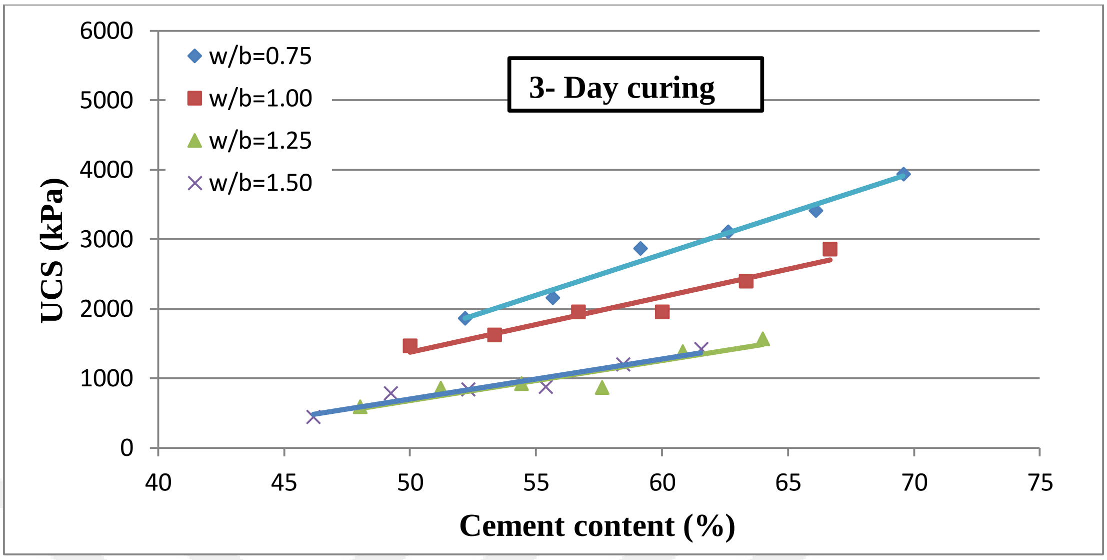

Figure 6. 19: UCS-cement content relations at all w/b ratios for 3 day curing (WMP)

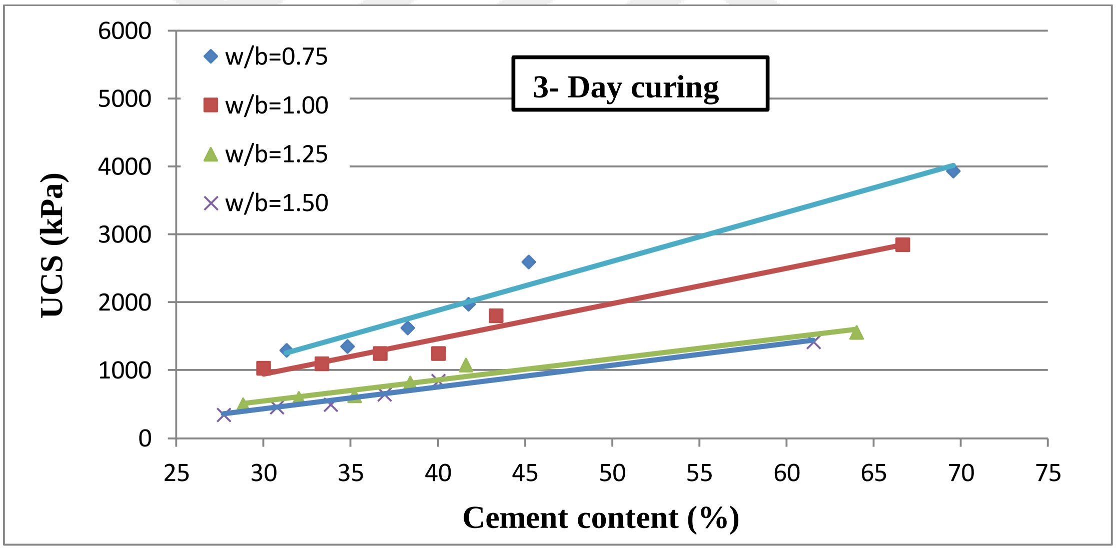

Figure 6. 20: UCS-cement content relations at all w/b ratios for 3 day curing (WMP + FA)

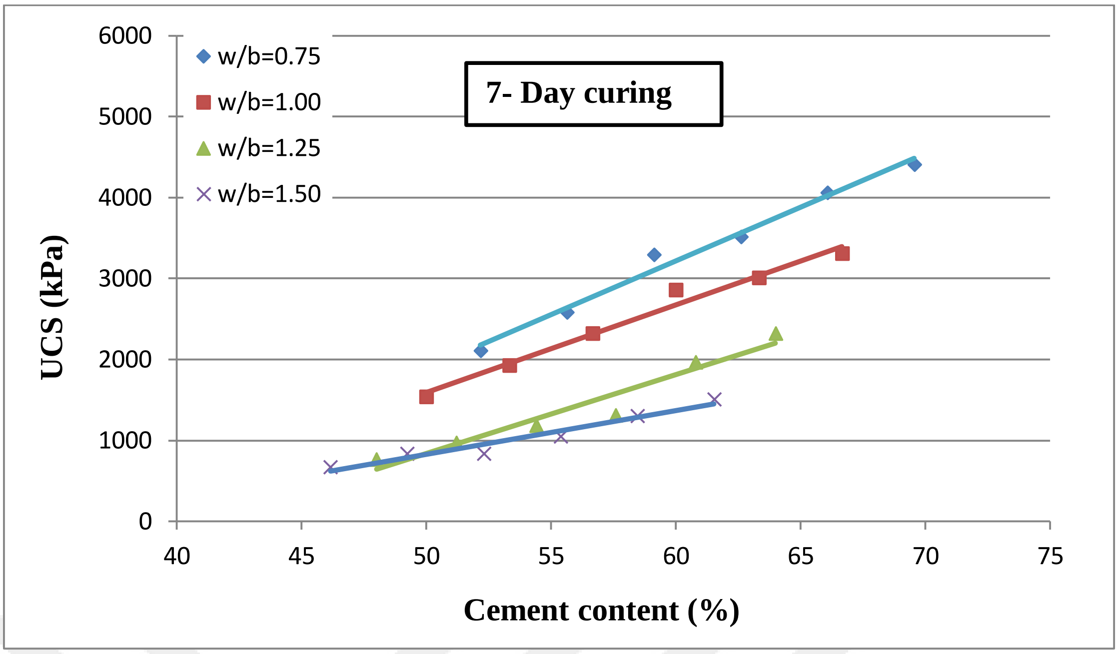

Figure 6. 21: UCS-cement content relations at all w/b ratios for 7 day curing (WMP)

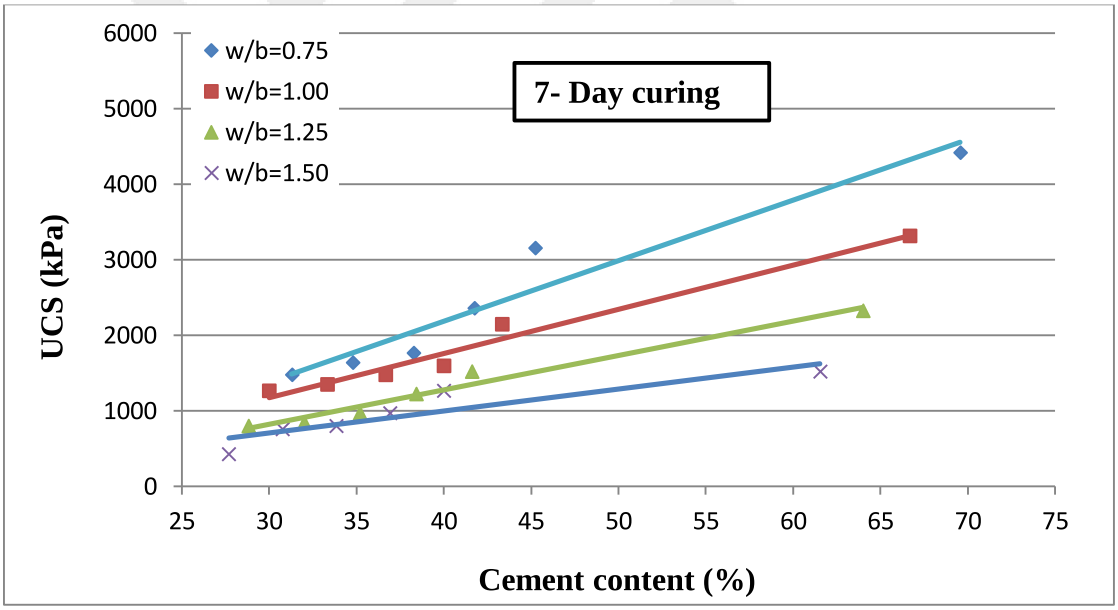

Figure 6. 22: UCS-cement content relations at all w/b ratios for 7 day curing (WMP + FA)

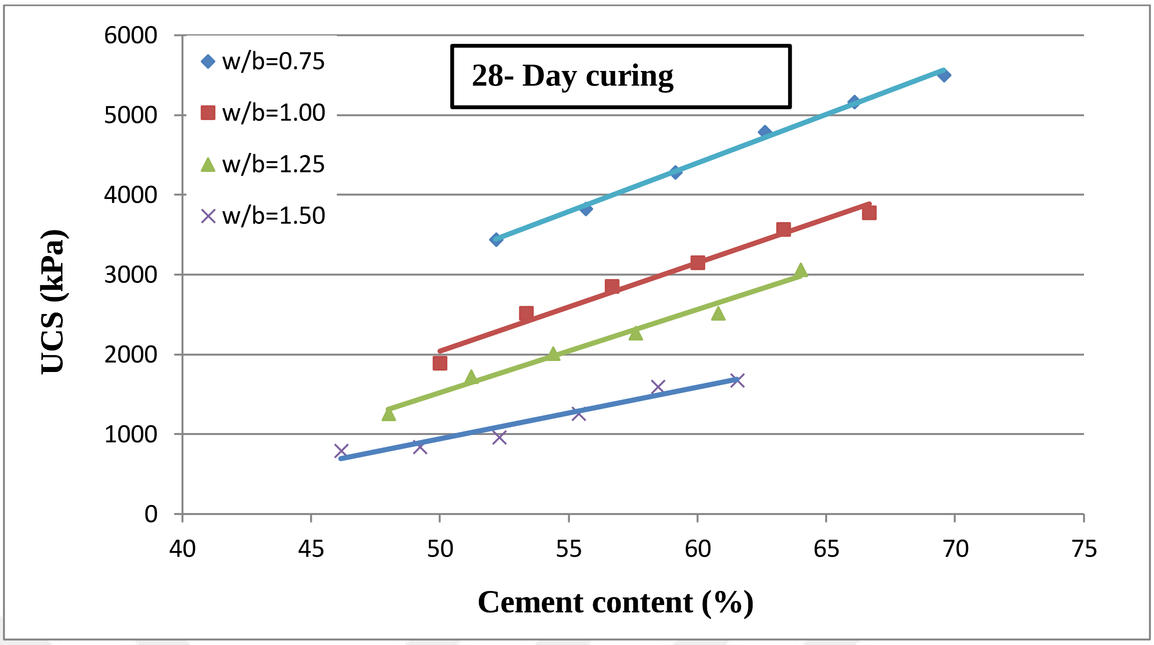

Figure 6. 23: UCS-cement content relations at all w/b ratios for 28 day curing (WMP)

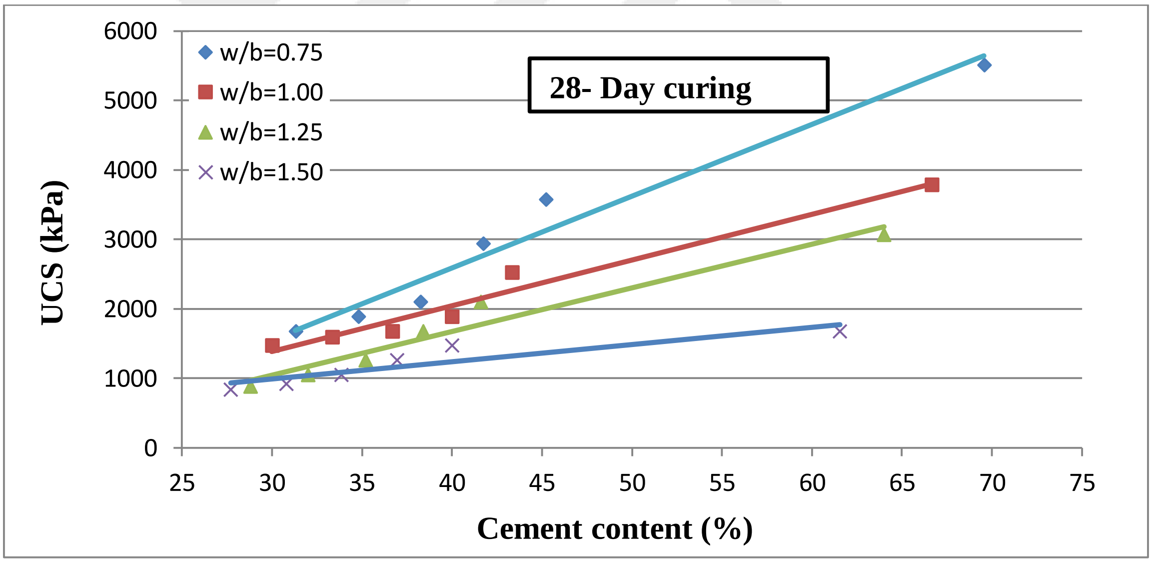

Figure 6. 24: UCS-cement content relations at all w/b ratios for 28 day curing (WMP + FA)

The water–binder ratio is supposed as an important parameter effecting the mechanical properties of cement–clay mixtures (Miura et al., 2001). UCS of clay–cement mixtures reduces remarkably because of increasing of the initial water amount of natural soil. The impact of the cementing agent, by which the strength of the clay–cement mixture is controlled, is generally affected by water– cement ratio (w/c). More cement amount is required by higher initial water content in order to attain any important impact during the stabilisation of the clay. As it is known in general that UCS importantly reduces with increasing w/c rate of a clay–cement mixture (Hassan, 2009; Miura et al., 2001). In Figure 6.25 w/c rates were given different from w/b ratio. Different w/c ratios were used in this study as it is show in Table 6.2. This behaviour can be clearly seen also from the results obtained in this study as shown in Figure 6.25. Therefore, increasing of w/c ratio from 0.75 to 2.00 and 0.72 to 3.35 decreased the UCS of the soilcretes samples at 28 day curing time.

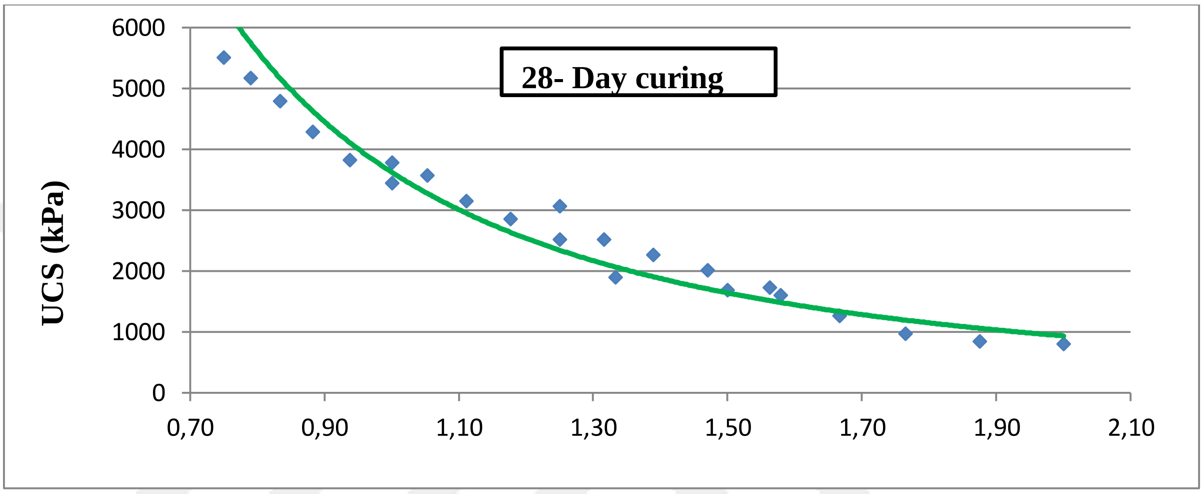

a.

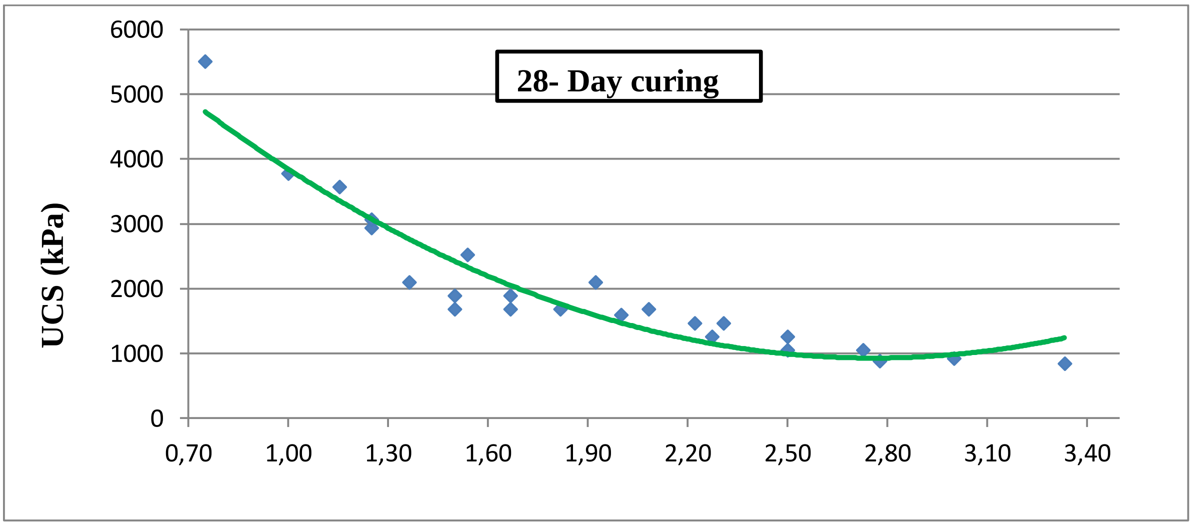

b.

Figure 6. 25: UCS-water/cement ratio relations for all mixtures at 28 day curing a. WMP b. WMP+FA

6.3.2. Elastic modulus results of the soilcretes

The elastic modulus results of all soilcrete samples at 3,7 and 28 days (a. WMP, b. WMP+FA at various water/binder rates; 0.75, 1.00, 1.25 and 1.50 respectively) are presented in Figure 6.26. All elastic modulus values of the soilcrete samples were obtained from the stress–strain curves of the specimens resulted from the UCS test.

For the low water/binder rate, the supplement of WMP and FA in the binder resulted in higher values for the modulus of elasticity than the reference samples. Elastic modulus changing range with respect to w/b ratio, curing time and WMP and FA amount is similar to UCS behaviour of the soilcretes sample. These soilcretes include much more amount of clay samples. This may cause more brittle behaviour. Figure 6.27 shows the all curing-day modulus of elasticity of the soilcretes in relation to the UCS. As it visible clearly, though there is some scatter around the optimal line, the impact of soil-binder ratio is less pronounced.

This is likely due to the impacts of w/b rate. As illustrates in Table 6.3, the E/qu ratios from soilcrete samples were lower than the suitable amount from the slurry clay–cement mixtures given by Lee et al. (2005). The E/qu ratio of soilcretes for all curing time and w/b ratio were also somewhat similar to values reported in deep cement mixing studies ranging from 130 to 500 (Asano et al., 1996; Futaki et al., 1996). As it is clearly seen Figure 6.27 that modulus of elasticity of the mixtures (Eo) exponentially increases with increase of UCS of samples protected in this study. There is a slightly correlation between UCS value of the mixtures and elastic modulus. The behavior and ranges of the mixtures are repetitive with literature. Also, E/qu values of all mixtures at 3,7 and 28 day curing time decreases with increasing of w/b ratio.

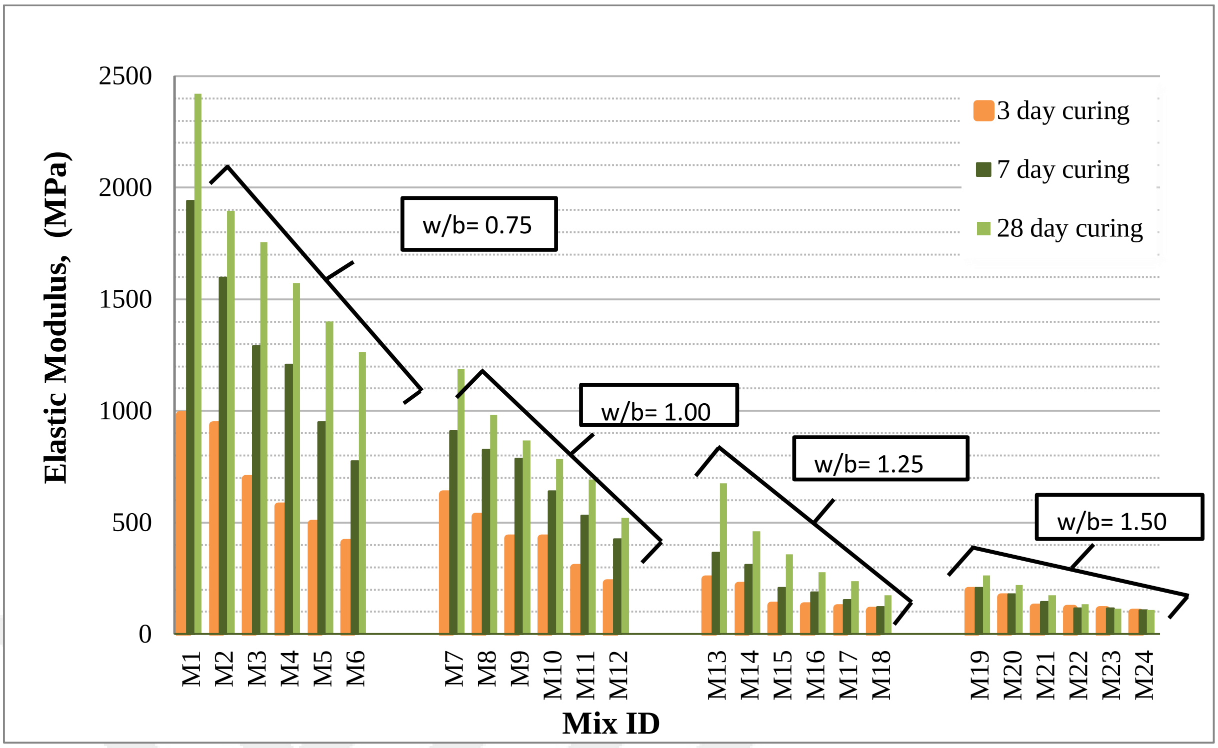

a.

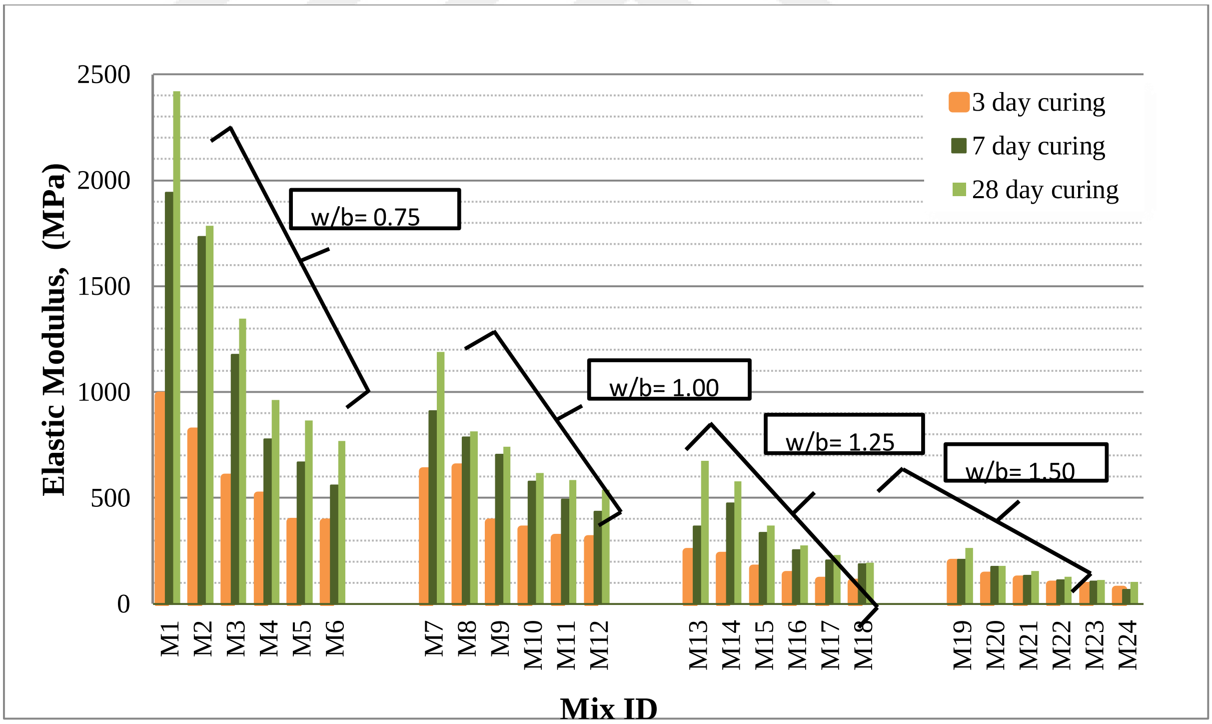

b.

Figure 6. 26: Elastic modulus results of all soilcrete samples at 3,7 and 28 days (a. WMP, b. WMP+FA at various water/binder rates; 0.75, 1.00, 1.25 and 1.50 respectively).

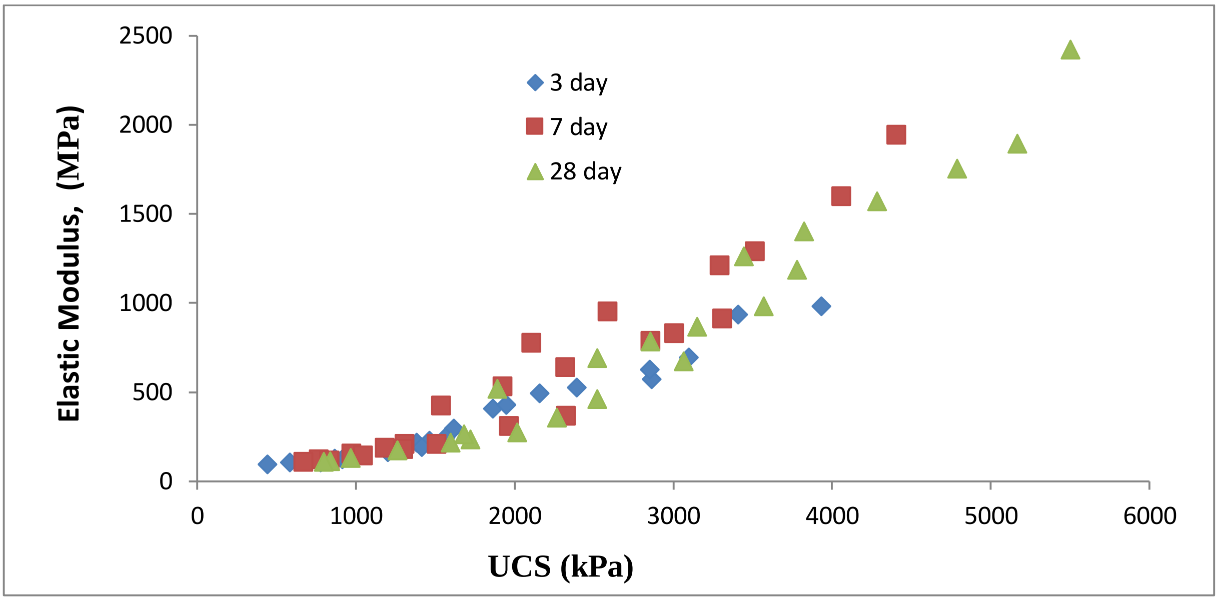

a.

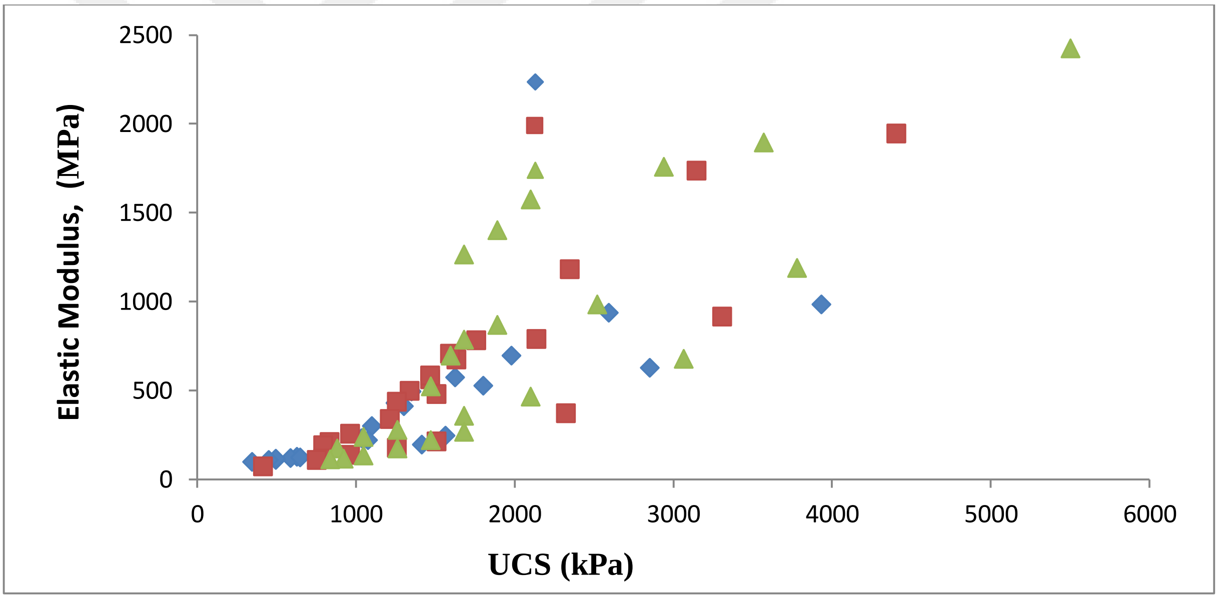

b.

Figure 6. 27: Correlations between UCS and elastic modulus of the soilcretes.
a.WMP b.WMP+FA

Table 6. 3: Summary of E0/qu ratios.

a. WMP

Condition of Soilcrete samples	Avarage E_0/q_u		
	3 day curing	7 day curing	28 day curing
at w/b=0.75	236	388	382
at w/b=1.00	208	275	283
at w/b=1.25	153	157	170
at w/b=1.50	144	140	142

b. WMP+FA

Condition of Soilcrete samples	Avarage E_0/q_u		
	3 day curing	7 day curing	28 day curing
at w/b=0.75	288	463	461
at w/b=1.00	282	351	347
at w/b=1.25	192	238	232
at w/b=1.50	164	139	130

6.3.3. Bleeding test results of the soilcretes

The bleeding test results of all mixtures at all w/b ratios and curing days was checked. According to the test results, the increment of water/binder rate increases the settlement of the mixtures. Moreover, bleeding value of the mixtures reduces incorporating with WMP for w/c = 1.25 and 1.5. Because of having a higher surface area of WMP and FA comparing to cement, WMP can absorb much more amount of water than amount of cement. Hence, increasing of WMP and FA amount in the mixtures led to decrease the settlement that was observed as soon as mixing procedure had been completed. The settlement of M23 mixture that was obtained after the bleeding test was completed is clearly seen in Figure 6.1(b).

Figure 6. 28: Failure criteria of the soilcretes samples for 28 day curing. (WMP)

Figure 6. 29: Failure criteria of the soilcretes samples for 28 day curing (WMP+FA)

6.3.4. Failure models after UCS tests for the soilcretes

Brittle crystalline materials contain initial damage, micro cracks, etc. and under compression (e.g. UCS), undergo a complex sequential process of crack closure, crack initiation, stable crack growth, and unsta- ble cracking and eventually fail (Bieniawski, 1989; Brace et al.,1966; Eberhardt et al., 1998; Jaeger et al., 2007; Lajtai and Lajtai, 1974; Li et al., 2003). Many works have been conducted to investigate the failure patterns in sort of cementitious materials under UCS test (Jaeger and Cook, 1979; Klein and Polivka, 1958; Santarelli and Brown, 1989). According to this study, test results are very closed to each other. Cementitious materials generally fail as axial splitting after UCS test is conducted. The failure modes of rock materials obtained from UCS test may maintain beneficial information such as safety and economic conditions for design of different engineering works. A total of 432 soilcretes samples were tested with UCS in this study. Different examples of failure were observed in soilstone samples (Figure 6.28, Figure 6.29). The test results showed that most specimens failed along foliations. In this study, similar failure modes observed in all types of soilcretes are shown as axial splitting. There are various failure behaviours for materials under compressive loads (i.e. shearing along a single plane, Y-shaped, along foliation, multiple fracturing, double shear, and axial splitting). Due to the fact that the soilcretes that were produced from cementitious materials generally are broken as axial splitting type after axial loading (Basu et al., 2013) any effect, which was derived from increasing of w/b ratio and curing time, on the failure models of the soilcrete samples could not be observed clearly (see Figure 6.28, Figure 6. 29).

6.4. Conclusion

Several findings that have been concluded from this study were given as following; The UCS test results of the mixtures prepared for this study were observed at the range of 400 kPa and 5.5 Mpa. These results are seen very similar to the results that were obtained from the past studies. And also, as it is clearly seen from the test results, the UCS values of the samples for 28 day curing are higher than 1 Mpa except 1.5 w/b ratio. As it is known that 1 MPa compressive strength value for soils is accepted as higher value and these types of soils are known as very stiff soils. Therefore, this study shows that WMP and FA could be used as mineral additives in grouting applications for improvement of very soft soils. On the other hand, the E/qu ratio obtained from soilcrete mixtures was less than the corresponding value from slurry clay–cement mixtures. The E/qu ratio of soilcretes for all curing time and w/b ratio were also somewhat similar to noticed rates in deep cement mixing experiments ranging from 150 to 500. The settlement of the mixtures increased with an increase amount of w/b ratio; however, these bleeding values decreased with an increase of WMP and FA amount. Thus, all bleeding test results are lower than the level of .5%. This means that the stability of all mixtures prepared for this study seems to be in acceptable range. Most of the mixtures prepared for this study failed along foliations. This is the expected behaviour for these types of materials. In this study, similar failure modes observed in all types of soilcretes are indicated as axial splitting.

CHAPTER 7

CONCLUSIONS AND RECOMMENDATIONS

7.1. Conclusion

The results have inferred from this study was given as following;

- The rheological properties of the CBGs importantly have been improved by the addition of WMP to grout mix at various w/b ratios. Strongly shear thickening attitude was got from the CBG mixture the all w/b ratios and all WMP content.
- The increment in the percentage of WMP in the CBG mixture incremented the plastic viscosity at all w/b proportion. Moreover, the increase in w/b rate reduced the viscosity of the CBG for all WMP content.
- The increment in the percentage of WMP in the grout mixture reduced the mini-slump flow diameter. In a constant the percentage of WMP, the increment in water-binder rate incremented the mini-slump flow diameter because of the impact of water. Moreover, the MCFT reduced with an increase in water - binder ratio for a constant waste marble powder content. The workability and flowability of the CBG importantly changed with the increase in the water-binder rate in CBG containing WMP.
- The rheological characteristics (the plastic viscosity and the yield stress) of the CBG got from the modified Bingham model also illustrates a good correlation with the MCFT and mini-slump flow of the grout (R^2 = 0.83, R^2=0.84). On the other hand, no correlation was found between yield stress and Lombardi PCM test.
- The rheological properties of the CBGs importantly have been improved by the addition of WMP+ FA all percentage of to grout mix at all water/binder rates. Strongly shear thickening attitude was got from the CBG mixture all mix WMP+ FA contents
- The increment in the percentage of WMP in the CBG mixture incremented the plastic viscosity.

- According to the control sample, the increment in the percentage of WMP (10-25%) amount increased the mini-slump flow diameter for constant FA (25%) content.
- Especially, FA increased the fluidity of CBG, when the WMP showed negative effect in increase the MCFT in WMP+FA content.
- The rheological properties (the plastic viscosity and the yield stress) of the CBG got from the modified Bingham model also illustrates a good correlation with the MCFT and mini-slump flow of the CBG (R^2= 0.82, R^2= 0.86). On the other hand, no correlation was found between yield stress and Lombardi PCM test.
- The UCS test results of the mixtures prepared for this study were observed at the range of 400 kPa and 5.5 Mpa. These results are seen very similar to the results that were obtained from the past studies.
- As it can be concluded from the study, for the lower water/binder rate, the addition of WMP in the binder resulted in higher values in comparison to the higher water/binder rates. When w/b ratio increases, the UCS of the soilcretes gradually decreases. As expected, the higher w/b ratio is the higher is the reduction for the calculated average compressive strength of soilcrete samples at all curing days.
- The supplement of WMP in the binder ensued in lower values for the found average compressive strength of soilcrete specimens at all curing times, in comparison to the reference specimens (M1, M7, M13, M19)
- With an increasing amount of WMP and WMP+FA in soilcrete samples at all curing soilcretes decrease at all curing days and w/b raions. This consistent pattern for all the composites has been explained as being a result of the low rate of pozzolanic reaction at those early ages.
- The maximum UCS value in soilcrete samples was observed as 6 Mpa when constitution of WMP was 0% at w/b 0.75 and 28 day curing. Moreover the minimum UCS of the samples was determined as 400 kPa for WMP, 250 kPa for WMP+FA.
- The compressive strength of soilcretes obtained in this study have been found to increase significantly with increasing curing time. The increase in the compressive strength of soilcretes is rapid early in curing period and then slows down over time.

- It is clearly seen from the test results, the UCS values of the samples for 28 day curing are higher than 1 Mpa except 1.5 w/b ratio. As it is known that 1 MPa compressive strength value for soils is accepted as higher value and these types of soils are known as very stiff soils. Therefore, this study shows that WMP and FA could be used as mineral additives in grouting applications for improvement of very soft soils.
- Test results showed that cement content had an important influence because of increasing compressive strenght of the mixtures at all w/b ratios and curing time. The incresing ranges are sam efor all curing time and w/b ratios.
- According to this thesis, increase of w/c ratio of the grout mixtures dramaticaly reduced the compressive strength of the mixtures same as the literature mentioned before chapters.
- While w/c ratio was incresing from 0.7 to 3.3, UCS of soilcretes samples at curing 28 day exponenetialy decreased and at high w/c ratios reduction range in ucs started to change slightly. This means that high w/c ratios have very little effect on compressive strength of grout mixtures.
- On the other hand, the E/qu ratio obtained from soilcrete mixtures was less than the corresponding value from slurry clay–cement mixes. The E/qu ratio of soilcretes for all curing time and w/b ratio were also somewhat similar to reported values in deep cement mixing studies, which ranged from 150 to 500.
- Modulus of elasticity of the mixtures exponentially increases with increase of unconfined compressive strength of samples prodected in this study. There is directly relation between unconfined compressive strength value of the mixtures and elastic modulus.
- The settlement of the mixtures increased with an increase amount of w/b ratio; however these bleeding values decreased with an increase of WMP and FA amount. Thus, all bleeding test results are lower than the level of .5%. This means that the stability of all mixtures prepared for this study seems to be in acceptable range.
- Most of the mixtures prepared for this study failed along foliations. This is the expected behaviour for these types of materials. The similar failure modes observed in all soilcretes types in this study are shown as axial splitting.

- According to fresh and hardened properties test results; Waste Marble Powder can be suitable for use in substitution cement in proportions up to 15% for w/b ratios below 1.25. Also, Waste Marble Powder and Fly Ash can be suitable for use in substitution cement in proportions up to 20% and %25 for w/b ratios below 1.25. For this reason, CO_2 emissions and cost decreased by this total rate.

7.2. Recommendations

The thesis work results demonstrate that WMP using as a filler additive and FA using as a pozzolanic additive for modifying the cementitious grout is an significant work. This experimental study can be enlarged depending on application field study. In any geotechnical work real permation or jet grout columns can be produced with the cement based grouts incorporating with WMP and FA at various w/b ratios. And then, the soilcretes samples can be taken from the permetion or jet grout columns. Also, mechanical characters of soilcretes can be examined comparing with laboratory test conducted. Moreover, the rheological characters (especially viscosity and workability) of the grout mixtures incorporated with WMP and FA at various w/b ratios can be observed and comparing with experimental results.

REFERENCE

Aitcin, P.C., Ballivy, G., Parizeau, R. (1984). The use of condensed silica fume in grouts: Innovative cement grouting, SP-83. *American Concrete Institute,* **83**, 1–18.

Aliabdo, A. A., Elmoaty, A. E. M. A. E., Auda, E. M. (2014). Re-use of waste marble dust in the production of cement and concrete. *Construction and Building Materials*, **50**, 28e41.

Alyamac, K. E., Ghafari, E., Ince, R. (2017). Development of eco-efficient self-compacting concrete with waste marble powder using the response surface method. *Journal of Cleaner Production*, **144**, 192-202.

Alyamac, K. E., Ince, R. A. (2009). Preliminary concrete mix design for SCC with marble powders. *Construction and Building Materials*, **23**, 1201–10.

Alyousef, R., Benjeddou, O., Khadimallah, M. A., Mohamed, A. M., Soussi, C. (2018). Study of the effects of marble powder amount on the self-compacting concretes properties by microstructure analysis on cement-marble powder pastes. *Advances in Civil Engineering*, **2018**, Article ID 6018613.

Alyousef, R., Khadimallah, M. A., Soussi, C., Benjeddou, O., Jedidi, M. (2018). Experimental and theoretical study of a new technique for mixing self-compacting concrete with marble sludge grout. *Advances in Civil Engineering*, **2018**, Article ID 3283451.

American Concrete Institute. 1984. Innovative Cement Grouting. Publications SP-83. Collection of papers presented at 1983 Fall Conv. Kansas City, Mo.

Andromalos, K. B., Gazaway, H. N. (1989). Jet grouting to construct a soilcrete wall using a twin stem system. *ASCE, Geotechnical and Construction Divisions Special Conference*, 25–29.

Arshad, A., Shahid, I., Anwar, U.H.C., Baig, M.N., Khan, S., Shakir, K. (2014). The wastes utility in concrete. *International Journal Environmental*, **8,** 1323–1328.

ASCE. American Society of Civil Engineers. 1982. Grouting in Geotechnical Engineering. p. 1017. New Orleans.

ASCE. American Society of Civil Engineers. 1985. Issues in Dam Grouting. p. 165. Denver.

ASCE. American Society of Civil Engineers. 1992. Grouting, Soil Improvement and Geosynthetics. p. 1451. New Orleans.

ASCE. American Society of Civil Engineers. 2003. Proceedings of the Third International Conference on Grouting and Ground Treatment. New Orleans, Louisiana. Geotechnical Special Publication No. 120.

Asano, J., Ban, K., Azuma, K., Takahashi, K. (1996). Deep mixing method of soil stabilization using coal ash. *Grouting and deep mixing. Proceedings IS Tokyo '96, second international conference on ground improvement geosystems*, pp. 393–398, Tokyo.

Ashish, D. K. (2018). Feasibility of waste marble powder in concrete as partial substitution of cement and sand amalgam for sustainable growth. *Journal of Build Engineering*, **15**, 236e242.

Ashish, D. K. (2019). Concrete made with waste marble powder and supplementary cementitious material for sustainable development. *Journal of Cleaner Production*, **211**, 716–729.

Asteris, P. G., Kolovos, K. G., Athanasopoulou, A., Plevris, V., Konstantakatos, G. (2017). Investigation of the mechanical behaviour of metakaolin-based sandcrete mixtures. *Euroean Journal of Environmental and Civil Engineering*.

ASTM C15/C150M-15. (2015). Standard specification for portland cement.

ASTM D4318-05. (2005). Standard test method for liquid limit, plastic limit, and plasticity index of soils.

ASTM D4546-08. (2008). Standard test methods for one-dimensional swell or collapse of cohesive soils.

ASTM D5102-09b. (2009). Standard test method for unconfined compressive strength of compacted soil–lime mixtures.

ASTM D698-12. (2012). Standard test methods for laboratory compaction characteristics of soil using standard effort.

ASTM D2166-13. (2013). Unconfined compressive strength of cohesive soil.

Axelsson, M., Gustafson, G. (2006). A robust method to determine the shear strength of cement-based injection grouts in the field. *Tunnelling and Underground Space Technology*, **21**, 499–503.

Baker, W. H. (1985). Embankment foundation densification by compaction grouting, proceedings, ıssues in dam grouting. *American Society of Civil Engineers*, p. 104-122.
New York.

Baker, W.H., Cording, E.J., MacPherson, H.H. (1983). Compaction grouting to control ground movements during tunnelling. *Underground Space*, **7**, 205-212.

Baltazar, L.G., Henriques, F.M.A., Jorne, F. (2012). Optimisation of flow behaviour and stability of superplasticized fresh hydraulic lime grouts through design of experiments. *Construction and Building Materials*, **35**, 838–845.

Banfill, P. (2006). Rheology of fresh cement and concrete. *Rheology Reviews*, 31–130.

Banfill, P. (2003). The rheology of fresh cement and concrete a review. *Proceeding of 11th International Cement Chemistry Congress*, Durban.

Bandimere, S. W. 1997. Compaction grout mechanism state of the practice grouting: compaction, remediation and testing. Geotechnical Special Publication No. 66, Edt. C. Vipulanandan, Proceedings of the ASCE Geo-Logan 97 Conference, ASCE, New York, pp. 18- 31

Barnes, H., (1995). A review of the slip (wall depletion) of polymer solutions, emulsions and particle suspensions in viscometers: its cause, character and cure. *Journal of Non-Newtonian Fluid Mechanics,* **56**, 221–231.

Barnes, H. (1997). Thixotropy–a review. *Journal of Non-Newtonian Fluid Mechanics,* **70**, 1–33.

Barnes, H. (1999). The yield stress–a review or 'panta roi'–everything flows. *Journal of Non-Newtonian Fluid Mechanics,* **81**, 133–178.

Bartos, P., Sonebi, M., Tamimi, A. Workability and rheology of fresh concrete: compendium of tests. Report of RILEM Technical Committee TC145 WSM, p. 86.

Basu, A., Mishra, D. A., Roychowdhury, K. (2013). Rock failure modes under uniaxial compression, Brazilian, and point load tests. *Bulletin of Engineering Geology and the Environment,* **72**, 457–475.

Belaidi, A. S. E., Azzouz, L., Kadri, E., Kenai, S. (2012). Effect of natural pozzolana and marble powder on the properties of self-compacting concrete. *Construction and Building Materials,* **31**, 251e257.

Benhamou, O. (1994). Comportement rhe´ologique des coulis de liants hydrauliquesultrafins destine´s a` l'injection. The`se pre´sente´e au Centre deGe´ologie de l'Inge´nieur de l'Ecole *Nationale supe´rieure des mines deParis*, Paris, 318 pp

Bieniawski, Z.T. (1989). Engineering rock mass classifications. New York, NY: Wiley.

Brace, W. F., Paulding, B. W., & Scholz, C. H. (1966). Dilatancy in the fracture of crystalline rocks. Journal of Geophysical Research, 71, 3939–3953.

Burgin, C. R. (1979). Investigation of the Physical Properties of Cement-Bentonite Grouts for Improvement of Dam Foundations. *Injection des Sols*. Eyrolles, Paris, 567.

Bustamante, M., & Gouvenot, D. (1983). Grouting: A method improving the bearing capacity of deep foundation. *Eight international conference on soil mechanics and foundations,* 264–278.

Caron, C. (1963). The Development of Grouts for the Injection of Fine Sands, Grouts and Drilling Muds in Engineering Practice, Butterworth, London.

Celik, F., Canakcı, H. (2015). An investigation of rheological properties of cement based grout mixed with rice husk ash (RHA). *Construction and Building Materials,* **91**, 187–194.

Cevik, A., Alzeebaree, R., Humur, G., Nis, A., Gülsan, M. E. (2018). Effect of nano-silica on the chemical durability and mechanical performance of fly ash based geopolymer concrete. *Ceramics Internatioanal*, **44**, 12253-12264.

Chao-Lung, H., Anh-Tuan, B. L., Chun-Tsun, C. (2011). Effect of rice husk ash on the strength and durability characteristics of concrete. *Construction and Building Materials*, **25**, 3768–3772.

Clarke, W. J., Royal, M. D., Helal, M. (1992). Ultrafine cement tests and dam test grouting. *Proceedings of the conference on grouting, soil improvement and geosynthetics*, 626–638, New Orleans, LA, New York, NY: ASCE.

Consoli, N.C., Rosa, D.A., Cruz, R. C., Rosa, A.D. (2011). Water content, porosity and cement content as parameters controlling strength of artificially cemented silty soil. *Engineering Geology*, **122**, 328–333.

Corinaldesi, V., Moriconi, G., Naik, T. R. (2010). Characterization of marble powder for its use in mortar and concrete. *Construction and Building Materials*, **24**, 113e117.

Coulter, S., Martin, C. D. (2006). Single fluid jet-grout strength and deformation properties. *Tunnelling and Underground Space Technology*, **21**, 690–695.

Coussot, P., Nguyen, Q. D., Huynh, H. T., Bonn, D. (2002). Avalanche behavior in yield stress fluids. *Physical review letters*, **88**, 175501.

Coussot, P., Nguyen, Q. D., Huynh, H. T., Bonn, D. (2002). Viscosity bifurcation in thixotropic, yielding fluids. *Journal of Rheology*, **46**, 573–589.

Çınar, M., Çelik, F., Çanakcı, H., Nassani, D. E. (2017). Fresh Properties of Cementitious Grout with Rice Husk Powder. *Arabian Journal for Science and Engineering*, **42**, 3819.

Danot, C., N. Derache. (2007). Grout injection in the laboratory. *International Symposium on Earth Reinforcement*, IS Kyushu.

Deere, D.U. (1982). Cement-Bentonite Grouting for Dam. *Proceeding of Conference on Grouting in Geotechnical Engineering*, New Orleans, Louisiana, pp. 279-300.

De Larrard, F., Ferraris, C. F., Sedran, T. (1998). Fresh concrete: a Herschel-Bulkley material. *Materials and Structures*, **31**, 494–498.

De Paoli, B., Bosco, B., Granata, R., Bruce, D. A. (1992). Fundamental observations on cement based grouts Traditional materials. *Proceedimgs of conference on grouting in geotechnical engineering* , 474–485. New Orleans, LA, New York, NY: ASCE

Domone, P. (2006). Mortar tests for self-consolidating concrete. Concrete Internatinal, 28(4), 39–45.

Eberhardt, E., Stead, D., Stimpson, B., & Read, R. S. (1998). Identifying crack initiation and propagation thresholds in brittle rock. *Canadian Geotechnical Journal*, **35**, 222–233.

Elyamany, H. E., Elmoaty, A., Elmoaty, M., Basma, A. M. (2014). Effect of filler types on physical, mechanical and microstructure of self compacting concrete and flow-able concrete. *Alexandria Engineering Journal,* **3**, 295e307.

Erdogan, T. Y. (2007). Beton. 2. Baskı. Ankara: Metu Press.

Ergun, A. (2011). Effects of the usage of diatomite and waste marble dust as partial replacement of cement on the mechanical properties of concrete. *Construction and Building Materials*, **25**, 806e812.

Ferraris, C. F., Obla, K. H., Hill, R. (2001). The influence of mineral admixtures on the rheology of cement paste and concrete. *Cement and Concrete Research*, **31**, 245–55.

Futaki, M., Nakano, K., Hagino, Y. (1996). Design Strength of Soil-Cement Columns as Foundation Ground for Structures. *Grouting and deep mixing. Proceedings of IS Tokyo '96, 2nd internatinal conference on ground improvement geosystems*, pp. 481–484. Tokyo.

Gelderloos, H.C., Bornhäuser, M. S., Brons, K. F. (1969). Het heffen van een verzakte caisson van de IJtunnel. *Bouw en Waterbouwkunde,* **15**, pp. 181-188.

Gencel, O., Ozel, C., Koksal, F., Erdogmus, E., Martínez-Barrerae, G., Brostow, W., (2012). Properties of concrete paving blocks made with waste marble. *Journal of Cleaner Production*, **21**, 62e70.

Gesoglu, M., Guneyisi, E., Kocabag, M. E., Bayram, V., Mermerdas, K. (2012). Fresh and hardened characteristics of self compacting concretes made with combined use of marble powder, limestone filler, and fly ash. *Construction and Building Materials*, **37**, 160e170.

Gettu, R., Gomes, P. C. C., Agullo, L., Josa, A. (2000). High-strength self-compacting concrete with fly ash: Development and utilization. In Malhotra, V. M., editor. *Proceedings of fifth CANMET/ACI international conference on recent advances in concrete technology* 507–522, Singapore.

Glossop, R., (1960). The invention and development of injection processes, *Geotechnique, London*, **10**, pp. 91-101.

Graf, E.D., (1969). Compaction grouting technique. *Journal of the Soil Mechanics and Foundations Division American Society of Civil Engineers*, **95**.

Gupta, P., Gupta, P., Srivastava, A., Gupta, R. (2008). Low cost concrete using marble slurry as cement replacement. *Proceedings of 5th International Engineering & Construction Conference, ASCE*, pp. 375–383.

Güllü, H., Cevik, A., Al-Ezzim, K. M. A., Gülsan, M. E. (2019). On the rheology of using geopolymer for grouting: A comparative study with cement-based grout included fly ash and cold bonded fly ash. *Construction and Building Materials*, **196**, 594-610.

Habeeb, G.A., Fayyadh, M.M. (2009). Rice husk ash concrete: The effect of RHA average particle size on mechanical properties and drying shrinkage. *Australian Journal of Basic and Applied Sciences*, **3**, 1616–1622.

Håkansson, U., Hässler, L., Stille, H. (1992). Rheological properties of microfine cement grouts. *Tunnelling and Underground Space Technology*, **7**, 453–458.

Håkansson, U. (1993). Rheology of fresh cement based grouts- PhD Thesis, Stockholm: *KTH Royal Institute of Technology*, Stockholm.

Håkansson, U., Rahman, M. (2009). Rheological properties of cement based grouts using the UVP-PD method. *Proceeding of Nordic Symposium of Rock Grouting*, Helsinki.

Hartnett, J. P., Hu, R. Y. Z. (1989). Technical note: The yield stres an engineering reality. *Journal of Rheology*, **33**, 671–679.

Hashmi, M., Ali, Hashmi, P. S. M. (2014). An experimental investigation on strengths characteristics of concrete with the partial replacement of cement by marble powder dust and sand by stone dust. *International Journal Of Engineering & Applied Sciences*, **4**, 203–209.

Hassan, M. (2009). Engineering characteristics of cement stabilized soft Finnish clays:a laboratory study (Licentiate's thesis). Helsinki University of Technology, Helsinki.

Hebhoub, H., Aoun, H., Belachia, M., Houari, H., Ghorbel, E. (2011). Use of waste marble aggregates in concrete. *Construction and Building Materials*, **25**, 1167–1171.

Helal, M., and Krizek R. J. (1992). Preferred Orientation of Pore Structure in Cement-Grouted Sand. Proceeding of Grouting. *Soil improvement and Geosynthetics*, **1**, 526-539.

Ichise, Y., Yamakado, A. (1974). High Pressure Jet Grouting Method, US Patent **3**,802-203.

Jaeger, J. C., Cook, N. G. W. (1979). Fundamentals of rock mechanics (3rd ed.). London: Chapman & Hall.

Jaeger, J. C., Cook, N. G. W., Zimmerman, R. W. (2007). Fundamentals of rock mechanics (4th ed.). Oxford: Blackwell.

James, A. E., Williams, D. J. A., Williams, P. R. (1987). Direct measurement of static yield properties of cohesive suspensions. *Rheologica acta*, **26**, 437–446.

Jaritngam, S., Swasdi, S. (2006). Improvement for soft soil by soilcement mixing. Proceedings of the Fourth international conference on soft soil engineering, 637–640, Vancouver, Canada.

Jiménez, V., León-Martínez, F., Montes-García, P., Gaona-Tiburcio, C., Chacon-Nava, J. (2013). Influence of sugar-cane bagasse ash and fly ash on the rheological behavior of cement pastes and mortars. *Construction and Building Materials*, **40**, 691-70.

Kamal, H., ElHawary, M., Abdul, J. A., AbdulSalam, S., Taha, M. (2011). Development of cement grout mixes for treatment of underground cavities in Kuwait. *International journal of civil and structural engineering*, **2**, 2.

Kantro, D.L. (1980). Influence of water reducing admixtures on properties of cement paste a miniature slump test. *Cement and concrete aggregates*, **2**, 95–102.

Karol, R.H. (1983). Chemical Grouting, Marcel Dekker Publ., New York, Basel. 465 pp.

Kauschınger, L. J., Perry, E. R., Hankour, R. (1992). Methods to estimate composition of jet grout bodies. Geo-congress New Orleans, Louisiana. Geotechnical Special Publication No. 30, 194–205. Mc Lean, VA: ASCE, .

Khan, M., Ali, M. (2019). Improvement in concrete behavior with fly ash, silica-fume and coconut fibres. *Construction and Building Materials*, **203**, 174-178.

Khayat, K. H., Yahia, A. (1997). Effect of Welan Gum-high-range water reducer combinations on rheology of cement grout. *ACI Materials Journal,* **94**, 365–72.

Kim, H., Park, Y. D., Noh, J., Song, Y., Han, C., Kang, S. (1997). Rheological properties of self compacting high-performance concrete. In V. M. Malhotra (Ed.), Proceedings of the third CANMET/ACI international conference, ACI International Conference on High Performance Concrete (pp. 653–668). Kuala Lumpur.

Kitazume, M., Terashi, M. (2013). The deep mixing method. London: CRC Press Taylor & Francis Group.

Klein, E., Baud, P., Reuschlé, T., Wong, T. F. (2001). Mechanical behaviour and failure mode of bentheim sandstone under triaxial compression. *Physics and Chemistry of the Earth, Part A: Solid Earth and Geodesy*, **26**, 21–25.

Klein, A., Polivka, M. (1958). The use of admixtures in cement. *Proceeding ASCE. Jour. of SMFE*, **84**, 1547.

Paper 1547.

Koerner, R. M. (1985). Construction and geotechnical methods in foundation engineering. McGraw-Hill Book Company.

Kolovos, K. G., Asteris, P. G., Cotsovos, D. M., Badogiannis, E., Tsivilis, S. (2013). Mechanical properties of soilcrete mixtures modified with metakaolin. *Construction and Building Materials*, **47**, 1026–1036.

Kolovos, K. G., Asteris, P. G., Tsivilis, S. (2016). Properties of sandcrete mixtures modified with metakaolin. *European Journal of Environmental and Civil Engineering*, **20**, 18–37.

Krizek, R.J., Liao, H. J., Borden, R. (1992). Mechanical properties of microfine cement/sodium grouted sand. *Grouting, Soil Improvement and Geosynthetics, Proceedings ASCE Geotech. Conference, Geotechnical Special Publication*, **30**, 688-699.

Kutzner, C. (1996). Grouting of Rock and Soil. Rotterdam: Balkema.

Lajtai, E. Z., Lajtai, V. N. (1974). The evolution of brittle fracture in rocks. *Journal of the Geological Society*, **130**, 1–16.

Lee, F. H., Lee, Y., Chew, S. H., Yong, K. Y. (2005). Strength and modulus of marine clay–cement mixes. *Journal of Geotechnical and Geoenvironmental Engineering*, **131**, 178–186.

Li, L., Lee, P. K. K., Tsui, Y., Tham, L. G., Tang, C. A. (2003). Failure process of granite. *International Journal of Geomechanics*, **3**, 84–98.

Littlejohn, G. S. (1982). Design of cement based grouts. Proceedings of conference on grouting in geotechnology and Engineering, New Orleans (pp. 35–48). New York, NY: ASCE.

Littlejohn, G. S. (1985). Chemical Grouting -1, Ground Engineering, pp. 13-16.

Lombardi, G., (1985). Some theoretical considerations on cement rock grouting. Lombardi Engineering Ltd.

Lowe, J., Standford, T. C. (1982). Special grouting at Tarbela dam project. Proceedings of conference on grouting in geotechnology and Engineering, New Orleans (pp. 152–171). New York, NY: ASCE.

Lunardi, P. (1997). Ground Improvement by means of Jet Grouting, *Ground Improvement*, **1**, 65-85.

Mahmud, H. B., Majuar, E., Zain, M. F. M., Hamid, N. B. A. A. (2004). Mechanical properties and durability of high strength concrete containing rice husk ash. In V. M. Malhotra (Ed.) Proceedings of the eighth CANMET/ACI international conference on fly ash, silica fume, slag and natural pozzolans in concrete, (pp. 751–765). Las Vegas, NV: Farmington Hills, Mich. : American Concrete Institute, c2004.

Mannheimer, R. (1991). Laminar and turbulent flow of cement slurries in large diameter pipe: A comparison with laboratory viscometers. *Journal of Rheology*, **35**, 113–133.

Martin, C. D. (1993). The strength of massive Lac du granite around underground openings (PhD thesis). University of Manitoba, Winnipeg.

Martin, C. D., Chandler, N. A. (1994). The progressive fracture of Lac du Bonnet granite. International Journal of Rock Mechanics and Mining Sciences & Geomechanics Abstracts, 31, 643–659.

Mehta, P. K., Monteiro, P. J. M. (2005). Concrete: Microstructure, properties, and materials (3rd ed.). New York, NY: McGraw-Hill.

Memon, S. A., Shaikh, M. A., Akbar, H. (2008). Production of low cost self compacting concrete using rice husk ash. first int. Conference on construction in develoing countries (pp. 260–269). Karachi, Pakistan.

Mezger, T.G. 2011. The Rheology Handbook. 3rd revised Edition Hanover:Vincentz Network, Germany.

Mikkelsen, P. E. (2002). Cement-bentonite grout backfill for borehole instruments. *Geotechnical and Instrumentation News,* **20**, 38–42.

Miltiadou, A. E. (1991). Etude des coulis hydrauliques pour la re´paration et lerenforcement des structures et des monuments historiques en mac¸onnie. *Etude et recherche des Laboratoires des Ponts et Chausse´es, Serieouvrages d'art*, **OA8**, 278.

Miura, N., Horpibulsuk, S., & Nagaraj, T. S. (2001). Engineering behavior of cement stabilized clay at high water content. *Soils Found Japan Geotechnical Society*, **41**, 3–10.

Moller, P., Fall, A., Chikkadi, V. (2009a). An attempt to categorize yield stress fluid behaviour. *Philosophical transactions of the royal society a-mathematical physical and engineering sciences,* **367**, 5139–5155.

Morel, J. C., Pkla, A., Walker, P. (2007). Compressive strength testing of compressed earth blocks. *Construction and Building Materials*, **21**, 303–309.

Moseley, M. P. (1993). Ground Improvement. Boynton Beach, FL: Blackie Academic and Professional.

Mujumdar, A., Beris, A. N., Metzner, A. B. (2002). Transient phenomena in thixotropic systems. *Journal of Non-Newtonian Fluid Mechanics.* **102**, 157–178.

Nagataki, S. (1993). Mineral admixtures in concrete: State of the art and trends. In Mehta, P. K. (Ed.), Proceedings of the V. Mohan Malhotra symposium on concrete technology: Past, present, and future (pp. 447–482). Berkeley, CA: University of California.

Nakanishi, W. (1974). Method for forming a underground wall comprising a plurality of columns in the earth and soil formation, *US Patent*, **3**,800-544

Nehdi, M., Duquette, J., Damatty, A. E. (2003). Performance of rice husk ash produced using a new technology as a mineral admixture in concrete. *Cement and Concrete Research*, **33**, 1203–1210.

Nehdi, M., Rahman, M. A. (2004). Estimating rheological properties of cement pastes using various rheological models for different test geometry, gap and surface friction. *Cement and Concrete Research*, **34**:1993–2007.

Nguyen, H. H. T., Quach, C. H. (2017). Mechanical behaviors of soilcrete created from soils of Tam Bang and Vam Dinh bridges simulating jet grouting technology. Proceedings of the conference on grouting, Honolulu, Hawaii (pp. 62–72). New York, NY: ASCE.

Nguyen, Q., Boger, D. (1983). Yield stress measurement for concentrated suspensions. *Journal of Rheology*, **27**, 321.

Nguyen, Q., Boger, D. (1987). Characterization of yield stress fluids with concentric cylinder viscometers. *Rheologica acta*, **26**, 508–515.

Nguyen, Q. D., Boger, D. V. (1985). Thixotropic behaviour of concentrated bauxite residue suspensions. *Rheologica Acta,* **24**, 427–437.

Nikbakhtan, B., Osanloo, M. (2009). Effect of grout pressure and grout flow on soil physical and mechanical properties in jet grouting operations. International Journal of Rock Mechanics and Mining Sciences, 46, 498–505.

Nonveiller E. 1989. Grouting, Theory and practice. Amsterdam: Elsevier.

Nonveiller, 1989. Grouting Theory and Practice, Developments in Geotechnical Engineering no. 57, Elsevier Science Publ, 250 pp.

Okamura, H., Ozawa, K. (1995). Mix design for self-compacting concrete. *Concrete Library JSCE*, **25**, 107–120.

Ozawa, K., Sakata, N., Okamura, H. (1995). Evaluation of self compactibility of fresh concrete using the funnel test. *Japan Society of Civil Engineers Concrete Library International*, **25**, 61–70.

Paoli, B. De., Bosco, B., Granata, R., Bruce, D. A. (1992a). Fundamental observations on cement based grouts (1): Traditional materials, Grouting. *Soil Improvement and Geosynthetics, Proceedings ASCE Geotech. Conference, Geotechnical Special Publication*, **30**, 474- 485.

Paoli, B. De., Bosco, B., Granata, R., Bruce, D. A. (1992b). Fundamental observations on cement based grouts (2): microfine cements and the Cemill process. *Grouting, Soil Improvement and Geosynthetics, Proceedings ASCE Geotech. Conference, Geotechnical Special Publication*, **30**, 486-499.

Pavlovic, M. N., Cotsovos, D. M., Dedic, M. M., Savidu, A. (2010a). Reinforced jet-grouted piles. Part 1: Analysis and design. *Proceedings of the Institution of Civil Engineers - Structures and Buildings*, **163**, 299–308.

Pavlovic, M. N., Cotsovos, D. M., Dedic, M. M., Savidu, A. (2010b). Reinforced jet-grouted piles. Part 2: Materials and tolerances. *Proceedings of the Institution of Civil Engineers - Structures and Buildings*, **163**, 309–315.

Perret, S., Khayat, K.H., Ballivy, G. (2000). The Effect of Degree of Saturation of Sand on Groutability – Experimental Simulation. *Ground Improvement*, **4**, 13-22.

Pooja, J. C., Prof, S. D. B. (2014). To Study the Behaviour of Marble Powder as Supplementry Cementitious Material in Concrete. *International. Journal of Engineering Research and Applications*, **4**, 377-381.

Porbaha, A., Shibuya, S., Kishida, T. (2000). State of the art in deep mixing technology. *Ground Improvment*, **4(3)**, 91–110.

Raffle, J. F., Greenwood, D. A. (1961). The Relationship Between the Rheological Characteristics of Grouts and Their Capacity to Permeate Soils. *Proceedings of 5th*

International Conference on Soil Mechanics and Foundation Engineering, **2**, 789-793.

Rai, B. K., Naushad, A. Kr., Rushad, T. (2011). Influence of marble powder/granules in concrete mix. *International Journal of Civil and Structural Engineering*, **1**, 827–834.

Ramezanianpour, A.A. (2009). Sustainable development in cement and concrete. *3rd International Conference on Concrete Development, Concrete Technology and Durability Research Center of Amirkabir University*.

Rana, A., Kalla, P., Csetenyi, L.J. (2015). Sustainable use of marble slurry in concrete. *Journal of Cleaner Production*, **94**, 304-311.

Rodrigues, R., de Brito, J., Sardinha, M. (2015). Mechanical properties of structural concrete containing very fine aggregates from marble cutting sludge. *Construction and Building Materials*, **77**, 349e356.

Rosquoe, F., Alexis, A., Khelidj, A., Phelipot, A. (2003). Experimental study of cement grout, Rheological behavior and sedimentation. *Cement and Concrete Research*, **33**, 713–722

Ruggiero, J.G. (1984). Low slump compactive tail shield grouting in soft ground shield driven tunnels. *Innovative Cement Grouting*, 103–114.

Sadati, S., Arezoumandi, M., Khayat, K. H., Volz, J. S. (2016) Shear performance of reinforced concrete beams incorporating recycled concrete aggregate and high-volume fly ash. *Journal of Cleaner Production*, **115**, 284e293.

Safiuddin, M. D. (2008). Development of self-consolidating high performance concrete incorporating rice husk ash (PhD thesis). Department of Civil and Environmental Engineering, University of Waterloo, Waterloo.

Safiuddin, M. D., West, J. S., Soudki, K. A. (2010). Hardened properties of self-consolidating high performance concrete including rice husk ash. *Cement and Concrete Composites*, **32**, 708–717.

Safiuddin, M. D., West, J. S., Soudki, K. A. (2011). Flowing ability of the mortars formulated from self compacting concretes incorporating rice husk ash. *Construction and Building Materials*, **25**, 973–978.

Sahmaran, M., Özkan, N., Keskin, S. B., Uzal, B., Yaman, I.Ö., Erdem, T.K. (2008). Evaluation of natural zeolite as a viscosity-modifying agent for cement-based grouts. *Cement and Concrete Research,* **38**, 930–937.

Sant, G., Ferraris, C. F., Weiss, J. (2008). Rheological properties of cement pastes: A discussion of structure formation and mechanical property development. *Cement and Concrete Research*, **38**, 1286–1296.

Santarelli, F. J., Brown, E. T. (1989). Failure of three sedimentary rocks in triaxial and hollow cylinder compression tests. *International Journal of Rock Mechanics and Mining Sciences & Geomechanics Abstracts,* **26**, 401–413.

Saraswathy, V., Song, H. W. (2007). Corrosion performance of rice husk ash blended concrete. *Construction and Building Materials*, **21(8)**, 1779–1784.

Schurz, J. (1990). The yield stres an empirical reality. *Rheologica acta*, **29**, 170–171.

Schwarz, L. G., Krizek, R. J. (1992). Effect of mixing on rheological properties of microfine cement grouts. Proceedings of the conference on grouting, soil improvement and geosynthetics, New Orleans (pp. 512–525). New York, NY: ASCE.

Sha, F., Li, S., Liu, R., Li, Z., Zhang, Q. (2018). Experimental study on performance of cement-based grouts admixed with fly ash, bentonite, superplasticizer and water glass. *Construction and Building Materials*, **161**, 282-291.

Shirule, P.A., Rahman, A., Gupta, R. D. (2012). Partial replacement of cement with marble dust powder. *International Journal of Advanced Engineering Research and Studies*, **1**, 175e177.

Shroff, A.V., Joshi N.H., Shah D.L. (1996). Rheological Properties of Microfine Cement Dust Grouts. *Proceedings of Second International Conference on Grouting and Deep Mixing*, Tokyo, 77-81. Balkema.

Singh, M., Srivastava, A., Bhunia, D. (2019). Long term strength and durability parameters of hardened concrete on partially replacing cement by dried waste marble powder slurry. *Construction and Building Materials*, **198**, 553-569.

Singh, M., Srivastava, A., Bhunia, D. (2017). An investigation on effect of partial replacement of cement by waste marble slurry. *Construction and Building Materials*, **134**, 471-488.

Soliman, N. M. (2013). Effect of using marble powder in concrete mixes on the behavior and strength of R.C. slabs. *International Journal of Current Engineering and Technology*, **3** (5).

Sonebi, M. (2002). Experimental design to optimize high-volume of fly ash grout in the presence of welan gum and superplasticizer. *Materials and Structures*, **35(250)**, 373–380.

Sonebi, M., Lachemi, M., Hossain, K. M. A. (2013). Optimisation of rheological parameters and mechanical properties of superplasticised cement grouts containing metakaolin and viscosity modifying admixture. *Construction and Building Materials*, **38**, 126–138.

Sonebi, M., Schmidt, W., Khatib, J. (2013). Influence of the type of viscosity-modifying admixtures and metakaolin on the rheology of grouts. *In International Congress on Materials & Structural Stability* CMSS-2013, Rabat, Morocco.

Tinoco, J., Correia, A. G., & Cortez, P. (2016). Jet grouting column diameter prediction based on a data-driven approach. European Journal of Environmental and Civil Engineering.

Tomiolo, A. (1982). Principles of Grouting. Short Course on Soil and Rock Improvement, Techniques Including Geotextiles, Reinforced Earth and Modern Piling Method. *Asian Institute of Technology*, Thailand.

Topcu, I. B., Canbaz, M. (2007). Effect of different fibers on the mechanical properties of concrete containing fly ash. *Construction and Building Materials*, **21** (7), 1486e1491.

Topçu, I. B., Bilir, T., Uygunoglu, T. (2009). Effect of waste marble dust content as filler on properties of self-compacting concrete. *Construction and Building Materials*, **23** (5), 1947e1953.

Uddin, K., Balasubramaniam, A. S., Bergado, D. T. (1997). Engineering behavior of cement-treated Bangkok soft clay. *Geotechnical Engineering – SEAGS*, **28(1)**, 89–119.

USCE. U.S. Corps of Engineers. 1956. Pressure Grouting Fine Fissures. Tech. Report No. 6-437, October, W.E.S. Vicksburg, Miss.

Uysal, M., Yılmaz, K. (2011). Effect of mineral admixtures on properties of selfcompacting concrete. *Cement and Concrete Composites*, **33** (7), 771e776.

Uysal, M., Sumer, M. (2011). Performance of self-compacting concrete containing different mineral admixtures. *Construction and Building Materials,* **25** (11), 4112e4120.

Vardhan, K., Goyal, S., Siddique, R., Singh, M. (2015). Mechanical properties and microstructural analysis of cement mortar incorporating marble powder as partial replacement of cement, *Construction and Building Materials*, **96**, 615–621.

Vipulanandan, C., Shenoy, S. (1992). Properties of cement grouts and grouted sands with additives. *Grouting, Soil Improvement and Geosynthetics, Proceedings ASCE Geotech. Conference, Geotechnical Special Publication*, **30**, 500-511.

Wallevik, J. E. (2009). Rheological properties of cement paste: Thixotropic behavior and structural breakdown. *Cement and Concrete Research*, **39**, 14–29.

Warner, J. (1972). Strength properties of chemically solidified soils. *Journal of the Soil Mechanics and Foundation Devision, ASCE,* **11**, 1163-1185

Warner, J., Brown, D. (1974). Planning and performing compaction grouting. *ASCE, Journal of Geotechnical Engineers*, 10606.

Warner, J. (1978). Compaction grouting A significant case history. *ASCE, Journal of Geotechnical Engineers*, **104**, 13897.

Warner, J. (1992). Compaction grout; rheology vs. effectiveness. *Grouting, Soil Improvement and Geosynthetics, Proceedings ASCE Geotech. Conference, Geotechnical Special Publication*, **30**, 229-239.

Warner, J., Schmidt, N., Reed, J., Shepardson, D., Lamb, R., Wong, S. (1992). Recent advances ın compaction grouting technology. *Grouting, Soil Improvement and Geosynthetics, Proceedings ASCE Geotech. Conference, Geotechnical Special Publication*, **30**, 252-264.

Warner, J. (1997). Compaction Grout Mechanism What do we know?. *Grouting: Compaction, Remediation and Testing; Geotechnical Special Publication*, **66**, 1 – 17.

Weaver, K. D., Evans, J. C., Pancoski, S.E. (1990) Grout testing for a hazardous waste application. *Concrete International*, **12**, 45–47.

Weaver, K., Bruce, D. (1991). Dam foundation grouting.

Wedding, P. A., Kantro, D. L. (1980). Influence of water reducing admixtures on properties of cement paste a miniature slump test. *Cement and Concrete Aggregate*, **2**, 95–102.

Welsh, J. P. (1986). Construction consideration for ground modification projects. Proceeding *of The International Conference on Deep Foundation*, Beijing, China.

Woodward, R. J., Miller, E. (1990). Grouting post-tensioned concrete bridges: The prevention of voids. *China Journal of Highway and Transport*, **37**, 9– 17.

Yahia, A., Khayat, K. H. (2003). Applicability of rheological models to high-performance grouts containing supplementary cementitious materials and viscosity enhancing admixture. *Materials and Structures,* **36**, 402–412.

Yao, Z.T., Ji, X.S., Sarker, P.K., Tang, J.H., Ge, L.Q., Xia, M.S., Xi, Y.Q. (2015). A comprehensive review on the applications of coal fly ash. *Earth-Science Reviews,* **141**, 105e121.

Yeon, K.S., Han, M. Y. Fundamental properties of polymer–cement mortars for concrete repair. *Proceedings of the 7th International Conference on Structural Faults and Repair*.

Yoon, S., Abu-Farsakh, M. (2009). Laboratory investigation on the strength characteristics of cement-sand as base material. *KSCE Journal of Civil Engineering*, **13**, 15–22.

Zain, M. F. M., Islam, M. N., Mahmud, F., Jamil, M. (2011). Production of rice husk ash for use in concrete as a supplementary cementitious material. *Construction and Building Materials*, **25**, 798–805.

Zerbino, R., Giaccio, G., Isaia, G. C. (2011). Concrete incorporating rice-husk ash without processing. *Construction and Building Materials*, **25**, 371–378.

Zhang, M. H., Malhotra, V. M. (1996). High-performance concrete incorporating rice husk ash as a supplementary cementing material. *ACI Materias Journal*, **93(6)**, 629–636.

Zhang, Y., Kong, X., Gao, L., Wang, J. (2016). Rheological behaviors of fresh cement pastes with polycarboxylate superplasticizer. *Journal of Wuhan University of Technology Materials Science*, **31**, 286-299

APPENDIX A

VISCOSITY TEST RESULT FOR WMP MIX

Table A-1: For MP0WB075 mix

Sample number	MP0WB075		Density	1,628			
Measuring point	Temperature [°C]	Viscosity [Pa.s]	Shear rate [1/s]	Shear stress [Pa]	Torque [mNm]	Speed [1/min]	Cinematic viscosity [mm²/s]
1	19,9	0,0303	50	1,5	0,14	50	0,019
2	20,0	0,0147	100	1,5	0,13	100	0,009
3	19,9	0,0132	150	2,0	0,18	150	0,008
4	19,9	0,0113	200	2,3	0,21	200	0,007
5	19,9	0,0118	250	3,0	0,27	250	0,007
6	19,9	0,0136	300	4,1	0,37	300	0,008
7	19,9	0,0145	350	5,1	0,46	350	0,009
8	19,9	0,0145	400	5,8	0,54	400	0,009
9	19,9	0,0148	450	6,6	0,60	450	0,009
10	19,8	0,0152	500	7,6	0,69	500	0,009
11	19,9	0,0164	550	9,0	0,82	550	0,010
12	19,9	0,0161	600	9,7	0,88	600	0,010
13	19,8	0,0164	650	10,6	0,97	650	0,010
14	19,9	0,0165	700	11,6	1,05	700	0,010
15	19,9	0,0168	750	12,6	1,15	750	0,010
16	19,8	0,0172	800	13,8	1,25	800	0,011
17	19,8	0,0179	850	15,2	1,38	850	0,011
18	19,8	0,0184	900	16,6	1,51	900	0,011
19	19,7	0,0189	950	18,0	1,63	950	0,012
20	19,8	0,0198	1000	19,8	1,80	1000	0,012
21	19,8	0,0195	1000	19,5	1,77	1000	0,012
22	19,8	0,0191	950	18,1	1,65	950	0,012
23	19,8	0,0186	900	16,7	1,52	900	0,011
24	19,8	0,0180	850	15,3	1,39	850	0,011
25	19,8	0,0153	800	12,3	1,12	800	0,009
26	19,8	0,0171	750	12,8	1,16	750	0,010
27	19,8	0,0151	700	10,6	0,96	700	0,009
28	19,8	0,0161	650	10,5	0,95	650	0,010
29	19,8	0,0155	600	9,3	0,85	600	0,010
30	19,8	0,0151	550	8,3	0,76	550	0,009
31	19,8	0,0147	500	7,3	0,67	500	0,009
32	19,8	0,0143	450	6,5	0,59	450	0,009
33	19,8	0,0138	400	5,5	0,50	400	0,008
34	19,8	0,0143	350	5,0	0,46	350	0,009
35	19,8	0,0131	300	3,9	0,36	300	0,008
36	19,8	0,0120	250	3,0	0,27	250	0,007
37	19,8	0,0111	200	2,2	0,20	200	0,007
38	19,8	0,0120	150	1,8	0,16	150	0,007
39	19,8	0,0133	100	1,3	0,12	100	0,008
40	19,7	0,0136	50	0,7	0,06	50	0,008

Table A-2: For MP5WB075 mix

Sample number	MP5WB075		Density	1,625			
Measuring point	**Temperature [°C]**	**Viscosity [Pa.s]**	**Shear rate [1/s]**	**Shear stress [Pa]**	**Torque [mNm]**	**Speed [1/min]**	**Cinematic viscosity [mm²/s]**
1	19,4	0,0350	50	1,8	0,16	50	0,022
2	19,4	0,0222	100	2,2	0,20	100	0,014
3	19,3	0,0188	150	2,8	0,26	150	0,012
4	19,3	0,0167	200	3,3	0,30	200	0,010
5	19,4	0,0161	250	4,0	0,37	250	0,010
6	19,4	0,0173	300	5,2	0,47	300	0,011
7	19,5	0,0179	350	6,3	0,57	350	0,011
8	19,5	0,0186	400	7,4	0,68	400	0,011
9	19,5	0,0195	450	8,8	0,80	450	0,012
10	19,4	0,0201	500	10,0	0,91	500	0,012
11	19,5	0,0200	550	11,0	1,00	550	0,012
12	19,5	0,0203	600	12,2	1,11	600	0,013
13	19,4	0,0203	650	13,2	1,20	650	0,012
14	19,4	0,0211	700	14,7	1,34	700	0,013
15	19,5	0,0214	750	16,1	1,46	750	0,013
16	19,5	0,0215	800	17,2	1,56	800	0,013
17	19,4	0,0218	850	18,6	1,69	850	0,013
18	19,5	0,0222	900	20,0	1,81	900	0,014
19	19,4	0,0228	950	21,6	1,97	950	0,014
20	19,4	0,0232	1000	23,2	2,11	1000	0,014
21	19,4	0,0232	1000	23,2	2,11	1000	0,014
22	19,4	0,0226	950	21,5	1,95	950	0,014
23	19,5	0,0222	900	20,0	1,81	900	0,014
24	19,4	0,0218	850	18,5	1,68	850	0,013
25	19,4	0,0215	800	17,2	1,57	800	0,013
26	19,4	0,0205	750	15,4	1,40	750	0,013
27	19,4	0,0208	700	14,6	1,32	700	0,013
28	19,5	0,0200	650	13,0	1,18	650	0,012
29	19,4	0,0200	600	12,0	1,09	600	0,012
30	19,4	0,0204	550	11,2	1,02	550	0,013
31	19,4	0,0191	500	9,5	0,87	500	0,012
32	19,4	0,0191	450	8,6	0,78	450	0,012
33	19,5	0,0187	400	7,5	0,68	400	0,012
34	19,4	0,0178	350	6,2	0,57	350	0,011
35	19,4	0,0172	300	5,2	0,47	300	0,011
36	19,4	0,0161	250	4,0	0,37	250	0,010
37	19,5	0,0157	200	3,1	0,29	200	0,010
38	19,4	0,0179	150	2,7	0,24	150	0,011
39	19,4	0,0212	100	2,1	0,19	100	0,013
40	19,4	0,0313	50	1,6	0,14	50	0,019

Table A-3: For MP10WB075 mix

Sample number	MP10WB075		Density	1,621			
Measuring point	Temperature [°C]	Viscosity [Pa.s]	Shear rate [1/s]	Shear stress [Pa]	Torque [mNm]	Speed [1/min]	Cinematic viscosity [mm²/s]
1	18,7	0,0192	50	1,0	0,09	50	0,012
2	18,7	0,0180	100	1,8	0,16	100	0,011
3	1,9	0,0148	150	2,2	0,20	150	0,009
4	18,8	0,0132	200	2,6	0,24	200	0,008
5	18,8	0,0135	250	3,4	0,31	250	0,008
6	18,8	0,0150	300	4,5	0,41	300	0,009
7	18,8	0,0154	350	5,4	0,49	350	0,009
8	18,7	0,0159	400	6,4	0,58	400	0,010
9	18,7	0,0166	450	7,5	0,68	450	0,010
10	18,7	0,0175	500	8,7	0,79	500	0,011
11	18,7	0,0170	550	9,3	0,85	550	0,010
12	18,7	0,0173	600	10,4	0,94	600	0,011
13	18,7	0,0182	650	11,8	1,07	650	0,011
14	18,7	0,0183	700	12,8	1,17	700	0,011
15	18,7	0,0188	750	14,1	1,28	750	0,012
16	18,7	0,0184	800	14,7	1,34	800	0,011
17	18,7	0,0195	850	16,6	1,51	850	0,012
18	18,7	0,0203	900	18,3	1,66	900	0,013
19	18,7	0,0209	950	19,9	1,81	950	0,013
20	18,7	0,0215	1000	21,5	1,95	1000	0,013
21	18,6	0,0214	1000	21,4	1,95	1000	0,013
22	18,7	0,0206	950	19,6	1,78	950	0,013
23	18,7	0,0201	900	18,1	1,65	900	0,012
24	18,7	0,0199	850	16,9	1,54	850	0,012
25	18,7	0,0192	800	15,4	1,40	800	0,012
26	18,7	0,0167	750	12,6	1,14	750	0,010
27	18,7	0,0179	700	12,5	1,14	700	0,011
28	18,7	0,0175	650	11,3	1,03	650	0,011
29	18,7	0,0170	600	10,2	0,93	600	0,010
30	18,7	0,0164	550	9,0	0,82	550	0,010
31	18,7	0,0166	500	8,3	0,76	500	0,010
32	18,6	0,0160	450	7,2	0,65	450	0,010
33	18,6	0,0158	400	6,3	0,57	400	0,010
34	18,6	0,0150	350	5,2	0,48	350	0,009
35	18,6	0,0134	300	4,0	0,37	300	0,008
36	18,5	0,0124	250	3,1	0,28	250	0,008
37	18,6	0,0125	200	2,5	0,23	200	0,008
38	18,6	0,0135	150	2,0	0,18	150	0,008
39	18,6	0,0156	100	1,6	0,14	100	0,010
40	18,6	0,0192	50	1,0	0,09	50	0,012

Table A-4: For MP15WB075 mix

Sample number	**MP15WB075**		**Density**	**1,617**			
Measuring point	**Temperature [°C]**	**Viscosity [Pa.s]**	**Shear rate [1/s]**	**Shear stress [Pa]**	**Torque [mNm]**	**Speed [1/min]**	**Cinematic viscosity [mm²/s]**
1	17,8	0,0040	50	0,2	0,10	50	0,002
2	18,0	0,0114	100	1,1	0,10	100	0,007
3	18,2	0,0095	150	1,4	0,13	150	0,006
4	18,4	0,0088	200	1,8	0,16	200	0,005
5	18,4	0,0105	250	2,6	0,24	250	0,007
6	18,5	0,0113	300	3,4	0,31	300	0,007
7	18,5	0,0123	350	4,3	0,39	350	0,008
8	18,5	0,0128	400	5,1	0,46	400	0,008
9	18,5	0,0131	450	5,9	0,54	450	0,008
10	18,4	0,0139	500	7,0	0,63	500	0,009
11	18,4	0,0143	550	7,9	0,71	550	0,009
12	18,4	0,0145	600	8,7	0,79	600	0,009
13	18,4	0,0149	650	9,7	0,88	650	0,009
14	18,5	0,0151	700	10,6	0,96	700	0,009
15	18,4	0,0153	750	11,4	1,04	750	0,009
16	18,4	0,0165	800	13,2	1,20	800	0,010
17	18,5	0,0172	850	14,6	1,33	850	0,011
18	18,5	0,0177	900	15,9	1,45	900	0,011
19	18,5	0,0182	950	17,3	1,57	950	0,011
20	18,5	0,0190	1000	19,0	1,73	1000	0,012
21	18,5	0,0189	1000	18,9	1,72	1000	0,012
22	18,5	0,0182	950	17,3	1,57	950	0,011
23	18,5	0,0177	900	16,0	1,45	900	0,011
24	18,5	0,0172	850	14,7	1,33	850	0,011
25	18,5	0,0167	800	13,4	1,22	800	0,010
26	18,5	0,0156	750	11,7	1,07	750	0,010
27	18,4	0,0155	700	10,8	0,98	700	0,010
28	18,4	0,0149	650	9,7	0,88	650	0,009
29	18,4	0,0142	600	8,5	0,77	600	0,009
30	18,4	0,0134	550	7,4	0,67	550	0,008
31	18,4	0,0129	500	6,5	0,59	500	0,008
32	18,4	0,0129	450	5,8	0,53	450	0,008
33	18,4	0,0128	400	5,1	0,46	400	0,008
34	18,4	0,0121	350	4,2	0,38	350	0,007
35	18,4	0,0114	300	3,4	0,31	300	0,007
36	18,3	0,0105	250	2,6	0,24	250	0,007
37	18,3	0,0092	200	1,8	0,17	200	0,006
38	18,4	0,0089	150	1,3	0,12	150	0,005
39	18,4	0,0100	100	1,0	0,09	100	0,006
40	18,3	0,0098	50	0,5	0,04	50	0,006

Table A-5: For MP20WB075 mix

Sample number	**MP20WB075**		**Density**	**1,613**			
Measuring point	**Temperature [°C]**	**Viscosity [Pa.s]**	**Shear rate [1/s]**	**Shear stress [Pa]**	**Torque [mNm]**	**Speed [1/min]**	**Cinematic viscosity [mm²/s]**
1	18,1	0,0061	50	0,3	0,03	50	0,0038
2	18,2	0,0133	100	1,3	0,12	100	0,0083
3	18,3	0,0117	150	1,8	0,16	150	0,0072
4	18,4	0,0113	200	2,3	0,21	200	0,0070
5	18,5	0,0120	250	3,0	0,27	250	0,0075
6	18,5	0,0130	300	3,9	0,35	300	0,0080
7	18,5	0,0135	350	4,7	0,43	350	0,0084
8	18,4	0,0139	400	5,6	0,51	400	0,0086
9	18,5	0,0142	450	6,4	0,58	450	0,0088
10	18,5	0,0147	500	7,3	0,67	500	0,0091
11	18,4	0,0150	550	8,3	0,75	550	0,0093
12	18,4	0,0153	600	9,2	0,84	600	0,0095
13	18,4	0,0157	650	10,2	0,93	650	0,0098
14	18,4	0,0164	700	11,5	1,04	700	0,0102
15	18,4	0,0165	750	12,4	1,12	750	0,0102
16	18,4	0,0166	800	13,3	1,21	800	0,0103
17	18,4	0,0171	850	14,5	1,32	850	0,0106
18	18,4	0,0175	900	15,7	1,43	900	0,0108
19	18,4	0,0181	950	17,2	1,57	950	0,0112
20	18,4	0,0185	1000	18,5	1,68	1000	0,0115
21	18,3	0,0188	1000	18,8	1,70	1000	0,0116
22	18,4	0,0180	950	17,1	1,55	950	0,0111
23	18,4	0,0175	900	15,7	1,43	900	0,0108
24	18,4	0,0172	850	14,7	1,33	850	0,0107
25	18,4	0,0168	800	13,4	1,22	800	0,0104
26	18,4	0,0151	750	11,3	1,03	750	0,0093
27	18,4	0,0161	700	11,3	1,02	700	0,0100
28	18,4	0,0168	650	10,9	0,99	650	0,0104
29	18,4	0,0153	600	9,2	0,83	600	0,0095
30	18,4	0,0151	550	8,3	0,76	550	0,0094
31	18,4	0,0145	500	7,2	0,66	500	0,0090
32	18,4	0,0142	450	6,4	0,58	450	0,0088
33	18,4	0,0133	400	5,3	0,49	400	0,0083
34	18,4	0,0135	350	4,7	0,43	350	0,0084
35	18,4	0,0125	300	3,8	0,34	300	0,0078
36	18,3	0,0124	250	3,1	0,28	250	0,0077
37	18,4	0,0113	200	2,3	0,21	200	0,0070
38	18,4	0,0114	150	1,7	0,15	150	0,0070
39	18,4	0,0128	100	1,3	0,12	100	0,0080
40	18,4	0,0173	50	0,9	0,08	50	0,0107

Table A-6: For MP25WB075 mix

Sample number	MP25WB075		Density	1,609			
Measuring point	Temperature [°C]	Viscosity [Pa.s]	Shear rate [1/s]	Shear stress [Pa]	Torque [mNm]	Speed [1/min]	Cinematic viscosity [mm²/s]
1	18,1	0,0080	50	0,4	0,04	50	0,0050
2	18,2	0,0133	100	1,3	0,12	100	0,0083
3	18,4	0,0117	150	1,8	0,16	150	0,0073
4	18,4	0,0101	200	2,0	0,18	200	0,0063
5	18,5	0,0115	250	2,9	0,26	250	0,0071
6	18,5	0,0127	300	3,8	0,35	300	0,0079
7	18,5	0,0133	350	4,6	0,42	350	0,0082
8	18,5	0,0136	400	5,4	0,49	400	0,0084
9	18,5	0,0141	450	6,4	0,58	450	0,0088
10	18,4	0,0147	500	7,3	0,67	500	0,0091
11	18,4	0,0150	550	8,2	0,75	550	0,0093
12	18,4	0,0153	600	9,2	0,83	600	0,0095
13	18,5	0,0155	650	10,1	0,92	650	0,0096
14	18,4	0,0157	700	11,0	1,00	700	0,0097
15	18,4	0,0162	750	12,2	1,11	750	0,0101
16	18,4	0,0167	800	13,4	1,22	800	0,0104
17	18,4	0,0172	850	14,6	1,33	850	0,0107
18	18,4	0,0175	900	15,8	1,43	900	0,0109
19	18,4	0,0177	950	16,8	1,53	950	0,0110
20	18,2	0,0182	1000	18,2	1,66	1000	0,0113
21	18,4	0,0185	1000	18,5	1,68	1000	0,0115
22	18,3	0,0178	950	16,9	1,54	950	0,0110
23	18,4	0,0174	900	15,7	1,43	900	0,0108
24	18,3	0,0168	850	14,3	1,30	850	0,0104
25	18,4	0,0163	800	13,0	1,18	800	0,0101
26	18,4	0,0161	750	12,0	1,10	750	0,0100
27	18,4	0,0165	700	11,5	1,05	700	0,0102
28	18,4	0,0165	650	10,7	0,97	650	0,0102
29	18,4	0,0150	600	9,0	0,82	600	0,0093
30	18,4	0,0147	550	8,1	0,74	550	0,0091
31	18,4	0,0143	500	7,2	0,65	500	0,0089
32	18,4	0,0140	450	6,3	0,57	450	0,0087
33	18,4	0,0139	400	5,6	0,51	400	0,0087
34	18,5	0,0133	350	4,6	0,42	350	0,0082
35	18,4	0,0131	300	3,9	0,36	300	0,0082
36	18,4	0,0115	250	2,9	0,26	250	0,0071
37	18,4	0,0108	200	2,2	0,20	200	0,0067
38	18,4	0,0117	150	1,8	0,16	150	0,0073
39	18,4	0,0152	100	1,5	0,14	100	0,0094
40	18,5	0,0173	50	0,9	0,08	50	0,0108

Table A-7: For MP0WB100 mix

Sample number	**MP0WB100**		**Density**	**1,508**			
Measuring point	**Temperature [°C]**	**Viscosity [Pa.s]**	**Shear rate [1/s]**	**Shear stress [Pa]**	**Torque [mNm]**	**Speed [1/min]**	**Cinematic viscosity [mm²/s]**
1	18,7	0,0000	50	0,0	0,00	50	0,0000
2	18,7	0,0000	100	0,0	0,00	100	0,0000
3	18,9	0,0012	150	0,2	0,01	150	0,0008
4	19,0	0,0029	200	0,6	0,05	200	0,0019
5	19,0	0,0044	250	1,1	0,10	250	0,0029
6	19,0	0,0052	300	1,6	0,14	300	0,0035
7	19,0	0,0053	350	1,8	0,17	350	0,0035
8	19,0	0,0060	400	2,4	0,22	400	0,0040
9	19,0	0,0070	450	3,1	0,29	450	0,0046
10	19,0	0,0072	500	3,6	0,33	500	0,0048
11	19,0	0,0078	550	4,3	0,39	550	0,0051
12	19,0	0,0082	600	4,9	0,45	600	0,0054
13	19,0	0,0085	650	5,5	0,50	650	0,0056
14	19,1	0,0094	700	6,6	0,60	700	0,0062
15	19,0	0,0104	750	7,8	0,71	750	0,0069
16	19,0	0,0102	800	8,2	0,74	800	0,0068
17	19,1	0,0109	850	9,2	0,84	850	0,0072
18	19,1	0,0112	900	10,0	0,91	900	0,0074
19	19,0	0,0116	950	11,1	1,01	950	0,0077
20	19,1	0,0120	1000	12,0	1,10	1000	0,0080
21	19,0	0,0124	1000	12,4	1,13	1000	0,0082
22	19,0	0,0117	950	11,1	1,01	950	0,0078
23	19,1	0,0112	900	10,1	0,92	900	0,0074
24	19,1	0,0106	850	9,0	0,82	850	0,0070
25	19,1	0,0103	800	8,2	0,75	800	0,0068
26	19,1	0,0096	750	7,2	0,59	750	0,0064
27	19,1	0,0095	700	6,6	0,67	700	0,0063
28	19,1	0,0089	650	5,8	0,47	650	0,0059
29	19,0	0,0084	600	5,0	0,46	600	0,0055
30	19,1	0,0083	550	4,6	0,42	550	0,0055
31	19,0	0,0070	500	3,5	0,32	500	0,0047
32	19,1	0,0068	450	3,1	0,28	450	0,0045
33	19,0	0,0061	400	2,4	0,22	400	0,0041
34	19,0	0,0051	350	1,8	0,16	350	0,0034
35	19,0	0,0043	300	1,3	0,12	300	0,0028
36	19,0	0,0036	250	0,9	0,08	250	0,0024
37	19,0	0,0025	200	0,5	0,04	200	0,0016
38	19,0	0,0015	150	0,2	0,01	150	0,0010
39	19,0	0,0000	100	0,0	0,00	100	0,0000
40	19,0	0,0000	50	0,0	0,00	50	0,0000

Table A-8: For MP5WB100 mix

Sample number	MP5WB100		Density	1,505			
Measuring point	**Temperature [°C]**	**Viscosity [Pa.s]**	**Shear rate [1/s]**	**Shear stress [Pa]**	**Torque [mNm]**	**Speed [1/min]**	**Cinematic viscosity [mm²/s]**
1	18,0	0,0001	50	0,01	0,00	50	0,0001
2	18,1	0,0003	100	0,03	0,00	100	0,0002
3	18,2	0,0013	150	0,2	0,00	150	0,0009
4	18,4	0,0020	200	0,4	0,04	200	0,0013
5	18,4	0,0036	250	0,9	0,08	250	0,0024
6	18,4	0,0043	300	1,3	0,12	300	0,0028
7	18,4	0,0057	350	2,0	0,18	350	0,0038
8	18,4	0,0064	400	2,5	0,23	400	0,0042
9	18,3	0,0066	450	3,0	0,27	450	0,0044
10	18,4	0,0079	500	3,9	0,36	500	0,0052
11	18,4	0,0084	550	4,6	0,42	550	0,0056
12	18,5	0,0086	600	5,2	0,47	600	0,0057
13	18,5	0,0096	650	6,2	0,57	650	0,0064
14	18,5	0,0098	700	6,9	0,69	700	0,0065
15	18,4	0,0100	750	7,5	0,64	750	0,0067
16	18,4	0,0101	800	8,1	0,74	800	0,0067
17	18,4	0,0105	850	8,9	0,81	850	0,0070
18	18,5	0,0108	900	9,8	0,89	900	0,0072
19	18,4	0,0117	950	11,1	1,01	950	0,0078
20	18,5	0,0121	1000	12,1	1,10	1000	0,0080
21	18,5	0,0120	1000	12,0	1,09	1000	0,0080
22	18,5	0,0115	950	10,9	0,99	950	0,0076
23	18,5	0,0111	900	9,9	0,90	900	0,0073
24	18,4	0,0107	850	9,1	0,83	850	0,0071
25	18,5	0,0098	800	7,9	0,71	800	0,0065
26	18,4	0,0100	750	7,5	0,68	750	0,0066
27	18,5	0,0110	700	7,7	0,70	700	0,0073
28	18,4	0,0079	650	5,1	0,46	650	0,0052
29	18,4	0,0083	600	5,0	0,45	600	0,0055
30	18,5	0,0071	550	3,9	0,35	550	0,0047
31	18,4	0,0070	500	3,5	0,32	500	0,0047
32	18,4	0,0063	450	2,8	0,26	450	0,0042
33	18,5	0,0054	400	2,2	0,20	400	0,0036
34	18,4	0,0054	350	1,9	0,17	350	0,0036
35	18,4	0,0044	300	1,3	0,12	300	0,0029
36	18,4	0,0031	250	0,8	0,07	250	0,0021
37	18,4	0,0025	200	0,5	0,04	200	0,0016
38	18,3	0,0008	150	0,1	0,00	150	0,0005
39	18,4	0,0003	100	0,03	0,00	100	0,0002
40	18,4	0,0001	50	0,00	0,00	50	0,0001

Table A-9: For MP10WB100 mix

Sample number	MP10WB100		Density	1,502			
Measuring point	Temperature [°C]	Viscosity [Pa.s]	Shear rate [1/s]	Shear stress [Pa]	Torque [mNm]	Speed [1/min]	Cinematic viscosity [mm²/s]
1	18,0	0,0001	50	0,01	0,00	50	0,0001
2	18,1	0,0003	100	0,03	0,00	100	0,0002
3	18,2	0,0017	150	0,3	0,00	150	0,0011
4	18,2	0,0027	200	0,5	0,05	200	0,0018
5	18,2	0,0038	250	1,0	0,09	250	0,0026
6	18,2	0,0049	300	1,5	0,13	300	0,0033
7	18,2	0,0050	350	1,8	0,16	350	0,0033
8	18,2	0,0059	400	2,4	0,21	400	0,0039
9	18,2	0,0070	450	3,1	0,29	450	0,0047
10	18,2	0,0076	500	3,8	0,39	500	0,0051
11	18,2	0,0080	550	4,4	0,40	550	0,0053
12	18,3	0,0081	600	4,9	0,39	600	0,0054
13	18,3	0,0094	650	6,1	0,55	650	0,0062
14	18,2	0,0098	700	6,9	0,62	700	0,0065
15	18,2	0,0105	750	7,9	0,71	750	0,0070
16	18,2	0,0112	800	8,9	0,81	800	0,0074
17	18,1	0,0112	850	9,5	0,87	850	0,0075
18	18,1	0,0117	900	10,6	0,96	900	0,0078
19	18,1	0,0122	950	11,6	1,05	950	0,0081
20	18,1	0,0127	1000	12,7	1,15	1000	0,0084
21	18,1	0,0128	1000	12,8	1,17	1000	0,0085
22	18,1	0,0121	950	11,5	1,05	950	0,0081
23	18,1	0,0118	900	10,6	0,96	900	0,0078
24	18,1	0,0115	850	9,5	0,89	850	0,0076
25	18,1	0,0107	800	8,6	0,78	800	0,0072
26	18,1	0,0102	750	7,6	0,69	750	0,0068
27	18,1	0,0102	700	7,2	0,65	700	0,0068
28	18,2	0,0089	650	5,8	0,53	650	0,0059
29	18,2	0,0087	600	5,2	0,47	600	0,0058
30	18,2	0,0085	550	4,7	0,43	550	0,0057
31	18,2	0,0073	500	3,7	0,33	500	0,0049
32	18,2	0,0067	450	3,0	0,27	450	0,0044
33	18,2	0,0059	400	2,4	0,21	400	0,0039
34	18,2	0,0051	350	1,8	0,16	350	0,0034
35	18,1	0,0040	300	1,2	0,11	300	0,0026
36	18,2	0,0027	250	0,7	0,06	250	0,0018
37	18,2	0,0018	200	0,4	0,03	200	0,0012
38	18,2	0,0008	150	0,1	0,00	150	0,0005
39	18,2	0,0004	100	0,04	0,00	100	0,0003
40	18,2	0,0001	50	0,01	0,00	50	0,0001

Table A-10: For MP15WB100 mix

Sample number	MP15WB100		Density	1,499			
Measuring point	Temperature [°C]	Viscosity [Pa.s]	Shear rate [1/s]	Shear stress [Pa]	Torque [mNm]	Speed [1/min]	Cinematic viscosity [mm²/s]
1	18,3	0,00003	50	0,002	0,00	50	0,00002
2	18,4	0,0002	100	0,02	0,00	100	0,0001
3	18,4	0,0015	150	0,2	0,01	150	0,0010
4	18,5	0,0029	200	0,6	0,05	200	0,0020
5	18,5	0,0048	250	1,2	0,11	250	0,0032
6	18,5	0,0054	300	1,6	0,15	300	0,0036
7	18,5	0,0057	350	2,0	0,18	350	0,0038
8	18,5	0,0062	400	2,5	0,23	400	0,0042
9	18,4	0,0071	450	3,2	0,29	450	0,0047
10	18,4	0,0078	500	3,9	0,31	500	0,0052
11	18,4	0,0080	550	4,4	0,40	550	0,0053
12	18,4	0,0089	600	5,3	0,49	600	0,0059
13	18,4	0,0090	650	5,8	0,46	650	0,0060
14	18,4	0,0097	700	6,8	0,68	700	0,0065
15	18,3	0,0103	750	7,7	0,70	750	0,0069
16	18,3	0,0107	800	8,6	0,78	800	0,0071
17	18,2	0,0112	850	9,5	0,86	850	0,0074
18	18,2	0,0114	900	10,3	0,93	900	0,0076
19	18,2	0,0117	950	11,2	1,01	950	0,0078
20	18,2	0,0123	1000	12,3	1,12	1000	0,0082
21	18,2	0,0126	1000	12,6	1,14	1000	0,0084
22	18,2	0,0117	950	11,2	1,01	950	0,0078
23	18,2	0,0114	900	10,2	0,93	900	0,0076
24	18,2	0,0110	850	9,4	0,85	850	0,0074
25	18,2	0,0105	800	8,4	0,76	800	0,0070
26	18,2	0,0102	750	7,7	0,57	750	0,0068
27	18,2	0,0102	700	7,1	0,65	700	0,0068
28	18,2	0,0097	650	6,3	0,46	650	0,0065
29	18,2	0,0094	600	5,7	0,40	600	0,0063
30	18,3	0,0086	550	4,7	0,43	550	0,0057
31	18,2	0,0074	500	3,7	0,34	500	0,0049
32	18,3	0,0071	450	3,2	0,29	450	0,0047
33	18,2	0,0065	400	2,6	0,24	400	0,0043
34	18,3	0,0053	350	1,8	0,17	350	0,0035
35	18,2	0,0049	300	1,5	0,13	300	0,0033
36	18,3	0,0042	250	1,1	0,10	250	0,0028
37	18,3	0,0027	200	0,5	0,05	200	0,0018
38	18,2	0,0008	150	0,1	0,01	150	0,0005
39	18,2	0,0002	100	0,02	0,00	100	0,0001
40	18,2	0,0001	50	0,00	0,00	50	0,00005

Table A-11: For MP20WB100 mix

Sample number	MP20WB100		Density	1,496			
Measuring point	Temperature [°C]	Viscosity [Pa.s]	Shear rate [1/s]	Shear stress [Pa]	Torque [mNm]	Speed [1/min]	Cinematic viscosity [mm²/s]
1	18,1	0,0001	50	0,01	0,00	50	0,0001
2	18,2	0,0003	100	0,03	0,00	100	0,0002
3	18,2	0,0013	150	0,2	0,00	150	0,0009
4	18,3	0,0027	200	0,5	0,05	200	0,0018
5	18,4	0,0040	250	1,0	0,09	250	0,0027
6	18,5	0,0049	300	1,5	0,13	300	0,0033
7	18,4	0,0057	350	2,0	0,18	350	0,0038
8	18,4	0,0062	400	2,5	0,23	400	0,0042
9	18,3	0,0068	450	3,1	0,28	450	0,0045
10	18,3	0,0072	500	3,6	0,33	500	0,0048
11	18,3	0,0083	550	4,5	0,41	550	0,0055
12	18,4	0,0093	600	5,6	0,40	600	0,0062
13	18,4	0,0096	650	6,2	0,45	650	0,0064
14	18,4	0,0105	700	7,3	0,67	700	0,0070
15	18,2	0,0107	750	8,0	0,66	750	0,0071
16	18,3	0,0109	800	8,7	0,72	800	0,0073
17	18,2	0,0113	850	9,6	0,80	850	0,0076
18	18,3	0,0118	900	10,6	0,88	900	0,0079
19	18,3	0,0120	950	11,4	1,04	950	0,0080
20	18,3	0,0123	1000	12,3	1,12	1000	0,0082
21	18,3	0,0129	1000	12,9	1,17	1000	0,0086
22	18,3	0,0119	950	11,3	1,03	950	0,0080
23	18,3	0,0115	900	10,4	0,94	900	0,0077
24	18,3	0,0109	850	9,2	0,84	850	0,0073
25	18,3	0,0106	800	8,5	0,77	800	0,0071
26	18,2	0,0102	750	7,6	0,69	750	0,0068
27	18,3	0,0112	700	7,9	0,71	700	0,0075
28	18,3	0,0099	650	6,4	0,46	650	0,0066
29	18,2	0,0087	600	5,2	0,47	600	0,0058
30	18,3	0,0072	550	3,9	0,36	550	0,0048
31	18,2	0,0074	500	3,7	0,34	500	0,0050
32	18,2	0,0063	450	2,8	0,26	450	0,0042
33	18,2	0,0055	400	2,2	0,20	400	0,0037
34	18,3	0,0054	350	1,9	0,17	350	0,0036
35	18,2	0,0041	300	1,2	0,11	300	0,0028
36	18,2	0,0033	250	0,8	0,07	250	0,0022
37	18,2	0,0025	200	0,5	0,04	200	0,0016
38	18,2	0,0013	150	0,2	0,00	150	0,0009
39	18,2	0,0004	100	0,04	0,00	100	0,0003
40	18,2	0,0001	50	0,00	0,00	50	0,0001

Table A-12: For MP25WB100 mix

Sample number	**MP25WB100**		**Density**	**1,493**			
Measuring point	**Temperature [°C]**	**Viscosity [Pa.s]**	**Shear rate [1/s]**	**Shear stress [Pa]**	**Torque [mNm]**	**Speed [1/min]**	**Cinematic viscosity [mm²/s]**
1	18,0	0,00004	50	0,002	0,00	50	0,00003
2	18,1	0,0003	100	0,03	0,00	100	0,0002
3	18,3	0,0018	150	0,26	0,00	150	0,0012
4	18,4	0,0029	200	0,59	0,05	200	0,0020
5	18,5	0,0044	250	1,10	0,10	250	0,0029
6	18,5	0,0054	300	1,61	0,15	300	0,0036
7	18,5	0,0055	350	1,94	0,18	350	0,0037
8	18,5	0,0064	400	2,54	0,23	400	0,0043
9	18,5	0,0074	450	3,33	0,30	450	0,0050
10	18,5	0,0078	500	3,89	0,35	500	0,0052
11	18,5	0,0087	550	4,78	0,43	550	0,0058
12	18,5	0,0091	600	5,43	0,49	600	0,0061
13	18,5	0,0096	650	6,22	0,51	650	0,0064
14	18,5	0,0104	700	7,29	0,66	700	0,0070
15	18,5	0,0107	750	8,04	0,73	750	0,0072
16	18,5	0,0111	800	8,87	0,88	800	0,0074
17	18,6	0,0117	850	9,95	0,90	850	0,0078
18	18,6	0,0120	900	10,79	0,98	900	0,0080
19	18,5	0,0126	950	11,95	1,09	950	0,0084
20	18,5	0,0132	1000	13,16	1,20	1000	0,0088
21	18,5	0,0130	1000	13,02	1,18	1000	0,0087
22	18,5	0,0125	950	11,86	1,08	950	0,0084
23	18,5	0,0122	900	10,97	1,00	900	0,0082
24	18,5	0,0118	850	10,00	0,91	850	0,0079
25	18,5	0,0112	800	8,92	0,81	800	0,0075
26	18,5	0,0108	750	8,13	0,74	750	0,0073
27	18,5	0,0101	700	7,06	0,64	700	0,0068
28	18,5	0,0091	650	5,94	0,54	650	0,0061
29	18,5	0,0090	600	5,38	0,49	600	0,0060
30	18,5	0,0081	550	4,45	0,40	550	0,0054
31	18,5	0,0079	500	3,94	0,36	500	0,0053
32	18,5	0,0070	450	3,15	0,29	450	0,0047
33	18,4	0,0065	400	2,59	0,24	400	0,0043
34	18,4	0,0054	350	1,89	0,17	350	0,0036
35	18,5	0,0046	300	1,38	0,13	300	0,0031
36	18,4	0,0040	250	1,00	0,09	250	0,0027
37	18,4	0,0025	200	0,49	0,04	200	0,0016
38	18,4	0,0015	150	0,22	0,01	150	0,0010
39	18,3	0,0002	100	0,02	0,00	100	0,0001
40	18,4	0,0001	50	0,004	0,00	50	0,00005

Table A-13: For MP0WB125 mix

Sample number	**MP0WB125**		**Density**	**1,426**			
Measuring point	**Temperature [°C]**	**Viscosity [Pa.s]**	**Shear rate [1/s]**	**Shear stress [Pa]**	**Torque [mNm]**	**Speed [1/min]**	**Cinematic viscosity [mm²/s]**
1	18,9	0,0000	50	0,00	0,00	50	0,00000
2	18,9	0,0000	100	0,00	0,00	100	0,0000
3	18,9	0,0000	150	0,00	0,00	150	0,0000
4	19,0	0,0013	200	0,26	0,00	200	0,0009
5	19,0	0,0014	250	0,35	0,03	250	0,0010
6	19,0	0,0024	300	0,73	0,07	300	0,0017
7	19,0	0,0038	350	1,33	0,12	350	0,0027
8	19,0	0,0047	400	1,89	0,17	400	0,0033
9	19,0	0,0050	450	2,26	0,21	450	0,0035
10	19,0	0,0065	500	3,24	0,29	500	0,0045
11	19,0	0,0064	550	3,65	0,32	550	0,0045
12	19,0	0,0073	600	4,36	0,40	600	0,0051
13	19,0	0,0076	650	4,92	0,45	650	0,0053
14	19,0	0,0079	700	5,52	0,50	700	0,0055
15	19,0	0,0084	750	6,32	0,57	750	0,0059
16	19,0	0,0091	800	7,29	0,66	800	0,0064
17	19,0	0,0097	850	8,27	0,75	850	0,0068
18	19,1	0,0101	900	9,11	0,83	900	0,0071
19	19,0	0,0106	950	10,04	0,91	950	0,0074
20	19,0	0,0109	1000	10,88	0,99	1000	0,0076
21	19,0	0,0112	1000	11,16	1,01	1000	0,0078
22	19,0	0,0106	950	10,09	0,92	950	0,0074
23	19,0	0,0101	900	9,11	0,83	900	0,0071
24	19,0	0,0105	850	8,94	0,74	850	0,0074
25	19,0	0,0102	800	8,13	0,74	800	0,0071
26	19,0	0,0098	750	7,34	0,60	750	0,0069
27	19,1	0,0096	700	6,73	0,61	700	0,0067
28	19,0	0,0084	650	5,47	0,38	650	0,0059
29	19,0	0,0074	600	4,45	0,40	600	0,0052
30	19,0	0,0066	550	3,65	0,28	550	0,0047
31	19,0	0,0059	500	2,96	0,27	500	0,0042
32	19,0	0,0052	450	2,36	0,21	450	0,0037
33	19,0	0,0040	400	1,61	0,15	400	0,0028
34	19,0	0,0034	350	1,19	0,11	350	0,0024
35	19,0	0,0029	300	0,86	0,08	300	0,0020
36	19,0	0,0014	250	0,35	0,03	250	0,0010
37	19,0	0,0000	200	0,00	0,00	200	0,0000
38	19,0	0,0000	150	0,00	0,00	150	0,0000
39	19,0	0,0000	100	0,00	0,00	100	0,0000
40	18,8	0,0000	50	0,00	0,00	50	0,00000

Table A-14: For MP5WB125 mix

Sample number	MP5WB125		Density	1,424			
Measuring point	**Temperature [°C]**	**Viscosity [Pa.s]**	**Shear rate [1/s]**	**Shear stress [Pa]**	**Torque [mNm]**	**Speed [1/min]**	**Cinematic viscosity [mm²/s]**
1	19,0	0,0000	50	0,00	0,00	50	0,0000
2	19,0	0,0000	100	0,00	0,00	100	0,0000
3	19,1	0,0000	150	0,00	0,00	150	0,0000
4	19,1	0,0000	200	0,00	0,00	200	0,0000
5	19,1	0,0019	250	0,46	0,02	250	0,0013
6	19,0	0,0024	300	0,73	0,07	300	0,0017
7	19,0	0,0035	350	1,24	0,11	350	0,0025
8	19,0	0,0040	400	1,61	0,15	400	0,0028
9	18,9	0,0049	450	2,22	0,20	450	0,0035
10	18,9	0,0058	500	2,90	0,22	500	0,0041
11	18,8	0,0061	550	3,33	0,30	550	0,0043
12	18,8	0,0069	600	4,13	0,43	600	0,0048
13	18,8	0,0076	650	4,91	0,33	650	0,0053
14	18,9	0,0080	700	5,57	0,57	700	0,0056
15	18,8	0,0082	750	6,18	0,56	750	0,0058
16	18,9	0,0088	800	6,78	0,61	800	0,0062
17	18,7	0,0090	850	7,67	0,69	850	0,0063
18	18,8	0,0094	900	8,46	0,77	900	0,0066
19	18,7	0,0098	950	9,25	0,85	950	0,0069
20	18,7	0,0109	1000	10,93	0,93	1000	0,0077
21	18,8	0,0106	1000	10,55	0,96	1000	0,0074
22	18,7	0,0097	950	9,25	0,84	950	0,0068
23	18,7	0,0094	900	8,46	0,77	900	0,0066
24	18,7	0,0090	850	7,67	0,70	850	0,0063
25	18,7	0,0085	800	6,78	0,62	800	0,0060
26	18,8	0,0080	750	6,03	0,62	750	0,0056
27	18,8	0,0076	700	5,34	0,49	700	0,0054
28	18,7	0,0071	650	4,59	0,42	650	0,0050
29	18,8	0,0067	600	4,03	0,37	600	0,0047
30	18,8	0,0056	550	3,10	0,28	550	0,0040
31	18,8	0,0056	500	2,78	0,25	500	0,0039
32	18,9	0,0048	450	2,17	0,20	450	0,0034
33	18,8	0,0043	400	1,70	0,15	400	0,0030
34	18,8	0,0033	350	1,14	0,10	350	0,0023
35	18,8	0,0024	300	0,73	0,07	300	0,0017
36	18,7	0,0016	250	0,40	0,04	250	0,0011
37	18,8	0,0000	200	0,00	0,00	200	0,0000
38	18,8	0,0000	150	0,00	0,00	150	0,0000
39	18,8	0,0000	100	0,00	0,00	100	0,0000
40	18,8	0,0000	50	0,00	0,00	50	0,00000

Table A-15: For MP10WB125 mix

Sample number	MP10WB125		Density	1,421			
Measuring point	Temperature [°C]	Viscosity [Pa.s]	Shear rate [1/s]	Shear stress [Pa]	Torque [mNm]	Speed [1/min]	Cinematic viscosity [mm²/s]
1	18,4	0,0000	50	0,00	0,00	50	0,0000
2	18,5	0,0000	100	0,00	0,00	100	0,0000
3	18,7	0,0000	150	0,00	0,00	150	0,0000
4	18,9	0,0011	200	0,23	0,00	200	0,0008
5	18,8	0,0012	250	0,31	0,03	250	0,0009
6	18,7	0,0023	300	0,68	0,06	300	0,0016
7	18,8	0,0034	350	1,19	0,11	350	0,0024
8	18,8	0,0043	400	1,70	0,15	400	0,0030
9	18,7	0,0045	450	2,03	0,18	450	0,0032
10	18,8	0,0065	500	3,24	0,29	500	0,0046
11	19,0	0,0065	550	3,58	0,32	550	0,0046
12	18,9	0,0068	600	4,08	0,37	600	0,0048
13	18,8	0,0077	650	5,01	0,46	650	0,0054
14	18,9	0,0078	700	5,48	0,49	700	0,0055
15	18,9	0,0087	750	6,51	0,46	750	0,0061
16	18,8	0,0088	800	7,06	0,64	800	0,0062
17	18,9	0,0093	850	7,90	0,72	850	0,0065
18	18,8	0,0097	900	8,74	0,79	900	0,0068
19	18,9	0,0101	950	9,58	0,87	950	0,0071
20	18,9	0,0105	1000	10,46	0,95	1000	0,0074
21	18,8	0,0107	1000	10,74	0,98	1000	0,0076
22	18,8	0,0100	950	9,53	0,87	950	0,0071
23	18,8	0,0096	900	8,64	0,79	900	0,0068
24	18,9	0,0090	850	7,67	0,70	850	0,0063
25	18,8	0,0084	800	6,72	0,76	800	0,0059
26	18,8	0,0084	750	6,27	0,57	750	0,0059
27	18,9	0,0077	700	5,38	0,49	700	0,0054
28	18,8	0,0067	650	4,36	0,40	650	0,0047
29	18,8	0,0071	600	4,27	0,39	600	0,0050
30	18,8	0,0067	550	3,66	0,33	550	0,0047
31	18,8	0,0058	500	2,91	0,26	500	0,0041
32	18,8	0,0050	450	2,26	0,21	450	0,0035
33	18,8	0,0041	400	1,66	0,15	400	0,0029
34	18,8	0,0033	350	1,14	0,10	350	0,0023
35	18,8	0,0023	300	0,68	0,06	300	0,0016
36	18,8	0,0012	250	0,31	0,03	250	0,0009
37	18,8	0,0000	200	0,00	0,00	200	0,0000
38	18,7	0,0000	150	0,00	0,00	150	0,0000
39	18,7	0,0000	100	0,00	0,00	100	0,0000
40	18,7	0,0000	50	0,00	0,00	50	0,00000

Table A-16: For MP15WB125 mix

Sample number	MP15WB125		Density	1,419			
Measuring point	Temperature [°C]	Viscosity [Pa.s]	Shear rate [1/s]	Shear stress [Pa]	Torque [mNm]	Speed [1/min]	Cinematic viscosity [mm²/s]
1	18,9	0,0000	50	0,00	0,00	50	0,0000
2	19,0	0,0000	100	0,00	0,00	100	0,0000
3	19,0	0,0000	150	0,00	0,00	150	0,0000
4	19,1	0,0000	200	0,00	0,00	200	0,0000
5	19,1	0,0010	250	0,26	0,02	250	0,0007
6	19,1	0,0024	300	0,73	0,07	300	0,0017
7	19,0	0,0031	350	1,10	0,10	350	0,0022
8	19,0	0,0041	400	1,66	0,15	400	0,0029
9	19,0	0,0052	450	2,36	0,21	450	0,0037
10	19,0	0,0057	500	2,87	0,26	500	0,0040
11	19,0	0,0059	550	3,22	0,28	550	0,0041
12	19,0	0,0065	600	3,89	0,35	600	0,0046
13	19,0	0,0075	650	4,87	0,44	650	0,0053
14	19,0	0,0077	700	5,39	0,43	700	0,0054
15	18,9	0,0085	750	6,35	0,59	750	0,0060
16	18,8	0,0086	800	6,87	0,62	800	0,0061
17	18,8	0,0091	850	7,76	0,71	850	0,0064
18	18,7	0,0096	900	8,60	0,78	900	0,0067
19	18,7	0,0101	950	9,58	0,87	950	0,0071
20	18,7	0,0103	1000	10,32	0,94	1000	0,0073
21	18,9	0,0106	1000	10,55	0,96	1000	0,0074
22	18,8	0,0098	950	9,34	0,85	950	0,0069
23	18,7	0,0093	900	8,41	0,76	900	0,0066
24	18,7	0,0092	850	7,85	0,71	850	0,0065
25	18,8	0,0084	800	6,69	0,61	800	0,0059
26	18,8	0,0087	750	6,55	0,60	750	0,0062
27	18,8	0,0078	700	5,48	0,50	700	0,0055
28	18,9	0,0079	650	5,15	0,47	650	0,0056
29	18,9	0,0069	600	4,13	0,38	600	0,0048
30	19,0	0,0057	550	3,15	0,29	550	0,0040
31	18,9	0,0056	500	2,82	0,26	500	0,0040
32	18,9	0,0046	450	2,08	0,19	450	0,0033
33	19,0	0,0040	400	1,61	0,15	400	0,0028
34	19,0	0,0035	350	1,24	0,11	350	0,0025
35	19,0	0,0023	300	0,68	0,06	300	0,0016
36	18,9	0,0005	250	0,12	0,01	250	0,0003
37	18,9	0,0000	200	0,00	0,00	200	0,0000
38	19,0	0,0000	150	0,00	0,00	150	0,0000
39	19,0	0,0000	100	0,00	0,00	100	0,0000
40	18,9	0,0000	50	0,00	0,00	50	0,00000

Table A-17: For MP20WB125 mix

Sample number	**MP20WB125**		**Density**	**1,417**			
Measuring point	**Temperature [°C]**	**Viscosity [Pa.s]**	**Shear rate [1/s]**	**Shear stress [Pa]**	**Torque [mNm]**	**Speed [1/min]**	**Cinematic viscosity [mm²/s]**
1	19,0	0,0000	50	0,00	0,00	50	0,0000
2	19,0	0,0000	100	0,00	0,00	100	0,0000
3	19,1	0,0000	150	0,00	0,00	150	0,0000
4	19,1	0,0004	200	0,07	0,01	200	0,0003
5	19,2	0,0020	250	0,49	0,04	250	0,0014
6	19,2	0,0030	300	0,91	0,08	300	0,0021
7	19,2	0,0039	350	1,38	0,13	350	0,0028
8	19,2	0,0047	400	1,89	0,17	400	0,0033
9	19,2	0,0054	450	2,45	0,22	450	0,0038
10	19,2	0,0056	500	2,79	0,23	500	0,0039
11	19,0	0,0068	550	3,75	0,34	550	0,0048
12	19,0	0,0076	600	4,55	0,41	600	0,0053
13	19,0	0,0079	650	5,13	0,44	650	0,0056
14	19,1	0,0085	700	5,94	0,54	700	0,0060
15	19,0	0,0086	750	6,44	0,58	750	0,0061
16	19,0	0,0092	800	7,39	0,67	800	0,0065
17	19,0	0,0095	850	8,09	0,74	850	0,0067
18	19,0	0,0099	900	8,88	0,81	900	0,0070
19	19,0	0,0104	950	9,86	0,90	950	0,0073
20	19,0	0,0108	1000	10,79	0,98	1000	0,0076
21	19,0	0,0113	1000	11,30	1,03	1000	0,0080
22	19,0	0,0104	950	9,86	0,90	950	0,0073
23	19,0	0,0098	900	8,83	0,80	900	0,0069
24	19,0	0,0097	850	8,25	0,73	850	0,0068
25	19,0	0,0096	800	7,70	0,77	800	0,0068
26	19,0	0,0089	750	6,64	0,60	750	0,0063
27	19,1	0,0081	700	5,66	0,51	700	0,0057
28	19,0	0,0079	650	5,15	0,41	650	0,0056
29	19,0	0,0073	600	4,36	0,40	600	0,0051
30	19,0	0,0069	550	3,80	0,35	550	0,0049
31	19,0	0,0059	500	2,96	0,27	500	0,0042
32	19,0	0,0055	450	2,50	0,23	450	0,0039
33	19,0	0,0045	400	1,80	0,16	400	0,0032
34	19,0	0,0041	350	1,42	0,13	350	0,0029
35	19,0	0,0035	300	1,05	0,10	300	0,0025
36	19,0	0,0023	250	0,59	0,05	250	0,0017
37	19,0	0,0008	200	0,17	0,02	200	0,0006
38	19,0	0,0000	150	0,00	0,00	150	0,0000
39	19,1	0,0000	100	0,00	0,00	100	0,0000
40	19,0	0,0000	50	0,00	0,00	50	0,0000

Table A-18: For MP25WB125 mix

Sample number	MP25WB125		Density	1,414			
Measuring point	**Temperature [°C]**	**Viscosity [Pa.s]**	**Shear rate [1/s]**	**Shear stress [Pa]**	**Torque [mNm]**	**Speed [1/min]**	**Cinematic viscosity [mm²/s]**
1	18,7	0,0000	50	0,00	0,00	50	0,0000
2	18,7	0,0000	100	0,00	0,00	100	0,0000
3	18,8	0,0000	150	0,00	0,00	150	0,0000
4	18,9	0,0000	200	0,00	0,00	200	0,0000
5	18,8	0,0012	250	0,31	0,03	250	0,0009
6	18,9	0,0024	300	0,73	0,07	300	0,0017
7	18,8	0,0035	350	1,24	0,11	350	0,0025
8	18,8	0,0045	400	1,80	0,16	400	0,0032
9	18,7	0,0050	450	2,26	0,21	450	0,0036
10	18,8	0,0059	500	2,95	0,22	500	0,0042
11	18,8	0,0063	550	3,47	0,32	550	0,0045
12	18,8	0,0066	600	3,99	0,36	600	0,0047
13	18,7	0,0073	650	4,77	0,32	650	0,0052
14	18,7	0,0079	700	5,52	0,50	700	0,0056
15	18,7	0,0080	750	5,96	0,51	750	0,0056
16	18,7	0,0083	800	6,64	0,60	800	0,0059
17	18,7	0,0087	850	7,43	0,68	850	0,0062
18	18,7	0,0090	900	8,13	0,74	900	0,0064
19	18,7	0,0093	950	8,88	0,81	950	0,0066
20	18,7	0,0100	1000	10,00	0,91	1000	0,0071
21	18,7	0,0100	1000	10,04	0,91	1000	0,0071
22	18,7	0,0091	950	8,69	0,79	950	0,0065
23	18,7	0,0087	900	7,85	0,71	900	0,0062
24	18,7	0,0084	850	7,15	0,65	850	0,0060
25	18,7	0,0084	800	6,73	0,68	800	0,0059
26	18,7	0,0075	750	5,61	0,58	750	0,0053
27	18,7	0,0070	700	4,92	0,51	700	0,0050
28	18,7	0,0070	650	4,54	0,41	650	0,0049
29	18,7	0,0066	600	3,94	0,36	600	0,0046
30	18,7	0,0057	550	3,15	0,29	550	0,0040
31	18,7	0,0056	500	2,82	0,26	500	0,0040
32	18,7	0,0051	450	2,31	0,21	450	0,0036
33	18,7	0,0044	400	1,75	0,16	400	0,0031
34	18,7	0,0033	350	1,14	0,10	350	0,0023
35	18,7	0,0026	300	0,77	0,07	300	0,0018
36	18,7	0,0018	250	0,45	0,04	250	0,0013
37	18,7	0,0000	200	0,00	0,00	200	0,0000
38	18,7	0,0000	150	0,00	0,00	150	0,0000
39	18,7	0,0000	100	0,00	0,00	100	0,0000
40	18,7	0,0000	50	0,00	0,00	50	0,0000

Table A-19: For MP0WB150 mix

Sample number	MP0WB150		Density	1,366			
Measuring point	**Temperature [°C]**	**Viscosity [Pa.s]**	**Shear rate [1/s]**	**Shear stress [Pa]**	**Torque [mNm]**	**Speed [1/min]**	**Cinematic viscosity [mm²/s]**
1	18,5	0,0000	50	0,00	0,00	50	0,0000
2	18,7	0,0000	100	0,00	0,00	100	0,0000
3	18,7	0,0000	150	0,00	0,00	150	0,0000
4	18,7	0,0000	200	0,00	0,00	200	0,0000
5	18,7	0,0003	250	0,07	0,01	250	0,0002
6	18,7	0,0010	300	0,31	0,03	300	0,0007
7	18,7	0,0022	350	0,77	0,07	350	0,0016
8	18,7	0,0030	400	1,19	0,11	400	0,0022
9	18,7	0,0037	450	1,66	0,15	450	0,0027
10	18,7	0,0040	500	2,02	0,14	500	0,0030
11	18,7	0,0046	550	2,54	0,23	550	0,0034
12	18,7	0,0052	600	3,14	0,23	600	0,0038
13	18,7	0,0056	650	3,66	0,39	650	0,0041
14	18,7	0,0058	700	4,08	0,37	700	0,0043
15	18,7	0,0061	750	4,60	0,35	750	0,0045
16	18,6	0,0068	800	5,48	0,50	800	0,0050
17	18,7	0,0070	850	5,99	0,54	850	0,0052
18	18,6	0,0073	900	6,64	0,60	900	0,0053
19	18,6	0,0077	950	7,34	0,67	950	0,0057
20	18,6	0,0079	1000	8,64	0,72	1000	0,0058
21	18,6	0,0086	1000	8,64	0,79	1000	0,0063
22	18,7	0,0051	950	4,87	0,44	950	0,0038
23	18,7	0,0074	900	6,64	0,60	900	0,0054
24	18,6	0,0070	850	5,99	0,54	850	0,0052
25	18,6	0,0066	800	5,24	0,48	800	0,0048
26	18,7	0,0063	750	4,73	0,43	750	0,0046
27	18,6	0,0058	700	4,03	0,30	700	0,0042
28	18,6	0,0055	650	3,57	0,32	650	0,0040
29	18,7	0,0049	600	2,96	0,27	600	0,0036
30	18,6	0,0041	550	2,26	0,21	550	0,0030
31	18,6	0,0038	500	1,89	0,17	500	0,0028
32	18,6	0,0035	450	1,56	0,14	450	0,0025
33	18,7	0,0027	400	1,10	0,10	400	0,0020
34	18,6	0,0017	350	0,59	0,05	350	0,0012
35	18,6	0,0010	300	0,31	0,03	300	0,0007
36	18,6	0,0008	250	0,20	0,01	250	0,0006
37	18,6	0,0000	200	0,00	0,00	200	0,0000
38	18,6	0,0000	150	0,00	0,00	150	0,0000
39	18,7	0,0000	100	0,00	0,00	100	0,0000
40	18,7	0,0000	50	0,00	0,00	50	0,0000

Table A-20: For MP5WB150 mix

Sample number	MP5WB150		Density	1,364			
Measuring point	Temperature [°C]	Viscosity [Pa.s]	Shear rate [1/s]	Shear stress [Pa]	Torque [mNm]	Speed [1/min]	Cinematic viscosity [mm²/s]
1	18,7	0,0000	50	0,00	0,00	50	0,0000
2	18,8	0,0000	100	0,00	0,00	100	0,0000
3	18,9	0,0000	150	0,00	0,00	150	0,0000
4	18,9	0,0000	200	0,00	0,00	200	0,0000
5	19,0	0,0005	250	0,11	0,01	250	0,0003
6	19,0	0,0019	300	0,56	0,02	300	0,0014
7	19,0	0,0021	350	0,73	0,07	350	0,0015
8	19,0	0,0031	400	1,24	0,11	400	0,0023
9	19,0	0,0032	450	1,42	0,13	450	0,0023
10	19,0	0,0043	500	2,16	0,15	500	0,0032
11	19,0	0,0048	550	2,64	0,24	550	0,0035
12	19,0	0,0051	600	3,07	0,39	600	0,0037
13	19,0	0,0053	650	3,47	0,32	650	0,0039
14	19,0	0,0064	700	4,45	0,47	700	0,0047
15	19,0	0,0065	750	4,86	0,49	750	0,0047
16	19,0	0,0075	800	6,04	0,55	800	0,0055
17	19,0	0,0079	850	6,35	0,61	850	0,0058
18	18,9	0,0085	900	7,53	0,69	900	0,0062
19	18,9	0,0087	950	8,23	0,75	950	0,0063
20	18,8	0,0091	1000	9,34	0,82	1000	0,0066
21	18,8	0,0093	1000	9,34	0,85	1000	0,0068
22	18,8	0,0087	950	8,23	0,75	950	0,0063
23	18,9	0,0084	900	7,53	0,68	900	0,0061
24	18,8	0,0083	850	7,03	0,61	850	0,0061
25	18,9	0,0079	800	6,35	0,65	800	0,0058
26	18,9	0,0072	750	5,43	0,49	750	0,0053
27	18,9	0,0070	700	4,87	0,44	700	0,0051
28	18,8	0,0063	650	4,08	0,37	650	0,0046
29	18,9	0,0054	600	3,24	0,29	600	0,0040
30	18,9	0,0045	550	2,45	0,22	550	0,0033
31	18,9	0,0044	500	2,22	0,20	500	0,0032
32	18,9	0,0041	450	1,84	0,17	450	0,0030
33	18,9	0,0030	400	1,19	0,11	400	0,0022
34	18,9	0,0023	350	0,82	0,07	350	0,0017
35	18,9	0,0015	300	0,45	0,04	300	0,0011
36	18,9	0,0003	250	0,07	0,01	250	0,0002
37	18,9	0,0000	200	0,00	0,00	200	0,0000
38	18,9	0,0000	150	0,00	0,00	150	0,0000
39	18,9	0,0000	100	0,00	0,00	100	0,0000
40	18,8	0,0000	50	0,00	0,00	50	0,0000

Table A-21: For MP10WB150 mix

Sample number	MP10WB150		Density	1,363			
Measuring point	Temperature [°C]	Viscosity [Pa.s]	Shear rate [1/s]	Shear stress [Pa]	Torque [mNm]	Speed [1/min]	Cinematic viscosity [mm²/s]
1	19,2	0,0000	50	0,00	0,00	50	0,0000
2	19,3	0,0000	100	0,00	0,00	100	0,0000
3	19,3	0,0000	150	0,00	0,00	150	0,0000
4	19,3	0,0000	200	0,00	0,00	200	0,0000
5	19,3	0,0002	250	0,05	0,01	250	0,0001
6	19,3	0,0015	300	0,45	0,04	300	0,0011
7	19,3	0,0025	350	0,86	0,08	350	0,0018
8	19,3	0,0033	400	1,33	0,12	400	0,0024
9	19,3	0,0038	450	1,70	0,15	450	0,0028
10	19,3	0,0042	500	2,11	0,15	500	0,0031
11	19,3	0,0052	550	2,87	0,26	550	0,0038
12	19,3	0,0054	600	3,24	0,29	600	0,0040
13	19,3	0,0057	650	3,71	0,34	650	0,0042
14	19,2	0,0062	700	4,36	0,40	700	0,0046
15	19,2	0,0068	750	5,24	0,32	750	0,0050
16	19,2	0,0071	800	5,80	0,52	800	0,0052
17	19,2	0,0078	850	6,69	0,60	850	0,0057
18	19,2	0,0082	900	7,34	0,67	900	0,0060
19	19,2	0,0085	950	8,09	0,74	950	0,0062
20	19,2	0,0090	1000	9,67	0,82	1000	0,0066
21	19,2	0,0097	1000	9,67	0,88	1000	0,0071
22	19,2	0,0085	950	8,04	0,73	950	0,0062
23	19,1	0,0082	900	7,34	0,67	900	0,0060
24	19,1	0,0079	850	6,69	0,61	850	0,0058
25	19,1	0,0073	800	5,80	0,53	800	0,0053
26	19,2	0,0070	750	5,24	0,48	750	0,0051
27	19,1	0,0062	700	4,31	0,33	700	0,0045
28	19,2	0,0059	650	3,85	0,35	650	0,0043
29	19,2	0,0052	600	3,15	0,29	600	0,0039
30	19,2	0,0046	550	2,54	0,23	550	0,0034
31	19,2	0,0037	500	1,87	0,26	500	0,0027
32	19,1	0,0031	450	1,39	0,17	450	0,0023
33	19,2	0,0030	400	1,19	0,11	400	0,0022
34	19,2	0,0021	350	0,73	0,07	350	0,0015
35	19,2	0,0013	300	0,40	0,04	300	0,0010
36	19,2	0,0001	250	0,03	0,01	250	0,0001
37	19,2	0,0000	200	0,00	0,00	200	0,0000
38	19,2	0,0000	150	0,00	0,00	150	0,0000
39	19,2	0,0000	100	0,00	0,00	100	0,0000
40	19,2	0,0000	50	0,00	0,00	50	0,0000

Table A-22: For MP15WB150 mix

Sample number	MP15WB150		Density	1,361			
Measuring point	Temperature [°C]	Viscosity [Pa.s]	Shear rate [1/s]	Shear stress [Pa]	Torque [mNm]	Speed [1/min]	Cinematic viscosity [mm²/s]
1	19,3	0,0000	50	0,00	0,00	50	0,0000
2	19,3	0,0000	100	0,00	0,00	100	0,0000
3	19,3	0,0000	150	0,00	0,00	150	0,0000
4	19,3	0,0000	200	0,00	0,00	200	0,0000
5	19,3	0,0001	250	0,03	0,01	250	0,0001
6	19,3	0,0016	300	0,49	0,04	300	0,0012
7	19,2	0,0022	350	0,77	0,07	350	0,0016
8	19,2	0,0031	400	1,24	0,11	400	0,0023
9	19,2	0,0040	450	1,80	0,16	450	0,0029
10	19,2	0,0045	500	2,23	0,25	500	0,0033
11	19,2	0,0050	550	2,77	0,25	550	0,0037
12	19,2	0,0052	600	3,09	0,30	600	0,0038
13	19,1	0,0052	650	3,38	0,31	650	0,0038
14	19,1	0,0056	700	3,94	0,36	700	0,0041
15	19,1	0,0062	750	4,68	0,43	750	0,0046
16	19,0	0,0074	800	5,90	0,54	800	0,0054
17	19,0	0,0078	850	6,60	0,60	850	0,0057
18	19,1	0,0083	900	7,43	0,68	900	0,0061
19	19,1	0,0086	950	8,13	0,74	950	0,0063
20	19,0	0,0089	1000	8,88	0,81	1000	0,0065
21	19,1	0,0093	1000	9,30	0,85	1000	0,0068
22	19,1	0,0085	950	8,04	0,73	950	0,0062
23	19,1	0,0081	900	7,29	0,66	900	0,0060
24	19,0	0,0077	850	6,55	0,60	850	0,0057
25	19,1	0,0071	800	5,66	0,51	800	0,0052
26	19,1	0,0070	750	5,24	0,48	750	0,0051
27	19,1	0,0064	700	4,50	0,32	700	0,0047
28	19,0	0,0063	650	4,13	0,38	650	0,0047
29	19,0	0,0059	600	3,52	0,32	600	0,0043
30	19,1	0,0046	550	2,54	0,23	550	0,0034
31	19,0	0,0042	500	2,12	0,19	500	0,0031
32	19,0	0,0039	450	1,75	0,16	450	0,0029
33	19,0	0,0032	400	1,28	0,12	400	0,0024
34	19,0	0,0028	350	0,98	0,06	350	0,0021
35	19,0	0,0012	300	0,35	0,03	300	0,0009
36	19,0	0,0003	250	0,07	0,01	250	0,0002
37	19,0	0,0000	200	0,00	0,00	200	0,0000
38	19,1	0,0000	150	0,00	0,00	150	0,0000
39	19,1	0,0000	100	0,00	0,00	100	0,0000
40	19,1	0,0000	50	0,00	0,00	50	0,0000

Table A-23: For MP20WB150 mix

Sample number	MP20WB150		Density	1,359			
Measuring point	Temperature [°C]	Viscosity [Pa.s]	Shear rate [1/s]	Shear stress [Pa]	Torque [mNm]	Speed [1/min]	Cinematic viscosity [mm²/s]
1	19,0	0,0000	50	0,00	0,00	50	0,0000
2	19,1	0,0000	100	0,00	0,00	100	0,0000
3	19,1	0,0000	150	0,00	0,00	150	0,0000
4	19,0	0,0000	200	0,00	0,00	200	0,0000
5	19,1	0,0001	250	0,03	0,01	250	0,0001
6	19,0	0,0015	300	0,45	0,04	300	0,0011
7	19,0	0,0027	350	0,96	0,09	350	0,0020
8	19,0	0,0034	400	1,38	0,13	400	0,0025
9	19,0	0,0043	450	1,94	0,18	450	0,0032
10	19,0	0,0048	500	2,40	0,22	500	0,0035
11	19,0	0,0058	550	3,19	0,24	550	0,0043
12	19,0	0,0059	600	3,52	0,32	600	0,0043
13	19,0	0,0063	650	4,13	0,38	650	0,0047
14	19,0	0,0068	700	4,73	0,43	700	0,0050
15	19,0	0,0075	750	5,66	0,58	750	0,0056
16	19,0	0,0077	800	6,18	0,56	800	0,0057
17	19,0	0,0080	850	6,78	0,62	850	0,0059
18	19,0	0,0085	900	7,62	0,69	900	0,0062
19	19,0	0,0088	950	8,36	0,76	950	0,0065
20	19,0	0,0092	1000	9,20	0,84	1000	0,0068
21	19,0	0,0096	1000	9,58	0,87	1000	0,0070
22	19,0	0,0088	950	8,32	0,76	950	0,0064
23	19,0	0,0085	900	7,62	0,69	900	0,0062
24	19,0	0,0080	850	6,83	0,62	850	0,0059
25	19,0	0,0078	800	6,26	0,64	800	0,0058
26	19,0	0,0073	750	5,48	0,50	750	0,0054
27	19,0	0,0066	700	4,64	0,42	700	0,0049
28	19,0	0,0060	650	3,89	0,41	650	0,0044
29	19,0	0,0058	600	3,47	0,32	600	0,0043
30	19,0	0,0048	550	2,64	0,24	550	0,0035
31	19,0	0,0042	500	2,12	0,19	500	0,0031
32	19,0	0,0042	450	1,89	0,17	450	0,0031
33	19,0	0,0032	400	1,28	0,12	400	0,0024
34	19,0	0,0022	350	0,77	0,07	350	0,0016
35	19,0	0,0013	300	0,40	0,04	300	0,0010
36	19,0	0,0011	250	0,27	0,01	250	0,0008
37	19,0	0,0000	200	0,00	0,00	200	0,0000
38	19,0	0,0000	150	0,00	0,00	150	0,0000
39	19,0	0,0000	100	0,00	0,00	100	0,0000
40	19,0	0,0000	50	0,00	0,00	50	0,0000

Table A-24: For MP25WB150 mix

Sample number	MP25WB150		Density	1,357			
Measuring point	Temperature [°C]	Viscosity [Pa.s]	Shear rate [1/s]	Shear stress [Pa]	Torque [mNm]	Speed [1/min]	Cinematic viscosity [mm²/s]
1	19,0	0,0000	50	0,00	0,00	50	0,0000
2	19,1	0,0000	100	0,00	0,00	100	0,0000
3	19,1	0,0000	150	0,00	0,00	150	0,0000
4	19,2	0,0000	200	0,00	0,00	200	0,0000
5	19,2	0,0000	250	0,00	0,01	250	0,0000
6	19,2	0,0011	300	0,34	0,04	300	0,0008
7	19,1	0,0025	350	0,86	0,08	350	0,0018
8	19,1	0,0033	400	1,33	0,12	400	0,0025
9	19,1	0,0040	450	1,80	0,16	450	0,0029
10	19,1	0,0046	500	2,30	0,16	500	0,0034
11	19,1	0,0056	550	3,05	0,28	550	0,0041
12	19,0	0,0060	600	3,61	0,33	600	0,0044
13	19,1	0,0063	650	4,08	0,31	650	0,0046
14	19,0	0,0067	700	4,69	0,43	700	0,0049
15	19,1	0,0077	750	5,76	0,52	750	0,0057
16	19,1	0,0079	800	6,29	0,56	800	0,0058
17	19,0	0,0081	850	6,92	0,63	850	0,0060
18	19,0	0,0085	900	7,62	0,69	900	0,0062
19	19,0	0,0089	950	8,46	0,77	950	0,0066
20	19,0	0,0094	1000	9,39	0,85	1000	0,0069
21	19,0	0,0098	1000	9,81	0,89	1000	0,0072
22	19,0	0,0091	950	8,69	0,79	950	0,0067
23	19,0	0,0085	900	7,67	0,70	900	0,0063
24	19,1	0,0083	850	7,01	0,64	850	0,0061
25	19,0	0,0078	800	6,22	0,57	800	0,0057
26	19,0	0,0071	750	5,34	0,49	750	0,0052
27	19,0	0,0070	700	4,92	0,32	700	0,0052
28	19,0	0,0066	650	4,27	0,45	650	0,0048
29	19,0	0,0054	600	3,61	0,29	600	0,0040
30	19,0	0,0049	550	3,05	0,24	550	0,0036
31	19,0	0,0048	500	2,40	0,22	500	0,0035
32	19,0	0,0037	450	1,66	0,15	450	0,0027
33	19,0	0,0030	400	1,19	0,11	400	0,0022
34	19,0	0,0023	350	0,82	0,07	350	0,0017
35	19,0	0,0010	300	0,31	0,03	300	0,0008
36	19,0	0,0000	250	0,00	0,01	250	0,0000
37	19,0	0,0000	200	0,00	0,00	200	0,0000
38	19,0	0,0000	150	0,00	0,00	150	0,0000
39	19,0	0,0000	100	0,00	0,00	100	0,0000
40	19,0	0,0000	50	0,00	0,00	50	0,0000

APPENDIX B

VISCOSITY TEST RESULT FOR WMP+FA MIX

Table B-1: For MP0FA0WB075 mix

Sample number	MP0FA0WB075		Density	1,628			
Measuring point	**Temperature [°C]**	**Viscosity [Pa.s]**	**Shear rate [1/s]**	**Shear stress [Pa]**	**Torque [mNm]**	**Speed [1/min]**	**Cinematic viscosity [mm²/s]**
1	19,9	0,0303	50	1,5	0,14	50	0,019
2	20,0	0,0147	100	1,5	0,13	100	0,009
3	19,9	0,0132	150	2,0	0,18	150	0,008
4	19,9	0,0113	200	2,3	0,21	200	0,007
5	19,9	0,0118	250	3,0	0,27	250	0,007
6	19,9	0,0136	300	4,1	0,37	300	0,008
7	19,9	0,0145	350	5,1	0,46	350	0,009
8	19,9	0,0145	400	5,8	0,54	400	0,009
9	19,9	0,0148	450	6,6	0,60	450	0,009
10	19,8	0,0152	500	7,6	0,69	500	0,009
11	19,9	0,0164	550	9,0	0,82	550	0,010
12	19,9	0,0161	600	9,7	0,88	600	0,010
13	19,8	0,0164	650	10,6	0,97	650	0,010
14	19,9	0,0165	700	11,6	1,05	700	0,010
15	19,9	0,0168	750	12,6	1,15	750	0,010
16	19,8	0,0172	800	13,8	1,25	800	0,011
17	19,8	0,0179	850	15,2	1,38	850	0,011
18	19,8	0,0184	900	16,6	1,51	900	0,011
19	19,7	0,0189	950	18,0	1,63	950	0,012
20	19,8	0,0198	1000	19,8	1,80	1000	0,012
21	19,8	0,0195	1000	19,5	1,77	1000	0,012
22	19,8	0,0191	950	18,1	1,65	950	0,012
23	19,8	0,0186	900	16,7	1,52	900	0,011
24	19,8	0,0180	850	15,3	1,39	850	0,011
25	19,8	0,0153	800	12,3	1,12	800	0,009
26	19,8	0,0171	750	12,8	1,16	750	0,010
27	19,8	0,0151	700	10,6	0,96	700	0,009
28	19,8	0,0161	650	10,5	0,95	650	0,010
29	19,8	0,0155	600	9,3	0,85	600	0,010
30	19,8	0,0151	550	8,3	0,76	550	0,009
31	19,8	0,0147	500	7,3	0,67	500	0,009
32	19,8	0,0143	450	6,5	0,59	450	0,009
33	19,8	0,0138	400	5,5	0,50	400	0,008
34	19,8	0,0143	350	5,0	0,46	350	0,009
35	19,8	0,0131	300	3,9	0,36	300	0,008
36	19,8	0,0120	250	3,0	0,27	250	0,007
37	19,8	0,0111	200	2,2	0,20	200	0,007
38	19,8	0,0120	150	1,8	0,16	150	0,007
39	19,8	0,0133	100	1,3	0,12	100	0,008
40	19,7	0,0136	50	0,7	0,06	50	0,008

Table B-2: For MP10FA25WB075 mix

Sample number	MP10FA25WB075		Density	1,596			
Measuring point	**Temperature [°C]**	**Viscosity [Pa.s]**	**Shear rate [1/s]**	**Shear stress [Pa]**	**Torque [mNm]**	**Speed [1/min]**	**Cinematic viscosity [mm²/s]**
1	18,2	0,0015	50	0,1	0,01	50	0,001
2	18,4	0,0063	100	0,6	0,06	100	0,004
3	18,6	0,0070	150	1,1	0,10	150	0,004
4	18,7	0,0078	200	1,6	0,14	200	0,005
5	18,7	0,0098	250	2,4	0,22	250	0,006
6	18,7	0,0106	300	3,2	0,29	300	0,007
7	18,7	0,0121	350	4,2	0,38	350	0,008
8	18,8	0,0128	400	5,1	0,46	400	0,008
9	18,8	0,0129	450	5,8	0,53	450	0,008
10	18,8	0,0137	500	6,8	0,62	500	0,009
11	18,8	0,0147	550	8,1	0,74	550	0,009
12	18,8	0,0147	600	8,8	0,80	600	0,009
13	18,8	0,0150	650	9,8	0,89	650	0,009
14	18,8	0,0155	700	10,8	0,98	700	0,010
15	18,8	0,0159	750	11,9	1,08	750	0,010
16	18,8	0,0163	800	13,0	1,18	800	0,010
17	18,9	0,0168	850	14,3	1,30	850	0,011
18	18,9	0,0174	900	15,6	1,42	900	0,011
19	18,8	0,0179	950	17,0	1,54	950	0,011
20	18,9	0,0180	1000	18,0	1,64	1000	0,011
21	18,9	0,0184	1000	18,4	1,67	1000	0,012
22	18,8	0,0176	950	16,7	1,52	950	0,011
23	18,9	0,0170	900	15,3	1,39	900	0,011
24	18,9	0,0166	850	14,1	1,28	850	0,010
25	18,9	0,0162	800	13,0	1,18	800	0,010
26	18,9	0,0158	750	11,9	1,08	750	0,010
27	18,8	0,0155	700	10,8	0,98	700	0,010
28	18,9	0,0149	650	9,7	0,88	650	0,009
29	18,9	0,0145	600	8,7	0,79	600	0,009
30	18,8	0,0139	550	7,7	0,70	550	0,009
31	18,9	0,0135	500	6,7	0,61	500	0,008
32	18,8	0,0130	450	5,8	0,53	450	0,008
33	18,9	0,0125	400	5,0	0,46	400	0,008
34	18,9	0,0115	350	4,0	0,37	350	0,007
35	18,9	0,0106	300	3,2	0,29	300	0,007
36	18,9	0,0096	250	2,4	0,22	250	0,006
37	18,9	0,0078	200	1,6	0,14	200	0,005
38	18,9	0,0067	150	1,0	0,09	150	0,004
39	19,0	0,0049	100	0,5	0,04	100	0,003
40	18,9	0,0108	50	0,5	0,05	50	0,007

Table B-3: For MP15FA25WB075 mix

Sample number	**MP15FA25WB075**		**Density**	**1,592**			
Measuring point	**Temperature [°C]**	**Viscosity [Pa.s]**	**Shear rate [1/s]**	**Shear stress [Pa]**	**Torque [mNm]**	**Speed [1/min]**	**Cinematic viscosity [mm²/s]**
1	18,5	0,0145	50	0,7	0,07	50	0,009
2	18,6	0,0045	100	0,4	0,04	100	0,003
3	18,7	0,0055	150	0,8	0,07	150	0,003
4	18,7	0,0078	200	1,6	0,14	200	0,005
5	18,7	0,0089	250	2,2	0,20	250	0,006
6	18,7	0,0100	300	3,0	0,27	300	0,006
7	18,7	0,0114	350	4,0	0,36	350	0,007
8	18,7	0,0118	400	4,7	0,43	400	0,007
9	18,7	0,0120	450	5,4	0,49	450	0,008
10	18,7	0,0124	500	6,2	0,57	500	0,008
11	18,7	0,0138	550	7,6	0,69	550	0,009
12	18,7	0,0136	600	8,2	0,74	600	0,009
13	18,7	0,0152	650	9,9	0,90	650	0,010
14	18,7	0,0153	700	10,7	0,97	700	0,010
15	18,7	0,0167	750	12,5	1,14	750	0,010
16	18,7	0,0134	800	10,7	0,98	800	0,008
17	18,7	0,0160	850	13,6	1,23	850	0,010
18	18,7	0,0162	900	14,6	1,32	900	0,010
19	18,7	0,0166	950	15,7	1,43	950	0,010
20	18,7	0,0172	1000	17,2	1,57	1000	0,011
21	18,7	0,0174	1000	17,4	1,58	1000	0,011
22	18,7	0,0169	950	16,1	1,46	950	0,011
23	18,7	0,0162	900	14,6	1,32	900	0,010
24	18,7	0,0157	850	13,3	1,21	850	0,010
25	18,7	0,0133	800	10,6	0,96	800	0,008
26	18,7	0,0148	750	11,1	1,01	750	0,009
27	18,7	0,0137	700	9,6	0,87	700	0,009
28	18,7	0,0134	650	8,7	0,79	650	0,008
29	18,7	0,0136	600	8,1	0,74	600	0,009
30	18,7	0,0125	550	6,9	0,62	550	0,008
31	18,7	0,0125	500	6,3	0,57	500	0,008
32	18,7	0,0118	450	5,3	0,48	450	0,007
33	18,7	0,0112	400	4,5	0,41	400	0,007
34	18,7	0,0110	350	3,8	0,35	350	0,007
35	18,7	0,0100	300	3,0	0,27	300	0,006
36	18,7	0,0089	250	2,2	0,20	250	0,006
37	18,7	0,0083	200	1,7	0,15	200	0,005
38	18,7	0,0051	150	0,8	0,07	150	0,003
39	18,7	0,0040	100	0,4	0,04	100	0,003
40	18,7	0,0043	50	0,2	0,02	50	0,003

Table B-4: For MP20FA25WB075 mix

Sample number	**MP20FA25WB075**		**Density**	**1,588**			
Measuring point	**Temperature [°C]**	**Viscosity [Pa.s]**	**Shear rate [1/s]**	**Shear stress [Pa]**	**Torque [mNm]**	**Speed [1/min]**	**Cinematic viscosity [mm²/s]**
1	18,4	0,0266	50	1,3	0,12	50	0,017
2	18,4	0,0054	100	0,5	0,05	100	0,003
3	18,5	0,0070	150	1,1	0,10	150	0,004
4	18,6	0,0081	200	1,6	0,15	200	0,005
5	18,7	0,0104	250	2,6	0,24	250	0,007
6	18,7	0,0113	300	3,4	0,31	300	0,007
7	18,7	0,0114	350	4,0	0,36	350	0,007
8	18,7	0,0118	400	4,7	0,43	400	0,007
9	18,7	0,0127	450	5,7	0,52	450	0,008
10	18,7	0,0134	500	6,7	0,61	500	0,008
11	18,7	0,0138	550	7,6	0,69	550	0,009
12	18,7	0,0139	600	8,3	0,76	600	0,009
13	18,7	0,0146	650	9,5	0,86	650	0,009
14	18,7	0,0139	700	9,7	0,88	700	0,009
15	18,7	0,0158	750	11,9	1,08	750	0,010
16	18,7	0,0164	800	13,1	1,19	800	0,010
17	18,7	0,0170	850	14,4	1,31	850	0,011
18	18,7	0,0175	900	15,7	1,43	900	0,011
19	18,6	0,0182	950	17,3	1,57	950	0,011
20	18,7	0,0187	1000	18,7	1,70	1000	0,012
21	18,6	0,0188	1000	18,8	1,71	1000	0,012
22	18,7	0,0180	950	17,1	1,55	950	0,011
23	18,6	0,0174	900	15,6	1,42	900	0,011
24	18,7	0,0169	850	14,4	1,31	850	0,011
25	18,6	0,0148	800	11,9	1,08	800	0,009
26	18,6	0,0159	750	12,0	1,09	750	0,010
27	18,6	0,0149	700	10,5	0,95	700	0,009
28	18,7	0,0149	650	9,7	0,88	650	0,009
29	18,6	0,0140	600	8,4	0,76	600	0,009
30	18,7	0,0144	550	7,9	0,72	550	0,009
31	18,6	0,0129	500	6,5	0,59	500	0,008
32	18,7	0,0127	450	5,7	0,52	450	0,008
33	18,6	0,0123	400	4,9	0,45	400	0,008
34	18,7	0,0110	350	3,8	0,35	350	0,007
35	18,7	0,0105	300	3,1	0,29	300	0,007
36	18,7	0,0092	250	2,3	0,21	250	0,006
37	18,7	0,0074	200	1,5	0,13	200	0,005
38	18,7	0,0064	150	1,0	0,09	150	0,004
39	18,7	0,0068	100	0,7	0,06	100	0,004
40	18,7	0,0117	50	0,6	0,05	50	0,007

Table B-5: For MP25FA25WB075 mix

Sample number	**MP25FA25WB075**		**Density**	**1,584**			
Measuring point	**Temperature [°C]**	**Viscosity [Pa.s]**	**Shear rate [1/s]**	**Shear stress [Pa]**	**Torque [mNm]**	**Speed [1/min]**	**Cinematic viscosity [mm²/s]**
1	18,2	0,0005	50	0,0	0,00	50	0,0003
2	18,2	0,0012	100	0,1	0,01	100	0,0008
3	18,3	0,0027	150	0,4	0,04	150	0,0017
4	18,3	0,0064	200	1,3	0,12	200	0,0041
5	18,4	0,0076	250	1,9	0,17	250	0,0048
6	18,3	0,0083	300	2,5	0,23	300	0,0052
7	18,3	0,0087	350	3,1	0,28	350	0,0055
8	18,3	0,0097	400	3,9	0,35	400	0,0061
9	18,3	0,0106	450	4,8	0,43	450	0,0067
10	18,4	0,0108	500	5,4	0,49	500	0,0068
11	18,4	0,0116	550	6,4	0,58	550	0,0073
12	18,4	0,0122	600	7,3	0,66	600	0,0077
13	18,4	0,0131	650	8,5	0,77	650	0,0083
14	18,3	0,0129	700	9,0	0,82	700	0,0081
15	18,3	0,0135	750	10,1	0,92	750	0,0085
16	18,3	0,0140	800	11,2	1,02	800	0,0088
17	18,2	0,0142	850	12,1	1,10	850	0,0090
18	18,2	0,0145	900	13,1	1,19	900	0,0092
19	18,1	0,0149	950	14,2	1,29	950	0,0094
20	18,1	0,0154	1000	15,4	1,40	1000	0,0097
21	18,3	0,0161	1000	16,1	1,46	1000	0,0101
22	18,2	0,0149	950	14,2	1,29	950	0,0094
23	18,2	0,0145	900	13,1	1,19	900	0,0092
24	18,1	0,0142	850	12,0	1,10	850	0,0089
25	18,2	0,0137	800	11,0	1,00	800	0,0087
26	18,2	0,0130	750	9,8	0,89	750	0,0082
27	18,3	0,0129	700	9,1	0,82	700	0,0082
28	18,3	0,0124	650	8,1	0,74	650	0,0079
29	18,4	0,0120	600	7,2	0,65	600	0,0076
30	18,4	0,0118	550	6,5	0,59	550	0,0075
31	18,4	0,0109	500	5,4	0,49	500	0,0069
32	18,3	0,0107	450	4,8	0,44	450	0,0068
33	18,4	0,0098	400	3,9	0,36	400	0,0062
34	18,4	0,0093	350	3,2	0,29	350	0,0058
35	18,4	0,0086	300	2,6	0,24	300	0,0054
36	18,4	0,0072	250	1,8	0,16	250	0,0045
37	18,4	0,0055	200	1,1	0,10	200	0,0035
38	18,4	0,0039	150	0,6	0,05	150	0,0025
39	18,4	0,0012	100	0,1	0,01	100	0,0008
40	18,4	0,0000	50	0,0	0,00	50	0,0000

Table B-6: For MP30FA25WB075 mix

Sample number	**MP30FA25WB075**		**Density**	**1,581**			
Measuring point	**Temperature [°C]**	**Viscosity [Pa.s]**	**Shear rate [1/s]**	**Shear stress [Pa]**	**Torque [mNm]**	**Speed [1/min]**	**Cinematic viscosity [mm²/s]**
1	19,4	0,0220	50	1,1	0,10	50	0,0139
2	19,4	0,0128	100	1,3	0,12	100	0,0081
3	19,4	0,0110	150	1,7	0,15	150	0,0070
4	19,3	0,0097	200	1,9	0,18	200	0,0061
5	19,3	0,0111	250	2,8	0,25	250	0,0070
6	19,3	0,0117	300	3,5	0,32	300	0,0074
7	19,4	0,0126	350	4,4	0,40	350	0,0080
8	19,3	0,0131	400	5,2	0,48	400	0,0083
9	19,3	0,0132	450	5,9	0,54	450	0,0084
10	19,3	0,0139	500	7,0	0,63	500	0,0088
11	19,3	0,0144	550	7,9	0,72	550	0,0091
12	19,3	0,0145	600	8,7	0,79	600	0,0092
13	19,2	0,0147	650	9,6	0,87	650	0,0093
14	19,2	0,0134	700	9,4	0,85	700	0,0085
15	19,2	0,0152	750	11,4	1,04	750	0,0096
16	19,2	0,0158	800	12,6	1,15	800	0,0100
17	19,2	0,0161	850	13,7	1,24	850	0,0102
18	19,2	0,0164	900	14,8	1,34	900	0,0104
19	19,2	0,0165	950	15,7	1,43	950	0,0104
20	19,2	0,0170	1000	17,0	1,54	1000	0,0107
21	19,2	0,0173	1000	17,3	1,57	1000	0,0109
22	19,2	0,0165	950	15,7	1,43	950	0,0104
23	19,2	0,0162	900	14,6	1,32	900	0,0102
24	19,2	0,0158	850	13,4	1,22	850	0,0100
25	19,3	0,0156	800	12,5	1,14	800	0,0099
26	19,2	0,0151	750	11,3	1,03	750	0,0096
27	19,2	0,0137	700	9,6	0,87	700	0,0087
28	19,2	0,0147	650	9,6	0,87	650	0,0093
29	19,2	0,0143	600	8,6	0,78	600	0,0091
30	19,2	0,0139	550	7,6	0,69	550	0,0088
31	19,2	0,0136	500	6,8	0,62	500	0,0086
32	19,3	0,0133	450	6,0	0,54	450	0,0084
33	19,2	0,0128	400	5,1	0,46	400	0,0081
34	19,2	0,0127	350	4,5	0,40	350	0,0080
35	19,2	0,0124	300	3,7	0,34	300	0,0078
36	19,1	0,0120	250	3,0	0,27	250	0,0076
37	19,2	0,0106	200	2,1	0,19	200	0,0067
38	19,2	0,0101	150	1,5	0,14	150	0,0064
39	19,2	0,0124	100	1,2	0,11	100	0,0078
40	19,2	0,0154	50	0,8	0,07	50	0,0098

Table B-7: For MP0FA0WB100 mix

Sample number	MP0FA0WB100		Density	1,508			
Measuring point	**Temperature [°C]**	**Viscosity [Pa.s]**	**Shear rate [1/s]**	**Shear stress [Pa]**	**Torque [mNm]**	**Speed [1/min]**	**Cinematic viscosity [mm²/s]**
1	18,7	0,0000	50	0,0	0,00	50	0,0000
2	18,7	0,0000	100	0,0	0,00	100	0,0000
3	18,9	0,0012	150	0,2	0,01	150	0,0008
4	19,0	0,0029	200	0,6	0,05	200	0,0019
5	19,0	0,0044	250	1,1	0,10	250	0,0029
6	19,0	0,0052	300	1,6	0,14	300	0,0035
7	19,0	0,0053	350	1,8	0,17	350	0,0035
8	19,0	0,0060	400	2,4	0,22	400	0,0040
9	19,0	0,0070	450	3,1	0,29	450	0,0046
10	19,0	0,0072	500	3,6	0,33	500	0,0048
11	19,0	0,0078	550	4,3	0,39	550	0,0051
12	19,0	0,0082	600	4,9	0,45	600	0,0054
13	19,0	0,0085	650	5,5	0,50	650	0,0056
14	19,1	0,0094	700	6,6	0,60	700	0,0062
15	19,0	0,0104	750	7,8	0,71	750	0,0069
16	19,0	0,0102	800	8,2	0,74	800	0,0068
17	19,1	0,0109	850	9,2	0,84	850	0,0072
18	19,1	0,0112	900	10,0	0,91	900	0,0074
19	19,0	0,0116	950	11,1	1,01	950	0,0077
20	19,1	0,0120	1000	12,0	1,10	1000	0,0080
21	19,0	0,0124	1000	12,4	1,13	1000	0,0082
22	19,0	0,0117	950	11,1	1,01	950	0,0078
23	19,1	0,0112	900	10,1	0,92	900	0,0074
24	19,1	0,0106	850	9,0	0,82	850	0,0070
25	19,1	0,0103	800	8,2	0,75	800	0,0068
26	19,1	0,0096	750	7,2	0,59	750	0,0064
27	19,1	0,0095	700	6,6	0,67	700	0,0063
28	19,1	0,0089	650	5,8	0,47	650	0,0059
29	19,0	0,0084	600	5,0	0,46	600	0,0055
30	19,1	0,0083	550	4,6	0,42	550	0,0055
31	19,0	0,0070	500	3,5	0,32	500	0,0047
32	19,1	0,0068	450	3,1	0,28	450	0,0045
33	19,0	0,0061	400	2,4	0,22	400	0,0041
34	19,0	0,0051	350	1,8	0,16	350	0,0034
35	19,0	0,0043	300	1,3	0,12	300	0,0028
36	19,0	0,0036	250	0,9	0,08	250	0,0024
37	19,0	0,0025	200	0,5	0,04	200	0,0016
38	19,0	0,0015	150	0,2	0,01	150	0,0010
39	19,0	0,0000	100	0,0	0,00	100	0,0000
40	19,0	0,0000	50	0,0	0,00	50	0,0000

Table B-8: For MP10FA25WB100 mix

Sample number	**MP10FA25WB100**		**Density**	**1,486**			
Measuring point	**Temperature [°C]**	**Viscosity [Pa.s]**	**Shear rate [1/s]**	**Shear stress [Pa]**	**Torque [mNm]**	**Speed [1/min]**	**Cinematic viscosity [mm²/s]**
1	18,1	0,0000	50	0,00	0,00	50	0,0000
2	18,2	0,0000	100	0,00	0,00	100	0,0000
3	18,4	0,0000	150	0,0	0,00	150	0,0000
4	18,4	0,0022	200	0,4	0,04	200	0,0015
5	18,4	0,0033	250	0,8	0,07	250	0,0022
6	18,4	0,0046	300	1,4	0,13	300	0,0031
7	18,5	0,0047	350	1,7	0,15	350	0,0032
8	18,5	0,0060	400	2,4	0,22	400	0,0040
9	18,5	0,0060	450	2,7	0,24	450	0,0040
10	18,6	0,0056	500	2,8	0,25	500	0,0037
11	18,5	0,0078	550	4,3	0,39	550	0,0052
12	18,5	0,0086	600	5,2	0,47	600	0,0058
13	18,5	0,0089	650	5,8	0,52	650	0,0060
14	18,5	0,0093	700	6,5	0,59	700	0,0063
15	18,5	0,0097	750	7,3	0,66	750	0,0065
16	18,5	0,0104	800	8,3	0,76	800	0,0070
17	18,5	0,0108	850	9,2	0,84	850	0,0073
18	18,4	0,0113	900	10,1	0,92	900	0,0076
19	18,4	0,0116	950	11,0	1,00	950	0,0078
20	18,3	0,0120	1000	12,0	1,10	1000	0,0081
21	18,5	0,0124	1000	12,4	1,12	1000	0,0083
22	18,5	0,0116	950	11,0	1,00	950	0,0078
23	18,4	0,0113	900	10,1	0,92	900	0,0076
24	18,4	0,0107	850	9,1	0,83	850	0,0072
25	18,4	0,0102	800	8,1	0,74	800	0,0068
26	18,5	0,0098	750	7,3	0,67	750	0,0066
27	18,5	0,0104	700	7,3	0,66	700	0,0070
28	18,5	0,0076	650	5,0	0,45	650	0,0051
29	18,5	0,0082	600	4,9	0,45	600	0,0055
30	18,5	0,0079	550	4,4	0,40	550	0,0053
31	18,5	0,0066	500	3,3	0,30	500	0,0044
32	18,5	0,0062	450	2,8	0,25	450	0,0041
33	18,5	0,0058	400	2,3	0,21	400	0,0039
34	18,5	0,0050	350	1,8	0,16	350	0,0034
35	18,5	0,0038	300	1,1	0,10	300	0,0026
36	18,5	0,0025	250	0,6	0,06	250	0,0017
37	18,5	0,0015	200	0,3	0,03	200	0,0010
38	18,5	0,0000	150	0,0	0,00	150	0,0000
39	18,5	0,0000	100	0,00	0,00	100	0,0000
40	18,5	0,0000	50	0,00	0,00	50	0,0000

Table B-9: For MP15FA25WB100 mix

Sample number	**MP15FA25WB100**		**Density**	**1,483**			
Measuring point	**Temperature [°C]**	**Viscosity [Pa.s]**	**Shear rate [1/s]**	**Shear stress [Pa]**	**Torque [mNm]**	**Speed [1/min]**	**Cinematic viscosity [mm²/s]**
1	18,5	0,0000	50	0,00	0,00	50	0,0000
2	18,5	0,0000	100	0,00	0,00	100	0,0000
3	18,5	0,0000	150	0,0	0,00	150	0,0000
4	18,5	0,0029	200	0,6	0,05	200	0,0020
5	18,5	0,0046	250	1,1	0,10	250	0,0031
6	18,5	0,0051	300	1,5	0,14	300	0,0034
7	18,5	0,0051	350	1,8	0,16	350	0,0035
8	18,6	0,0059	400	2,4	0,21	400	0,0040
9	18,6	0,0070	450	3,1	0,29	450	0,0047
10	18,5	0,0081	500	4,0	0,37	500	0,0054
11	18,6	0,0083	550	4,6	0,42	550	0,0056
12	18,6	0,0080	600	4,8	0,44	600	0,0054
13	18,6	0,0099	650	6,4	0,58	650	0,0066
14	18,6	0,0105	700	7,3	0,67	700	0,0071
15	18,6	0,0091	750	6,8	0,62	750	0,0061
16	18,6	0,0106	800	8,5	0,77	800	0,0071
17	18,6	0,0110	850	9,3	0,85	850	0,0074
18	18,7	0,0114	900	10,3	0,93	900	0,0077
19	18,7	0,0118	950	11,3	1,02	950	0,0080
20	18,7	0,0122	1000	12,2	1,11	1000	0,0082
21	18,6	0,0124	1000	12,4	1,13	1000	0,0084
22	18,6	0,0119	950	11,3	1,03	950	0,0081
23	18,6	0,0114	900	10,2	0,93	900	0,0077
24	18,7	0,0110	850	9,5	0,85	850	0,0074
25	18,6	0,0104	800	8,3	0,76	800	0,0070
26	18,6	0,0098	750	7,4	0,67	750	0,0066
27	18,6	0,0096	700	6,7	0,61	700	0,0064
28	18,6	0,0079	650	5,2	0,47	650	0,0053
29	18,6	0,0085	600	5,1	0,46	600	0,0057
30	18,6	0,0081	550	4,5	0,40	550	0,0055
31	18,6	0,0073	500	3,7	0,33	500	0,0049
32	18,6	0,0067	450	3,0	0,27	450	0,0045
33	18,6	0,0060	400	2,4	0,22	400	0,0040
34	18,5	0,0049	350	1,7	0,15	350	0,0033
35	18,6	0,0038	300	1,1	0,10	300	0,0026
36	18,6	0,0031	250	0,8	0,07	250	0,0021
37	18,5	0,0018	200	0,4	0,03	200	0,0012
38	18,6	0,0000	150	0,0	0,00	150	0,0000
39	18,6	0,0000	100	0,00	0,00	100	0,0000
40	18,6	0,0000	50	0,00	0,00	50	0,0000

Table B-10: For MP20FA25WB100 mix

Sample number	MP20FA25WB100		Density	1,480			
Measuring point	Temperature [°C]	Viscosity [Pa.s]	Shear rate [1/s]	Shear stress [Pa]	Torque [mNm]	Speed [1/min]	Cinematic viscosity [mm²/s]
1	18,1	0,00000	50	0,000	0,00	50	0,00000
2	18,2	0,00000	100	0,00	0,00	100	0,0000
3	18,3	0,00018	150	0,0	0,00	150	0,0001
4	18,4	0,00200	200	0,4	0,04	200	0,0013
5	18,5	0,00309	250	0,8	0,07	250	0,0021
6	18,5	0,00428	300	1,3	0,12	300	0,0029
7	18,5	0,00553	350	1,9	0,18	350	0,0037
8	18,5	0,00612	400	2,4	0,22	400	0,0041
9	18,5	0,00668	450	3,0	0,27	450	0,0045
10	18,5	0,00779	500	3,9	0,35	500	0,0053
11	18,5	0,00809	550	4,5	0,40	550	0,0055
12	18,5	0,00866	600	5,2	0,47	600	0,0059
13	18,5	0,00936	650	6,1	0,55	650	0,0063
14	18,5	0,01002	700	7,0	0,64	700	0,0068
15	18,5	0,00892	750	6,7	0,61	750	0,0060
16	18,5	0,01191	800	9,5	0,87	800	0,0080
17	18,5	0,01110	850	9,4	0,86	850	0,0075
18	18,4	0,01173	900	10,6	0,96	900	0,0079
19	18,4	0,01194	950	11,3	1,03	950	0,0081
20	18,4	0,01242	1000	12,4	1,13	1000	0,0084
21	18,4	0,01260	1000	12,6	1,15	1000	0,0085
22	18,4	0,01189	950	11,3	1,03	950	0,0080
23	18,4	0,01137	900	10,2	0,93	900	0,0077
24	18,4	0,01110	850	9,4	0,86	850	0,0075
25	18,4	0,01086	800	8,7	0,79	800	0,0073
26	18,4	0,01028	750	7,7	0,70	750	0,0069
27	18,4	0,01128	700	7,9	0,72	700	0,0076
28	18,4	0,00757	650	4,9	0,45	650	0,0051
29	18,4	0,00758	600	4,5	0,41	600	0,0051
30	18,5	0,00759	550	4,2	0,38	550	0,0051
31	18,4	0,00751	500	3,8	0,34	500	0,0051
32	18,4	0,00648	450	2,9	0,26	450	0,0044
33	18,4	0,00577	400	2,3	0,21	400	0,0039
34	18,4	0,00567	350	2,0	0,18	350	0,0038
35	18,4	0,00444	300	1,3	0,12	300	0,0030
36	18,4	0,00346	250	0,9	0,08	250	0,0023
37	18,4	0,00246	200	0,5	0,04	200	0,0017
38	18,4	0,00000	150	0,0	0,00	150	0,0000
39	18,4	0,00000	100	0,00	0,00	100	0,0000
40	18,5	0,00000	50	0,00	0,00	50	0,00000

Table B-11: For MP25FA25WB100 mix

Sample number	**MP25FA25WB100**		**Density**	**1,477**			
Measuring point	**Temperature [°C]**	**Viscosity [Pa.s]**	**Shear rate [1/s]**	**Shear stress [Pa]**	**Torque [mNm]**	**Speed [1/min]**	**Cinematic viscosity [mm²/s]**
1	17,8	0,0000	50	0,00	0,00	50	0,0000
2	17,9	0,0000	100	0,00	0,00	100	0,0000
3	17,9	0,0000	150	0,0	0,00	150	0,0000
4	18,1	0,0022	200	0,4	0,04	200	0,0015
5	18,1	0,0038	250	1,0	0,09	250	0,0026
6	18,1	0,0047	300	1,4	0,13	300	0,0032
7	18,1	0,0051	350	1,8	0,16	350	0,0035
8	18,1	0,0058	400	2,3	0,21	400	0,0039
9	18,1	0,0066	450	3,0	0,27	450	0,0045
10	18,1	0,0064	500	3,2	0,29	500	0,0043
11	18,2	0,0073	550	4,0	0,37	550	0,0050
12	18,2	0,0081	600	4,9	0,44	600	0,0055
13	18,1	0,0083	650	5,4	0,49	650	0,0056
14	18,1	0,0099	700	6,9	0,63	700	0,0067
15	18,1	0,0105	750	7,9	0,71	750	0,0071
16	18,1	0,0099	800	7,9	0,72	800	0,0067
17	18,1	0,0103	850	8,7	0,79	850	0,0070
18	18,1	0,0106	900	9,6	0,87	900	0,0072
19	18,1	0,0114	950	10,8	0,98	950	0,0077
20	18,1	0,0118	1000	11,8	1,07	1000	0,0080
21	18,1	0,0120	1000	12,0	1,09	1000	0,0081
22	18,1	0,0115	950	10,9	0,99	950	0,0078
23	18,1	0,0110	900	9,9	0,90	900	0,0074
24	18,1	0,0104	850	8,8	0,80	850	0,0070
25	18,1	0,0109	800	8,7	0,79	800	0,0074
26	18,1	0,0100	750	7,5	0,68	750	0,0068
27	18,1	0,0096	700	6,7	0,61	700	0,0065
28	18,1	0,0086	650	5,6	0,51	650	0,0058
29	18,1	0,0068	600	4,1	0,37	600	0,0046
30	18,1	0,0072	550	4,0	0,36	550	0,0049
31	18,1	0,0069	500	3,5	0,32	500	0,0047
32	18,1	0,0064	450	2,9	0,26	450	0,0043
33	18,1	0,0054	400	2,2	0,20	400	0,0037
34	18,1	0,0050	350	1,8	0,16	350	0,0034
35	18,1	0,0040	300	1,2	0,11	300	0,0027
36	18,1	0,0035	250	0,9	0,08	250	0,0023
37	18,1	0,0027	200	0,5	0,05	200	0,0018
38	18,1	0,0000	150	0,0	0,00	150	0,0000
39	18,1	0,0000	100	0,00	0,00	100	0,0000
40	18,1	0,0000	50	0,00	0,00	50	0,0000

Table B-12: For MP30FA25WB100 mix

Sample number	**MP30FA25WB100**		**Density**	**1,475**			
Measuring point	**Temperature [°C]**	**Viscosity [Pa.s]**	**Shear rate [1/s]**	**Shear stress [Pa]**	**Torque [mNm]**	**Speed [1/min]**	**Cinematic viscosity [mm²/s]**
1	17,9	0,00000	50	0,000	0,00	50	0,00000
2	17,9	0,00000	100	0,00	0,00	100	0,0000
3	18,0	0,00000	150	0,00	0,00	150	0,0000
4	18,1	0,00223	200	0,45	0,04	200	0,0015
5	18,1	0,00383	250	0,96	0,09	250	0,0026
6	18,1	0,00459	300	1,38	0,13	300	0,0031
7	18,2	0,00540	350	1,89	0,17	350	0,0037
8	18,1	0,00647	400	2,59	0,24	400	0,0044
9	18,1	0,00710	450	3,19	0,29	450	0,0048
10	18,1	0,00685	500	3,43	0,31	500	0,0046
11	18,1	0,00826	550	4,55	0,41	550	0,0056
12	18,1	0,00882	600	5,29	0,48	600	0,0060
13	18,1	0,00964	650	6,27	0,57	650	0,0065
14	18,1	0,01135	700	7,95	0,72	700	0,0077
15	18,1	0,01053	750	7,90	0,72	750	0,0071
16	18,1	0,01104	800	8,83	0,80	800	0,0075
17	18,1	0,01143	850	9,72	0,88	850	0,0078
18	18,1	0,01209	900	10,88	0,99	900	0,0082
19	18,1	0,01248	950	11,86	1,08	950	0,0085
20	18,1	0,01302	1000	13,02	1,18	1000	0,0088
21	18,1	0,01307	1000	13,07	1,19	1000	0,0089
22	18,1	0,01239	950	11,77	1,07	950	0,0084
23	18,1	0,01188	900	10,69	0,97	900	0,0081
24	18,1	0,01160	850	9,86	0,90	850	0,0079
25	18,1	0,01121	800	8,97	0,82	800	0,0076
26	18,1	0,00886	750	6,64	0,60	750	0,0060
27	18,1	0,01022	700	7,15	0,65	700	0,0069
28	18,1	0,00921	650	5,99	0,54	650	0,0062
29	18,1	0,00944	600	5,66	0,51	600	0,0064
30	18,1	0,00843	550	4,64	0,42	550	0,0057
31	18,1	0,00835	500	4,17	0,38	500	0,0057
32	18,1	0,00689	450	3,10	0,28	450	0,0047
33	18,1	0,00659	400	2,64	0,24	400	0,0045
34	18,1	0,00553	350	1,94	0,18	350	0,0038
35	18,1	0,00506	300	1,52	0,14	300	0,0034
36	18,0	0,00365	250	0,91	0,08	250	0,0025
37	18,1	0,00200	200	0,40	0,04	200	0,0014
38	18,1	0,00018	150	0,03	0,00	150	0,0001
39	18,1	0,00000	100	0,00	0,00	100	0,0000
40	18,1	0,00000	50	0,000	0,00	50	0,00000

Table B-13: For MP0FA0WB125 mix

Sample number	**MP0FA0WB125**		**Density**	**1,426**			
Measuring point	**Temperature [°C]**	**Viscosity [Pa.s]**	**Shear rate [1/s]**	**Shear stress [Pa]**	**Torque [mNm]**	**Speed [1/min]**	**Cinematic viscosity [mm²/s]**
1	18,9	0,0000	50	0,00	0,00	50	0,00000
2	18,9	0,0000	100	0,00	0,00	100	0,0000
3	18,9	0,0000	150	0,00	0,00	150	0,0000
4	19,0	0,0013	200	0,26	0,00	200	0,0009
5	19,0	0,0014	250	0,35	0,03	250	0,0010
6	19,0	0,0024	300	0,73	0,07	300	0,0017
7	19,0	0,0038	350	1,33	0,12	350	0,0027
8	19,0	0,0047	400	1,89	0,17	400	0,0033
9	19,0	0,0050	450	2,26	0,21	450	0,0035
10	19,0	0,0065	500	3,24	0,29	500	0,0045
11	19,0	0,0064	550	3,65	0,32	550	0,0045
12	19,0	0,0073	600	4,36	0,40	600	0,0051
13	19,0	0,0076	650	4,92	0,45	650	0,0053
14	19,0	0,0079	700	5,52	0,50	700	0,0055
15	19,0	0,0084	750	6,32	0,57	750	0,0059
16	19,0	0,0091	800	7,29	0,66	800	0,0064
17	19,0	0,0097	850	8,27	0,75	850	0,0068
18	19,1	0,0101	900	9,11	0,83	900	0,0071
19	19,0	0,0106	950	10,04	0,91	950	0,0074
20	19,0	0,0109	1000	10,88	0,99	1000	0,0076
21	19,0	0,0112	1000	11,16	1,01	1000	0,0078
22	19,0	0,0106	950	10,09	0,92	950	0,0074
23	19,0	0,0101	900	9,11	0,83	900	0,0071
24	19,0	0,0105	850	8,94	0,74	850	0,0074
25	19,0	0,0102	800	8,13	0,74	800	0,0071
26	19,0	0,0098	750	7,34	0,60	750	0,0069
27	19,1	0,0096	700	6,73	0,61	700	0,0067
28	19,0	0,0084	650	5,47	0,38	650	0,0059
29	19,0	0,0074	600	4,45	0,40	600	0,0052
30	19,0	0,0066	550	3,65	0,28	550	0,0047
31	19,0	0,0059	500	2,96	0,27	500	0,0042
32	19,0	0,0052	450	2,36	0,21	450	0,0037
33	19,0	0,0040	400	1,61	0,15	400	0,0028
34	19,0	0,0034	350	1,19	0,11	350	0,0024
35	19,0	0,0029	300	0,86	0,08	300	0,0020
36	19,0	0,0014	250	0,35	0,03	250	0,0010
37	19,0	0,0000	200	0,00	0,00	200	0,0000
38	19,0	0,0000	150	0,00	0,00	150	0,0000
39	19,0	0,0000	100	0,00	0,00	100	0,0000
40	18,8	0,0000	50	0,00	0,00	50	0,00000

Table B-14: For MP10FA25WB125 mix

Sample number	MP10FA25WB125		Density	1,410			
Measuring point	Temperature [°C]	Viscosity [Pa.s]	Shear rate [1/s]	Shear stress [Pa]	Torque [mNm]	Speed [1/min]	Cinematic viscosity [mm²/s]
1	18,1	0,0000	50	0,00	0,00	50	0,0000
2	18,2	0,0000	100	0,00	0,00	100	0,0000
3	18,4	0,0000	150	0,00	0,00	150	0,0000
4	18,4	0,0004	200	0,00	0,01	200	0,0003
5	18,5	0,0012	250	0,31	0,03	250	0,0009
6	18,4	0,0024	300	0,73	0,07	300	0,0017
7	18,4	0,0029	350	1,00	0,09	350	0,0020
8	18,5	0,0036	400	1,42	0,13	400	0,0025
9	18,4	0,0047	450	2,12	0,19	450	0,0033
10	18,5	0,0066	500	3,29	0,30	500	0,0047
11	18,4	0,0061	550	3,38	0,31	550	0,0044
12	18,4	0,0065	600	3,89	0,35	600	0,0046
13	18,4	0,0061	650	3,94	0,36	650	0,0043
14	18,4	0,0081	700	5,66	0,51	700	0,0057
15	18,4	0,0080	750	5,99	0,54	750	0,0057
16	18,4	0,0082	800	6,78	0,60	800	0,0058
17	18,4	0,0088	850	7,67	0,68	850	0,0062
18	18,4	0,0095	900	8,51	0,77	900	0,0067
19	18,4	0,0097	950	9,25	0,84	950	0,0069
20	18,4	0,0101	1000	10,14	0,92	1000	0,0072
21	18,3	0,0104	1000	10,37	0,94	1000	0,0074
22	18,4	0,0096	950	9,11	0,83	950	0,0068
23	18,4	0,0092	900	8,32	0,76	900	0,0066
24	18,4	0,0089	850	7,53	0,68	850	0,0063
25	18,4	0,0100	800	8,04	0,73	800	0,0071
26	18,4	0,0079	750	5,90	0,54	750	0,0056
27	18,4	0,0082	700	5,76	0,52	700	0,0058
28	18,4	0,0072	650	4,68	0,43	650	0,0051
29	18,4	0,0065	600	3,89	0,35	600	0,0046
30	18,3	0,0061	550	3,33	0,30	550	0,0043
31	18,4	0,0049	500	2,45	0,22	500	0,0035
32	18,4	0,0046	450	2,08	0,19	450	0,0033
33	18,4	0,0036	400	1,42	0,13	400	0,0025
34	18,4	0,0034	350	1,19	0,11	350	0,0024
35	18,4	0,0018	300	0,54	0,05	300	0,0013
36	18,4	0,0010	250	0,26	0,02	250	0,0007
37	18,4	0,0000	200	0,00	0,00	200	0,0000
38	18,4	0,0000	150	0,00	0,00	150	0,0000
39	18,4	0,0000	100	0,00	0,00	100	0,0000
40	18,4	0,0000	50	0,00	0,00	50	0,00000

Table B-15: For MP15FA25WB125 mix

Sample number	MP15FA25WB125		Density	1,408			
Measuring point	Temperature [°C]	Viscosity [Pa.s]	Shear rate [1/s]	Shear stress [Pa]	Torque [mNm]	Speed [1/min]	Cinematic viscosity [mm²/s]
1	17,4	0,0000	50	0,00	0,00	50	0,0000
2	17,6	0,0000	100	0,00	0,00	100	0,0000
3	17,7	0,0000	150	0,00	0,00	150	0,0000
4	17,8	0,0000	200	0,00	0,00	200	0,0000
5	17,9	0,0003	250	0,07	0,01	250	0,0002
6	17,8	0,0015	300	0,45	0,04	300	0,0011
7	17,8	0,0033	350	1,14	0,10	350	0,0023
8	17,8	0,0040	400	1,61	0,15	400	0,0029
9	17,7	0,0046	450	2,08	0,19	450	0,0033
10	17,7	0,0050	500	2,50	0,23	500	0,0035
11	17,7	0,0059	550	3,24	0,29	550	0,0042
12	17,6	0,0048	600	2,87	0,26	600	0,0034
13	17,5	0,0053	650	3,47	0,32	650	0,0038
14	17,6	0,0070	700	4,92	0,45	700	0,0050
15	17,5	0,0079	750	5,94	0,54	750	0,0056
16	17,4	0,0084	800	6,69	0,61	800	0,0059
17	17,4	0,0087	850	7,39	0,67	850	0,0062
18	17,3	0,0093	900	8,36	0,76	900	0,0066
19	17,2	0,0099	950	9,44	0,86	950	0,0071
20	17,2	0,0104	1000	10,37	0,94	1000	0,0074
21	17,3	0,0102	1000	10,23	0,93	1000	0,0073
22	17,3	0,0099	950	9,39	0,85	950	0,0070
23	17,3	0,0092	900	8,27	0,75	900	0,0065
24	17,3	0,0090	850	7,62	0,69	850	0,0064
25	17,3	0,0096	800	7,67	0,70	800	0,0068
26	17,2	0,0080	750	6,04	0,55	750	0,0057
27	17,3	0,0082	700	5,76	0,52	700	0,0058
28	17,3	0,0073	650	4,73	0,43	650	0,0052
29	17,3	0,0049	600	2,96	0,27	600	0,0035
30	17,2	0,0060	550	3,29	0,30	550	0,0042
31	17,3	0,0053	500	2,64	0,24	500	0,0037
32	17,2	0,0043	450	1,94	0,18	450	0,0031
33	17,2	0,0036	400	1,42	0,13	400	0,0025
34	17,3	0,0033	350	1,14	0,10	350	0,0023
35	17,3	0,0016	300	0,49	0,04	300	0,0012
36	17,4	0,0012	250	0,31	0,03	250	0,0009
37	17,4	0,0000	200	0,00	0,00	200	0,0000
38	17,4	0,0000	150	0,00	0,00	150	0,0000
39	17,5	0,0000	100	0,00	0,00	100	0,0000
40	17,6	0,0000	50	0,00	0,00	50	0,00000

Table B-16: For MP20FA25WB125 mix

Sample number	MP20FA25WB125		Density	1,405			
Measuring point	Temperature [°C]	Viscosity [Pa.s]	Shear rate [1/s]	Shear stress [Pa]	Torque [mNm]	Speed [1/min]	Cinematic viscosity [mm²/s]
1	17,5	0,0000	50	0,00	0,00	50	0,0000
2	17,6	0,0000	100	0,00	0,00	100	0,0000
3	17,6	0,0000	150	0,00	0,00	150	0,0000
4	17,7	0,0000	200	0,00	0,00	200	0,0000
5	17,8	0,0010	250	0,26	0,02	250	0,0007
6	17,7	0,0024	300	0,73	0,07	300	0,0017
7	17,7	0,0034	350	1,19	0,11	350	0,0024
8	17,7	0,0046	400	1,84	0,17	400	0,0033
9	17,7	0,0052	450	2,36	0,21	450	0,0037
10	17,7	0,0068	500	3,38	0,31	500	0,0048
11	17,7	0,0066	550	3,61	0,33	550	0,0047
12	17,7	0,0066	600	3,99	0,36	600	0,0047
13	17,7	0,0076	650	4,92	0,45	650	0,0054
14	17,7	0,0093	700	6,50	0,59	700	0,0066
15	17,7	0,0085	750	6,41	0,58	750	0,0061
16	17,7	0,0073	800	5,80	0,53	800	0,0052
17	17,6	0,0095	850	8,09	0,74	850	0,0068
18	17,6	0,0098	900	8,78	0,80	900	0,0069
19	17,7	0,0103	950	9,76	0,89	950	0,0073
20	17,7	0,0107	1000	10,74	0,98	1000	0,0076
21	17,7	0,0110	1000	10,97	1,00	1000	0,0078
22	17,7	0,0104	950	9,86	0,90	950	0,0074
23	17,7	0,0100	900	8,97	0,82	900	0,0071
24	17,7	0,0094	850	7,99	0,73	850	0,0067
25	17,7	0,0102	800	8,13	0,74	800	0,0072
26	17,7	0,0094	750	7,01	0,64	750	0,0067
27	17,7	0,0067	700	4,69	0,43	700	0,0048
28	17,7	0,0079	650	5,10	0,46	650	0,0056
29	17,7	0,0069	600	4,13	0,38	600	0,0049
30	17,7	0,0065	550	3,57	0,32	550	0,0046
31	17,7	0,0065	500	3,24	0,29	500	0,0046
32	17,7	0,0053	450	2,40	0,22	450	0,0038
33	17,7	0,0046	400	1,84	0,17	400	0,0033
34	17,7	0,0034	350	1,19	0,11	350	0,0024
35	17,7	0,0027	300	0,82	0,07	300	0,0019
36	17,7	0,0014	250	0,35	0,03	250	0,0010
37	17,7	0,0000	200	0,00	0,00	200	0,0000
38	17,7	0,0000	150	0,00	0,00	150	0,0000
39	17,7	0,0000	100	0,00	0,00	100	0,0000
40	17,7	0,0000	50	0,00	0,00	50	0,00000

Table B-17: For MP25FA25WB125 mix

Sample number	**MP25FA25WB125**		**Density**	**1,403**			
Measuring point	**Temperature [°C]**	**Viscosity [Pa.s]**	**Shear rate [1/s]**	**Shear stress [Pa]**	**Torque [mNm]**	**Speed [1/min]**	**Cinematic viscosity [mm²/s]**
1	17,6	0,0000	50	0,00	0,00	50	0,0000
2	17,7	0,0000	100	0,00	0,00	100	0,0000
3	17,8	0,0000	150	0,00	0,00	150	0,0000
4	17,9	0,0006	200	0,12	0,01	200	0,0004
5	17,9	0,0022	250	0,54	0,05	250	0,0015
6	18,0	0,0030	300	0,91	0,08	300	0,0022
7	18,0	0,0047	350	1,66	0,15	350	0,0034
8	18,0	0,0057	400	2,26	0,21	400	0,0040
9	18,1	0,0059	450	2,64	0,24	450	0,0042
10	18,1	0,0069	500	3,47	0,32	500	0,0050
11	18,1	0,0082	550	4,50	0,41	550	0,0058
12	18,1	0,0080	600	4,82	0,44	600	0,0057
13	18,1	0,0081	650	5,24	0,48	650	0,0057
14	18,1	0,0097	700	6,78	0,62	700	0,0069
15	18,1	0,0108	750	8,09	0,74	750	0,0077
16	18,1	0,0117	800	9,34	0,85	800	0,0083
17	18,1	0,0106	850	8,97	0,82	850	0,0075
18	18,0	0,0110	900	9,90	0,90	900	0,0078
19	18,1	0,0115	950	10,88	0,99	950	0,0082
20	18,1	0,0118	1000	11,81	1,07	1000	0,0084
21	18,1	0,0120	1000	12,00	1,09	1000	0,0086
22	18,1	0,0114	950	10,83	0,98	950	0,0081
23	18,1	0,0108	900	9,72	0,88	900	0,0077
24	18,1	0,0104	850	8,83	0,80	850	0,0074
25	18,1	0,0112	800	8,97	0,82	800	0,0080
26	18,1	0,0099	750	7,43	0,68	750	0,0071
27	18,1	0,0108	700	7,57	0,69	700	0,0077
28	18,1	0,0077	650	5,01	0,46	650	0,0055
29	18,1	0,0082	600	4,92	0,45	600	0,0058
30	18,1	0,0080	550	4,41	0,40	550	0,0057
31	18,1	0,0069	500	3,47	0,32	500	0,0050
32	18,1	0,0060	450	2,68	0,24	450	0,0042
33	18,1	0,0050	400	1,98	0,18	400	0,0035
34	18,1	0,0046	350	1,61	0,15	350	0,0033
35	18,1	0,0035	300	1,05	0,10	300	0,0025
36	18,1	0,0025	250	0,63	0,06	250	0,0018
37	18,1	0,0001	200	0,03	0,00	200	0,0001
38	18,1	0,0000	150	0,00	0,00	150	0,0000
39	18,1	0,0000	100	0,00	0,00	100	0,0000
40	18,1	0,0000	50	0,00	0,00	50	0,0000

Table B-18: For MP30FA25WB125 mix

Sample number	**MP30FA25WB125**		**Density**	**1,401**			
Measuring point	**Temperature [°C]**	**Viscosity [Pa.s]**	**Shear rate [1/s]**	**Shear stress [Pa]**	**Torque [mNm]**	**Speed [1/min]**	**Cinematic viscosity [mm²/s]**
1	17,9	0,0000	50	0,00	0,00	50	0,0000
2	18,0	0,0000	100	0,00	0,00	100	0,0000
3	18,0	0,0000	150	0,00	0,00	150	0,0000
4	18,1	0,0000	200	0,00	0,00	200	0,0000
5	18,1	0,0007	250	0,17	0,02	250	0,0005
6	18,1	0,0021	300	0,63	0,06	300	0,0015
7	18,1	0,0038	350	1,33	0,12	350	0,0027
8	18,1	0,0041	400	1,66	0,15	400	0,0030
9	18,1	0,0054	450	2,45	0,22	450	0,0039
10	18,1	0,0061	500	3,05	0,28	500	0,0044
11	18,2	0,0061	550	3,33	0,30	550	0,0043
12	18,1	0,0067	600	4,03	0,37	600	0,0048
13	18,1	0,0077	650	5,01	0,46	650	0,0055
14	18,1	0,0094	700	6,55	0,60	700	0,0067
15	18,1	0,0087	750	6,50	0,59	750	0,0062
16	18,1	0,0099	800	7,90	0,72	800	0,0070
17	18,1	0,0096	850	8,18	0,74	850	0,0069
18	18,1	0,0101	900	9,06	0,82	900	0,0072
19	18,1	0,0104	950	9,86	0,90	950	0,0074
20	18,1	0,0109	1000	10,93	0,99	1000	0,0078
21	18,1	0,0111	1000	11,07	1,01	1000	0,0079
22	18,1	0,0104	950	9,90	0,90	950	0,0074
23	18,1	0,0099	900	8,92	0,81	900	0,0071
24	18,1	0,0095	850	8,09	0,74	850	0,0068
25	18,1	0,0107	800	8,60	0,78	800	0,0077
26	18,1	0,0089	750	6,64	0,60	750	0,0063
27	18,1	0,0093	700	6,50	0,59	700	0,0066
28	18,1	0,0079	650	5,10	0,46	650	0,0056
29	18,1	0,0063	600	3,80	0,35	600	0,0045
30	18,1	0,0073	550	4,03	0,37	550	0,0052
31	18,1	0,0059	500	2,96	0,27	500	0,0042
32	18,1	0,0049	450	2,22	0,20	450	0,0035
33	18,2	0,0046	400	1,84	0,17	400	0,0033
34	18,1	0,0033	350	1,14	0,10	350	0,0023
35	18,1	0,0030	300	0,91	0,08	300	0,0022
36	18,1	0,0010	250	0,26	0,02	250	0,0007
37	18,1	0,0000	200	0,00	0,00	200	0,0000
38	18,2	0,0000	150	0,00	0,00	150	0,0000
39	18,2	0,0000	100	0,00	0,00	100	0,0000
40	18,1	0,0000	50	0,00	0,00	50	0,0000

Table B-19: For MP0FA0WB125 mix

Sample number	**MP0FA0WB150**		**Density**	**1,366**			
Measuring point	**Temperature [°C]**	**Viscosity [Pa.s]**	**Shear rate [1/s]**	**Shear stress [Pa]**	**Torque [mNm]**	**Speed [1/min]**	**Cinematic viscosity [mm²/s]**
1	18,5	0,0000	50	0,00	0,00	50	0,0000
2	18,7	0,0000	100	0,00	0,00	100	0,0000
3	18,7	0,0000	150	0,00	0,00	150	0,0000
4	18,7	0,0000	200	0,00	0,00	200	0,0000
5	18,7	0,0003	250	0,07	0,01	250	0,0002
6	18,7	0,0010	300	0,31	0,03	300	0,0007
7	18,7	0,0022	350	0,77	0,07	350	0,0016
8	18,7	0,0030	400	1,19	0,11	400	0,0022
9	18,7	0,0037	450	1,66	0,15	450	0,0027
10	18,7	0,0040	500	2,02	0,14	500	0,0030
11	18,7	0,0046	550	2,54	0,23	550	0,0034
12	18,7	0,0052	600	3,14	0,23	600	0,0038
13	18,7	0,0056	650	3,66	0,39	650	0,0041
14	18,7	0,0058	700	4,08	0,37	700	0,0043
15	18,7	0,0061	750	4,60	0,35	750	0,0045
16	18,6	0,0068	800	5,48	0,50	800	0,0050
17	18,7	0,0070	850	5,99	0,54	850	0,0052
18	18,6	0,0073	900	6,64	0,60	900	0,0053
19	18,6	0,0077	950	7,34	0,67	950	0,0057
20	18,6	0,0079	1000	8,64	0,72	1000	0,0058
21	18,6	0,0086	1000	8,64	0,79	1000	0,0063
22	18,7	0,0051	950	4,87	0,44	950	0,0038
23	18,7	0,0074	900	6,64	0,60	900	0,0054
24	18,6	0,0070	850	5,99	0,54	850	0,0052
25	18,6	0,0066	800	5,24	0,48	800	0,0048
26	18,7	0,0063	750	4,73	0,43	750	0,0046
27	18,6	0,0058	700	4,03	0,30	700	0,0042
28	18,6	0,0055	650	3,57	0,32	650	0,0040
29	18,7	0,0049	600	2,96	0,27	600	0,0036
30	18,6	0,0041	550	2,26	0,21	550	0,0030
31	18,6	0,0038	500	1,89	0,17	500	0,0028
32	18,6	0,0035	450	1,56	0,14	450	0,0025
33	18,7	0,0027	400	1,10	0,10	400	0,0020
34	18,6	0,0017	350	0,59	0,05	350	0,0012
35	18,6	0,0010	300	0,31	0,03	300	0,0007
36	18,6	0,0008	250	0,20	0,01	250	0,0006
37	18,6	0,0000	200	0,00	0,00	200	0,0000
38	18,6	0,0000	150	0,00	0,00	150	0,0000
39	18,7	0,0000	100	0,00	0,00	100	0,0000
40	18,7	0,0000	50	0,00	0,00	50	0,0000

Table B-20: For MP10FA25WB150 mix

Sample number	MP10FA25WB150		Density	1,354			
Measuring point	Temperature [°C]	Viscosity [Pa.s]	Shear rate [1/s]	Shear stress [Pa]	Torque [mNm]	Speed [1/min]	Cinematic viscosity [mm²/s]
1	20,3	0,0000	50	0,00	0,00	50	0,0000
2	20,4	0,0000	100	0,00	0,00	100	0,0000
3	20,3	0,0000	150	0,00	0,00	150	0,0000
4	20,3	0,0000	200	0,00	0,00	200	0,0000
5	20,3	0,0003	250	0,07	0,01	250	0,0002
6	20,3	0,0015	300	0,45	0,04	300	0,0011
7	20,3	0,0023	350	0,82	0,07	350	0,0017
8	20,3	0,0036	400	1,42	0,13	400	0,0026
9	20,3	0,0038	450	1,70	0,15	450	0,0028
10	20,3	0,0042	500	2,12	0,19	500	0,0031
11	20,3	0,0048	550	2,64	0,24	550	0,0035
12	20,3	0,0057	600	3,43	0,31	600	0,0042
13	20,3	0,0053	650	3,43	0,31	650	0,0039
14	20,3	0,0070	700	4,92	0,45	700	0,0052
15	20,3	0,0076	750	5,71	0,52	750	0,0056
16	20,2	0,0076	800	6,08	0,55	800	0,0056
17	20,3	0,0081	850	6,35	0,62	850	0,0060
18	20,3	0,0086	900	7,53	0,70	900	0,0063
19	20,2	0,0090	950	8,50	0,77	950	0,0066
20	20,2	0,0094	1000	9,34	0,85	1000	0,0069
21	20,2	0,0096	1000	9,58	0,87	1000	0,0071
22	20,2	0,0090	950	8,50	0,77	950	0,0066
23	20,3	0,0087	900	7,81	0,71	900	0,0064
24	20,3	0,0081	850	6,92	0,63	850	0,0060
25	20,3	0,0091	800	7,25	0,66	800	0,0067
26	20,3	0,0063	750	4,73	0,43	750	0,0047
27	20,2	0,0067	700	4,69	0,43	700	0,0049
28	20,2	0,0051	650	3,33	0,30	650	0,0038
29	20,3	0,0058	600	3,47	0,32	600	0,0043
30	20,1	0,0058	550	3,19	0,29	550	0,0043
31	20,2	0,0046	500	2,31	0,21	500	0,0034
32	20,2	0,0043	450	1,94	0,18	450	0,0032
33	20,2	0,0036	400	1,42	0,13	400	0,0026
34	20,2	0,0021	350	0,73	0,07	350	0,0015
35	20,1	0,0010	300	0,31	0,03	300	0,0008
36	20,2	0,0000	250	0,00	0,00	250	0,0000
37	20,3	0,0000	200	0,00	0,00	200	0,0000
38	20,2	0,0000	150	0,00	0,00	150	0,0000
39	20,2	0,0000	100	0,00	0,00	100	0,0000
40	20,1	0,0000	50	0,00	0,00	50	0,0000

Table B-21: For MP15FA25WB150 mix

Sample number	**MP15FA25WB150**		**Density**	**1,352**			
Measuring point	**Temperature [°C]**	**Viscosity [Pa.s]**	**Shear rate [1/s]**	**Shear stress [Pa]**	**Torque [mNm]**	**Speed [1/min]**	**Cinematic viscosity [mm²/s]**
1	18,5	0,0000	50	0,00	0,00	50	0,0000
2	18,8	0,0000	100	0,00	0,00	100	0,0000
3	19,0	0,0000	150	0,00	0,00	150	0,0000
4	19,1	0,0000	200	0,00	0,00	200	0,0000
5	19,1	0,0000	250	0,00	0,00	250	0,0000
6	19,2	0,0012	300	0,35	0,03	300	0,0009
7	19,3	0,0017	350	0,59	0,05	350	0,0012
8	19,3	0,0031	400	1,24	0,11	400	0,0023
9	19,2	0,0039	450	1,75	0,16	450	0,0029
10	19,3	0,0054	500	2,68	0,24	500	0,0040
11	19,3	0,0050	550	2,73	0,25	550	0,0037
12	19,3	0,0052	600	3,15	0,29	600	0,0039
13	19,3	0,0043	650	2,82	0,26	650	0,0032
14	19,3	0,0065	700	4,55	0,41	700	0,0048
15	19,3	0,0070	750	5,24	0,48	750	0,0052
16	19,3	0,0075	800	5,80	0,55	800	0,0056
17	19,4	0,0080	850	6,69	0,62	850	0,0059
18	19,3	0,0082	900	7,34	0,67	900	0,0060
19	19,3	0,0087	950	8,27	0,75	950	0,0064
20	19,3	0,0091	1000	9,67	0,82	1000	0,0067
21	19,3	0,0093	1000	9,30	0,85	1000	0,0069
22	19,3	0,0086	950	8,18	0,74	950	0,0064
23	19,3	0,0083	900	7,43	0,68	900	0,0061
24	19,4	0,0078	850	6,64	0,60	850	0,0058
25	19,3	0,0072	800	5,76	0,52	800	0,0053
26	19,3	0,0069	750	5,15	0,47	750	0,0051
27	19,3	0,0076	700	5,29	0,48	700	0,0056
28	19,3	0,0059	650	3,85	0,35	650	0,0044
29	19,3	0,0053	600	3,19	0,29	600	0,0039
30	19,3	0,0052	550	2,87	0,26	550	0,0039
31	19,3	0,0045	500	2,26	0,21	500	0,0033
32	19,2	0,0034	450	1,52	0,14	450	0,0025
33	19,2	0,0027	400	1,10	0,10	400	0,0020
34	19,2	0,0022	350	0,77	0,07	350	0,0016
35	19,2	0,0009	300	0,26	0,02	300	0,0006
36	19,2	0,0000	250	0,00	0,00	250	0,0000
37	19,3	0,0000	200	0,00	0,00	200	0,0000
38	19,2	0,0000	150	0,00	0,00	150	0,0000
39	19,2	0,0000	100	0,00	0,00	100	0,0000
40	19,2	0,0000	50	0,00	0,00	50	0,0000

Table B-22: For MP20FA25WB150 mix

Sample number	**MP20FA25WB150**		**Density**	**1,351**			
Measuring point	**Temperature [°C]**	**Viscosity [Pa.s]**	**Shear rate [1/s]**	**Shear stress [Pa]**	**Torque [mNm]**	**Speed [1/min]**	**Cinematic viscosity [mm²/s]**
1	19,4	0,0000	50	0,00	0,00	50	0,0000
2	19,5	0,0000	100	0,00	0,00	100	0,0000
3	19,5	0,0000	150	0,00	0,00	150	0,0000
4	19,6	0,0000	200	0,00	0,00	200	0,0000
5	19,7	0,0000	250	0,00	0,00	250	0,0000
6	19,6	0,0010	300	0,31	0,03	300	0,0008
7	19,6	0,0017	350	0,59	0,05	350	0,0012
8	19,6	0,0025	400	1,00	0,09	400	0,0019
9	19,5	0,0035	450	1,56	0,14	450	0,0026
10	19,6	0,0038	500	1,89	0,17	500	0,0028
11	19,5	0,0050	550	2,77	0,25	550	0,0037
12	19,5	0,0039	600	2,36	0,21	600	0,0029
13	19,5	0,0045	650	2,91	0,26	650	0,0033
14	19,5	0,0068	700	4,78	0,43	700	0,0051
15	19,5	0,0068	750	5,10	0,46	750	0,0050
16	19,5	0,0071	800	5,66	0,51	800	0,0052
17	19,4	0,0074	850	6,32	0,57	850	0,0055
18	19,4	0,0079	900	7,11	0,65	900	0,0058
19	19,4	0,0082	950	7,81	0,71	950	0,0061
20	19,4	0,0085	1000	8,51	0,77	1000	0,0063
21	19,5	0,0092	1000	9,16	0,83	1000	0,0068
22	19,5	0,0081	950	7,71	0,70	950	0,0060
23	19,4	0,0078	900	7,01	0,64	900	0,0058
24	19,5	0,0076	850	6,50	0,59	850	0,0057
25	19,4	0,0078	800	6,27	0,57	800	0,0058
26	19,4	0,0071	750	5,34	0,49	750	0,0053
27	19,4	0,0068	700	4,73	0,43	700	0,0050
28	19,4	0,0060	650	3,89	0,35	650	0,0044
29	19,4	0,0052	600	3,15	0,29	600	0,0039
30	19,4	0,0050	550	2,73	0,25	550	0,0037
31	19,4	0,0042	500	2,08	0,19	500	0,0031
32	19,4	0,0037	450	1,66	0,15	450	0,0027
33	19,4	0,0029	400	1,14	0,10	400	0,0021
34	19,4	0,0015	350	0,54	0,05	350	0,0011
35	19,4	0,0007	300	0,21	0,02	300	0,0005
36	19,4	0,0000	250	0,00	0,00	250	0,0000
37	19,4	0,0000	200	0,00	0,00	200	0,0000
38	19,4	0,0000	150	0,00	0,00	150	0,0000
39	19,4	0,0000	100	0,00	0,00	100	0,0000
40	19,4	0,0000	50	0,00	0,00	50	0,0000

Table B-23: For MP25FA25WB150 mix

Sample number	**MP25FA25WB150**		**Density**	**1,349**			
Measuring point	**Temperature [°C]**	**Viscosity [Pa.s]**	**Shear rate [1/s]**	**Shear stress [Pa]**	**Torque [mNm]**	**Speed [1/min]**	**Cinematic viscosity [mm²/s]**
1	18,2	0,0000	50	0,00	0,00	50	0,0000
2	18,3	0,0000	100	0,00	0,00	100	0,0000
3	18,4	0,0000	150	0,00	0,00	150	0,0000
4	18,5	0,0000	200	0,00	0,00	200	0,0000
5	18,5	0,0000	250	0,00	0,00	250	0,0000
6	18,6	0,0010	300	0,31	0,03	300	0,0008
7	18,6	0,0018	350	0,63	0,06	350	0,0013
8	18,6	0,0030	400	1,19	0,11	400	0,0022
9	18,6	0,0031	450	1,38	0,13	450	0,0023
10	18,6	0,0031	500	1,56	0,14	500	0,0023
11	18,5	0,0051	550	2,82	0,26	550	0,0038
12	18,5	0,0053	600	3,19	0,29	600	0,0039
13	18,6	0,0058	650	3,80	0,35	650	0,0043
14	18,5	0,0062	700	4,36	0,40	700	0,0046
15	18,6	0,0084	750	6,27	0,57	750	0,0062
16	18,6	0,0088	800	7,01	0,64	800	0,0065
17	18,6	0,0077	850	6,55	0,60	850	0,0057
18	18,6	0,0079	900	7,15	0,65	900	0,0059
19	18,6	0,0083	950	7,85	0,71	950	0,0061
20	18,6	0,0088	1000	8,83	0,80	1000	0,0065
21	18,6	0,0090	1000	9,02	0,82	1000	0,0067
22	18,5	0,0084	950	7,95	0,72	950	0,0062
23	18,5	0,0079	900	7,15	0,65	900	0,0059
24	18,5	0,0076	850	6,45	0,59	850	0,0056
25	18,5	0,0086	800	6,87	0,62	800	0,0064
26	18,5	0,0067	750	5,06	0,46	750	0,0050
27	18,6	0,0062	700	4,36	0,40	700	0,0046
28	18,5	0,0057	650	3,71	0,34	650	0,0042
29	18,5	0,0053	600	3,19	0,29	600	0,0039
30	18,5	0,0042	550	2,31	0,21	550	0,0031
31	18,6	0,0049	500	2,45	0,22	500	0,0036
32	18,5	0,0039	450	1,75	0,16	450	0,0029
33	18,5	0,0027	400	1,10	0,10	400	0,0020
34	18,5	0,0017	350	0,59	0,05	350	0,0012
35	18,5	0,0007	300	0,21	0,02	300	0,0005
36	18,5	0,0000	250	0,00	0,00	250	0,0000
37	18,5	0,0000	200	0,00	0,00	200	0,0000
38	18,5	0,0000	150	0,00	0,00	150	0,0000
39	18,6	0,0000	100	0,00	0,00	100	0,0000
40	18,5	0,0000	50	0,00	0,00	50	0,0000

Table B-24: For MP30FA25WB150 mix

Sample number	MP30FA25WB150		Density	1,347			
Measuring point	**Temperature [°C]**	**Viscosity [Pa.s]**	**Shear rate [1/s]**	**Shear stress [Pa]**	**Torque [mNm]**	**Speed [1/min]**	**Cinematic viscosity [mm²/s]**
1	18,0	0,0000	50	0,00	0,00	50	0,0000
2	18,2	0,0000	100	0,00	0,00	100	0,0000
3	18,2	0,0000	150	0,00	0,00	150	0,0000
4	18,3	0,0000	200	0,00	0,00	200	0,0000
5	18,4	0,0000	250	0,00	0,00	250	0,0000
6	18,4	0,0012	300	0,35	0,03	300	0,0009
7	18,5	0,0022	350	0,77	0,07	350	0,0016
8	18,4	0,0030	400	1,19	0,11	400	0,0022
9	18,4	0,0039	450	1,75	0,16	450	0,0029
10	18,5	0,0035	500	1,75	0,16	500	0,0026
11	18,5	0,0051	550	2,82	0,26	550	0,0038
12	18,4	0,0057	600	3,43	0,31	600	0,0042
13	18,4	0,0046	650	3,01	0,27	650	0,0034
14	18,4	0,0079	700	5,52	0,50	700	0,0059
15	18,4	0,0058	750	4,36	0,40	750	0,0043
16	18,4	0,0077	800	6,18	0,56	800	0,0057
17	18,4	0,0083	850	7,01	0,64	850	0,0061
18	18,3	0,0085	900	7,67	0,70	900	0,0063
19	18,4	0,0090	950	8,55	0,78	950	0,0067
20	18,3	0,0094	1000	9,39	0,85	1000	0,0070
21	18,5	0,0095	1000	9,53	0,87	1000	0,0071
22	18,4	0,0088	950	8,36	0,76	950	0,0065
23	18,4	0,0084	900	7,57	0,69	900	0,0062
24	18,4	0,0080	850	6,78	0,62	850	0,0059
25	18,4	0,0094	800	7,48	0,68	800	0,0069
26	18,4	0,0073	750	5,48	0,50	750	0,0054
27	18,4	0,0079	700	5,52	0,50	700	0,0059
28	18,4	0,0062	650	4,03	0,37	650	0,0046
29	18,5	0,0056	600	3,61	0,30	600	0,0041
30	18,5	0,0050	550	3,05	0,25	550	0,0037
31	18,5	0,0054	500	2,68	0,24	500	0,0040
32	18,5	0,0035	450	1,56	0,14	450	0,0026
33	18,5	0,0027	400	1,10	0,10	400	0,0020
34	18,5	0,0025	350	0,86	0,08	350	0,0018
35	18,6	0,0012	300	0,35	0,03	300	0,0009
36	18,5	0,0000	250	0,00	0,00	250	0,0000
37	18,6	0,0000	200	0,00	0,00	200	0,0000
38	18,6	0,0000	150	0,00	0,00	150	0,0000
39	18,6	0,0000	100	0,00	0,00	100	0,0000
40	18,6	0,0000	50	0,00	0,00	50	0,0000

CURRICULUM VITAE

PERSONAL INFORMATION

Name and Surname: Muhammet ÇINAR

Natioality: Turkish

Birth place and date: DENİZLİ / 11.09.1989

Phone number: +90 545 464 89 89

Email: muhammet.cinar@hku.edu.tr and mcinar.ce@gmail.com

EDUCATION

Graduate school	Year
Master: Hasan Kalyoncu University (Occupational Health and Safety)	2017
Master: Hasan Kalyoncu University (Civil Engineering)	2015
Bachelor: Gaziantep University (Civil Engineering)	2013
High School: Durmuş Ali Çoban High School	2006

WORK EXPERIENCE

	Place	Enrollment
2014- Present	Hasan Kalyoncu University	Teaching Assistant
2013-2014	TÜBİTAK 1001	Researche Assistant

PUBLICATIONS

Articles:

Çınar, M., Çelik, F., Çanakcı, H., Nassani, D.E. (2017). "Fresh Properties of Cementitious Grout with Rice Husk Powder". Arabian Journal for Science and Engineering **42 (9)**, 3819-3827 (SCI-Exp)

Çınar, M., Karpuzcu, M., Çanakcı, H. (2019). "Effect of Waste Marble Powder and Fly Ash on The Rheological Characteristics of Cement-Based Grout". Civil Engineering Journal, **5 (4)**, XX (Emerging SCI- WoS)

Çınar, M., Karpuzcu, M., Çanakcı, H. (2019). "The Measurement of Fresh Properties of Cement-Based Grout Containing Waste Marble Powder". Journal of the International Measurement Confederation (Measurement), XX (SCI-Exp- Under Review)

<u>Proceedings at international and national conferences:</u>

Çınar, M., Çelik, F., Çanakcı, H. (2015). "Effect of Rice Husk Powder Content with Different Water-Cement Ratios on Rheological Properties of Cement-Based Grouts". International Conference on Computational and Experimental Science and Engineering (ICCESEN 2015) 14-19 Oct. 2015, Antalya Türkiye

Çelik, F., **Çınar, M**., Çanakcı, H. (2015). "Çimento Katkılı Grout'un Reolojik ve Akışkanlık Özelliklerine Pirinç Kabuğu Külünün Etkisi" 6. Geoteknik Sempozyumu 26-27 Kasım 2015, Çukurova Üniversitesi, Adana

Altunhan, İ., **Çınar, M**., Çanakcı, H. (2015). "Investigating geotechnic properties of materials gypsum and anyhdrite that developing depending on geological structure in sivas basin hafik formation" International Conference on Computational and Experimental Science and Engineering (ICCESEN 2015) 14-19 Oct. 2015, Antalya Türkiye